Investigations on (photo) reactions of cosmetic UV filters towards skin proteins

Dissertation zur Erlangung des Doktorgrades
der Naturwissenschaften (Dr. rer. nat.)

Fakultät Naturwissenschaften
Universität Hohenheim

Institut für Lebensmittelchemie

vorgelegt von

Constanze Stiefel

aus Leonberg

2014

Dekan:	Prof. Dr. Heinz Breer
1. berichtende Person, 1. Prüfer:	Prof. Dr. Wolfgang Schwack
2. berichtende Person, 2. Prüfer:	Prof. Dr. Gertrud Morlock
3. Prüfer:	Prof. Dr. Heinz-Dieter Isengard

Eingereicht am:	07.10.2014
Mündliche Prüfung am:	17.02.2015

Die vorliegende Arbeit wurde am 02.02.2015 von der Fakultät Naturwissenschaften der Universität Hohenheim als „Dissertation zur Erlangung des Doktorgrades der Naturwissenschaften“ angenommen.

Danksagungen

Ganz herzlich möchte ich mich bei all jenen bedanken, die zum guten Gelingen dieser Arbeit beigetragen haben:

- Prof. Dr. Wolfgang Schwack für das spannende Thema dieser Arbeit, die stete Diskussionsbereitschaft und Erreichbarkeit bei jeglichen Fragenstellungen, die beständige Hilfe während des gesamten Publikationsprozesses sowie die Möglichkeit einer flexiblen Einteilung der Arbeit, so dass die Fertigstellung der Dissertation parallel zum bereits begonnenen Arbeitsverhältnis problemlos möglich war

- Prof. Dr. Gerda Morlock für die Übernahme des Mitberichts, die stete Bereitschaft zum wissenschaftlichen Austausch und die stets aufbauenden und inspirierenden Gespräche

- Prof. Dr. Heinz-Dieter Isengard für die Bereitschaft, als 3. Prüfer zur Verfügung zu stehen

- Sylvia Maître, Lilli Sawitzki und Yen-Thi Hai Nguyen, die mich bei meiner experimentellen Arbeit unterstützt haben

- bei allen Mitarbeitern des Instituts für Lebensmittelchemie für eine wirklich tolle Zeit und viele schöne gemeinsame Erlebnisse und Erinnerungen

Ein ganz besonderer Dank gilt meinen Eltern, die immer für mich da sind, mich stets unterstützen, motivieren und fördern und ohne die das Gelingen dieser Arbeit nicht möglich gewesen wäre; meinem Freund Frank für seine ruhige und besonnene Art und seine stete Unterstützung; meiner Patentante Bruni und ihrem Mann Herbert, die extra zum Strand gefahren sind, um mir Sand und Meerwasser von der Ostsee zu schicken; all meinen guten Freunden, die mich immer wieder motiviert und während der ganzen Zeit begleitet haben und mich nie haben vergessen lassen, dass man den Computer irgendwann auch mal ausschalten kann.

Table of contents

Preliminary remarks

The work presented in this doctoral thesis was carried out under the supervision of Prof. Dr. Wolfgang Schwack between August 2007 and October 2014 at the Institute of Food Chemistry, University of Hohenheim, Stuttgart, Germany.

Parts of this thesis have already been published in the following international peer-reviewed journals, or were presented at international conferences as oral or poster presentations:

Full publications

1. C. Stiefel and W. Schwack (2013) Rapid screening method to study the reactivity of UV filter substances towards skin proteins by high-performance thin-layer chromatography. *International Journal of Cosmetic Science* 35, 588-599.
2. Constanze Stiefel and Wolfgang Schwack (2013) Reactions of cosmetic UV filters with skin proteins: model studies of ketones with primary amines. *Trends in Photochemistry and Photobiology* 15, 63-75.
3. Constanze Stiefel and Wolfgang Schwack (2013) Reactions of cosmetic UV filters with skin proteins: model studies of esters with primary amines. *Trends in Photochemistry and Photobiology* 15, 106-116.
4. C. Stiefel and W. Schwack (2014) Reactivity of cosmetic UV filters towards skin proteins: Model studies with Boc-lysine, Boc-Gly-Phe-Gly-Lys-OH, BSA and gelatin. *International Journal of Cosmetic Science* 36, 561-570.
5. C. Stiefel, W. Schwack (2015) Photoprotection in changing times – UV filter efficacy and safety, sensitization processes and regulatory aspects. *International Journal of Cosmetic Science* 37, 2-30.
6. C. Stiefel and W. Schwack (2015) Photostability of Cosmetic UV Filters on Mammalian Skin Under UV Exposure. *Photochemistry and Photobiology* 91, 84-91.

Oral presentations

1. Constanze Stiefel, Wolfgang Schwack: Schnelles HPTLC-Screening zur Reaktivität von UV-Filtern gegenüber Hautproteinen, Jahrestagung der Regionalverbände Nord und Südwest der Lebensmittelchemischen Gesellschaft, Karlsruhe, March 19-20, 2013.

Poster presentations

1. Constanze Stiefel, Wolfgang Schwack: Modellstudien zur Reaktivität von UV Filtersubstanzen gegenüber Proteinen. 38. Deutscher Lebensmittelchemikertag, 14. - 16. September, 2009, Berlin, Deutschland.

2. Constanze Stiefel, Wolfgang Schwack: Modellstudien zur Bildung von UV-Filter-Proteinaddukten, Lebensmittelchemische Gesellschaft, Arbeitstagung der Regionalverbände Süd-West und Bayer, 08. - 09. März 2010, Erlangen, Deutschland.

3. Constanze Stiefel, Wolfgang Schwack: Modellstudien zur Bildung von UV Filter-Protein-Addukten, Lebensmittelchemische Gesellschaft, Arbeitstagung der Regionalverbände Nord und Südwest, 14. - 15. März 2011, Kassel, Deutschland.

4. Constanze Stiefel, Wolfgang Schwack: Fast HPTLC screening to study the reactivity of UV filter substances towards skin proteins, 22. International Symposium for High-Performance Thin-Layer Chromatography, 02. – 04. July 2014, Lyon, France.

Chapter I-VI of this thesis are in form and content identical with the full publications 1-6. Styles and figures were adapted to the consecutive layout of the thesis.

Except for figure 1 in chapter I, which is used with friendly permission of OpenStax College, all other images, pictures and illustations in this work were created by the author.

Contributions

The participation and contributions of the authors to the specified full publications are as follows:

Ms. **Constanze Stiefel** performed all the essential practical and analytical work. The analysis and interpretation of the obtained data was carried out by herself, as was the conception and preparation of the original manuscripts that lead to the specified publications.

Prof. Dr. Wolfgang Schwack was the supervisor of this work and he proofread and corrected the manuscripts in terms of structure, comprehensibility, and text credibility and readability. Prof. Dr. Wolfgang Schwack advised in clarifying analytical questions, functioned as an advisor throughout the publication process, and was responsible for the formal aspects of the publications.

Ms. **Yen-Thi Hai Nguyen** assisted Ms. Constanze Stiefel in the preparation and analysis of porcine skin samples during her diploma thesis.

I Photoprotection in changing times – UV filter efficacy and safety, sensitization processes and regulatory aspects

Constanze Stiefel, Wolfgang Schwack

Reprinted with permission from: *International Journal of Cosmetic Science* 2014, 37, 2-30.

Synopsis

As excessive sun exposure is tightly associated with different pathological changes of the skin, for example premature skin ageing or the development of skin cancer, an appropriate protection of the skin against UV radiation is of particular importance. Sun protection products and UV filter substances have evolved continuously in the past few decades. New developments and improved technical conditions of production have led to increasingly effective and efficient products with broadband protection ability. Accordingly, legal requirements have also changed and expanded. Although certain trends exist to harmonize the regulation of sunscreens at a global level, there are still large differences how UV absorbers are approved, which testing methods are prescribed, and which general requirements sun protection products must fulfil. Modern UV filters provide efficient protection against UVA and UVB radiation, are heat and photostable, user-friendly, cost-effective, water resistant and non-toxic. As inorganic and organic UV filters are topically applied to the skin in relatively high concentrations (up to 25%), especially the assessment of their (photo)sensitization potential is of particular importance. Accordingly, skin sensitization is a key endpoint for the legally required safety assessment of cosmetic ingredients in Europe and many other countries. This review will summarize the current regulatory status of different approved UV filters, will describe their beneficial and adverse properties and will give an overview of how the efficacy of sunscreens can be evaluated. Finally, an insight into the basic mechanism of (photo)allergic reactions and existing skin sensitization test methods will be provided.

Keywords: safety testing, skin barrier, skin physiology/structure, skin sensitization, sun protection, UV absorbers

General introduction

In addition to the desired effects of sun radiation, such as the increase of general well-being [1], vitamin D3 synthesis [2] and positive therapeutic effects on some skin diseases, for example psoriasis [3], excessive UV radiation is mainly responsible for several types of severe skin damage. In addition to the direct visible acute damages such as sunburn or polymorphic light eruption, the undesirable long-term effects, most notably skin cancer, are a special cause for concern [4-6]. Today, it is generally accepted that a main environmental risk factor for skin cancer is the exposure to sunlight or UV radiation [7, 8]. This finding, however, prevailed only gradually during the 20th century.

Until the end of the 19th century, there was no real market for sun protection products. A pale skin colour was considered elegant and begat prosperity. With industrialization, the centuries-old ideal of beauty changed fundamentally. An improved living standard with more leisure time, a less-restricted style of dress and medical health advice to spend more time outdoors led to increased sun exposure and the initial need for skin protection [9, 10].

Still, at the beginning of the 20th century, it was believed that solar heat was the actual cause of sunburn. Only in 1922 did Karl Eilham Hausser und Wilhelm Vahle observe that not heat but ultraviolet radiation between 280 and 315 nm was responsible for the formation of sunburn [11]. This finding was the cornerstone of sunscreen development.

Already in the middle of the 1930s, Franz Greiter and Eugene Schueller, the later founders of Piz Buin and L'Oreal, brought the first, simple sunscreens on the market. These products were mainly focused on the prevention of sunburn, that is ultraviolet (UVB) protection. Due to the success of the first sunscreens, there was a decreasing fear of sunburn, and sunbathing became increasingly popular [12, 13]. However, with the extended exposure to the sun, the incidence of skin cancer also increased [14, 15].

In Germany alone, the cases of cutaneous melanoma have nearly tripled between 1976 and 2003 [16] with approximately 140 000 new cases of skin cancer every year [17]. Recent increases in skin cancer incidence may directly reflect the change in leisure behaviour over the last decades associated with shortterm excessive tanning, especially during the summer holidays or due to the usage of tanning devices [18–20]. Here, it must be mentioned that sunscreens with higher sun protection factor (SPF) may offer better protection ability, but conversely also entice the user to stay longer in the sun [21, 22]. Furthermore, there has been a gradual depletion of the stratospheric ozone layer ('ozone hole') since the 1970s [23], which has led to increased UVB intensity at the surface associated with a rising number of skin cancer cases [24, 25].

To avoid damage from UV radiation, the human body has developed different protection mechanisms, for example a thickening of the stratum corneum (hyperkeratosis) or skin pigmentation [26, 27]. However, the body's protective mechanisms are not sufficient for long-term UV exposure, and additional protective measures are required.

The widespread sun protection campaigns since the 1980s have led to improved education of the population about the risks of excessive sun exposure and the importance of sunscreen usage [28–30]. This laid the foundation for a growing market of sun protection products, which have been continuously improved and adapted to consumer needs and the scientific progress. With increasing awareness of the harmful effects of sunlight, the demand for higher sun protection factors (SPFs) has continued to grow in recent decades. At the end of the 1970s, an SPF of about 20 was the maximum attainable SPF with existing technological capabilities and the limited number of available UV filters. Today, there is a variety of organic and inorganic UV filters, which are combined to reach a balanced UVA/UVB protection while maintaining a high SPF of greater than 50 due to an increase in the number of UV filters and their concentration in the products [31, 32].

Furthermore, the usage of cosmetic UV filter substances has expanded to a large number of daily skin and hair care products [33, 34]. It is therefore not surprising that more than 10 000 tons of UV filters are produced annually for the global market [35]. As a result, the skin is in constant contact with high quantities of UV filters throughout the entire year. This increased usage must be studied critically, not only because of the increasing release of the UV filters into the environment [36, 37] and their possible ecological impacts [38, 39], but also due to their behaviour on the skin.

Because of the particular application type and the typical chemical structure of organic UV filters, the assessment of their photostability is of great importance [40]. Photodegradation can lead to a loss of UV protection and the formation of photo products [41–43]. Additionally, due to the chemical structure of the most common organic UV filters and their known photodegradation products, various reactions, for example with protein structures of the skin, are conceivable but not yet sufficiently investigated [44].

Structure of the human skin

The largest human organ is the skin with a surface area of about 2 m^2 and a weight of about 3 kg for an average adult, calculated without subcutaneous adipose tissue. The skin consists of several layers of epithelial tissue with an average thickness of between approximately 0.5 and 2 mm (palms and soles up to 4 mm) [45]. The skin fulfils several important vital functions. As an outer barrier, it protects the inner body against pathogens and mechanical, chemical and physical impacts. With various sensory receptors, which are responsive against mechanical stimuli and temperature, the skin is an important sense organ. In addition, the skin prevents the uncontrolled loss of water and minerals and protects the human body against hypothermia. Finally, the skin is responsible for the production of vitamin D [46, 47]. The human skin consists of three main definable layers, the epidermis, the dermis and the subcutis (Fig. 1).

The epidermis can be further divided into five sublayers: the stratum basale, stratum spinosum, stratum granulosum, stratum lucidum and stratum corneum [48]. The basal/germinal layer (stratum basale) shows the highest mitotic activity of the skin. It is composed mainly of nonproliferating and proliferating keratinocytes (KCs; ‘stem cells’); proliferating KCs undergo constant cell division and are the origin of the corneocytes, which are finally exfoliated at skin surface [49]. Each basal cell has a large nucleus, numerous free ribosomes, a few mitochondria, a small Golgi complex and a rough endoplasmic reticulum (rER). Additionally, several Merkel cells (touch receptors) and the melanocytes are located in this layer. In the multilayered spinous layer (stratum spinosum), a gradual transformation of KCs took place, and they become larger, polygonal and flattened in the upper part of the layer. The cells of the stratum spinosum synthesize intermediate filaments (cytokeratins), which are grouped into bundles, called tonofilaments. KCs are connected to each other by multiple, prickle-like intercellular bridges (desmosomes) where the tonofilaments are anchored to the cell membrane.

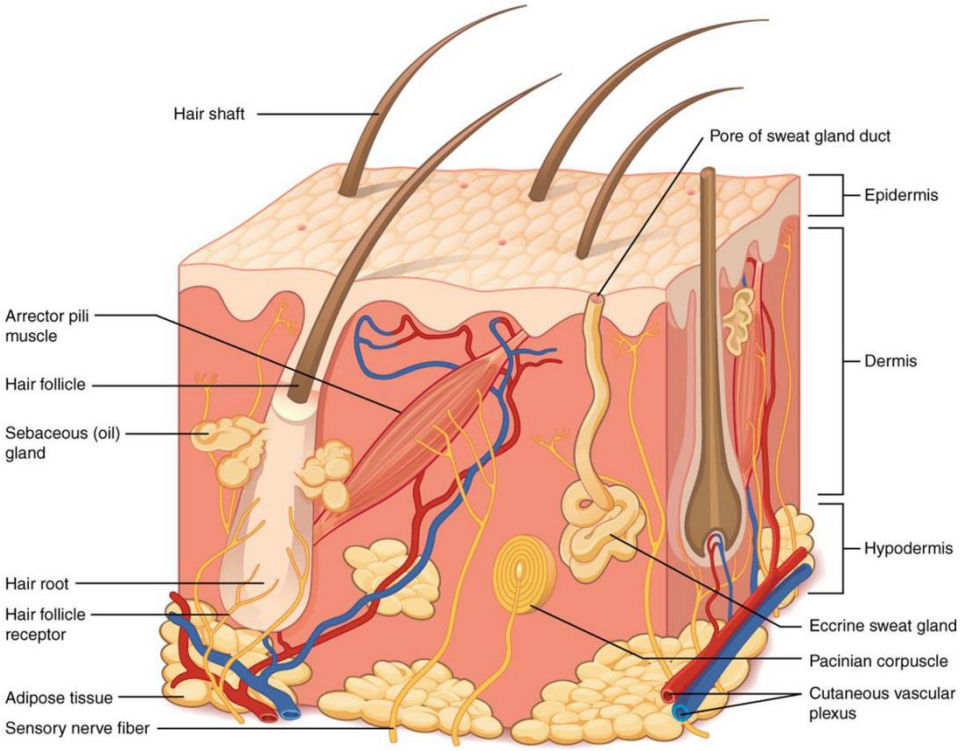

Figure 1 Layers of skin: the skin is composed of two main layers: the epidermis, made of closely packed epithelial cells, and the dermis, made of dense, irregular connective tissue that houses blood vessels, hair follicles, sweat glands and other structures. Beneath the dermis lies the hypodermis, which is composed mainly of loose connective and fatty tissues. (This content is available for free at http://cnx.org/content/col11496/latest) [419].

This reticulated structure gives the layer its typical name. In the stratum spinosum, the immune cells of the lymphatic system (Langerhans cells) are located. The increased synthesis of keratohyalin in KCs of the granular layer (stratum granulosum) initiates the cornification (keratinization) of the cells. This is accompanied by a simultaneous loss of other cell organelles (e.g. the nucleus). Lipids contained within lamellar bodies of KCs are released into the extracellular space and form the lipid barrier of the skin. What follows is the stratum lucidum. The clear and thin layer of dead skin cells is only present in the palms and soles. The outer layer is the cornified/horny layer (stratum corneum) consisting of 10–30 layers of polyhedral, enucleated corneocytes. Corneocytes are surrounded by an envelope of cornified proteins (e.g. loricrin, involucrin and filaggrins) filled with water-retaining keratin proteins. The corneocytes stick together through corneodesmosomes and are surrounded by hydrophobic lipids [50]. The intercellular organization of the lipids plays an important role in the barrier function of the skin [51, 52]. They form two lamellar phases, with periodicities of approximately 6 and 13 nm [53]. The lipids inhibit both an inside–out water loss and the permeation of hydrophilic substances with a molecular weight of more than about 500 Dalton (DA) [54]. The main barrier functions of the epidermis are attributed to the stratum corneum, which prevents water loss from the body and provides mechanical protection, although the cell–cell junctions and the associated cytoskeletal proteins in the deeper layers also provide important protection ability [55–57]. In adult epidermis, there is a balance of cell proliferation and cell desquamation with a complete renewal approximately every 28 days [58].

The cell proliferation in the stratum basale is followed by the differentiation of the cells in the stratum spinosum and granulosum, which ends with the transition in the horny layer. The dermis is tightly connected to the epidermis through the basal layer. The main structural components of the dermis are collagen, elastic and extrafibrillar matrix fibres (connective tissue), which give the skin its mechanical stability. The hair follicles, sweat glands, sebaceous glands and apocrine glands are located in the dermis. The dermis also contains numerous lymphatic vessels and blood vessels, which nourish both dermal and epidermal cells and are important for waste removal. Various immune cells, such as macrophages, lymphocytes and mast cells, are also located in the dermis. The dermis can be divided in the stratum papillare and the stratum reticulare [47]. With age, the human skin becomes thinner, more and more wrinkled, and loses some of its elasticity. The main reasons for this are the dehydration of the stratum corneum, an extensive crosslinking of collagen and the degeneration of the elastic fibres [59, 60]. The subcutis or hypodermis lies below the dermis. It attaches the skin to underlying bones and muscles and contains the bigger blood vessels and nerves. It consists of loose connective tissue and elastin. The main cell types are fibroblasts, macrophages and adipocytes. Adipose tissue serves as thermal isolation, provides energy storage and offers mechanical protection [61].

Natural sunlight

The spectrum of natural sunlight covers most of the electromagnetic spectrum with the highest intensity in the range of visible light. At the top of the earth's atmosphere, sunlight has a power of 1366 watts m 2 and is comprised of about 50% infrared (IR) light, 40% visible light (VIS) and 10% ultraviolet (UV) light [62] (Fig. 2).

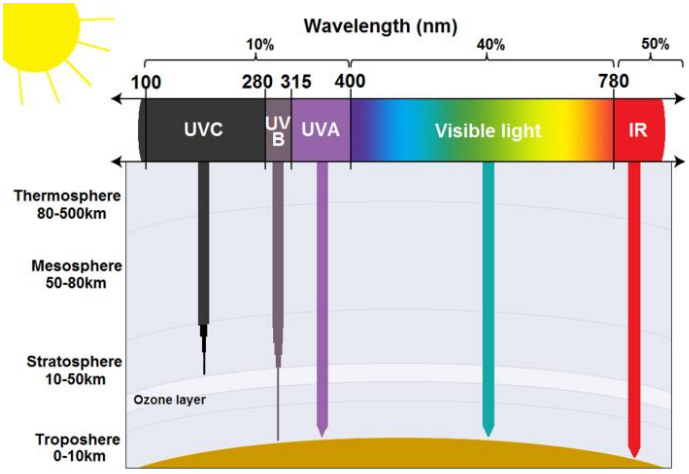

Figure 2 Spectrum of natural sunlight and the light-filtering effect of the atmosphere (according to data of [62,63,65]).

Whereas humans sense IR radiation as heat and VIS radiation optically, UV radiation is not directly perceivable. Depending on the wavelength, UV radiation can be divided into UVC (200–280 nm), UVB (280–315 nm) and UVA radiation (315–400 nm) [63]. Only part of UV radiation reaches the surface and depends on the location, the season, the clouds, the air pollution and the humidity [64]. The majority of UVC and UVB radiation is absorbed by oxygen and ozone in the atmosphere.

On average, approximately 20 times more UVA rays than UVB rays reach the earth's surface [65]. Due to their different wavelengths, UV rays can penetrate the skin to different depths and can cause cellular changes (Fig. 3) [66, 67].

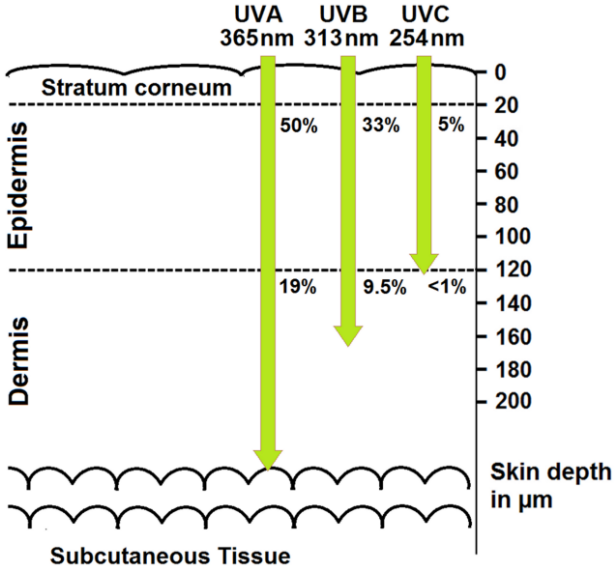

Figure 3 Percent transmittance of UVA, UVB, and UVC radiation (according to data of [67]).

In addition to natural sources, artificial sources must also be mentioned. Except for occupational exposure, sun lamps and tanning beds are the most common source of artificial UV light in everyday life [68, 69]. Commercial tanning beds emit high UVA levels and variable amounts of UVB (1–5%) [70]. Because children and adolescents in particular show a higher vulnerability to UV radiation [71, 72], some EU countries, including Germany, the United Kingdom and Austria, have adopted legal provisions that prohibit adolescents under 18 years from indoor tanning [73].

Positive effects

Limited quantities of UV rays have different positive effects on human well-being and are described as relaxing and enjoyable. Most positive effects of solar radiation are seen in the context of UVB-induced production of vitamin D3 in the skin [2, 74]. By incident sunlight, 7-dehydrocholesterol, present in the plasma membranes of epidermal KCs and dermal fibroblasts, is converted into previtamin D3. By the rearrangement of double bonds (thermal isomerization), stable vitamin D3 is formed and ejected into the extracellular space where it binds to the vitamin D-binding protein and thus enters the circulatory system. With protein binding, vitamin D3 is converted into 25-hydroxyvitamin D3 (25(OH) D). After being transported to the kidney, 25(OH)D is metabolized to 1,25–dihydroxyvitamin D3 ($1,25(OH)_2D$), its biologically active form [75].

During prolonged UV radiation, pre-vitamin D3 is photoisomerized to the two biologically inactive isomers, lumisterol and tachysterol, and vitamin D3 is converted to suprasterols I and II and 5,6-transvitamin D3, to prevent vitamin D intoxication [75, 76].

Vitamin D3 is required for the intestinal absorption of calcium and phosphorus and is therefore essential for healthy bone growth. Without vitamin D3, only 10–15% of dietary calcium and about 60% of phosphorus are absorbed [77, 78]. In childhood, severe vitamin D insufficiency can lead to growth retardation and skeletal deformities, such as rickets [79]. In adults, vitamin D deficiency leads to reduced bone mineral density and ultimately to osteoporosis [80, 81]. In addition, as skeletal muscles have receptors for $1,25(OH)_2D$, the hormonally active form of vitamin D, some studies suggest that vitamin D deficiency may also be related to muscle weakness [82, 83].

For most people, approximately 90% of the human vitamin D requirement is covered by exposure to sunlight. Therefore, elderly people staying indoors most of the time, heavily veiled women, and strong pigmented persons are especially affected by deficiencies [84–86]. The application of sunscreens with high SPF can also decrease vitamin D production [87].

In addition to its positive effects on the bone health, vitamin D can have many other positive effects on the human body. These include the stimulation of insulin production, effects on myocardial contractility, modulation of T and B lymphocyte function, prevention of inflammatory disease, promotion of hormone secretion, and decreased risk of developing colon cancer and rheumatoid arthritis [74, 87, 88].

In addition, UV radiation is also successfully used to treat several skin diseases, for example psoriasis and eczema [89, 90]. Such treatment occurs under medical supervision, and the benefits of the treatment and the risk of extensive UV radiation are weighed against each other at the beginning [91]. In general, balanced exposure to sunlight is essential to make optimal use of positive health effects without unnecessarily burdening the skin.

Negative effects

UVB radiation

The basis of the biological effects of UV rays is their absorption by endogenous molecules and an associated excitation or even ionization of specific amino acids or nucleic acids. With decreasing wavelengths, the energy of the radiation and the damaging effects strongly increase.

Energy-rich, short wave UVB rays mainly act in the epidermis and are the main cause of probably the best known and most obvious acute negative effect of extensive sun exposure, the sunburn (erythema). In comparison with skin reddening that occurs immediately and is mainly caused by a temporary widening of blood vessels and an associated increase in circulation, UVB-induced erythema occurs some hours after UV exposure. Sunburn is seen as an inflammatory skin reaction, which can be associated with swelling, itching and even blistering [5, 92].

With strong damage to skin cells or genetic material, the cells are subject to programmed cell death known as apoptosis. The consequence of this process is skin peeling and renewal of the skin after strong sunburn. This renewal is a kind of protection mechanism that prevents the replication of malignant cells and the formation of skin cancer [93–95].

UVB radiation has a strong carcinogenic effect. It causes direct damage to the DNA and RNA and leads to the generation of thymine–thymine cyclobutane pyrimidine dimers (TT-CPDs) (Fig. 4) and pyrimidine–pyrimidine (6-4) adducts (6-4 PPs) (Fig. 5) [6, 96, 97].

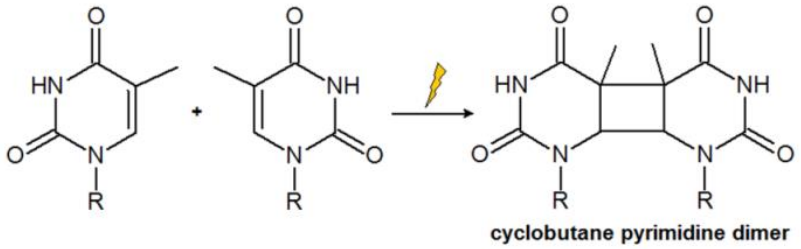

Figure 4 Formation of thymine cyclobutane dimers (according to [420]).

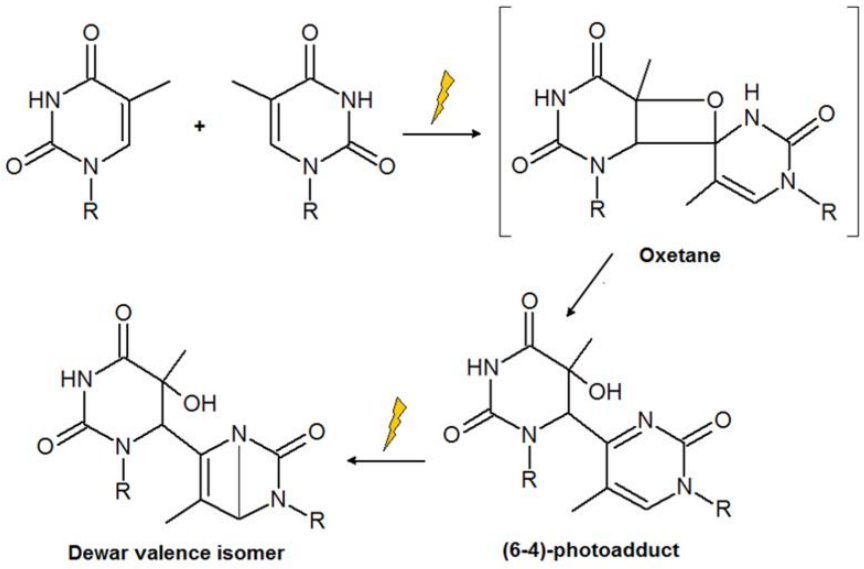

Figure 5 Formation of the pyrimidine (6-4) pyrimidone photoproduct (according to [420]).

DNA photoproducts can be excised and replaced by different endogenous repair enzymes (specific endonucleases), which restore the original structure. However, if the repair mechanisms fail or the damage is too extensive, apoptosis is initiated by the tumour suppressor protein p53 (TP53). However, if the suppressor protein has also been damaged due to UV radiation, apoptosis does not occur. As consequence, it can come to an accumulation of mutations in the DNA during cell division, particularly to C-to-T or CC-to-TT transitions (‘UV signature mutations’) [6, 98]. In squamous cell carcinoma and partly basal cell carcinoma, these mutations are mainly found in the TP53 gene [99–101]. Furthermore, there is also a direct association between exposure to UVB radiation and the formation of eye disease. Photokeratitis and photoconjunctivitis (inflammation of the cornea and conjunctiva) are known reversible acute effects [102, 103], whether pathological changes such as cataracts, pterygia conjunctiva or macular degeneration develop only gradually [104, 105]. Therefore, appropriate protection of the skin and also the eyes is important in bright sunlight.

UVA radiation

UVA radiation plays a major role in photoageing of the skin. Today, it is generally assumed that UVA radiation leads to a balance shift towards the collagen-degrading matrix metalloproteinases (MMPs) and a simultaneous downregulation of their tissue-specific inhibitors [106, 107]. The consequences are an accelerated and increasing degradation of collagen fibres with the concurrent inhibition of the formation of collagen and hyaluronic acid. This leads to an increased formation of deep skin folds, wrinkles and a loss of turgor [108, 109].

Photoageing has also been shown to be correlated with the increased formation of mutations of the mitochondrial DNA, triggered by the formation of reactive oxygen species (ROS), for example superoxide radical, hydrogen peroxide or hydroxyl radical [110, 111]. This mutagenesis mainly affects the dermis and therefore the non-proliferating part of the skin, so that the UV-damaged skin cells cannot be eliminated by the endogenous repair mechanisms. This results in the dose-dependent accumulation of the damages of the mitochondrial genome [112, 113]. However, the ageing process is not limited to the dermis, but also affects the epidermis. The proliferation of healthy KCs is strongly disturbed in the presence of fibroblasts with a high content of mitochondrial DNA deletions, which show up in a weakening of the barrier functions of the skin [114].

Naturally, the skin has endogenous enzymatic antioxidants (e.g. superoxide dismutase or catalase) and non-enzymatic antioxidants (e.g. coenzyme Q10, glutathione or vitamin E), which provide protection against ROS [115, 116]. However, UV radiation leads to a decrease in antioxidant enzymatic activity in cultured fibroblasts [117], and repeated UV exposure before enzyme activity fully returns can lead to additional damage to the skin tissue [118].

In addition, UVA radiation and the formation of ROS not only influence skin ageing but also play a central role in the formation of cancer [119, 120]. ROS are formed via absorption of the UV rays by cellular chromophores such as NADH or porphyrins. They can cause punctual DNA mutations, chromatid exchange, chromosome aberrations or single-strand breaks, which explains their cytotoxic and carcinogenic potential [6, 111, 121].

Singlet oxygen is considered to be the most important ROS that oxidizes the guanine nucleotide to 8-hydroxy-2'-deoxyguanosine (8-oxodG), which is the main marker of oxidative DNA damages [122, 123]. As a result, G-to-T or T-to-G transitions occur, which can be seen as typical UVA fingerprint mutations in keratinocytederived tumours and especially in melanoma [124–126].

Squamous cell and basal cell carcinoma

The occurrence of squamous cell and basal cell carcinoma provides evidence for the influence of long-term UV radiation on their formation. Both skin cancer types extend from the epidermis and are mainly found in skin areas exposed to extensive sun light. Accordingly, more than 80% of basal cell carcinomas and more than 75% of squamous cell carcinomas are found on the head, neck or the hands [127].

They mostly grow there continuously at the same position, and a delocalization is rather rare, more often observed in cases of squamous cell carcinoma (approximately 5%). Actinic keratosis is often seen as a precursor of squamous cell carcinoma and is associated with the first skin changes of sun-exposed areas with scaly, thickened or crusty skin patches [128].

Depending on the different penetration depths of UVA and UVB rays, UVA fingerprint mutations are preferentially found in the basal layer, whereas UVB fingerprint mutations concentrate particularly on superficial layers [125]. Although UVB radiation is believed to play a greater role in the formation of non-melanoma skin cancer, also UVA radiation seems to be an important risk factor [120, 129–131].

Another carcinogenic effect of both UVA and UVB radiation is its suppressive effect on the immune system of the skin [132]. In the skin, different cell types are responsible for immune defence: KCs, monocytes, epidermal T cells, dermal macrophages and Langherhans cells (LCs). These cells interact with a complex network of mediators such as prostaglandins and cytokines that coordinate a balanced immune response [133]. This complex organization is deeply altered by UV irradiation, which leads to the increased release of immune suppressive cytokines, for example interleukin 4 and 10 (IL-4, IL-10), hepatocyte growth factor (HGF), tumour necrosis factor alpha (TNF-α), or transforming growth factor-beta1 (TGF-β-1), and the development of suppressive T regulatory cells [134, 135].

In addition, UV light can alter and damage the LCs embedded between KCs in the epidermis. LCs normally identify exogenous substances through their surface profile, activate resting T lymphocytes and therefore initiate a specific immune response against the exogenous substances. With increasing radiation time and intensity, the number and functionality of LCs decreases. LCs from irradiated skin show a reduced expression of major histocompatibility complex (MHC) proteins of class II and have reduced antigen-presenting ability, probably due to a UV-induced reduction of costimulatory molecules such as cluster of differentiation antigens (CD 80 and CD 86) [136, 137]. Thus, malignant, degenerated cells cannot be detected and are not rejected by the immune system [138].

Cis-Urocanic acid (UCA), the photoisomere of *trans*-UCA, can also promote systemic suppressive effects [139, 140]. In mice with a histidine-rich diet, the total UCA concentration increased significantly. Under subsequent UVB irradiation, these test animals showed significantly higher suppression of contact hypersensitivity compared to normally fed mice [141]. The actual underlying mechanisms of UCA action are still unclear, but it is thought that UCA acts via different pathways. For example, *cis*-UCA both has an effect on granulocytes and natural killer cells (NK) and reduces the number of LCs by at least 50% [142]. In addition, it can also modulate the action of different cytokines such as TNF-α, IL-6 or IL-8, and may initiate the formation of intracellular ROS [143–145].

Thus, UV radiation has a dual role: first, the induction of the carcinogenicity through direct and indirect DNA damage; and second, the additional suppression of the immunological tumour defence.

Malignant melanoma

Melanoma is a highly malignant tumour of the skin arising from the melanocytes. In 2012, there were more than 3 500 000 new cases of cancer across Europe, including more than 100 000 cases of melanoma [146]. Particularly, alarming is especially the fast growth rates. In Europe and the U.S.A., the incidence rates for cutaneous melanoma (CM) have tripled or quadrupled since the 1970s. With 40–60 new cases per 100 000 inhabitants every year, Australia and New Zealand have the highest incidence rates worldwide [147, 148].

CM tends to metastasize in an early stage and is the world's most lethal skin disease [149]. The formation of CM in genetically susceptible individuals is directly associated with different risk factors include family history, nevi and the exposure to UV radiation from sunlight or artificial sources [150]. In contrast to the basal cell carcinoma and the squamous cell carcinoma, where mainly sun-exposed skin areas are affected and chronic cumulative sun exposure leads to the pathological skin changes, intermittent sun exposure of the skin seems to play a crucial role in the formation of acute malignant melanoma. Higher, for example job-related, moderate sun exposure seems to have an inverse association with the occurrence of melanoma [151]. It seems that skin's own protective mechanisms, such as skin pigmentation or the thickening of the horny layer, can partially prevent the formation of melanoma. In contrast, the skin of persons who are abruptly exposed to extensive sunlight is caught unprepared and is therefore more vulnerable. Accordingly, skin areas that are only intermittently exposed to extensive sunlight (e.g. the back or the inner thighs) and persons who work mostly inside are most frequently affected by melanoma [152].

Unprotected UV exposure and sunburns in childhood and adolescence increase the risk of skin cancer formation in adulthood. Anamneses of five or more sunburns in childhood can double the risk of subsequent melanoma formation [153, 154]. The significance of premature sunburn was also confirmed by different animal studies, for example the HGF transgenic mouse model [155]. Here, neonatal test animals were exposed to erythemal doses of UV radiation, whereupon they developed melanocytic tumours in the form of early lesions up to metastases similar to human cutaneous malignant melanoma [156]. These results emphasize the critical role of early sunlight exposure for the formation of human melanoma.

Although UV radiation is seen as one of the most important risk factors in the formation of melanoma, the role of UVA and UVB radiation is still controversial [157, 158]. Nevertheless, today it is generally accepted that both wavelength areas contribute in different ways to the development of the tumour [159, 160].

A recent published study in 2012 found that there is a pigment-independent pathway initiated by UVB radiation through direct DNA damages and a second, pigment-dependent pathway under the influence of UVA radiation that causes indirect oxidative DNA damages in the melanocytes via ROS [161].

While after UVB radiation the typical markers TT-CPD and 6-4 PP are found in epidermal cells of both pigmented and unpigmented test animals, after UVA radiation only a low level of TT-CPD lesions is detectable. Instead, in pigmented test animals, 8-Oxo-7,8-dihydro-2'-deoxyguanosine (8-oxodG) was found in the nuclei of extra-follicular melanocytes at the dermal/epidermal junction. This indicates a strong photooxidative interaction between UVA light and the melanin in the melanocytes and confirms that the presence of pigmented nevi is a strong risk factor for melanoma.

Because the uncontrolled proliferation of melanocytes is seen as a first critical step in the formation of melanoma, the expressions of different growth factors seem to have an important influence on the aetiology of melanoma [162]. Melanocytes carry different growth factor receptors whereby the corresponding ligands are produced by the surrounding KCs in the epidermis and the fibroblasts in the dermis. The growth factors regulate survival, growth and pigment production of the melanocytes. Mitogen-activated protein kinases (MAPK) are responsible for the homeostatic balance between melanocytes, KCs and fibroblasts, and regulate cell growth and cell survival via the cascaded protein kinases, namely the rat sarcoma (RAS) kinase, the rapidly accelerated fibrosarcoma (RAF) kinase, the extracellular signalregulated protein kinase (ERK) and the MAPK/ERK kinase (MEK) [163]. In over 60% of malignant melanoma, somatic mutations of the B-RAF protein (an isoform of the RAF kinase) or the BRAF gene can be found [164, 165]. The mutated B-RAF protein has an up to 800-fold increased kinase activity, resulting in an overactivation of the MAPK signalling pathway and a misdirected expression of different growth factors, for example increased production of basic fibroblast growth factor (bFGF), endothelin-1 (ET-1) and stem cell factor (SCF) in KCs and of bFGF, HGF and TGF-β in the fibroblasts [166, 167]. This results in the activation of the melanocytes via paracrine ways and the uncontrolled proliferation of melanocytes. For advanced melanoma cells, which increasingly produce a variety of cytokines and growth factors endogenously (e.g. bFGF) and thus ensure their own survival, growth and spread via autocrine ways, increased independence from exogenous growth factors could be observed [168]. Finally, it must be noted that the molecular processes that are responsible for the formation of the different types of skin cancer are very complex and multifaceted, and even after numerous studies, the detailed processes are still not fully understood and require further research to advance possible medical treatment options.

Natural photoprotection of the skin

The human skin has developed different natural protection mechanisms against UV radiation. The most important protection is the pigmentation of the skin by formation of melanin (Fig. 6), which acts as radical scavenger and ensures light absorption up to the visible range [169].

Melanogenesis starts tyrosinase catalysed with the formation of tyrosine to the catechol L-DOPA. By subsequent oxidation, orthoquinone is formed. The non-enzymatic cycling step to leucodopachrome follows the tyrosinase-dependent transformation to dopachrome.

Decarboxylation of dopachrome leads to 5,6-dihydroxyindole (DHI) and its oxidation to the 5,6-indolequinone or by direct oxidation of dopachrome to 5,6-dihydroxyindole-2-carbonic acid (DHICA).

Polymerization of these units finally leads to eumelanin. In the presence of cysteine or glutathione, dopaquinone is converted to cysteinyldopa. Subsequently, the yellow-red pigment pheomelanin is formed through oxidative polymerization of cysteinyldopa via benzothiazinylalanine [170].

UVA radiation is mainly responsible for the immediate and persistent pigment darkening (IPD and PPD) by photooxidation of melanin precursors, which are already present in the skin. These reactions take place within a few minutes or hours but are mostly reversible, so that the tanning of the skin diminishes within a few days. UVB radiation results in delayed tanning reaction (DTR). Pigment formation takes place in the basal layer and is based on the proliferation of specific enzymes, especially tyrosinase. The melanocytes are stimulated to form melanin, which is transported to KCs to protect the cell nuclei in particular. With the movement of the epidermis cells, the pigment also moves towards the skin surface. The formation of the suntan takes several days and lasts for a few weeks [171].

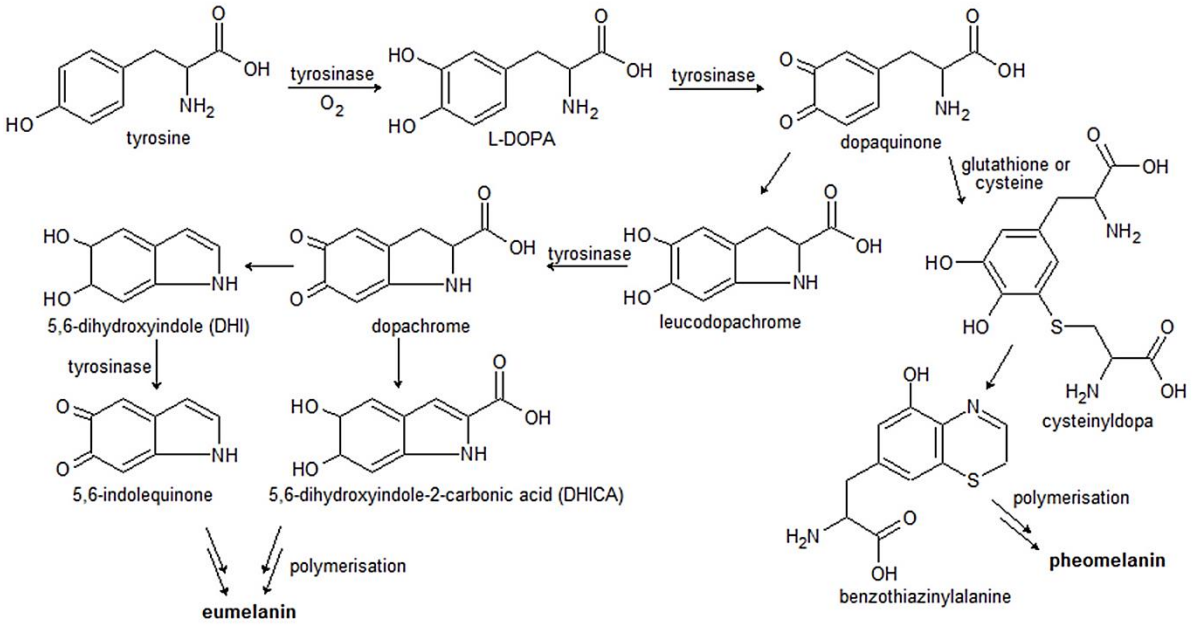

Figure 6 UV-induced transformation of tyrosine into pre-melanin metabolites and into melanin (according to [420,421]).

Under excessive sun exposure, also the enzymatic activity of histidinase, in addition to that of tyrosinase, increases. As a result, KCs of the horny layer increasingly form UCA out of histidine. UCA absorbs in the long-wave UVA range under *cis*/*trans*-isomerization [139]. In the past, UCA has been used as a UV filter in various sun protection products. However, when it turned out that its *cis*-form shows a strong immunosuppressive effect, the substance was banned in the EU and other countries. However, the question whether the beneficial or detrimental effects of UCA predominate is still cause of discussion [145, 172].

A further protection mechanism is the formation of the UVinduced hyperkeratosis. Under UV radiation (especially UVB light), the basal cells are stimulated to proliferate what causes a thickening of the horny layer. Without further exposure to UV radiation, the hyperkeratosis disappears [173].
Furthermore, there are the body's endogenous defence mechanisms, that is repair enzymes that are able to identify, cut and replace faulty DNA sequences. For strongly damaged cells – so-called sunburn cells – apoptosis can be initiated as a protection mechanism [174, 175]. And finally, there are endogenous redox systems, such as ubiquinone, glutathione and a-lipoic acids, which have an antioxidative effect and react efficiently with free radicals before they can damage other cell constituents, such as lipid membranes, proteins and nucleic acid. However, the quantities of these substances produced by the body itself are rapidly depleted under UV radiation by the formed ROS [176].

UV filter substances

As natural skin protection becomes ineffective after a short time (depending on the skin type, between 10 and 40 min) and a lasting tan develops only slowly, other protection measures, for example avoidance of direct midday sun, wearing of protective clothes and sunglasses, and usage of appropriate sun protection products, are needed for longer stays in the sun. To prevent sunburns and protect the skin from serious damage, sunscreens must meet certain criteria. They should be photostable, dissipate the absorbed light energy through photophysical and photochemical pathways without the formation of harmful reactive intermediates, be water resistant and well tolerated; in addition, they should not penetrate the skin [177, 178]. Normally, sunscreens contain a combination of organic filters and inorganic UV filters, which ensure effective protection across the whole UVA and UVB range [31]. As sun protection products are used in relatively high concentrations over the whole body surface, their tolerability is of particular importance in addition to good performance. Accordingly, appropriate dermatological tests are required as part of the safety assessment according to the European Cosmetics Regulation No. 1223/ 2009 [179]. Although all UV filter substances are tested for their (photo)irritative and (photo)sensitization potential, their actual allergic potential may only turn up after years of widespread usage in various products.

Legal requirements and recommendations

The legal status of sunscreen products differs from country to country, sometimes substantially. There is no overarching binding definition for sunscreens or UV filters worldwide, but many countries use the definition of the EU Cosmetics Regulation No. 1223/ 2009. Thereafter, UV filters are substances that are exclusively or mainly intended to protect the skin against UV radiation by absorbing, reflecting or scattering UV light. In some countries such as the European Union, China, India, South Africa, Japan, and the countries of the Association of Southeast Asian Nations (ASEAN) and Mercosur in South America, sunscreens are regulated as cosmetics. In contrast, in the U.S.A., Australia, and New Zealand, sunscreens are regulated as drugs.

The same applies for Canada, except for sunscreens that solely use titanium dioxide (TiO_2), zinc oxide (ZnO) or *p*-aminobenzoic acid as UV filters. They fall under the category 'Natural Health Products' (NHP) and are therefore less regulated. Which UV filters can be used for cosmetic products differs between countries (Table I). In Europe, Annex VI of the EU Cosmetics Regulation lists all UV filters allowed for cosmetic products in the EU with their respective maximum use concentrations. At the moment, the list contains 27 substances if considering the recent inclusion of the UV filter tris-biphenyl triazine [180] and the deletion of PABA according to directive 2008/123/EC [181]. ZnO is currently not yet listed as an approved UV filter, but due to a positive assessment of the Scientific Committee on Consumer Safety (SCCS), it is expected that ZnO will also be included during one of the next revisions of the Annexes. The lists of approved UV filters for China (numbering 28), India (numbering 27) and the ASEAN countries (numbering 28) are mainly oriented towards the European Cosmetics Regulation. In the U.S.A., only 16 UV filters are approved for sunscreens, of which only 10 are also approved for Europe, but with partially different maximum use concentrations [182]. Although the Food and Drug Administration (FDA) further accepted eight UV filters already approved in Europe for possible future submission in the time and extent application (TEA) process, there is no prospect of an imminent approval. For Australia and New Zealand, 29 UV filters have been approved, of which 23 substances are also part of the EU Cosmetics Regulation plus five UV filters also approved in the U.S.A. The Canadian Sunscreen Monograph is strongly oriented towards FDA requirements. The monograph lists currently 20 UV filters, which are approved drug medical ingredients or natural health products medicinal ingredients for sunscreens. In Japan, the usage of 34 UV filters is permitted. Some of them, such as benzophenone-9 or pentyl dimethyl PABA, are solely approved in Japan, whereas several UV filters that are approved within the EU or other Asian countries are forbidden. In the Mercosur countries, 33 UV filters are approved for usage in cosmetic products. A special case is South Africa (SA), which adopts nearly all UV filters approved by any reliable major organization. Therefore, in SA, there are currently 48 approved UV filter substances. For all of the above-mentioned countries, there are only nine UV filters, octocrylene (OCR), homosalate, benzophenone- 3 (BP-3), phenylbenzimidazole sulphonic acid (PBSA), ethylhexyl methoxycinnamate (EHMC), butyl methoxydibenzoylmethane (BMDBM) and ethylhexyl salicylate (EHS) that are approved worldwide but have different maximum limits, so it is nearly impossible for a manufacturer to use one uniform formulation in all markets. Sun protection products have an important protective function. Therefore, their efficacy and the basis on which the efficacy is claimed are important public health issues that must be controlled. The efficacy of sun protection products is first given by the sun protection factor (SPF), which is the quotient between the minimal erythema dose (MED) with applied sunscreen and the MED without sunscreen. Therefore, the SPF is an indicator of protection against UVB radiation. However, considering the erythemal action spectrum, also UVA-II (315–340 nm) seems to contribute to the formation of erythema to some extent [183].

Table I Approved UV filters worldwide with their maximum usage concentration

	EU (%)	**CN** (%)	**US** (%)	**AU** (%)	**CA** (%)	**JP** (%)	**IN** (%)	**ZA** (%)	**ASEAN** (%)	**Mercosur** (%)
PABA (and ist esters - JP)	-*	5	15	-	15	4	5	15	-	15
Camphor benzalkonium methosulphate	6	6	-	6	-	-	6	6	6	6
Homosalate	10	10	15	15	15	10	10	10	10	15
Benzophenone-3	10	10	8	10	6	5	10	10	10	10
Phenylbenzimidazole sulphonic acid	8	8	4	4	4	3	8	8	8	8
Terephthalylidene dicamphor sulfonic acid	10	10	-	10	10	10	10	10	10	10
Butyl methoxydibenzoylmethane	5	5	3	5	3	10	5	5	5	5
Benzylidene camphor sulphonic acid	6	6	-	6	-	-	6	6	6	6
Octocrylene	10	10	10	10	10	10	10	10	10	10
Polyacrylamidomethyl benzylidene camphor	6	6	-	-	-	-	6	6	6	6
Ethylhexyl methoxycinnamate	10	10	7.5	10	7.5	20	10	10	10	10
PEG-25 PABA	10	10	-	10	-	-	10	10	10	10
Isoamyl *p*-methoxycinnamate	10	10	-	10	-	-	10	10	10	10
Ethylhexyl triazone	5	5	-	5	-	5	5	5	5	5
Drometrizole trisiloxane	15	15	-	15	15	15	15	15	15	15
Diethylhexyl butamido triazone	10	10	-	-	-	-	10	10	10	10
4-Methylbenzylidene camphor	4	4	-	4	6	-	4	4	4	4
3-Benzylidene camphor	2	2	-	-	-	-	2	2	2	2
Ethylhexyl salicylate	5	5	5	5	5	10	5	5	5	5
Ethylhexyl dimethyl PABA	8	8	8	8	8	10	8	8	8	8
Benzophenone-4	5**	5**	10	10	10	10	5**	10	5**	10
Benzophenone-5			-	10	-	10		5		5
MBBT	10	10	-	10	-	10	10	10	10	10
DPDT	10	10	-	10	-	-	10	10	10	10
BEMT	10	10	-	10	-	3	10	10	10	10
Polysilicone-15	10	10	-	10	-	10	10	10	10	10
Titanium dioxide	25	25	25	25	25	N.I.	25	25	25	25
DHHB	10	10	-	10	-	10	10	10	10	10
Tris-biphenyl triazine (nano)	10	-	-	-	-	-		-	-	-
Zinc oxide	†	25	25	N.I.	25	N.I.	-	25	25	25
Menthyl anthranilate	-	-	5	5	5	-	-	5	5	5
Cinoxate	-	-	3	6	3	5	-	5	-	3
Benzophenone-8	-	-	3	3	3	-	-	3	-	3
TEA salicylate	-	-	12	12	12	-	-	12	-	12
Diethanolamine methoxycinnamate	-	-	-	-	10	-	-	8	-	-
Benzophenone-1	-	-	-	-	-	10	-	10	-	-
Benzophenone-2	-	-	-	-	-	10	-	10	-	-
Benzophenone-6	-	-	-	-	-	10	-	5	-	-
Benzophenone-9	-	-	-	-	-	10	-	N.I.	-	-
Methyl-2,5-diisopropylcinnamate	-	-	-	-	-	10	-	10	-	-
1-(3,4-Dimethoxyphenyl)-4,4-dimethyl-1,3-pentadiene	-	-	-	-	-	7	-	7	-	-
Ethylhexyl dimethoxybenzylidene dioxoimidazolinepropionate	-	-	-	-	-	3	-	3	-	-
Ferulic acid	-	-	-	-	-	10	-	10	-	-
4-(2-Beta-Glucopyranosiloxy)propoxy-2-hydroxybenzophenone	-	-	-	-	-	5	-	-	-	-
Glyceryl ethylhexanoate dimethoxycinnamate	-	-	-	-	-	10	-	10	-	-
Glyceryl PABA	-	-	-	-	-	4	-	5	-	-
Isopentyl trimethoxycinnamate trisiloxane	-	-	-	-	-	7.5	-	7.5	-	-
Mixture: Isopropyl *p*-methoxycinnamate + Ethyl diisopropylcinnamate + Methyl-2,4-diisopropylcinnamate	-	-	-	-	-	10	-	10	-	-
Pentyl dimethyl PABA	-	-	-	-	-	10	-	-	-	-
Digalloyl trioleate	-	-	-	-	-	-	-	5	-	-
Ethyl dihydroxypropyl PABA	-	-	-	-	-	-	-	5	-	-

PABA: para-4-Aminobenzoic acid; MBBT: Methylene bis-benzotriazolyl tetramethylbutylphenol;
BEMT: Bis-Ethylhexyloxyphenol methoxyphenyl triazine; DPDT: Disodium phenyl dibenzimidazole tetrasulphonate;
DHHB: Diethylamino hydroxybenzoyl hexyl benzoate. *Banned since 2008 (2008/123/EC);
** sum of benzophenone-4 and benzophenone-5; † inclusion in annex VI expected; N.I.: No limit.

In 1956, the radiation physicist Rudolf Schulze first introduced the term ‘protection factor’, which was initially only used among dermatologists [184]. In 1962, the chemist Franz Greiter picked up the term and defined it precisely in the way we know ‘SPF’ today [185]. The SPF should allow the consumer a direct and easily understandable comparison. However, as *in vivo* SPF determinations depend on different parameters such as number and selection of the test persons, kind of application, and irradiation source or the exact waiting time to evaluate the skin reddening, the need for a uniform methodology soon arose. In 1976, the US Food and Drug Administration (FDA) proposed the first standardized method to determine the SPF of sunscreens [186]. Further standards similar to the FDA method followed, for example by the Standards Association of Australia (SAA) in 1986 [187] and by the Japan Cosmetic Industry Association (JCIA) in 1991 [188]. The first standardized method in Europe was the COLIPA SPF Test Method, developed in collaboration with major European manufacturers of sun protection products and contract testing laboratories in 1994 [189]. In 2003, COLIPA (since 2012: Cosmetics Europe), JCIA and the South African Cosmetic, Toiletry & Fragrance Association (CTFA-SA) published the jointly improved International SPF Test Method (ISPF) [190], which was revised in 2006 with the additional participation of the Cosmetic, Toiletry and Fragrance Association of the United States (CTFA-USA) [191]. In December 2010, the International Organization for Standardization (ISO) published the ISO Standard ‘Cosmetics – Sun protection test methods – *In vivo* determination of the sun protection factor (SPF)’, which replaced the earlier test method [192].

Today, Korea, Columbia, the Mercosur Countries (Argentina, Brazil, Paraguay and Uruguay), Australia, New Zealand, Canada and the ASEAN countries (Indonesia, Malaysia, the Philippines, Singapore, Thailand, Brunei, Myanmar, Cambodia, Laos and Vietnam) have adopted methods referring to FDA or ISO standards. China is also considering an adoption of a SPF standard. The standardized amount of sunscreen applied in the *in vivo* test situation is 2 mg cm^{-2}. However, different studies have shown that the actual ‘in-use’ levels of applied sunscreens are often significantly lower, which decreases their protection ability [193, 194], so that the SPF claimed on the product cannot be reached [195]. In general, the protection capability of a sunscreen depends on other factors in addition to the SPF and the actual amount of sunscreen applied. These include the respective skin type of the user, the frequency of re-application, the subsequent activities (swimming, drying of the skin, contact with sand, etc.) and the total formulation of the product [196].

For a long time, the efficacy of sun protection products was mainly concentrated on a high SPF, giving consumers a false sense of security and encouraging them to stay in the sun longer. Although a sunscreen of SPF 30 offers twice the protection of a sunscreen with SPF 15 (according to a halved UVB transmittance of 3.3% against 6.7%) and therefore allows to stay twice as long in the sun, a high SPF says almost nothing about UVA protection and during the prolonged exposure time, the skin is increasingly defenceless against UVA radiation, without any directly visible signs but an increased risk of melanoma [197, 198]. In addition, it is known that the determination of especially high SPFs is difficult due to the necessarily long irradiation time and the decreasing reproducibility [199, 200].

As it became clear throughout the years that UVA radiation is not only responsible for premature skin ageing but shows also mutagenic and carcinogenic properties, the development of sunscreen products with the best possible broadband protection was pushed forward [31, 198, 201]. In 2006, the European Commission (EC) issued a recommendation on the efficacy of sunscreen products including a UVA-PF/SPF ratio of at least 1 : 3 [202]. By doing so, the EC and the industry seek to further ensure that sunscreens protect consumers against both UVB and UVA radiation and that there are easy-to-understand efficacy levels based on standard criteria. Although not legally binding, European manufacturers consequently reformulated their products according to the recommendations. To indicate that a sunscreen product offers the recommended minimum UVA protection, COLIPA has issued a standardized UVA label, the 'UVA-seal'.

Depending on the respective country, different established methods are used to determine the UVA protection ability of a product (Table II). One possibility to determine the UVA protection performance of a sunscreen is the *in vivo* measuring of PPD or IPD after long-term or short-term UVA radiation [203, 204]. The PPD was originally developed in Japan where it is still the prescribed method to measure UVA protection [205]. Today there is also an ISO standard, which is based on the principles recommended by JCIA [206].

Another way to test the UVA or broad-spectrum protection ability of a product is by the usage of appropriate *in vitro* methods. In Europe, this development started with the determination of the UVA/UVB ratio, which compares the area under the curve in the UVB and in the UVA ranges, as well as the critical wavelength (CW) [207]. Both tests are based on the assessment of the UV transmittance of a thin sunscreen film spread over a defined area of a roughened substrate before and after controlled UV exposure. The CW describes the range of protection over the 'whole' UV spectrum (290–400 nm) and is the wavelength at which 90% of the cumulative area under the total absorbance curve from 290 to 400 nm occurs. The longer the critical wavelength is, the broader the UVA protection of a product. According to the FDA 2011 Final Rule, the determination of the CW is the prescribed standard method to define whether a product offers broad-spectrum protection (CW ≥ 370 nm) or not [208].

The internationally standardized ISO method 'Determination of sunscreen UVA photoprotection *in vitro*' [209] is also based on absorbance measurements. The ISO replaced the earlier reference method of COLIPA, first published in 2007 [210] and last updated 2011 [211] due to the results of a collaborative study concerning the roughness of the plate material used [212]. The aim was to determine the CW and the UVA protection factor (UVA-PF) by the convolution of the transmittance results with the PPD action spectrum and the spectrum of the UVA-filtered solar simulator. Due to the European recommendation, the UVA-PF/SPF ratio of an effective sunscreen is ≥0.33.

In Australia and New Zealand, for a long time, the 'Australian Standard' was the established *in vitro* method to determine UVA protection [213]. Once a sunscreen reduces the transmission in the range of 320–360 nm by at least 90%, a product could claim broadspectrum UV protection. For products with low or moderate SPF, the methods offers adequate protection, but with a higher SPF the ratio between UVA and UVB protection increases disproportionately.

In addition, the Australian Standard method excludes a large portion of the UVA-I spectrum (340–400 nm). Therefore, in the recent Australian and New Zealand Sunscreen Standard [214], the previous standard method was replaced by the ISO 24443:2012 [209].

All of the countries previously mentioned allow at least one of these UVA determination methods (Table II). However, a possible agreement on one common standard seems unlikely, at least for the near future.

Table II Overview of prescribed UVA determination methods in different countries

	UVA determination method
Europe	ISO 24442:2012 (PPD)
	ISO 24443:2011 (*in vitro*) + critical wavelength ≥ 370 nm
USA	FDA Final Rule 2011 – critical wavelength > 370 nm
Canada	FDA Final Rule 2011 – critical wavelength > 370 nm
	COLIPA *in vitro* method + critical wavelength
	ISO 24442:2012 (PPD)
	JCIA Standard (PPD)
China	JCIA Standard (PPD)
Japan	JCIA Standard (PPD)
ASEAN	ISO 24442:2012 (PPD)
	ISO 24443:2011 (*in vitro*) + critical wavelength ≥ 370 nm
Mercosur	FDA Final Rule 2011 – critical wavelength > 370 nm
	COLIPA *in vitro* method + critical wavelength
	ISO 24442:2012 (PPD)
	ISO 24443:2011 (*in vitro*) + critical wavelength ≥ 370 nm
	JCIA Standard (PPD)
South Africa	Documented test results of an acceptable authority, but broad spectrum ration UVA/UVB 2:5

Water resistance also has an influence on the efficacy of a sun protection product and can be reached by the usage of UV filters with only minimal water solubility, polymers and an appropriate emulsifier system. Since 2005, there is a standardized COLIPA testing method to determine the water resistance of a product [215]. It is based on the comparison of the SPF of a tested sunscreen product after a defined period of immersion in water with the original SPF. The term '(very) water resistant' can be used if the remaining SPF after 2 (4) baths of 20 min is ≥50% of the original SPF (IC 90%). The FDA method is similar in the methodology, but the big difference is that no decrease in the SPF level is allowed after the respective testing time.

As possible photodegradation may have a big influence on the efficacy of a sun protection product, a test of the photostability of a sunscreen over the whole UVA and UVB range is also required. One possibility to determine the photostability is the usage of an *in vivo* method in which a fixed amount of sunscreen is applied on the skin of a test subject followed by irradiation. The UV filters are recovered by tape stripping and extracted from the tapes, and their residual presence is quantified by high-performance liquid chromatography (HPLC) and spectrophotometry. The difference in the determined UV filter amount of an irradiated and non-irradiated sample allows a direct assessment of the photostability of a sun protection product. In 2004, COLIPA has issued a comparable *in vitro* testing guide-

line, which was also based on the HPLC determination of the UV filter amount of a tested sun protection product before and after UV irradiation [216].

The above-mentioned *in vitro* test methods for the determination of SPF, UVA protection and photodegradation are based on results obtained *in vitro* with the help of poly(methyl methacrylate) (PMMA) or roughened quartz plates. Whether these results can be transferred directly to the real conditions of the skin is questionable, as reactions of the skin under UV exposure or interactions of the products with the skin are not covered by the test conditions [217–220].

Besides the testing of the performance of UV filters and sunscreens, the issue of patent freedom has become a major concern for UV filter and sunscreen manufacturers worldwide. At the moment, all newly developed UV filters are patented before their introduction to the sunscreen market. For example, BASF holds several patents for the use of ZnO in sun care formulations in the U.S.A. or L'Oreal for the effective UVA filters Mexoryl SX and Mexoryl XL. Furthermore, the patents do not extend solely to the UV filters themselves, but also to the combinations of different UV filters (e.g. octocrylene and 4-MBC) or the underlying technologies. This strongly constrains the cosmetic usage of such ingredients for competitors and can even make usage impossible [221].

Inorganic UV filters

For these UV filters, the term 'physical UV filters' was initially used, attributed to their first known mechanism of sun blocking through the physical manner of reflection and scattering. However, small inorganic UV filter particles also absorb part of the incident light. The combination of absorption, reflection and scattering leads to a protection across both the UVA and UVB spectrum [222].

The best known inorganic UV filters are TiO_2 and ZnO. TiO_2 is listed in Annex VI of the Cosmetics Regulation as a permitted UV filter up to a concentration of 25% in the finished product. TiO_2 is known to exist in the three crystal forms, anatase (tetragonal), brookite (orthorhombic) and rutile (tetragonal) with different UVattenuating properties. ZnO is currently not listed in Annex VI as a permitted UV filter. So far, however, there were different national approvals, for example in the German Cosmetics Ordinance [223], which allowed the usage of ZnO as a UV filter. Currently, the EC is about to implement microfine and nanofine ZnO as UV filter in Annex VI of the Cosmetics Regulation based on the previous positive opinions of the Scientific Committee of Consumer Safety [224, 225].

In the past, mineral UV filters formed an opaque film on the skin that limited their cosmetic use. Due to technological advantages, micronized oxides are now obtained on a nanometric scale (<100 nm) and show other properties of light refraction and diffraction, resulting in a thin transparent layer that is easy to spread with even better protection abilities [226]. For both nano TiO_2 and nano ZnO, the SCCS concluded that their usage in sun protection products can be considered as safe [225, 227]. The only exception is made for the usage of ZnO and TiO_2 nanoparticles in spray products, because there is evidence that these particles can have severe effects in the lungs upon inhalation. Although very effective and positively evaluated by the SCCS, the usage of nanomaterials is still questioned critically.

The main points of criticism are the possible altered toxicological potential of extremely small particles, their conceivable penetration, especially through (sun)damaged skin, and their toxicological effects in the body [228, 229].

Toxic effects of ZnO and TiO_2 nanoparticles are seen in their ability to evade immunological defence mechanisms, to form complexes with proteins and in their photochemical activity [230, 231]. When exposed to UV radiation *in vitro*, nanoparticles emit electrons responsible for the formation of highly reactive oxygen species, for example hydroxyl radicals or hydrogen peroxide [232– 234]. In general, they are able to damage cell compounds such as cell membranes, proteins and DNA, and are therefore cytotoxic [235–237]. When comparing the three crystal forms of TiO_2, the anatase and the amorphous form show higher photoreactivity and cytotoxicity than the rutile form [238–240]. This finding is partly reassuring insofar as, in sunscreens, the rutile form is mainly used due to its higher UV absorption [241].

Of course, the results of those *in vitro* cell tests are not directly transferable to *in vivo* conditions, primarily because the increased formation of ROS at a viable cell level requires the penetration of the particles into the skin.

To reduce the undesirable photoreactivity of TiO_2 and ZnO nanoparticles, the surface activity of the particles can be reduced by an appropriate coating of the material with both inorganic (aluminium oxide, silica, zirconia) or organic (silanes, silicones, dimethicones) substances [242, 243]. An appropriate coating is stable over the whole production process, can help to ensure that the particles can be readily incorporated in the formulation and protects the particles against agglomeration (1–100 µm) and deposition [244].

Permeation of small particles through the stratum corneum may occur via different pathways: intracellular, intercellular or through the appendage route (i.e. along hair follicles, sweat pores or skin glands) [230]. Due to their low solubility and the impermeable character of corneocytes, intracellular penetration of TiO_2 or ZnO is rather unlikely [229]. Although aggregation of the small particles in hair follicles was observed [245, 246], the follicles must be seen as more similar to accumulation sites from which particles are gradually transported out with the sebum flow without further penetration in the living skin [247, 248]. What remains is the intercellular pathway, which is also limited due to the densely packed stratum corneum (SC) structure. Intercellular spaces between the SC corneocytes are likely small and measure between 0.5–7 and 20–30 nm [249]. However, the spaces can be expanded by the application of topical products [250] or after stress, for example caused by UV radiation [251, 252].

The penetration of nanoparticles in the skin has been subject of numerous studies, some of which have had different results. Most *in vitro* and *in vivo* studies using both animal and human skin verify that TiO_2 and ZnO nanoparticles do not penetrate the underlying layers of either intact or UV-damaged skin [253–259]. The penetration is mostly limited to the SC, and hence, systemic absorption is unlikely. One reason for this could be that nanoparticles tend to aggregate into larger structures (30–150 nm), which may reduce their ability to penetrate the skin [255, 260–263].

Nevertheless, as sunscreens are also applied especially to sunstressed or damaged skin with weakened barrier functions, there is a further need for substance-specific research.

Organic UV filters

The group of organic UV filters includes different substance classes, which can be divided into UVA and UVB filters due to their specific absorption characteristics. Most organic UV filters contain aromatic compounds conjugated with carbonyl groups. The excitation of electrons in the respective benzene ring leads to absorption in the UV range. The absorption range and strength of the different UV filter classes (Fig. 7) are additionally affected by further substituents [264].

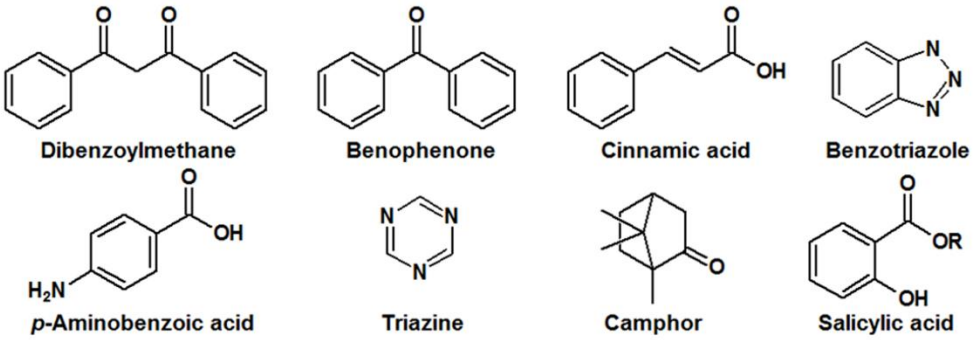

Figure 7 Basic chemical structures of commonly used UV filters.

The frequency of use of the different organic UV filters has changed significantly in the past 20 years due to scientific evidence and the development of new UV filter substances. To get an overview of the most commonly used UV filters in Germany in 2013 and 2014, we compared 178 sun protection products, 137 skincare products (e.g. face cream, hand cream, make-up) and 47 lip care products with UV protection, due to their ingredients declaration (Fig. 8).

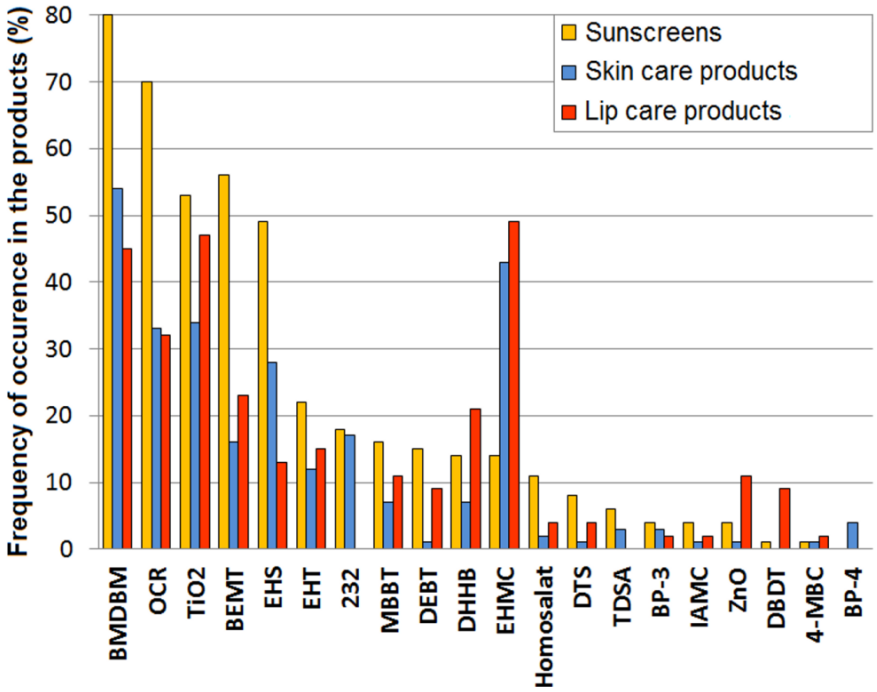

Figure 8 Overview of the most commonly used cosmetic UV filters, available on the German market in 2013 and 2014, divided into sunscreens, skin care products, and lip care products.

Dibenzoylmethane derivatives

Butyl methoxydibenzoylmethane (BMDBM) is the most common UVA filter in cosmetic products and is included in approximately 80% of the sun protection products in Germany (Fig. 8). With the worldwide recommendation of a balanced UVA/UVB protection, the usage of BMDBM has gained further importance. BMDBM has replaced the former 4-isopropyl dibenzoylmethane (I-DBM), the production of which was discontinued in 1993 due to its high photoallergic potential [265]. However, BMDBM is also a known contact allergen among the UV filters [266, 267]. Another critical point is the photoinstability of BMDBM, especially when it is used in combination with ethylhexyl methoxycinnamate (EHMC) [43, 268, 269]. The resulting photodegradation products also have a specific reaction potential and may be seen as further triggers for contact allergies [270]. However, with an appropriate UV filter combination, for example with octocrylene (OCR) or by encapsulation, photodegradation can be decreased to a minimum [271–274].

Benzophenone derivatives

The two UV filters benzophenone-3 (BP-3) and benzophenone-4 (BP-4), both approved in the EU, show very good photostability and broad-spectrum protection over the whole UVB and UVA ranges [275, 276]. Therefore, they are not only used in sunscreens and various skincare products, especially in non-European countries [277], but also as typical light stabilizers in plastics and coatings [278]. However, used alone they do not provide complete UVA protection. Several studies have demonstrated that BP-3 shows a clear tendency to penetrate the human skin and was found in urine and even mother's milk [279–281]. This is particularly critical because BP-3 is considered a substance with endocrine potential [282–284]. In addition, BP-3 and BP-4 are seen as the most common photoallergens among the UV filters [285–288]. Therefore, the usage of BP-3 and BP-4 in sun protection products in Germany decreased to a minimum (Fig. 8).

p-Aminobenzoate derivatives

The UVB filter 4-aminobenzoic acid (PABA) was one of the first commercially available and one of the most popular UV filters worldwide [289]. However, it soon became apparent that both PABA and its derivatives were known triggers of photoallergic reactions [290, 291]. In 2008, PABA was banned as a cosmetic UV filter in the EU. The usage of ethylhexyl *p*-aminobenzoic acid (OD-PABA) has also significantly decreased in the past 20 years, and nowadays, it has been almost completely replaced by other UV filters.

Salicylate derivatives

The UVB filters ethylhexyl salicylate (EHS) and homosalate are typical representatives of this group. Salicylate derivatives are rather weak UVB absorbers but are often used to augment other UVB filters. Due to their insolubility in water, they show good water resistance.

Cosmetically used salicylates are rarely associated with allergic or photoallergic reactions [267, 292, 293], and do not have notable oestrogenic activity [294, 295]. In addition, EHS shows only a slight tendency to penetrate the skin [296]. Therefore, especially EHS with its good photostability and solubility is a common ingredient in sunscreens (Fig. 8).

The UV absorber triethanolamine salicylate is water-soluble and is a typical photoprotective agent in hair care products.

Camphor derivatives

Due to their excellent photostability, the camphor derivatives 3-benzylidene camphor (3-BC) and 4-methylbenzylidene camphor (4-MBC) were popular UVB filters for a long time [297]. In 1994, 4-MBC was found in about 30% of the sun protection products [298]. Even in the period from 2004 to 2006, 4-MBC was still a typical sunscreen ingredient [299]. In the past several years, the camphor derivatives have been under more and more criticism due to their possible endocrine potential [282–284]. The increasing pressure of the public and different non-governmental organizations, for example Women in Europe for a Common Future (WECF) or the German Friends of the Earth (BUND), resulted in the near cessation of use of 3-BC and 4-MBC in sun protection products in Germany (Fig. 8). Terephthalylidene dicamphor sulphonic acid (TDSA, Mexoryl SX), a further camphor derivative, is an effective UVA filter, which was developed and patented by L'Oréal (Paris, France) in 1982 and was approved in 1991 as cosmetic ingredient in Europe. In 2006, Mexoryl SX was also approved by the FDA as part of the sunscreen 'Anthelios SX'. This was the first approval of a product with a new UV filter since 1988. TDSA shows good protection ability against the negative effects of UVA radiation, such as skin pigmentation, epidermal hyperplasia or the decrease of skin hydration and elasticity [300–302]. In addition, TDSA is photostable and shows no tendency for percutaneous absorption [303].

Cinnamate derivatives

Ethylhexyl methoxycinnamate (EHMC, octinoxate) is one of the most common UV filters worldwide and is often used in combination with other UVB filters to achieve high SPF values. EHMC is generally well tolerated but shows a certain photodegradation potential, especially in combination with BM-DBM, associated with a decrease of its protection ability [267, 304, 305]. However, encapsulation of EHMC can significantly improve its photostability [306, 307]. For EHMC, which is seen as another UVB filter with possible oestrogenic activity [282–284, 308] and a tendency to permeate the skin [296, 309], the frequency of use in Germany strongly decreased. In 1994, EHMC was an ingredient of about 65% of all sunscreens on the market [298]. We found it in about 15% of the observed sun protection products currently sold in Germany. However, EHMC is still one of the most important UVB filters in daily care products (Fig. 8). The UVB filter OCR also belongs to the group of cinnamates. Due to its good photostability and its photo-stabilizing effect, especially towards BMDBM [273, 310], OCR can be found in approximately 80% of all observed sunscreens in Germany (Fig. 8).

It is assumed that under irradiation, an energy transfer can occur between OCR and BMDBM in an exited state (triplet), which results in the very efficient deactivation of BMDBM from the triplet to the ground state via heat release and therefore stabilization [177]. However, due to its widespread usage, there is more and more evidence that OCR has developed into one of the most common photoallergens [311–314].

Triazones

Recently, the development of new UV filters is based on the socalled 500 Da rule [54]. With an increased molecular weight of more than 500 Da, skin penetration is reduced. This reduction is associated with increased safety and efficiency of such substances. Due to the extension and multiplication of their chromophoric groups, the UVB filter ethylhexyl triazone (EHT), the UVB filter diethylhexyl butamido triazone (DEBT, iscotrizinol, Uvasorb HEB) and the broad-spectrum UV filter bis-ethylhexyloxyphenol methoxyphenyl triazine (BEMT, bemotrizinol, Tinosorb S) have a molecular weight well above 500 Da. These UV filters show comparatively high absorption coefficients, significant anti-inflammatory effects and are highly efficient and very photostable [221, 315–317]. In addition, especially Tinosorb S can improve the photostability of other UV filter substances in a sunscreen [315]. Due to their various positive properties, triazones are incorporated in more and more sun protection and skincare products (Fig. 8). Recently, tris-biphenyl triazine (Tinosorb A2B) has been added to Annex VI of the EU Cosmetics Regulation [180]. It is the first UV filter with a particle size below 100 nm that is explicitly approved for the use in European cosmetics. It is a water-dispersible, broad-spectrum, micronized UV filter that protects the skin especially against UV radiation between 290 and 340 nm, thus closing the gap between ‘classical’, pure UVA or UVB filters. It is the first UV filer, which was newly added to Annex VI since 2005.

Benzotriazoles

Also the broad-spectrum UV filters drometrizole trisiloxane (DTS, Mexoryl XL) and methylene bis-benzotriazolyl tetramethylbutylphenol (MBBT, Bisoctrizole, Tinsorb M) fall under the 500 Da rule. Accordingly, their skin penetration is minimal and (photo)allergic reactions to these UV filters also appear to be further rare [318, 319]. Mexoryl XL was the first photostable UV filter, which offers protection over the whole UVB and UVA ranges. The combination of Mexoryl SX and XL has an additional synergistic effect on their protection abilities [320]. Tinosorb M is manufactured in the form of organic microfine particles and can be dispersed in the water phase of a sunscreen. Accordingly, it combines the properties of organic and inorganic UV filters, and scatters, reflects and absorbs UV radiation. Tinosorb M shows a good photostability and broad-spectrum ability over the whole UVB, UVA-I and UVA-II range [321, 322].

Development of allergic and photoallergic reactions

As described previously, several organic UV filters are known triggers of allergic and photoallergic reactions responsible for approximately 55–80% of the positive photopatch test results [286, 291, 323]. Their mostly lipophilic character and their small molecular size allow sufficient skin penetration, which is the basic requirement to initiate an allergic response.

Mechanism of sensitization

Allergic contact dermatitis (ACD) is a type IV hypersensitivity response (delayed type) and is the result of a T-lymphocyte-mediated immune response to an allergenic substance that comes into contact with the skin. Hence, in contrast to other allergic reactions, ACD is not antibody mediated but is cell mediated [324]. ACD consists of two phases: the induction (sensitization) phase and the elicitation (expression) phase (Fig. 9). The first phase may take from a few days to a few years, depending on the allergic potential of the substance. After sensitization, the second phase takes approximately 1–2 days to fully develop, hence the name 'delayed type'. In the first phase, small molecules with allergenic potential (haptens) penetrate through the skin.

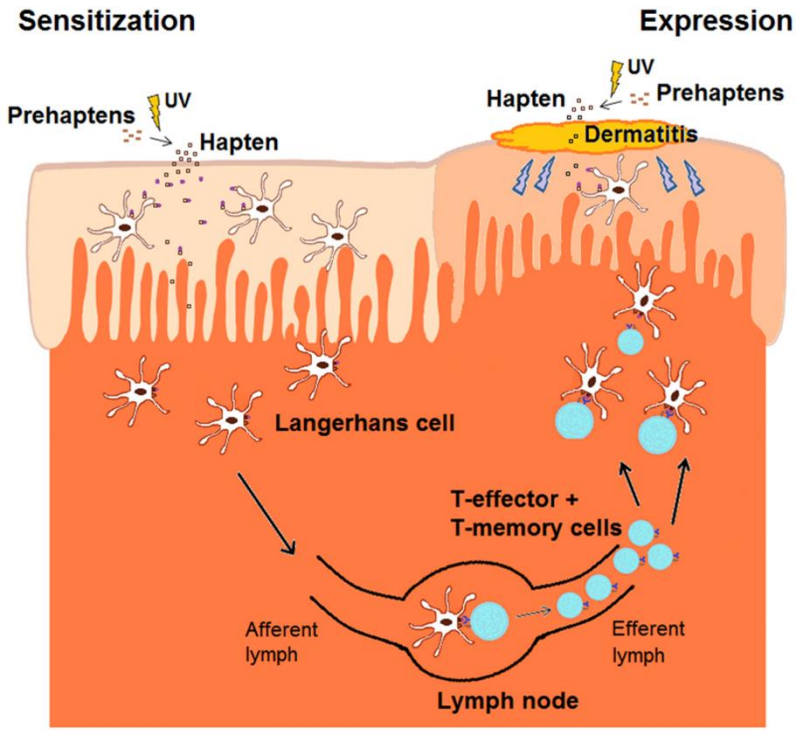

Figure 9 Schematic illustration of the sequence of an allergic response (mechanism according to [422])

Some substances are initially non-immunogenic but become potent haptens due to enzymatic processes in or on the skin (prohaptens) or due to non-enzymatic processes, for example oxidation or photoactivation (pre-haptens) [325, 326]. In the skin, the haptens bind covalently to nucleophilic amino acid side chains (mainly lysine and/or cysteine residues) of MHC proteins, which are carrier proteins, and form an antigenic complex, which is internalized and processed by dendritic LCs [327].

At the same time, an uptake of haptens by KCs activates the release of different cytokines, for example the interleukins IL-1β, IL-1α and IL-18, and different growth factors, for example tumour necrosis factor alpha (TNF-α) and granulocyte–macrophage colonystimulating factor (GM-CSF) [328]. In addition, the contact of KCs with haptens induces different protective pathways such as the oxidative stress response pathway [329–331]. This pathway is mediated by the antioxidant response element (ARE), which is an enhancer sequence that transcriptionally regulates different genes that encode phase two enzymes to maintain the cellular redox status and to protect against oxidative damage. Activation of ARE is regulated by the specific transcription factor, nuclear factor (erythroid- derived 2)-like 2 (Nrf2), which in turn is negatively controlled by the Kelch-like ECH-associated protein (Keap1), a protein that binds Nrf2. Keap1 is redox sensitive, and the cysteine groups in its structure can easily be oxidized, which decreases its affinity for Nrf2. As a result, Nrf2 is released from Keap1, translocates to the nucleus where it binds to ARE, and induces the transcription of different antioxidative genes [332]. An allergenic substance can also induce the release of Nrf2 due to its binding to the cysteine side chains of the Keap1 protein [333].

Additionally, KCs show metabolic potential and supply enzymes (e.g. cytochrome P450), which are involved in the activation of prohaptens to immunologically effective haptens [334]. Under the influence of the released cytokines and chemokines, the loaded LCs migrate towards the regional lymph nodes. There, LCs present the hapten–protein complex to naive T cells, which recognize the antigen and start the cascade of antigen-specific commitment. The proliferation of memory and effector T lymphocytes is initiated, which migrate in the peripheral tissue. Upon re-exposure to the same or a very similar hapten, the LCs become haptenized once more and are rapidly intercepted by the already-existing antigen- specific T cells in the epidermis (lower activation threshold). Proinflammatory cytokines and chemokines are released locally, which promote an inflammatory reaction with typical ACD symptoms such as redness, itching, swelling of the skin, formation of blisters and an oozing rash. Due to the development process, an ADC can be divided into skin penetration, possible metabolic activation, protein binding, activation and migration of LHCs, and proliferation of T cells [324, 335–337].

Skin sensitization test methods

Allergic contact reactions have become frequent skin complaints with increasing incidence rates during recent years. It is estimated that the prevalence of contact allergies is about 15–20% in the general population [338, 339]. Therefore, the evaluation of the sensitization potential of chemical substances, especially cosmetic ingredients that are intentionally applied directly on the skin, is of great importance. Accordingly, manufacturers of cosmetics are legally obliged to secure the safe usage of their products before they are placed on the market. In addition, many chemical substances, including cosmetic ingredients, must be assessed under the European Chemicals Regulation REACH (1907/2006/EC) [340]. The evaluation of skin sensitization is one mandatory endpoint when producing or importing a ton or more of a substance in or to Europe.

For a long time, sensitization was tested using different animal methods, for example guinea pig-based tests such as the Guinea pig maximization test (GPMT), the Buehler Test or the local lymph node assay (LLNA). Even today, these methods are the only generally recognized test systems currently authorized by the Organization for Economic Cooperation and Development (OECD) [341–344]. For the original LLNA, radiolabeled thymidine is used as a marker to determine the cellular proliferation in the auricular lymph node of the test animals after repeated topical application of the test chemical [345]. Today, several variants of the LLNA have been developed in which the radioactive materials are replaced, for example by 5-bromo-2-deoxyuridine in the LLNA:BrdU-ELISA [346]. By testing a minimum of three different concentrations of the test substance, it is not only possible to differentiate between sensitizers and nonsensitizers, but also to assess the respective sensitizing potential via the EC3 value, the effective concentration of a test chemical to provoke a threefold increase in lymph node cell proliferation. Guinea pig tests are based on a visual assessment of a skin reaction induced after topical application (Buehler test) [347] or intradermal and topical application of the test substance (GPMT) [348]. The latter two can only provide information as to whether a substance is a sensitizer or not and have limitations when the sensitization potency of a substance must be assessed.

Even today, the above-mentioned OECD methods are the only validated tests that are currently implemented in the REACH regulation or the corresponding Test Methods Regulation (EC) No. 440/2008 [349]. Nevertheless, REACH expressly requires and promotes the usage of appropriate alternative test methods. Moreover, since 11 July 2013, the new cosmetics regulation completely bans animal testing for both finished cosmetic products and cosmetic raw materials. Therefore, it is not surprising that in the last 15 years, great efforts have been made to develop promising animal-free testing methods. According to the five accepted mechanistic key events, that is skin penetration/bioavailability (1), peptide reactivity/ haptenation (2), epidermal inflammation (3), dendritic cell activation and migration (4), and T-cell proliferation (5), different approaches were followed. It is likely that a combination of different analysis methods using different endpoints may offer an overall high accuracy for prediction [350].

Bioavailability

In the case of sensitization, bioavailability describes the ability of a substance to penetrate the skin and the possible activation of a weak or non-sensitizing substance into a sensitizer. The chemical structure and the physical properties of a substance allow an initial assessment. For example, a low molecular weight (<500 Da) and melting point (<200°C), and an octanol/water partition coefficient (log KOW) between 1 and 5 suggest a certain penetration potential [351]. Therefore, the consideration of such data can be useful for in silico structure–activity relationship (SAR) tools.

Most of the data on the skin penetration have been obtained by *in vitro* or ex vivo studies using Franz diffusion cells and human or animal skin but also artificial skin constructs (ASC) [352].

Human skin models can be divided into skin equivalents, having both KCs and dermal substitutes (collagen and fibroblasts), and reconstituted human epidermis (RHE) models, consisting of multiple layers of KCs to mimic the epidermis. Several commercial RHE models are available, but these model systems lack dendritic cells or T lymphocytes, which are crucial for the sensitization process [353, 354]. Recently, a Japanese Research Group led by Uchino developed skin with an additional collagen/vitrigel layer, which contains KCs, fibroblasts and dentritic cells (DCs) (VG-KDF-Skin) [355]. However, although different RHE models such as EpiSkin, EpiDerm or SkinE- thic have already been implemented under the OECD guidelines as proven test systems for the endpoints of skin corrosion and skin irritation [356, 357], there is currently no approved method for the area of sensitization with these test systems. Although some studies show promising results, it turns out that the permeability of the available reconstructed skin models is much higher compared with human skin, especially for lipophilic substances [358–360]. Additionally, the test systems cannot currently achieve ASC that are comparable complex as human skin, especially considering skin-specific metabolic activation processes [361, 362]. Hence, also the European Union Reference Laboratory for alternatives to animal testing (EURL ECVAM), which promotes the scientific and regulatory acceptance of non-animal tests, concluded that the currently available models of human skin equivalents used to determine sensitization require further optimizations before they can be considered for evaluation by ECVAM.

Haptenation

For a majority of organic substances, the covalent binding to skin proteins is a crucial step during the sensitization process [363, 364]. Such reactions can be described as nucleophilic–electrophilic processes. Therefore, the assessment of the molecular structure of chemical substances allows a first estimation of their reactivity and is the basis of structure–activity relationship approaches [365–367]. To draw conclusions about the toxicity of a substance due to its structure, it is useful to group the substances into different reaction mechanistic domains such as Michael acceptors, Schiff base formers, SN2 and SNAr electrophiles and acylating agents, which were proposed by Aptula and Roberts [368]. Inclusion of quantitative assessments has led to different in silico quantitative structure–activity relationship (QSAR) models, for example the Toxtree and the DEREK NEXUS software, or the OECD (Q)SAR Application Toolbox to name only a few. These models use structural alerts and defined exclusion rules to assess the skin sensitization potential of a substance by performing a trend analysis and read across [369–371]. The additional inclusion of further physical– chemical parameters such as the log KOW can further improve the accuracy of the assessment.

Another approach is the usage of *in chemico* methods such as the direct peptide reactivity assay (DPRA), the peroxidase peptide reactivity assay (PPRA) or the electrophilic allergen screening assay (EASA) to generate data for the reactivity of chemicals towards model nucleophiles [372–375]. The DPRA uses two model peptides with lysine and cysteine as reaction targets. The depletion of the peptides, measured with HPLC-UV, is seen as an indicator for the sensitization potential of a substance.

Another possibility to determine the reactivity of chemicals towards model peptides is to detect unoccupied thiol or lysine binding sides after incubation with 5,5'-dithiobis-2-nitrobenzoic acid or fluorescamine [376].

In a new generation of DPRA, the peroxidase peptide reactivity assay (PPRA), horseradish peroxidase and hydrogen peroxides are additionally used to follow some metabolism and oxidation processes and to incorporate pro- or pre-haptens that require some kind of activation [374, 377]. The DPRA has completed validation by EURL ECVAM, which supports the development of an appropriate OECD Test Guideline (TG) [378]. Recently, a draft TG on DPRA is under discussion at OECD. To further extend the outcome of such peptide reactivity assays, an LC-MS/MS determination can be linked, which allows not only quantitative but also qualitative assessment due to the determination of possible adducts, dimerization processes, etc. [379, 380].

Epidermal inflammation

KCs are the dominating cell types in the epidermis and are the first skin cells, which come into contact with substances that penetrated through the stratum corneum. KCs show metabolic activity and are able to express various (pro)inflammatory cytokines (e.g. IL-1α or IL-18) and different adhesion and growth factors upon contact with sensitizers and photosensitizers [381, 382]. This is the basis of a whole series of proposed alternative methods, for example the cell-based AREn32 or NCTC 2544 IL-18 assays and the SenCeeTox, or SENS-IS assays [383–389]. With SENS-IS, for which human 3D reconstructed epidermis (EpiSkin) is used, a quantification of 62 biomarkers, which are split into three groups (irritation, ARE and SENS-IS), is possible [390]. SenCeeTox measures changes in gene transcription of up to six genes using different concentrations of the test substances and may not only identify sensitizers but also accurately predict their potency category [391, 392].

The contact of KCs with skin sensitizers can also induce cytoprotective cellular pathways, for example Nrf2–Keap1–ARE regulatory pathway, which plays an important role in the protection of cells against oxidative and xenobiotic damage [393]. Keap1, with its hapten-reactive cysteine residues, plays a crucial role here. Based on this approach, the KeratinoSens and the LuSens assays were developed to measure the keratinocyte activity by the induction of a luciferase gene under the control of the antioxidant response element (ARE) [394–396]. In February 2014, ECVAM published its recommendation on the KeratinoSens. It is expected that the recommendation will facilitate scientific discussions at OECD in view of developing further OECD Test Guidelines for skin sensitization [397].

Dendritic cell activation

During contact between an allergen and the skin, dermal dendritic cells and the immature dendritic LCs serve as antigen-presenting cells able to internalize and process the hapten–protein complex and present the allergen–MHC complex to naive T cells [398, 399]. As a key issue in the sensitization process, many investigators see potential for the use of dendritic cell lines for the development of animal-free alternative methods.

As LCs are only present in the skin in small numbers and tend to maturate during extraction and cultivation processes, other dendritic cell lines such as the human myeloid leukaemia cell lines THP-1, U-937, MUTZ-3 or KG-1 are isolated, cultivated and used under standardized conditions. Dendritic cell activation can be measured by chemokine (e.g. DC-CK1, CCCL5, CCL19 and MIP-1α) and cytokine secretion (e.g. IL-1β, IL-1α, IL-8 and TNF-α) and through the expression of cell surface markers (e.g. CD40, CD54, CD86 and C-C chemokine receptor type 7 (CCR7)) [400]. Under the available test systems, the myeloid U937 skin sensitization test (MUSST) and the human cell line activation test (h-CLAT) are the most advanced test systems in terms of both the number of tested substances and the standardization procedure. MUSST is based on changes in CD86 expression of the U937 cell line measured by flow cytometry [401, 402]. During h-CLAT, CD86 and CD54 expression of a THP-1 cell line is also measured using flow cytometry [403, 404]. Both methods are currently part of an ECVAM-coordinated pre-validation study. Another approach is the analysis of gene expression changes after the contact of DCs with allergens. The VITOSENS assay measures changes in gene expression of 13 genes, the cAMP-responsive element modulator (CREM) and the monocyte chemotactic protein-1 receptor (CCR2), determined as predictive biomarkers of CD34+ progenitor cells (CD34-DC) after contact with sensitizing chemicals [405, 406]. The Genomic Allergen Rapid Detection (GARD) assay utilizes genomic biomarker signatures based on the cellular responses of the human myeloid cell line MUTZ-3 towards sensitizers. The biomarker signatures provide measurements of numerous genes that are involved in immune response and cytoprotective mechanisms [407].
In addition, the increased cytokine/chemokine secretion upon contact with sensitizers is the basis of various other dendritic cell assays. For example, IL-8, as a sensitive biomarker, seems to be promising for distinguishing between sensitizers and non-sensitizers [408–410]. Quantification can be performed by enzyme-linked immunosorbent assay (ELISA), which allows high sample throughput for possible screening. However, only a limited number of chemicals have been tested so far, so that the results still do not allow conclusive assessment of the validity of these methods.

T-cell proliferation

As seen in the LLNA, the proliferation of naive T cells after contact with a chemical substance is a reliable indicator that a substance is immunogenic. Therefore, several publications concentrate on the feasibility of *in vitro* T-cell proliferation followed by a coculture of sensitizer-treated dendritic cells (DC/T-cell coculture protocols) and the expression of selected biomarkers [411–413]. Whereas the first generation of classical human T-cell priming assays (hTCPA) could only detect strong or extreme sensitizers, the usage of human peripheral blood with fewer regulatory cells increased the sensitivity of the methods and allows the determination of moderate and weak sensitizing properties [414, 415]. Although T-cell-based assays are complex and have limitations, they are seen as useful and valid future tools in the development of alternative methods [416].
It is generally accepted that no single approach of non-animal testing methods reflecting the key mechanisms of skin sensitization will be sufficient to predict the sensitization potential of a substance.

However, the combination of different approaches in a combined test battery has the potential of a full replacement toolkit [417]. So far, one of the most promising approaches is a test system combined and evaluated under the leadership of BASF. Bauch et al. combined the DPRA, the LuSens, or KeratinoSens assay and the mMUSST and h-CLAT. They reached an accuracy of 94% for 54 test substances with no false positive or false negative events and thus exceeded even the results of the LLNA [389, 418].

Conclusion

The compatibility and performance of sun protection products are essential for their safe use. The selection of (photo)stable UV filters, an appropriate combination of different UVA and UVB absorbers, and a cosmetically pleasant formulation provide the basis for effective protection against UV radiation. Unfortunately, a globally harmonized system for the evaluation, testing and approval of sunscreens is still missing, making it almost impossible for a manufacturer to formulate sun protection products that can be approved globally. The market for sun protection products is constantly changing based on the progress of scientific knowledge. Nevertheless, the approval of new UV absorbers is a major challenge, especially in certain countries, such as U.S.A. Although the role of sun protection products will further increase, the widespread use of UV filters in multiple cosmetic products should not be disregarded due to their impacts on compatibility and their fate in environment.

Acknowledgements

The authors declare no conflicts of interest.

References

1. Holick, M.F. A perspective on the beneficial effects of moderate exposure to sunlight: bone health, cancer prevention, mental health and well being. In *Comprehensive Series in Photosciences - Sun Protection in Man* (Giacomoni, P.U., ed.), pp. 11-37, Elsevier Science, Amsterdam (2001).
2. Hossein-nezhad, A. and Holick, M.F. Vitamin D for health: a global perspective. *Mayo Clin. Proc.* 88, 720-755 (2013).
3. Papoutsaki, M. and Costanzo, A. Treatment of psoriasis and psoriatic arthritis. *BioDrugs* 27, 3-12 (2013).
4. Matsumura, Y. and Ananthaswamy, H.N. Toxic effects of ultraviolet radiation on the skin. *Toxicol. Appl. Pharmacol.* 195, 298-308 (2004).
5. Polefka, T.G., Meyer, T.A., Agin, P.P., Bianchini, R.J. Effects of solar radiation on the skin. *J. Cosmet. Dermatol.* 11, 134-143 (2012).
6. Pfeifer, G.P. and Besaratinia, A. UV wavelength-dependent DNA damage and human non-melanoma and melanoma skin cancer. *Photochem. Photobiol. Sci.* 11, 90-97 (2012).
7. Narayanan, D.L., Saladi, R.N. and Fox, J.L. Ultraviolet radiation and skin cancer. *Int. J. Dermatol.* 49, 978-986 (2010).
8. Mason, R.S. and Reichrath, J. Sunlight, vitamin D and skin cancer. *Anticancer Agents Med. Chem.* 13, 83-97 (2013).
9. Randle, H.W. Suntanning: differences in perceptions throughout history. *Mayo Clin. Proc.* 72, 461-466 (1997).
10. Roelandts, R. History of Human Photobiology. In *Photodermatology* (Lim, H.W., Hönigsmann, H. and Hawk, J.L.M., eds.), pp. 1–13. CRC Press, Boca Raton (2007).
11. Hausser, K.W. and Vahle, W. Die Abhängigkeit des Lichterythems und der Pigmentbildung von der Schwingungszahl (Wellenlänge) der erregenden Strahlung. *Strahlentherapie* 13, 41-71 (1922).
12. Couteau, C. and Coiffard, L. History of sun protection. *Rev. Hist. Pharm. (Paris)* 58, 151-162 (2010).
13. Urbach, F. The historical aspects of sunscreens. *J. Photochem. Photobiol. B* 64, 99-104 (2001).
14. Dal, H., Boldemann, C. and Lindelöf, B. Does relative melanoma distribution by body site 1960-2004 reflect changes in intermittent exposure and intentional tanning in the Swedish population? *Eur. J. Dermatol*. 17, 428-434 (2007).
15. Bolanca, Z., Bolanca, I., Buljan, M., Blajic, I., Penavic, Z.J. and Situm, M. Trends, habits and attitudes towards suntanning. *Coll. Antropol.* 32, 143-146 (2008).

16. Lasithiotakis, K.G., Leiter, U., Gorkievicz, R., Eigentler,T., Breuninger, H., Metzler, G., Strobel, W. and Garbe, C. The incidence and mortality of cutaneous melanoma in Southern Germany: trends by anatomic site and pathologic characteristics, 1976 to 2003. *Cancer* 107, 1331-1339 (2006).
17. Association of Population-based Cancer Registries in Germany (GEKID). GEKID-Atlas. Available at: http://www.gekid.de, accessed 20 February 2014.
18. Petersen, B., Thieden, E., Philipsen, P.A., Heydenreich, J., Young, A.R. and Wulf, H.C. A sun holiday is a sunburn holiday. *Photodermatol. Photoimmunol. Photomed.* 29, 221-224 (2013).
19. Veierod, M.B., Weiderpass, E., Thorn, M., Hansson, J., Lund, E., Armstrong, B. and Adami, H.O. A prospective study of pigmentation, sun exposure, and risk of cutaneous malignant melanoma in women. *J. Natl. Cancer Inst.* 95, 1530-1538 (2003).
20. Veierod, M.B., Adami, H.O., Lund, E., Armstrong, B.K. and Weiderpass, E. Sun and solarium exposure and melanoma risk: effects of age, pigmentary characteristics, and nevi. *Cancer Epidemiol. Biomarkers Prev.* 19, 111-120 (2010).
21. Autier, P., Dore, J.F., Reis, A.C., Grivegnee, A., Ollivaud, L., Truchetet, F., Chamoun, E., Rotmensz, N., Severi, G. and Cesarini, J.P. Sunscreen use and intentional exposure to ultraviolet A and B radiation: a double blind randomized trial using personal dosimeters. *Br. J. Cancer* 83, 1243-1248 (2000).
22. Autier, P., Boniol, M. and Dore, J.F. Sunscreen use and increased duration of intentional sun exposure: still a burning issue. *Int. J. Cancer* 121, 1-5 (2007).
23. Andersen, S.O., Halberstadt, M.L. and Borgford-Parnell, N. Stratospheric ozone, global warming, and the principle of unintended consequences--an ongoing science and policy success story. *J. Air Waste Manag. Assoc.* 63, 607-647 (2013).
24. Kripke, M.L. Impact of ozone depletion on skin cancers. *J. Dermatol. Surg. Oncol.* 14, 853-857 (1988).
25. Lemus-Deschamps, L. and Makin, J.K. Fifty years of changes in UV Index and implications for skin cancer in Australia. *Int. J. Biometeorol.* 56, 727-735 (2012).
26. Young, A.R. and Sheehan, J.M. UV-induced pigmentation in human skin. In *Comprehensive Series in Photosciences - Sun Protection in Man* (Giacomoni, P.U., ed.), pp. 357-376, Elsevier Science, Amsterdam (2001).
27. Jablonski, N.G. and Chaplin, G. Colloquium paper: human skin pigmentation as an adaptation to UV radiation. *Proc. Natl. Acad. Sci. USA* 107(Suppl. 2), 8962-8968 (2010).
28. Breitbart, E.W., Greinert, R. and Volkmer, B. Effectiveness of information campaigns. *Prog Biophys. Mol. Biol.* 92, 167-172 (2006).

29. Makin, J.K., Warne, C.D., Dobbinson, S.J., Wakefield, M.A. and Hill, D.J. Population and age-group trends in weekend sun protection and sunburn over two decades of the SunSmart programme in Melbourne, Australia. *Br. J. Dermatol.* 168, 154-161 (2013).
30. Robinson, J.K., Rigel, D.S. and Amonette, R.A. Trends in sun exposure knowledge, attitudes, and behaviors: 1986 to 1996. *J. Am. Acad. Dermatol.* 37, 179-186 (1997).
31. Moyal,D. The development of efficient sunscreens. *Indian J. Dermatol. Venereol. Leprol.* 78, 31-34 (2012).
32. Wang, S.Q., Tanner, P.R., Lim, H.W. and Nash, J.F. The evolution of sunscreen products in the United States--a 12-year cross sectional study. *Photochem. Photobiol. Sci.* 12, 197-202 (2013).
33. Manova, E., von Goetz, N., Hauri, U., Bogdal, C. and Hungerbuhler, K. Organic UV filters in personal care products in Switzerland: a survey of occurrence and concentrations. *Int. J. Hyg. Environ. Health* 216, 508-514 (2013).
34. Seite,S., Fourtanier, A. and Rougier, A. Photoprotection in moisturizers and daily-care products. *G. Ital. Dermatol. Venereol.* 145, 631-636 (2010).
35. Shaat, N.A. and Shaat, M. Recent sunscreens market trends. In *Sunscreens, regulations and commercial development* (Shaat, N.A., ed.), pp. 929-940. Taylor & Francis, Boca Raton (2005).
36. Gago-Ferrero, P., Diaz-Cruz, M.S. and Barcelo, D. An overview of UV-absorbing compounds (organic UV filters) in aquatic biota. *Anal. Bioanal. Chem.* 404, 2597-2610 (2012).
37. Poiger, T., Buser, H.R., Balmer, M.E., Bergqvist, P.A. and Muller, M.D. Occurrence of UV filter compounds from sunscreens in surface waters: regional mass balance in two Swiss lakes. *Chemosphere* 55, 951-963 (2004).
38. Fent, K. and Kunz, P. Occurrence and Effects of Hormonally Active UV Filters in the Aquatic Environment. *SÖFW* 135, 2-12 (2009).
39. Giokas, D.L., Salvador, A. and Chisvert, A. (2007) UV filters: From sunscreens to human body and the environment. *Trends Anal. Chem.* 26, 360-374 (2007).
40. Nash, J.F. and Tanner, P.R. Relevance of UV filter/sunscreen product photostability to human safety. *Photodermatol. Photoimmunol. Photomed.* 30, 88-95 (2014).
41. Dondi,D., Albini,A. and Serpone,N. (2006) Interactions between different solar UVB/UVA filters contained in commercial suncreams and consequent loss of UV protection. *Photochem. Photobiol. Sci.* 5, 835-843 (2006).
42. Köhnlein, M. Untersuchungen zum photochemischen Verhalten des UV-B-Filters Octylmethoxycinnamat in Modellsystemen, Sonnenschutzmitteln sowie auf der Haut. PhD thesis, Institute of Food Chemistry, University of Hohenheim (2000).
43. Schwack, W. and Rudolph, T. Photochemistry of dibenzoyl methane UVA filters Part 1. *Photochem. Photobiol. B* 28, 229-234 (1995).

44. Karlsson, I., Persson, E., Mårtensson, J. and Börje, A. Investigation of the sunscreen octocrylene's interaction with amino acid analogs in the presence of UV radiation. *Photochem. Photobiol.* 88, 904-912 (2012).
45. Holbrook, K.A. and Odland, G.F. Regional differences in the thickness (cell layers) of the human stratum corneum: an ultrastructural analysis. *J. Invest. Dermatol*. 62, 415-422 (1974).
46. Sterry, W. *Kurzlehrbuch Dermatologie*, pp. 3-8. Thieme Verlag, Stuttgart (2011).
47. McGrath, J.A., Eady, R.A.J. and Pope, F.M. Chapter 3 - Anatomy and Organization of Human Skin. In *Rook's Textbook of Dermatology* (Burns, T., Breathnach, S., Cox, N. and Griffiths, C., eds.), pp. 1-53. John Wiley & Sons, Chichester, UK (2010).
48. Gauglitz G.G. and Schauber, J. Skin: Architecture and Function. In *Dermal Replacements in General, Burn, and Plastic Surgery* (Kamolz, L. and Lumenta, D.B., eds.), pp. 1-11. Springer-Verlag, Wien (2013).
49. Blanpain, C. Epidermal stem cells. *Bull Mem. Acad. R. Med. Belg.* 162, 418-424 (2007).
50. Wertz, P.W., Madison, K.C. and Downing, D.T. Covalently bound lipids of human stratum corneum. *J. Invest. Dermatol*. 92, 109-111 (1989).
51. Radner, F.P. and Fischer, J. The important role of epidermal triacylglycerol metabolism for maintenance of the skin permeability barrier function. *Biochim. Biophys. Acta.* 1841, 409-415 (2014).
52. Meckfessel, M.H. and Brandt, S. The structure, function, and importance of ceramides in skin and their use as therapeutic agents in skin-care products. *J. Am. Acad. Dermatol.* 71, 177-184 (2014).
53. Bouwstra, J., Pilgram, G., Gooris, G., Koerten, H. and Ponec, M. New aspects of the skin barrier organization. *Skin Pharmacol. Appl. Skin Physiol.* 14, 52-62 (2001).
54. Bos, J.D. and Meinardi, M.M. The 500 Dalton rule for the skin penetration of chemical compounds and drugs. *Exp. Dermatol.* 9, 165-169 (2000).
55. Wickett, R.R. and Visscher, M.O. Structure and function of the epidermal barrier. *Am. J. Infect. Control* 34, 98-110 (2006).
56. Baroni, A., Buommino, E., De Gregorio, V., Ruocco, E., Ruocco, V. and Wolf, R. Structure and function of the epidermis related to barrier properties. *Clin. Dermatol,* 30, 257-262 (2012).
57. Proksch, E., Brandner, J.M. and Jensen, J.M. The skin: an indispensable barrier. *Exp Dermatol.* 17, 1063-1072 (2008).
58. McCullough, J.L. and Kelly, K.M. Prevention and treatment of skin aging. *Ann. N. Y. Acad. Sci.* 1067, 323-331 (2006).

59. Langton, A.K., Griffiths, C.E., Sherratt, M.J. and Watson, R.E. Cross-linking of structural proteins in ageing skin: an in situ assay for the detection of amine oxidase activity. *Biogerontology* 14, 89-97 (2013).
60. Calleja-Agius, J., Brincat, M. and Borg, M. Skin connective tissue and ageing. *Best Pract. Res. Clin. Obstet. Gynaecol*. 27, 727-740 (2013).
61. Lai-Cheong, J.E. and McGrath, J.A. Structure and function of skin, hair and nails. *Medicine* 41, 317-320 (2013).
62. Qiang, F. Radiation (Solar). In *Encyclopedia of Atmospheric Sciences* (Holton, J.R., ed.), pp. 1859-1863. Academic Press, Oxford (2003).
63. ISO 21348:2007. Space environment (natural and artificial) -- Process for determining solar irradiances.
64. McKenzie, R.L., Björn, L.O., Bais, A., Ilyasad, M. Changes in biologically active ultraviolet radiation reaching the Earth's surface. *Photochem. Photobiol. Sci.* 2, 5-15 (2003).
65. Dupont, E., Gomez, J. and Bilodeau, D. Beyond UV radiation: a skin under challenge. *Int. J. Cosmet. Sci.* 35, 224-232 (2013).
66. Meinhardt, M., Krebs, R., Anders, A., Heinrich, U. and Tronnier, H. Wavelength-dependent penetration depths of ultraviolet radiation in human skin. *J. Biomed. Opt.* 13, 044030 (2008).
67. Bruls, W.A., Slaper, H., van der Leun, J.C. and Berrens, L. Transmission of human epidermis and stratum corneum as a function of thickness in the ultraviolet and visible wavelengths. *Photochem. Photobiol.* 40, 485-494 (1984).
68. International Agency for Research in Cancer (IARC). Exposure to artificial UV radiation and skin cancer / views and expert opinions of an IARC Working Group that met in Lyon, France 27-29 June (2005). Available at: http://www.iarc.fr/en/publications/pdfs-online/wrk/wrk1/ArtificialUVRad&SkinCancer.pdf, accessed 13 September 2014.
69. Gandini, S., Autier, P. and Boniol, M. Reviews on sun exposure and artificial light and melanoma. *Prog. Biophys. Mol. Biol.* 107, 362-366 (2011).
70. Nilsen, L.T.N., Aalerud, T.N. Hannevika, M. and Veierød, M.B. UVB and UVA irradiances from indoor tanning devices. *Photochem. Photobiol. Sci.* 10, 1129-1136 (2011).
71. Balk, S.J. and Geller, A.C. Teenagers and artificial tanning. *Pediatrics* 121, 1040-1042 (2008).
72. Balk, S.J. Ultraviolet radiation: a hazard to children and adolescents. *Pediatrics* 127, 791-817 (2011).
73. Pawlak, M.T., Bui, M., Amir, M., Burkhardt, D.L., Chen, A.K., Dellavalle, R.P. Legislation restricting access to indoor tanning throughout the world. *Arch. Dermatol.* 148, 1006-1012 (2012).

74. Holick, M.F. Sunlight and vitamin D for bone health and prevention of autoimmune diseases, cancers, and cardiovascular disease. *Am. J. Clin. Nutr.* 80, 1678-1688 (2004).
75. Bikle, D.D. Vitamin D metabolism and function in the skin. *Mol. Cell Endocrinol.* 347, 80-89 (2011).
76. Webb, A.R., de Costa, B.R., Holick, M.F. Sunlight regulates the cutaneous production of vitamin D3 by causing its photodegradation. *J. Clin. Endocrinol. Metab.* 68, 882–887 (1989).
77. Holick, M.F. Vitamin D deficiency. *N. Engl. J. Med.* 357, 266-281 (2007).
78. DeLuca, H.F. Overview of general physiologic features and functions of vitamin D. *Am. J. Clin. Nutr.* 80, 1689-1696 (2004).
79. Thacher, T.D. and Clarke, B.L. Vitamin D insufficiency. *Mayo Clin. Proc.* 86, 50-60 (2011).
80. Chen, J., Liu, W., Lin, Q., Chen, L., Yin, J. and Huang, H. Vitamin D deficiency and low bone mineral density in native Chinese rheumatoid arthritis patients. *Int. J. Rheum. Dis.* 17, 66-70 (2014).
81. Lips, P. and van Schoor, N.M. The effect of vitamin D on bone and osteoporosis. *Best Pract. Res. Clin. Endocrinol. Metab.* 25, 585-591 (2011).
82. Ceglia, L. and Harris, S.S. Vitamin D and its role in skeletal muscle. *Calcif. Tissue Int.* 92, 151-162 (2013).
83. Girgis, C.M., Clifton-Bligh, R.J., Hamrick, M.W., Holick, M.F. and Gunton, J.E. The roles of vitamin D in skeletal muscle: form, function, and metabolism. *Endocr. Rev.* 34, 33–83 (2013).
84. Taha, S.A., Dost, S.M. and Sedrani, S.H. 25-Hydroxyvitamin D and total calcium: extraordinarily low plasma concentrations in Saudi mothers and their neonates. *Pediatr. Res.* 18, 739-741 (1984).
85. Gloth, F.M. 3rd, Gundberg, C.M., Hollis, B.W., Haddad, J.G. Jr., and Tobin, J.D. Vitamin D deficiency in homebound elderly persons. *JAMA* 274, 1683-1686 (1995).
86. Clemens, T.L., Adams, J.S., Henderson, S.L. and Holick, M.F. Increased skin pigmentation reduces the capacity of skin to synthesise vitamin D3. *Lancet* 1, 74–76 (1982).
87. Matsuoka, L.Y., Ide, L., Wortsman, J., MacLaughlin, J.A. and Holick, M.F. Sunscreens suppress cutaneous vitamin D3 synthesis. *J. Clin. Endocrinol. Metab.* 64, 1165–1168 (1987).
88. Raiten, D.J. and Picciano, M.F. Vitamin D and health in the 21st century: bone and beyond. Executive summary. *Am. J. Clin. Nutr.* 80, 1673-1677 (2004).
89. Benakova, N. (2011) Phototherapy of psoriasis in the era of biologics: still in. *Acta Dermatovenerol. Croat.* 19, 195-205 (2011).

90. Reynolds, N.J., Franklin, V., Gray, J.C., Diffey, B.L. and Farr, P.M. Narrow-band ultraviolet B and broad-band ultraviolet A phototherapy in adult atopic eczema: a randomised controlled trial. *The Lancet* 357, 2012-2016 (2001).
91. Naldi, L. and Griffiths, C.E. Traditional therapies in the management of moderate to severe chronic plaque psoriasis: an assessment of the benefits and risks. *Br. J. Dermatol.* 152, 597-615 (2005).
92. Sklar, L.R., Almutawa, F., Lim, H.W. and Hamzavi, I. Effects of ultraviolet radiation, visible light, and infrared radiation on erythema and pigmentation: a review. *Photochem. Photobiol. Sci.* 12, 54-64 (2013).
93. Assefa, Z., Van Laethem, A., Garmyn, M. and Agostinis, P. Ultraviolet radiationinduced apoptosis in keratinocytes: on the role of cytosolic factors. *Biochim. Biophys. Acta* 1755, 90–106 (2005).
94. Claerhout, S., Van Laethem, A., Agostinis, P. and Garmyn, M. Pathways involved in sunburn cell formation: deregulation in skin cancer. *Photochem. Photobiol. Sci.* 5, 199-207 (2006).
95. Lippens, S., Hoste, E., Vandenabeele, P., Agostinis, P. and Declercq, W. Cell death in the skin. *Apoptosis* 14, 549-569 (2009).
96. Ravanat, J.L., Douki, T. and Cadet, J. UV damage to nucleic acid components. In *Comprehensive Series in Photosciences* (Giacomoni, P.U., ed.), pp. 207-230, Elsevier Science, Amsterdam (2001).
97. Ikehata, H. and Ono, T. The mechanisms of UV mutagenesis. *J. Radiat. Res.* 52, 115-125 (2011).
98. Wikonkal, N.M. and Brash, D.E. Ultraviolet radiation induced signature mutations in photocarcinogenesis. *J. Investig. Dermatol. Symp. Proc.* 4, 6-10 (1999).
99. Liu, J., Zhang, C. and Feng, Z. Tumor suppressor p53 and its gain-of-function mutants in cancer. *Acta Biochim. Biophys. Sin. (Shanghai)* 46, 170-179 (2014).
100. Giglia-Mari, G. and Sarasin, A. TP53 mutations in human skin cancers. *Hum. Mutat.* 21, 217-228 (2003).
101. Rivlin, N., Brosh, R., Oren, M. and Rotter, V. Mutations in the p53 Tumor Suppressor Gene: Important Milestones at the Various Steps of Tumorigenesis. *Genes Cancer* 2, 466-474 (2011).
102. Taylor, H.R. The biological effects of UV-B on the eye. *Photochem. Photobiol.* 50, 489-492 (1989).
103. Young, A.R. Acute effects of UVR on human eyes and skin. *Prog. Biophys. Mol. Biol.* 92, 80-85 (2006).
104. Roberts, J.E. Ultraviolet radiation as a risk factor for cataract and macular degeneration. *Eye Contact Lens* 37, 246-249 (2011).

105. Yam, J.C. and Kwok, A.K. Ultraviolet light and ocular diseases. *Int. Ophthalmol.* 34, 383-400 (2014).
106. Quan, T., Qin, Z., Xia, W., Shao, Y., Voorhees, J.J. and Fisher, G.J. Matrix-degrading metalloproteinases in photoaging. *J. Investig. Dermatol. Symp. Proc.* 14, 20-24 (2009).
107. Gilchrest, B.A. Photoaging. *J. Invest. Dermatol.* 133, E2-E6 (2013).
108. Rabe, J.H., Mamelak, A.J., McElgunn, P.J.S., Morison, W.L. and Sauder, D.N. Photoaging: mechanisms and repair. *J. Am. Acad. Dermatol.* 55, 1-19 (2006).
109. Baumann L. Skin ageing and its treatment. *J. Pathol.* 211, 241-251 (2007).
110. Berneburg, M., Plettenberg, H., Medve-Konig, K., Pfahlberg, A., Gers-Barlag, H., Gefeller, O. and Krutmann, J. Induction of the photoaging-associated mitochondrial common deletion in vivo in normal human skin. *J. Invest. Dermatol.* 122, 1277-1283 (2004).
111. Cadet, J. and Douki, T. Oxidatively generated damage to DNA by UVA radiation in cells and human skin. *J. Invest. Dermatol.* 131, 1005-1007 (2011).
112. Krutmann, J. and Schroeder, P. Role of mitochondria in photoaging of human skin: the defective powerhouse model. *J. Investig. Dermatol. Symp. Proc.* 14, 44-49 (2009).
113. Schroeder, P., Gremmel, T., Berneburg, M. and Krutmann, J. Partial depletion of mitochondrial DNA from human skin fibroblasts induces a gene expression profile reminiscent of photoaged skin. *J. Invest. Dermatol*. 128, 2297-2303 (2008).
114. Marionnet, C., Pierrard, C., Lejeune, F., Sok, J., Thomas, M. and Bernerd, F. Different oxidative stress response in keratinocytes and fibroblasts of reconstructed skin exposed to non extreme daily-ultraviolet radiation. *PLOS One* 5, e12059 (2010).
115. Shindo, Y., Witt, E., Han, D., Epstein, W. and Packer, L. Enzymic and non-enzymic antioxidants in epidermis and dermis of human skin. *J. Invest. Dermatol.* 102, 122-124 (1994).
116. Valko, M., Leibfritz, D., Moncol, J., Cronin, M.T., Mazur, M. and Telser, J. Free radicals and antioxidants in normal physiological functions and human disease. *Int. J. Biochem. Cell Biol.* 39, 44-84 (2007).
117. Leccia, M.T., Yaar, M., Allen, N., Gleason, M. and Gilchrest, B.A. Solar simulated irradiation modulates gene expression and activity of antioxidant enzymes in cultured human dermal fibroblasts. *Exp. Dermatol.* 10, 272-279 (2001).
118. Shindo, Y. and Hashimoto, T. Time course of changes in antioxidant enzymes in human skin fibroblasts after UVA irradiation. *J. Dermatol. Sci.* 14, 225-232 (1997).
119. Placzek, M., Przybilla, B., Kerkmann, U., Gaube, S. and Gilbertz, K. Effect of ultraviolet (UV) A, UVB or ionizing radiation on the cell cycle of human melanoma cells. *Br. J. Dermatol.* 156, 843-847 (2007).
120. De Gruijl, F.R. Photocarcinogenesis: UVA vs. UVB radiation. *Skin Pharmacol. Appl. Skin Physiol.* 15, 316-320 (2002).

121. Cadet, J., Sage, E. and Douki, T. Ultraviolet radiation-mediated damage to cellular DNA. *Mutat. Res*. 571, 3-17 (2005).
122. Pilger, A. and Rüdiger, H.W. 8-Hydroxy-2'-deoxyguanosine as a marker of oxidative DNA damage related to occupational and environmental exposures. *Int. Arch. Occup. Environ. Health* 80,1-15 (2006).
123. Valavanidis, A., Vlachogianni, T. and Fiotakis, C. 8-hydroxy-2'-deoxyguanosine (8-OHdG): A critical biomarker of oxidative stress and carcinogenesis. *J. Environ. Sci. Health C Environ. Carcinog. Ecotoxicol. Rev.* 27, 120-139 (2009).
124. Halliday, G,M., Agar, N.S., Barnetson, R.S., Ananthaswamy, H.N. and Jones, A.M. UV-A fingerprint mutations in human skin cancer. *Photochem. Photobiol.* 81, 3-8 (2005).
125. Agar, N.S., Halliday, G.M., Barnetson, R.S., Ananthaswamy, H.N., Wheeler, M. and Jones, A.M. The basal layer in human squamous tumors harbors more UVA than UVB fingerprint mutations: a role for UVA in human skin carcinogenesis. *Proc. Natl. Acad. Sci. USA* 101, 4954-4959 (2004).
126. Mouret, S., Forestier, A. and Douki, T. The specificity of UVA-induced DNA damage in human melanocytes. *Photochem. Photobiol. Sci.* 11, 155-162 (2012).
127. Van der Pols, J.C. Epidemiology of Basal Cell and Squamous Cell Carcinoma of the Skin. In *Skin Cancer - A World-Wide Perspective* (Dummer, R., Pittelkow, M.R., Iwatsuki, K., Green, A. and Elwan, N.M., eds.), pp. 3-12. Springer-Verlag Berlin Heidelberg (2011).
128. Fuchs, A. and Marmur, E. The kinetics of skin cancer: progression of actinic keratosis to squamous cell carcinoma. *Dermatol. Surg.* 33, 1099-1101 (2007).
129. Armstrong, B.K. and Kricker, A. The epidemiology of UV induced skin cancer. *J. Photochem. Photobiol. B.* 63, 8-18 (2001).
130. Situm, M., Buljan, M., Bulat, V., Lugović Mihić, L., Bolanca, Z. and Simić, D. The role of UV radiation in the development of basal cell carcinoma. *Coll. Antropol.* 32, 167-170 (2008).
131. Rünger, T.M. Role of UVA in the pathogenesis of melanoma and non-melanoma skin cancer. A short review. *Photodermatol. Photoimmunol. Photomed.* 15, 212-216 (1999).
132. Damian, D.L., Matthews, Y.J., Phan, T.A. and Halliday, G.M. An action spectrum for ultraviolet radiation-induced immunosuppression in humans. *Br. J. Dermatol.* 164, 657-659 (2011).
133. Meyer, T., Stockfleth, E. and Christophers, E. Immune response profiles in human skin. *Br. J. Dermatol.* 157, 1-7 (2007).
134. Schwarz, T. Mechanisms of UV-induced immunosuppression. *Keio J. Med.* 54: 165-171 (2005).
135. Rivas, J.M. and Ullrich, S.E. The role of IL-4, IL-10, and TNF-alpha in the immune suppression induced by ultraviolet radiation. *J. Leukoc. Biol.* 56, 769-775 (1994).

136. Amerio, P., Carbone, A., Auriemma, M., Varrati, S. and Tulli, A. UV induced skin immunosuppression. *Antiinflamm. Antiallergy Agents Med. Chem.* 8, 3-13 (2009).
137. Chomiczewska-Skóra, D., Adamus, A., Trznadel-Grodzka, E. and Rotsztejn, H. Effects of ultraviolet radiation on Langerhans cells. *Centr. Eur. J. Immunol.* 38, 393-398 (2013).
138. Aubin, F. Mechanisms involved in ultraviolet light-induced immunosuppression. *Eur. J. Dermatol.* 13, 515-523 (2003).
139. Gibbs, N.K., Tye, J. and Norval, M. Recent advances in urocanic acid photochemistry, photobiology and photoimmunology. *Photochem. Photobiol. Sci.* 7, 655-667 (2008).
140. Gibbs, N.K. and Norval, M. Photoimmunosuppression: a brief overview. *Photodermatol. Photoimmunol. Photomed.* 29, 57-64 (2013).
141. Reilly, S.K. and De Fabo, E.C. Dietary histidine increases mouse skin urocanic acid levels and enhances UVB-induced immune suppression of contact hypersensitivity. *Photochem. Photobiol.* 53, 431-438 (1991).
142. Kurimoto, I. and Streilein, J.W. Deleterious effects of cis-urocanic acid and UVB radiation on Langerhans cells and on induction of contact hypersensitivity are mediated by tumor necrosis factor-alpha. *J. Invest. Dermatol.* 99, 69-70 (1992).
143. Kaneko, K., Smetana-Just, U., Matsui, M., Young, A.R., John, S., Norval, M. and Walker, S.L. Cis-Urocanic acid initiates gene transcription in primary human keratinocytes. *J. Immunol.* 181, 217-224 (2008).
144. Moodycliffe, A.M., Bucana, C.D., Kripke, M.L., Norval, M. and Ullrich, S.E. Differential effects of a monoclonal antibody to cis-urocanic acid on the suppression of delayed and contact hypersensitivity following ultraviolet irradiation. *J. Immunol.* 157, 2891-2899 (1996).
145. Gibbs, N.K. and Norval, M. Urocanic acid in the skin: a mixed blessing? *J. Invest. Dermatol.* 131, 14-17 (2011).
146. Ferlay, J., Steliarova-Foucher, E., Lortet-Tieulent, J. *et al.* Cancer incidence and mortality patterns in Europe: estimates for 40 countries in 2012. *Eur. J. Cancer* 49, 1374-1403 (2013).
147. Australian Institute of Health and Welfare (AIHW) & Australian Association of Cancer Registries (AACR) Cancer in Australia: an overview. Cancer series no. 74 Cat. no. CAN 70, Canberra: AIHW (2012). Available at: http://www.aihw.gov.au/WorkArea/DownloadAsset.aspx?id=60129542353, accessed 13 September 2014.
148. Liang, J.J., Robinson, E. and Martin, R.C. Cutaneous melanoma in New Zealand: 2000-2004. *ANZ J. Surg.* 80, 312-316 (2010).
149. Garbe, C. and Leiter, U. Melanoma epidemiology and trends. *Clin. Dermatol.* 27, 3-9 (2009).

150. De Vries, E. and Coebergh, J.W. Cutaneous malignant melanoma in Europe. *Eur. J. Cancer* 40, 2355-2366 (2004).
151. Nelemans, P.J., Groenendal, H., Kiemeney, L.A., Rampen, F.H., Ruiter, D.J. and Verbeek, A.L. Effect of intermittent exposure to sunlight on melanoma risk among indoor workers and sun-sensitive individuals. *Environ. Health Perspect.* 101, 252 (1993).
152. Elwood, J.M. and Gallagher, R.P. Body site distribution of cutaneous malignant melanoma in relationship to patterns of sun exposure. *Int. J. Cancer* 78, 276-280 (1998).
153. Whiteman, D.C., Whiteman, C.A. and Green, A.C. Childhood sun exposure as a risk factor for melanoma: a systematic review of epidemiologic studies. *Cancer Causes Control* 12, 69-82 (2001).
154. Pustisek, N., Sikanic-Dugic, N., Hirsl-Hecej, V. and Domljan, M.L. (2010) Acute skin sun damage in children and its consequences in adults. *Coll. Antropol.* 34(Suppl 2), 233-237 (2010).
155. Walker, G.J., Soyer, H.P., Terzian, T. and Box, N.F. Modelling melanoma in mice. *Pigment Cell Melanoma Res.* 24, 1158-1176 (2011).
156. Gaffal, E., Landsberg, J., Bald, T., Sporleder, A., Kohlmeyer, J. and Tüting, T. Neonatal UVB exposure accelerates melanoma growth and enhances distant metastases in Hgf-Cdk4(R24C) C57BL/6 mice. *Int. J. Cancer* 129, 285-294 (2011).
157. Von Thaler, A.K., Kamenisch, Y. and Berneburg, M. The role of ultraviolet radiation in melanomagenesis. *Exp. Dermatol.* 19, 81-88 (2010).
158. Tucker, M.A. Is sunlight important to melanoma causation? *Cancer Epidemiol. Biomarkers Prev.* 17, 467-468 (2008).
159. Kanavy, H.E. and Gerstenblith, M.R. Ultraviolet radiation and melanoma. *Semin. Cutan. Med Surg.* 30, 222-228 (2011).
160. Mitchell, D. and Fernandez, A. The photobiology of melanocytes modulates the impact of UVA on sunlight-induced melanoma. *Photochem. Photobiol. Sci.* 11, 69-73 (2012).
161. Noonan, F.P., Zaidi, M.R., Wolnicka-Glubisz, A. *et al.* Melanoma induction by ultraviolet A but not ultraviolet B radiation requires melanin pigment. *Nat. Communic.* 3, 884 (2012).
162. Jhappan, C., Noonan, F.P. and Merlino, G. Ultraviolet radiation and cutaneous malignant melanoma. *Oncogene* 22, 3099-3112 (2003).
163. Dhillon, A.S., Hagan, S., Rath, O. and Kolch, W. MAP kinase signalling pathways in cancer. *Oncogene.* 26, 3279-3290 (2007).
164. Davies, H., Bignell, G.R., Cox, C. *et al.* Mutations of the BRAF gene in human cancer. *Nature* 417, 949-954 (2002).
165. Bauer, J., Büttner, P., Murali, R. *et al.* BRAF mutations in cutaneous melanoma are independently associated with age, anatomic site of the primary tumor, and the degree of solar elastosis at the primary tumor site. *Pigment Cell Melanoma Res.* 24, 345-351 (2011).

166. Brenner, M., Degitz, K., Besch, R. and Berking, C. Differential expression of melanoma-associated growth factors in keratinocytes and fibroblasts by ultraviolet A and ultraviolet B radiation. *Br. J. Dermatol.* 153, 733-739 (2005).

167. Muthusamy, V. and Piva, T.J. UVB-stimulated TNFα release from human melanocyte and melanoma cells is mediated by p38 MAPK. *Int. J. Mol. Sci.* 14, 17029-17054 (2013).

168. Rodeck, U. Growth factor independence and growth regulatory pathways in human melanoma development. *Cancer and Metastasis Rev.* 12, 219-226 (1993).

169. Brenner, M. and Hearing, V.J. The protective role of melanin against UV damage in human skin. *Photochem. Photobiol.* 84, 539-549 (2008).

170. Yamaguchi, Y., Brenner, M. and Hearing, V.J. The regulation of skin pigmentation. *J. Biol. Chem.*282, 27557-27561 (2007).

171. Maddodi, N., Jayanthy, A. and Setaluri, V. Shining light on skin pigmentation: the darker and the brighter side of effects of UV radiation. *Photochem. Photobiol.* 88, 1075-1082 (2012).

172. Tiwari, S. and Chand Mishra, P. Urocanic acid as an efficient hydroxyl radical scavenger: a quantum theoretical study. *J. Mol. Model.* 17, 59-72 (2011).

173. Grundmann, J.U. and Gollnick, H. Prevention of ultraviolet ray damage: external and internal sunscreens. *Ther. Umsch.* 56, 225-232 (1999).

174. Murphy, G., Young, A.R., Wulf, H.C., Kulms, D. and Schwarz, T. The molecular determinants of sunburn cell formation. *Exp. Dermatol.* 10, 155-160 (2001).

175. Yamaguchi, Y., Takahashi, K., Zmudzka, B.Z. *et al.* Human skin responses to UV radiation: pigment in the upper epidermis protects against DNA damage in the lower epidermis and facilitates apoptosis. *FASEB J*, 20(9), 1486-1488 (2006).

176. Afaq, F. and Mukhtar, H. Effects of solar radiation on cutaneous detoxification pathways. *J. Photochem. Photobiol. B* 63, 61-69 (2001).

177. Forestier, S. Rationale for sunscreen development. *J. Am. Acad. Dermatol.* 58, 133-138 (2008).

178. Antoniou, C., Kosmadaki, M.G., Stratigos, A.J. and Katsambas, A.D. Sunscreens--what's important to know. *J. Eur. Acad. Dermatol. Venereol.* 22, 1110-1118 (2008).

179. European Parliament and Council, 2009. Regulation (EC) No. 1223/2009 of the European. Parliament and of the Council of 30 November 2009 on cosmetic products. Official Journal of the European Union L 342/59 (2009). Available at: http://eur-lex.europa.eu/LexUriServ/LexUriServ.do?uri=OJ:L:2009:342:0059:0209:en:PDF, accessed 13 September 2014.

180. European Parliament and Council, 2014. Regulation (EU) No 866/2014 of 8 August 2014 amending Annexes III, V and VI to Regulation (EC) No 1223/2009 of the European Parliament and the Council on cosmetic products. Available at: http://eur-lex.europa.eu/legal-content/EN/TXT/PDF/?uri=CELEX:32014R0866&from=EN, accessed 13 September 2014.
181. Commission Directive 2008/123/EC of 18 December 2008 amending Council Directive 76/768/EEC, concerning cosmetic products, for the purpose of adapting Annexes II and VII thereto to technical progress. *Off. J. Eur. Union L* 340/71 (2008). Available at: http://ec.europa.eu/enterprise/tbt/tbt_repository/EEC217_EN_0_2.pdf, accessed 13 September 2014.
182. Food and Drug Administration (FDA) Sunscreen drug products for over-th-counter human use; final monograph. Federal Register 64/98, 27666-27693, USA (1999). Available at: http://www.fda.gov/ohrms/dockets/98fr/052199b.pdf, accessed 13 September 2014.
183. Osterwalder, U., Sohn, M. and Herzog, B. Global state of sunscreens. *Photodermatol. Photoimmunol. Photomed.* 30, 62-80 (2014).
184. Schulze, R. Einige Versuche und Bemerkungen zum Problem der handelsüblichen Lichtschutzmittel. *Parf. Kosm.* 37, 7 (1956).
185. Greiter, F. Sun protection factor - development methods. *Parf. Kosm.* 55, 70-75 (1974).
186. Food and Drug Administration (FDA). Sunscreen drug products for over-the-counter human use: proposed safety, effective and labeling conditions. Federal register 43/166, 38206-38269, USA (1978).
187. Australian Standards Association. Sunscreen products - evaluation and classification. AS 2604-1986.
188. Japan Cosmetic Industry Association (JCIA). Standard SPF Test Method (1991).
189. The European Cosmetic Toiletry and Perfumery Association (COLIPA). Sun protection factor test method. Ref 94/289 (1994).
190. The European Cosmetic Toiletry and Perfumery Association (COLIPA), Cosmetic Toiletry & Fragrance Association of South Africa (CTFA-SA), and Japan Cosmetic Industry Association (JCIA). International Sun Protection Factor (SPF) test method, 001-2003, February 2003.
191. Cosmetic Toiletry & Fragrance Association of South Africa (CTFA-SA), the European Cosmetic Toiletry and Perfumery Association (COLIPA), Japan Cosmetic Industry Association (JCIA), Cosmetic, Toiletry & Fragrance Association of the USA (CTFA-US). International Sun Protection Factor (SPF) test method, May 2006.

192. ISO 24444:2010. Cosmetics - Sun protection test methods - In vivo determination of the sun protection factor (SPF). Available at: http://www.iso.org/iso/catalogue_detail.htm?csnumber=46523, accessed 13 September 2014.
193. Bech-Thomsen, N. and Wulf, H.C. Sunbathers' application of sunscreen is probably inadequate to obtain the sun protection factor assigned to the preparation. *Photodermatol. Photoimmunol. Photomed.* 9, 242-244 (1992).
194. Petersen, B. and Wulf, H.C. Application of sunscreen--theory and reality. *Photodermatol. Photoimmunol. Photomed*. 30, 96-101 (2014).
195. Schalka, S., Dos Reis, V.M. and Cucé, L.C. The influence of the amount of sunscreen applied and its sun protection factor (SPF): evaluation of two sunscreens including the same ingredients at different concentrations. *Photodermatol. Photoimmunol. Photomed.* 25, 175-180 (2009).
196. Rai, R., Shanmuga, S.C. and Srinivas, C.R. Update on photoprotection. *Indian J. Dermatol.* 57, 335 (2012).
197. Haywood, R., Wardman, P., Sanders, R. and Linge, C. Sunscreens inadequately protect against ultraviolet-A-induced free radicals in skin: implications for skin aging and melanoma? *J. Invest. Dermatol.* 121, 862-868 (2003).
198. Moyal, D.D. and Fourtanier, A.M. Broad-spectrum sunscreens provide better protection from solar ultraviolet-simulated radiation and natural sunlight-induced immunosuppression in human beings. *J. Am. Acad. Dermatol.* 58, S149-S154 (2008).
199. Tronnier, H. Testprobleme bei der exakten Bestimmung hoher Lichtschutzfaktoren. *Apotheker Journal* 18, 6 (1996).
200. Finkel, P. Lichtschutzfaktor: Je höher, desto besser? *Parf. Kosm.* 78, 30-33 (1997).
201. Bernerd, F., Marionnet, C. and Duval, C. Solar ultraviolet radiation induces biological alterations in human skin in vitro: relevance of a well-balanced UVA/UVB protection. *Indian J. Dermatol. Venereol. Leprol.* 78, 15-23 (2012).
202. Official Journal of the European Union. Commission Recommendation on the efficacy of sunscreen products and the claims made relating thereto, L 265, pp. 39-43 (2006/647/EC). Available at: http://eur-lex.europa.eu/LexUriServ/LexUriServ.do?uri=OJ:L:2006:265:0039:0043:en:PDF, accessed 13 September 2014.
203. Hwang, Y.J., Park, H.J., Hahn, H.J. *et al.* Immediate pigment darkening and persistent pigment darkening as means of measuring the ultraviolet A protection factor in vivo: a comparative study. *Br. J. Dermatol.* 164, 1356-1361 (2011).

204. Moyal, D., Wichrowski, K. and Tricaud, C. In vivo persistent pigment darkening method: a demonstration of the reproducibility of the UVA protection factors results at several testing laboratories. *Photodermatol. Photoimmunol. Photomed.* 22, 124-128 (2006).
205. Japan Cosmetic Industry Association (JCIA). Technical Bulletin. Measurment standards for UVA protection efficacy (1996).
206. ISO 24442:2011. Cosmetics - Sun protection test methods - In vivo determination of sun-screen UVA protection. Available at: http://www.iso.org/iso/catalogue_detail.htm?csnumber=46521, accessed 13 September 2014.
207. Diffey, B.L. A method for broad spectrum classification of sunscreens. *Int. J. Cosmet. Sci.* 16, 47-52 (1994).
208. Food and Drug Administration (FDA). Sunscreen drug products for over-the-counter human use; final monograph. Federal Register 76/117, 35620-35665, USA (2011). Available at: http://www.gpo.gov/fdsys/pkg/FR-2011-06-17/pdf/2011-14766.pdf, accessed 13 September 2014.
209. ISO 24443:2012. Determination of sunscreen UVA photoprotection in vitro. Available at: http://www.iso.org/iso/catalogue_detail?csnumber=46522, accessed 13 September 2014.
210. The European Cosmetic Toiletry and Perfumery Association (COLIPA). Method for the in vitro determination of UVA protection provided by sunscreen products (2007).
211. The European Cosmetic Toiletry and Perfumery Association (COLIPA). In vitro method for the determination of the UVA protection factor and "critical wavelength" values of sunscreen products (2011).
212. Moyal, D., Alard, V., Bertin, C. *et al.* The revised COLIPA in vitro UVA method. *Int. J. Cosmet. Sci.* 35, 35-40 (2013).
213. Australian/New Zealand Standard. Sunscreen products - Evaluation and classification. AS/NZ 2604:1998.
214. Australian/New Zealand Standard. Sunscreen products - Evaluation and classification. AS/NZ 2604:2012.
215. The European Cosmetic Toiletry and Perfumery Association (COLIPA). Guidelines for evaluating sun product water resistance (2005). Available at: https://www.cosmeticseurope.eu/publications-cosmetics-europe-association/guidelines.html?view=item&id=18, accessed 13 September 2014.
216. The European Cosmetic Toiletry and Perfumery Association (COLIPA). Method for the in vitro determination of photostability of UV filters in cosmetic products (2004).
217. Schrader, K. Die Sonnenschutzfaktorbestimmung Kritische Bewertung aus der Sicht eines Prüfinstitutes. *Bundesgesundheitsblatt Gesundheitsforschung Gesundheitsschutz*, 44, 457-462 (2001).

218. Stokes, R. and Diffey, B. In vitro assessment of sunscreen photostability: the effect of radiation source, sunscreen application thickness and substrate. *Int. J. Cosmetic Sci.* 21, 341-351 (1999).

219. Garoli, D., Pelizzo, M.G., Nicolosi, P., Peserico, A., Tonin, E. and Alaibac, M. Effectiveness of different substrate materials for in vitro sunscreen tests. *J. Dermatol. Sci.* 56, 89-98 (2009).

220. Crovara Pescia, A., Astolfi, P., Puglia, C., Bonina, F., Perrotta, R., Herzog, B. and Damiani, E. On the assessment of photostability of sunscreens exposed to UVA irradiation: from glass plates to pig/human skin, which is best? Int. J. Pharm. 427, 217-223 (2012).

221. Shaath, N.A. Global developments in sun care ingredients. *Cosmetics & Toiletries*, 121, 57 (2006).

222. Dransfield, G.P. Inorganic Sunscreens. *Radiat. Prot. Dosim.* 91, 271-273 (2000).

223. German Cosmetics Ordinance of 7th October 1997 (Federal Gazette - BDBl. I. p.2410), last amended on 16th July 2014 (BGBl. I. p.1054). Available at: http://www.gesetze-im-internet.de/bundesrecht/kosmetikv_2014/gesamt.pdf, accessed 13 September 2014.

224. Scientific Committee on Consumer Safety (SCCS). Opinion on zinc oxide (nano form); SCCS/1489/12. Adopted at the 16th plenary meeting of 18 September 2012. Available at: http://ec.europa.eu/health/scientific_committees/consumer_safety/docs/sccs_o_103.pdf, accessed 13 September 2014.

225. Scientific Committee on Consumer Safety (SCCS). Addendum to the opinion SCCS/1489/12 on zinc oxide (nano form); SCCS/1518/13. Adopted by written procedure on 23 July 2013. Available at: http://ec.europa.eu/health/scientific_committees/consumer_safety/docs/sccs_o_137.pdf, accessed 13 September 2014.

226. Nohynek, G.J., Dufour, E.K. and Roberts, M.S. Nanotechnology, cosmetics and the skin: is there a health risk? *Skin Pharmacol. Physiol.* 21, 136-149 (2008).

227. Scientific Committee on Consumer Safety (SCCS). Opinion on titanium dioxide (nano form); SCCS/1516/13. Adopted by written procedure on 22 July 2013. Available at: http://ec.europa.eu/health/scientific_committees/consumer_safety/docs/sccs_o_136.pdf, accessed 13 September 2014.

228. Nohynek, G.J., Lademann, J., Ribaud, C. and Roberts, M.S. Grey goo on the skin? Nanotechnology, cosmetic and sunscreen safety. *Crit. Rev. Toxicol.* 37, 251-277 (2007).

229. Newman, M.D., Stotland, M. and Ellis, J.I. The safety of nanosized particles in titanium dioxide- and zinc oxide-based sunscreens. *J. Am. Acad. Dermatol.* 61, 685-692 (2009).

230. Smijs, T.G. and Pavel, S. Titanium dioxide and zinc oxide nanoparticles in sunscreens: focus on their safety and effectiveness. *Nanotechnol. Sci. Appl.* 4, 95-112 (2011).

231. Gilbert, E., Pirot, F., Bertholle, V., Roussel, L., Falson, F. and Padois, K. Commonly used UV filter toxicity on biological functions: review of last decade studies. *Int. J. Cosmet. Sci.* 35, 208-219 (2013).

232. Shukla, R.K., Sharma, V., Pandey, A.K., Singh, S., Sultana, S. and Dhawan, A. ROS-mediated genotoxicity induced by titanium dioxide nanoparticles in human epidermal cells. *Toxicol. In Vitro* 25, 231-241 (2011).

233. Buchalska, M., Kras, G., Oszajca, M., Łasocha, W. and Macyk, W. Singlet oxygen generation in the presence of titanium dioxide materials used as sunscreens in suntan lotions. *J. Photochem. Photobiol. A* 213, 158-163 (2010).

234. Sharma, V., Shukla, R.K., Saxena, N., Parmar, D., Das, M. and Dhawan, A. DNA damaging potential of zinc oxide nanoparticles in human epidermal cells. *Toxicol. Lett.* 185, 211-218 (2009).

235. Wang, C.C., Wang, S., Xia, Q., He, W., Yin, J.J., Fu, P.P. and Li, J.H. Phototoxicity of zinc oxide nanoparticles in HaCaT keratinocytes-generation of oxidative DNA damage during UVA and visible light irradiation. *J. Nanosci. Nanotechnol.* 13, 3880-3888 (2013).

236. Pan, Z., Lee, W., Slutsky, L., Clark, R.A., Pernodet, N. and Rafailovich, M.H. Adverse effects of titanium dioxide nanoparticles on human dermal fibroblasts and how to protect cells. *Small* 5, 511-520 (2009).

237. Jeng, H.A. and Swanson, J. Toxicity of metal oxide nanoparticles in mammalian cells. *J. Environ. Sci. Health A Tox. Hazard Subst. Environ. Eng.* 41, 2699-2711 (2006).

238. Tiano, L., Armeni, T., Venditti, E., Barucca, G., Mincarelli, L. and Damiani, E. Modified TiO(2) particles differentially affect human skin fibroblasts exposed to UVA light. *Free Radic. Biol. Med.* 49, 408-415 (2010).

239. Sayes, C.M., Wahi, R., Kurian, P.A. *et al.* Correlating nanoscale titania structure with toxicity: a cytotoxicity and inflammatory response study with human dermal fibroblasts and human lung epithelial cells. *Toxicol. Sci.* 92, 174-85 (2006).

240. Xue, C., Wu, J., Lan, F., Liu, W., Yang, X., Zeng, F. and Xu, H. Nano titanium dioxide induces the generation of ROS and potential damage in HaCaT cells under UVA irradiation. *J. Nanosci. Nanotechnol.* 10, 8500-8507 (2010).

241. Jaroenworaluck, A., Sunsaneeyametha, W., Kosachan, N. and Stevens, R. Characteristics of silica-coated TiO2 and its UV absorption for sunscreen cosmetic applications. *Surf. Interface Anal.* 38, 473-477 (2006).

242. Serpone, N., Salinaro, A., Horikoshi, S. and Hidaka, H. Beneficial effects of photo-inactive titanium dioxide specimens on plasmid DNA, human cells and yeast cells exposed to UVA/UVB simulated sunlight. *J. Photochem. Photobiol. A* 179, 200-212 (2006).

243. Siddiquey, I.A., Ukaji, E., Furusawa, T., Sato, M. and Suzuki, N. The effects of organic surface treatment by methacryloxypropyltrimethoxysilane on the photostability of TiO2. *Mater. Chem. Phys.* 105, 162-168 (2007).

244. Lademann, J., Weigmann, H., Schafer, H., Muller, G. and Sterry, W. Investigation of the stability of coated titanium microparticles used in sunscreens. *Skin Pharmacol. Appl. Skin Physiol.* 13, 258-264 (2000).

245. Senzui, M., Tamura, T., Miura, K., Ikarashi, Y., Watanabe, Y. and Fujii, M. Study on penetration of titanium dioxide (TiO(2)) nanoparticles into intact and damaged skin in vitro. *J. Toxicol. Sci.* 35, 107-113 (2010).

246. Zvyagin, A.V., Zhao, X., Gierden, A., Sanchez, W., Ross, J.A. and Roberts,M.S. Imaging of zinc oxide nanoparticle penetration in human skin in vitro and in vivo. *J. Biomed. Opt.* 13, 064031 (2008).

247. Lademann, J., Weigmann, H., Rickmeyer, C., Barthelmes, H., Schaefer, H., Mueller, G. and Sterry, W. Penetration of titanium dioxide microparticles in a sunscreen formulation into the horny layer and the follicular orifice. *Skin Pharmacol. Appl. Skin Physiol.* 12, 247-256 (1999).

248. Mavon, A., Miquel, C., Lejeune, O., Payre, B. and Moretto, P. In vitro percutaneous absorption and in vivo stratum corneum distribution of an organic and a mineral sunscreen. *Skin Pharmacol. Physiol.* 20, 10-20 (2007).

249. Cevc, G. and Vierl, U. Nanotechnology and the transdermal route: A state of the art review and critical appraisal. *J. Control Release* 141, 277-299 (2010).

250. Williams, A.C. and Barry, B.W. Penetration enhancers. *Adv. Drug Deliv. Rev.* 56, 603-618 (2004).

251. Kezic, S. and Nielsen, J.B. Absorption of chemicals through compromised skin. *Int. Arch. Occup. Environ. Health* 82, 677-688 (2009).

252. Jiang, S.J., Chu, A.W., Lu, Z.F., Pan, M.H., Che, D.F. and Zhou, X.J. Ultraviolet B-induced alterations of the skin barrier and epidermal calcium gradient. *Exp. Dermatol.* 16, 985-992 (2007).

253. Filipe, P., Silva, J.N., Silva, R. *et al.* Stratum corneum is an effective barrier to TiO2 and ZnO nanoparticle percutaneous absorption. *Skin Pharmacol. Physiol.* 22, 266-275 (2009).

254. Adachi, K., Yamada, N., Yoshida, Y. and Yamamoto, O. Subchronic exposure of titanium dioxide nanoparticles to hairless rat skin. *Exp. Dermatol.* 22, 278-283 (2013).

255. Sadrieh, N., Wokovich, A.M., Gopee, N.V. *et al.* Lack of significant dermal penetration of titanium dioxide from sunscreen formulations containing nano- and submicron-size TiO2 particles. *Toxicol. Sci.* 115, 156-166 (2010).

256. Gontier, E., Ynsa, M.D., Biro, T. *et al.* Is there penetration of titania nanoparticles in sunscreens through skin? A comparative electron and ion microscopy study. *Nanotoxicol.* 2, 218-231 (2008).

257. Monteiro-Riviere, N.A., Wiench, K., Landsiedel, R., Schulte, S., Inman, A.O. and Riviere, J.E. Safety evaluation of sunscreen formulations containing titanium dioxide and zinc oxide nanoparticles in UVB sunburned skin: an in vitro and in vivo study. *Toxicol. Sci.* 123, 264-280 (2011).

258. Lin, L.L., Grice, J.E., Butler, M.K. *et al.* Time-correlated single photon counting for simultaneous monitoring of zinc oxide nanoparticles and NAD(P)H in intact and barrier-disrupted volunteer skin. *Pharm. Res.* 28, 2920-2930 (2011).

259. Miquel-Jeanjean, C., Crepel, F., Raufast, V., Payre, B., Datas, L., Bessou-Touya, S. and Duplan, H. Penetration study of formulated nanosized titanium dioxide in models of damaged and sun-irradiated skins. *Photochem. Photobiol.* 88, 1513-1521 (2012).

260. Samontha, A., Shiowatana, J. and Siripinyanond, A. Particle size characterization of titanium dioxide in sunscreen products using sedimentation field-flow fractionation-inductively coupled plasma-mass spectrometry. *Anal. Bioanal. Chem.* 399, 973-978 (2011).

261. Schulz, J., Hohenberg, H., Pflücker, F. *et al.* Distribution of sunscreens on skin. *Adv. Drug Deliv. Rev.* 54, 157-163 (2002).

262. French,R.A., Jacobson,A.R., Kim,B., Isley,S.L., Penn,R.L. and Baveye,P.C. Influence of ionic strength, pH, and cation valence on aggregation kinetics of titanium dioxide nanoparticles. *Environ. Sci. Technol.* 43, 1354-1359 (2009).

263. Baveye, P. and Laba, M. Aggregation and toxicology of titanium dioxide nanoparticles. *Environ. Health Perspect.* 116, 152-153 (2008).

264. Bens, G. Sunscreens. In *Sunlight, Vitamin D and Skin Cancer* (Reichrath, J., ed.), pp. 137-161. Springer-Verlag, Berlin (2008).

265. Schauder, S. Lichtkrank durch Lichtschutz. *Deutsches Ärzteblatt* 92, 2008-2009 (1995).

266. Bryden, A.M., Moseley, H., Ibbotson, S.H. *et al.* Photopatch testing of 1155 patients: results of the U.K. multicentre photopatch study group. *Br. J. Dermatol.* 155, 737-747 (2006).

267. Kerr, A.C., Ferguson, J., Haylett, A.K. *et al.* A european multicentre photopatch test study. *Br. J. Dermatol*. 166, 1002-1009 (2012).

268. Mturi, G.J. and Martincigh, B.S. Photostability of the sunscreening agent 4- tert-butyl-4′-methoxydibenzoylmethane (avobenzone) in solvents of different polarity and proticity. *Photochem. Photobiol. A* 200, 410-420 (2008).

269. Sayre, R.M., Dowdy, J.C., Gerwig, A.J., Shields, W.J. and Lloyd, R.V. Unexpected photolysis of the sunscreen octinoxate in the presence of the sunscreen avobenzone. *Photochem. Photobiol.* 81, 452-456 (2005).

270. Karlsson, I., Hillerström, L., Stenfeldt, A.L., Mårtensson, J. and Börje, A. Photodegradation of dibenzoylmethanes: potential cause of photocontact allergy to sunscreens. *Chem. Res. Toxicol*. 22, 1881-1892 (2009).

271. Herzog, B., Wehrle, M. and Quass, K. (2009) Photostability of UV absorber systems in sunscreens. *Photochem. Photobiol.* 85, 869-878 (2009).

272. Lhiaubet-Vallet, V., Marin, M., Jimenez, O., Gorchs, O., Trullas, C. and Miranda, M.A. Filter-filter interactions. Photostabilization, triplet quenching and reactivity with singlet oxygen. *Photochem. Photobiol. Sci.* 9, 552-558 (2010).

273. Scalia, S. and Mezzena, M. Incorporation in lipid microparticles of the UVA filter, butyl methoxydibenzoylmethane combined with the UVB filter, octocrylene: effect on photostability. *AAPS PharmSciTech*. 10, 384-390 (2009).

274. Hanno, I., Anselmi, C. and Bouchemal, K. Polyamide nanocapsules and nano-emulsions containing Parsol® MCX and Parsol® 1789: in vitro release, ex vivo skin penetration and photo-stability studies. *Pharm. Res.* 29, 559-573 (2012).

275. Liu, Y., Ying, G., Shareef, A. and Kookana, R.S. Photostability of the UV filter benzophenone-3 and its effect on the photodegradation of benzotriazole in water. *Envir. Chem.* 8, 581-588 (2011).

276. Vanquerp, V., Rodriguez, C., Coiffard, C., Coiffard, L.J. and De Roeck-Holtzhauer, Y. High-performance liquid chromatographic method for the comparison of the photostability of five sunscreen agents. *J. Chromatogr. A* 832, 273-277 (1999).

277. Liao, C. and Kannan, K. Widespread Occurrence of Benzophenone-Type UV Light Filters in Personal Care Products from China and the United States: An Assessment of Human Exposure. *Environ. Sci. Technol.* 48, 4103-4109 (2014).

278. Pfaendner, R. How will additives shape the future of plastics? *Polym. Degrad. Stabil.* 91, 2249-2256 (2006).

279. Gustavsson Gonzalez, H., Farbrot, A.and Larkö, O. Percutaneous absorption of benzophenone-3, a common component of topical sunscreens. *Clin. Exp. Dermatol.* 27, 691-694 (2002).

280. Janjua, N.R., Kongshoj, B., Andersson, A.M. and Wulf H.C. Sunscreens in human plasma and urine after repeated whole-body topical application. *J. Eur. Acad. Dermatol. Venereol.* 22, 456-461 (2008).

281. Gonzalez, H., Farbrot, A., Larkö, O. and Wennberg, A.M. Percutaneous absorption of the sunscreen benzophenone-3 after repeated whole-body applications, with and without ultraviolet irradiation. *Br. J. Dermatol*. 154, 337-340 (2006).

282. Schlumpf, M., Cotton, B., Conscience, M., Haller, V., Steinmann, B. and Lichtensteiger, W. In vitro and in vivo estrogenicity of UV screens. Environ. *Health Perspect.* 109, 239-244 (2001).

283. Krause, M., Klit, A., Blomberg Jensen, M. *et al.* Sunscreens: are they beneficial for health? An overview of endocrine disrupting properties of UV-filters. *Int. J. Androl.* 35, 424-436 (2012).

284. Kunz, P.Y., Galicia, H.F. and Fent, K. Comparison of in vitro and in vivo estrogenic activity of UV filters in fish. *Toxicol. Sci.* 90, 349-361 (2006).

285. Pigatto, P.D., Guzzi, G., Schena, D. *et al.* Photopatch test: an Italian multicentre study from 2004-2006. *Contact Dermatitis* 59, 103-108 (2008).

286. Rodríguez, E., Valbuena, M., Rey, M. and Porras de Quintana, L. (2006) Causal agents of photoallergic contact dermatitis diagnosed in the national institute of dermatology of Colombia. *Photoderm. Photoimmunol. Photomed.* 22, 189-192 (2006).

287. Hughes, T.M. and Stone, N.M. Benzophenone 4: an emerging allergen in cosmetics and toiletries? *Contact Dermatitis* 56, 153-156 (2007).

288. Heurung, A.R., Raju, S.I. and Warshaw, E.M. Benzophenones. *Dermatitis* 25, 3-10 (2014).

289. Mackie, B.S. and Mackie, L.E. The PABA story. *Australas. J. Dermatol.* 40, 51-53 (1999).

290. Waters, A.J., Sandhu, D.R., Lowe, G. and Ferguson, J. Photocontact allergy to PABA in sunscreens: the need for continued vigilance. *Contact Dermatitis* 60, 172-173 (2009).

291. Greenspoon, J., Ahluwalia, R., Juma, N. and Rosen, C.F. Allergic and photoallergic contact dermatitis: a 10-year experience. *Dermatitis* 24, 29-32 (2013).

292. Avenel-Audran, M. Sunscreen products: finding the allergen... *Eur. J. Dermatol.* 20, 161-166 (2010).

293. Wong, T. and Orton, D. Sunscreen allergy and its investigation. *Clin. Dermatol.* 29, 306-310 (2011).

294. Jiménez-Díaz, I, Molina-Molina, J.M., Zafra-Gómez, A. *et al.* Simultaneous determination of the UV-filters benzyl salicylate, phenyl salicylate, octyl salicylate, homosalate, 3-(4-methylbenzylidene) camphor and 3-benzylidene camphor in human placental tissue by LC-MS/MS. Assessment of their in vitro endocrine activity. *J. Chromatogr. B Analyt. Technol. Biomed. Life Sci.* 936, 80-87 (2013).

295. Morohoshi, K., Yamamoto, H., Kamata, R, Shiraishi, F., Koda, T. and Morita, M. Estrogenic activity of 37 components of commercial sunscreen lotions evaluated by in vitro assays. *Toxicol. In Vitro* 19, 457-469 (2005).

296. Chatelain, E., Gabard, B. and Surber C. Skin penetration and sun protection factor of five UV filters: effect of the vehicle. *Skin Pharmacol. Appl. Skin Physiol.* 16, 28-35 (2003).

297. Deflandre, A and Lang, G. Photostability assessment of sunscreens. Benzylidene camphor and dibenzoylmethane derivatives. *Int. J. Cosmet. Sci.* 10, 53-62 (1988).

298. Schauder, S., Schrader, A. and Ippen, H. Göttinger Liste 1994 –Sonnenschutzkosmetik in Deutschland, 3rd edition, pp. 31-41. Blackwell Wissenschafts-Verlag, Berlin (1994).

299. Schlumpf, M., Kypke, K., Wittassek, M. *et al.* Exposure patterns of UV filters, fragrances, parabens, phthalates, organochlor pesticides, PBDEs, and PCBs in human milk: correlation of UV filters with use of cosmetics. *Chemosphere* 81, 1171-1183 (2010).

300. Séite, S., Moyal, D., Richard, S., de Rigal, J., Lévêque, J.L., Hourseau, C. and Fourtanier, A. Mexoryl SX: a broad absorption UVA filter protects human skin from the effects of repeated suberythemal doses of UVA. *J. Photochem. Photobiol. B* 44, 69-76 (1998).

301. Fourtanier, A., Moyal, D. and Seité, S. Sunscreens containing the broad-spectrum UVA absorber, Mexoryl SX, prevent the cutaneous detrimental effects of UV exposure: a review of clinical study results. *Photodermatol. Photoimmunol. Photomed.* 24, 164-174 (2008).

302. Moyal, D. Prevention of ultraviolet-induced skin pigmentation. *Photodermatol. Photoimmunol. Photomed.* 20, 243-247 (2004).

303. Benech-Kieffer, F., Meuling, W.J., Leclerc, C., Roza, L., Leclaire, J. and Nohynek, G. Percutaneous absorption of Mexoryl SX in human volunteers: comparison with in vitro data. *Skin Pharmacol. Appl. Skin Physiol.* 16, 343-355 (2003).

304. Pattanaargson, S. and Limphong, P. Stability of octyl methoxycinnamate and identification of its photo-degradation product. *Int. J. Cosmet. Sci.* 23, 153-160 (2001).

305. MacManus-Spencer, L.A., Tse, M.L., Klein, J.L. and Kracunas, A.E. Aqueous photolysis of the organic ultraviolet filter chemical octyl methoxycinnamate. *Environ. Sci. Technol.* 45, 3931-3937 (2011).

306. Trotta, V., Goios, F., Monteiro, H., Almeida, I.F. and Scalia, S. Influence of lipid microparticle encapsulation on in vitro efficacy, photostability and water resistance of the sunscreen agents, octyl methoxycinnamate and butyl methoxydibenzoylmethane. *Drug. Dev. Ind. Pharm.* 40, 1233-1239 (2014).

307. Perugini, P., Simeoni, S., Scalia, S., Genta, I., Modena, T., Conti, B.and Pavanetto, F. Effect of nanoparticle encapsulation on the photostability of the sunscreen agent, 2-ethylhexyl-p-methoxycinnamate. *Int. J. Pharm.* 246, 37-45 (2002).

308. Axelstad, M., Boberg, J., Hougaard, K.S. *et al.* Effects of pre- and postnatal exposure to the UV-filter octyl methoxycinnamate (OMC) on the reproductive, auditory and neurological development of rat offspring. *Toxicol. Appl. Pharmacol.* 250, 278-290 (2011).

309. Janjua, N.R., Mogensen, B., Andersson, A.M., Petersen, J.H., Henriksen, M., Skakkebaek, N.E. and Wulf, H.C. Systemic absorption of the sunscreens benzophenone-3, octyl-methoxycinnamate, and 3-(4-methyl-benzylidene) camphor after whole-body topical application and reproductive hormone levels in humans. *J. Invest. Dermatol.* 123, 57-61 (2004).

310. Gaspar, L.R. and Maia Campos, P.M. Evaluation of the photostability of different UV filter combinations in a sunscreen. *Int. J. Pharm.* 307, 123-128 (2006).

311. Avenel-Audran, M., Dutartre, H., Goossens, A. *et al.* Octocrylene, an emerging photoallergen. *Arch. Dermatol.* 146, 753-757 (2010).

312. Karlsson, I., Vanden Broecke, K., Mårtensson, J., Goossens, A. and Börje A. (2011) Clinical and experimental studies of octocrylene's allergenic potency. *Contact Dermatitis* 64, 343-352.

313. Travassos, A.R., Claes, L., Boey, L., Drieghe, J. and Goossens A. (2011) Non-fragrance allergens in specific cosmetic products. *Contact Dermatitis* 65, 276-285.

314. Gonçalo, M., Ferguson, J., Bonevalle, A. *et al.* (2013) Photopatch testing: recommendations for a European photopatch test baseline series. *Contact Dermatitis* 68, 239-243.

315. Chatelain, E. and Gabard, B. Photostabilization of butyl methoxydibenzoylmethane (Avobenzone) and ethylhexyl methoxycinnamate by bis-ethylhexyloxyphenol methoxyphenyl triazine (Tinosorb S), a new UV broadband filter. *Photochem. Photobiol.* 74, 401-406 (2011).

316. L'alloret, F., Candau, D., Seité, S. *et al.* New combination of ultraviolet absorbers in an oily emollient increases sunscreen efficacy and photostability. *Dermatol. Ther. (Heidelb.)* 2, 4 (2012).

317. Couteau, C., Chauvet, C., Paparis, E. and Coiffard, L. UV filters, ingredients with a recognized anti-inflammatory effect. *PLOS One* 7, e46187 (2012).

318. Durand, L., Habran, N., Henschel, V. and Amighi, K. In vitro evaluation of the cutaneous penetration of sprayable sunscreen emulsions with high concentrations of UV filters. *Int. J. Cosmet. Sci.* 31, 279-292 (2009).

319. Shaw, T., Simpson, B., Wilson, B., Oostman, H., Rainey, D. and Storrs F. True photoallergy to sunscreens is rare despite popular belief. *Dermatitis* 21, 185-198 (2010).

320. Moyal, D. Prevention of ultraviolet-induced skin pigmentation. *Photodermatol. Photoimmunol. Photomed.* 20, 243-247 (2004).

321. Herzog, B., Mongiat, S., Deshayes, C., Neuhaus, M., Sommer, K. and Mantler, A. In vivo and in vitro assessment of UVA protection by sunscreen formulations containing either butyl methoxy dibenzoyl methane, methylene bis-benzotriazolyl tetramethylbutylphenol, or microfine ZnO. *Int. J. Cosmet. Sci.* 24, 170-185 (2002).

322. Hojerová, J., Medovcíková, A. and Mikula, M. Photoprotective efficacy and photostability of fifteen sunscreen products having the same label SPF subjected to natural sunlight. *Int. J. Pharm.* 408, 27-38 (2011).

323. Cardoso, J., Canelas, M. Gonçalo, M. and Figueiredo, A. Photopatch testing with an extended series of photoallergens: a 5-year study. *Contact Dermatitis* 60, 314-319 (2009).

324. Orton, D.I and Willis, C.M. Contact Dermatitis. In *Allergy and Allergic Diseases* (Kay, A.B., Kaplan, A.P., Bousquet, J. and Holt, P.G., eds.), pp. 1831-1852. John Wiley & Sons, Chichester, UK (2008).

325. Lepoittevin, J.P. Metabolism versus chemical transformation or pro- versus prehaptens? *Contact Dermatitis* 54, 73-74 (2006).

326. Karlberg, A.T., Börje, A., Duus Johansen, J. *et al.* Activation of non-sensitizing or low-sensitizing fragrance substances into potent sensitizers - prehaptens and prohaptens. *Contact Dermatitis* 69, 323-334 (2013).

327. Divkovic, M., Peasel, C.K., Gerberick, G.F. and Basketter, D.A. Hapten–protein binding: from theory to practical application in the in vitro prediction of skin sensitization. *Contact Dermatitis* 53, 189–200 (2005).

328. Nishibu, A., Ward, B.R., Boes, M. and Takashima, A. Roles for IL-1 and TNF-alpha in dynamic behavioral responses of Langerhans cells to topical hapten application. *J. Dermatol. Sci.* 45, 23-30 (2007).

329. Natsch A. The Nrf2-Keap1-ARE toxicity pathway as a cellular sensor for skin sensitizers--functional relevance and a hypothesis on innate reactions to skin sensitizers. *Toxicol. Sci.* 113, 284-292 (2010).

330. Tkachev, V.O., Menshchikova, E.B. and Zenkov, N.K. Mechanism of the Nrf2/Keap1/ARE signaling system. *Biochemistry (Mosc)* 76, 407-422 (2011).

331. Kwak, M.K., Wakabayashi, N. and Kensler, T.W. Chemoprevention through the Keap1-Nrf2 signaling pathway by phase 2 enzyme inducers. *Mutat. Res.* 555, 133–148 (2004).

332. Dinkova-Kostova, A.T., Holtzclaw, W.D., Cole, R.N. *et al.* Direct evidence that sulfhydryl groups of Keap1 are the sensors regulating induction of phase 2 enzymes that protect against carcinogens and oxidants. *Proc. Natl Acad. Sci*. USA 99, 11908–11913 (2002).

333. Migdal, C., Botton, J., El Ali, Z. *et al.* Reactivity of chemical sensitizers toward amino acids in cellulo plays a role in the activation of the Nrf2-ARE pathway in human monocyte dendritic cells and the THP-1 cell line. *Toxicol. Sci.* 133, 259-274 (2013).

334. Hennen, J., Aeby, P., Goebel, C., Schettgen, T., Oberli, A., Kalmes, M. and Blömeke, B. Cross talk between keratinocytes and dendritic cells: impact on the prediction of sensitization. *Toxicol. Sci.* 123, 501-510 (2011).

335. Kerr, A. and Ferguson, J. Photoallergic contact dermatitis. *Photodermatol. Photoimmunol. Photomed.* 26, 56-65 (2010).

336. Karlberg, A.T., Bergström, M.A., Börje, A., Luthman, K. and Nilsson, J.L. Allergic contact dermatitis--formation, structural requirements, and reactivity of skin sensitizers. *Chem. Res. Toxicol.* 21, 53-69 (2008).

337. Basketter, D.A. Skin immunology and sensitization. In *Principles and Practice of Skin Toxicology* (Chilcott, R. and Price, S., eds.), pp. 151-168. John Wiley & Sons, Chichester (2008).

338. Thyssen, J.P., Linneberg, A., Menné, T. and Johansen, J.D. The epidemiology of contact allergy in the general population--prevalence and main findings. *Contact Dermatitis.* 57, 287-299 (2007).

339. Bieber, T. Atopic dermatitis. *N. Engl. J. Med.* 358, 1483-1494 (2008).

340. The European Parliament and the Council of the European Union. Regulation (EC) No 1907/2006 of the European Parliament and of the Council of 18 December 2006 concerning the Registration, Evaluation, Authorisation and Restriction of Chemicals (REACH), establishing a European Chemicals Agency, amending Directive 1999/45/EC and repealing Council Regulation (EEC) No 793/93 and Commission Regulation (EC) No 1488/94 as well as Council Directive 76/769/EEC and Commission Directives 91/155/EEC, 93/67/EEC, 93/105/EC and 2000/21/EC. *Off. J. Eur. Union L* 136, 3-17. Available at: http://eur-lex.europa.eu/legal-content/EN/TXT/PDF/?uri=CELEX:32006R1907&qid=1410618098058&from=EN, accessed 13 September 2014.
341. OECD Guidelines for the Testing of Chemicals, Section 4, Test No. 406: Skin Sensitisation, adopted 17th July 1992. Available at: http://www.oecd-ilibrary.org/environment/test-no-406-skin-sensitisation_9789264070660-en, accessed 13 September 2014.
342. OECD Guidelines for the Testing of Chemicals, Section 4, Test No. 442A: Skin Sensitization - Local Lymph Node Assay, adopted 23th July 2010. Available at: http://www.oecd-ilibrary.org/environment/test-no-442a-skin-sensitization_9789264090972-en, accessed 13 September 2014.
343. OECD Guidelines for the Testing of Chemicals, Section 4, Test No. 442B: Skin Sensitization - Local Lymph Node Assay: BrdU-ELISA, adopted 23th July 2010. Available at: http://www.oecd-ilibrary.org/environment/test-no-442b-skin-sensitization_9789264090996-en, accessed 13 September 2014.
344. OECD Guidelines for the Testing of Chemicals, Section 4, Test No. 429: Skin Sensitisation - Local Lymph Node Assay, adopted 23th July 2010. Available at: http://www.oecd-ilibrary.org/environment/test-no-429-skin-sensitisation_9789264071100-en, accessed 13 September 2014.
345. Kimber, I. and Basketter, D.A. The murine local lymph node assay: a commentary on collaborative trials and new directions. *Food Chem. Toxicol.* 30, 165-169 (1992).
346. Rovida, C., Ryan, C., Cinelli, S., Basketter, D., Dearman, R. and Kimber, I. The local lymph node assay (LLNA). *Curr. Protoc. Toxicol.* Chapter 20, Unit 20.7 (2012).
347. Buehler, E.V. Delayed contact hypersensitivity in the guinea pig. *Arch. Dermatol.* 91, 171-177 (1965).
348. Magnusson, B. and Kligman, A.M. The identification of contact aller-gens by animal assay. The guinea pig maximization test. *J. Invest. Dermatol.* 52, 268-276 (1969).

349. Regulation (EC) No 440/2008 of 30 May 2008 laying down test methods pursuant to Regulation (EC) No 1907/2006 of the European Parliament and of the Council on the Registration, Evaluation, Authorisation and Restriction of Chemicals (REACH). Official Journal of the European Union L 142, 1-739. Available at: http://eur-lex.europa.eu/LexUriServ/LexUriServ.do?uri=OJ:L:2008:142:0001:0739:en:PDF, accessed 13 September 2014.
350. Weltzien, H., Corsini, E., Gibbs, S. *et al.* Safe cosmetics without animal testing? Contributions of the EU Project Sens-it-iv. *J. für Verbrauch. Lebensm.* 4, 41-48 (2009).
351. Luanpitpong, S. and Rojanasakul, Y. Transdermal Drug Delivery. In: *Basic Physical Pharmacy* (Ma, J.K.H. and Hadzija, B., eds.), pp. 365-382. Jones & Bartlett Learning, Burlington, (2012).
352. Bartosova, L and Bajgar, J. Transdermal drug delivery in vitro using diffusion cells. *Curr. Med. Chem.* 19, 4671-4677 (2012).
353. Vandebriel, R.J.and van Loveren, H. Non-animal sensitization testing: state-of-the-art. *Crit. Rev. Toxicol.* 40, 389-404 (2010).
354. Adler, S., Basketter, D., Creton, S. *et al.* Alternative (non-animal) methods for cosmetics testing: current status and future prospects-2010. *Arch. Toxicol.* 85, 367-485 (2011).
355. Uchino, T., Takezawa, T. and Ikarashi, Y. Reconstruction of three-dimensional human skin model composed of dendritic cells, keratinocytes and fibroblasts utilizing a handy scaffold of collagen vitrigel membrane. *Toxicol. In Vitro* 23, 333-337 (2009).
356. OECD Guidelines for the Testing of Chemicals, Section 4, Test No. 431: In vitro skin corrosion: reconstructed human epidermis (RHE) test method, adopted 26th July 2013. Available at: http://www.oecd-ilibrary.org/environment/test-no-431-in-vitro-skin-corrosion-human-skin-model-test_9789264071148-en, accessed 13 September 2014.
357. OECD Guidelines for the Testing of Chemicals, Section 4, Test No. 439: In Vitro Skin Irritation - Reconstructed Human Epidermis Test Method, adopted 26th July 2013. Available at: http://www.oecd-ilibrary.org/environment/test-no-439-in-vitro-skin-irritation-reconstructed-human-epidermis-test-method_9789264203884-en, accessed 13 September 2014.
358. Schreiber, S., Mahmoud, A., Vuia, A. *et al.* Reconstructed epidermis versus human and animal skin in skin absorption studies. *Toxicol. In Vitro* 19, 813-822 (2005).
359. Schäfer-Korting, M., Bock, U., Diembeck, W. *et al.* The use of reconstructed human epidermis for skin absorption testing: Results of the validation study. *Altern. Lab. Anim.* 36, 161-187 (2008).
360. Hikima, T., Kaneda, N., Matsuo, K. and Tojo, K. Prediction of percutaneous absorption in human using three-dimensional human cultured epidermis LabCyte EPI-MODEL. *Biol. Pharm. Bull.* 35, 362-368 (2012).

361. Van Gele, M., Geusens, B., Brochez, L., Speeckaert, R. and Lambert, J. Three-dimensional skin models as tools for transdermal drug delivery: challenges and limitations. *Expert Opin. Drug Deliv.* 8, 705-720 (2011).

362. Küchler, S., Strüver, K. and Friess, W. Reconstructed skin models as emerging tools for drug absorption studies. *Expert Opin. Drug Metab. Toxicol.* 9, 1255-1263 (2013).

363. Roberts, D.W. and Aptula, A.O. Determinants of skin sensitisation potential. *J. Appl. Toxicol.* 28, 377-387 (2008).

364. Chipinda, I., Hettick, J.M. and Siegel, P.D. Haptenation: chemical reactivity and protein binding. *J. Allergy (Cairo)* 2011, 839682 (2011).

365. Dimitrov, S.D., Low, L.K., Patlewicz, G.Y. *et al.* Skin sensitization: modeling based on skin metabolism simulation and formation of protein conjugates. *Int. J. Toxicol.* 24, 189-204 (2005).

366. Maxwell, G., MacKay, C., Cubberley, R. *et al.* Applying the skin sensitisation adverse outcome pathway (AOP) to quantitative risk assessment. *Toxicol. In Vitro*. 28, 8-12(2014).

367. OECD Environment, Health and Safety Publications - Series on Testing and Assessment, No. 168: The adverse outcome pathway for skin sensitization initiated by covalent binding to proteins, Part 1: Scientific Evidence, ENV/JM/MONO(2012)10/PART1, May 2012. Available at: http://www.oecd.org/officialdocuments/publicdisplaydocumentpdf/?cote=env/jm/mono%282012%2910/part1&doclanguage=en, accessed 13 September 2014.

368. Aptula, A.O. and Roberts, D.W. Mechanistic applicability domains for nonanimal-based prediction of toxicological end points: general principles and application to reactive toxicity. *Chem. Res. Toxicol.* 19, 1097-1105 (2006).

369. Enoch, S.J., Madden, J.C. and Cronin, M.T. Identification of mechanisms of toxic action for skin sensitisation using a SMARTS pattern based approach. *SAR QSAR Environ. Res.* 19, 555-578 (2008).

370. Fedorowicz, A., Singh, H., Soderholm, S. and Demchuk, E. Structure-activity models for contact sensitization. *Chem. Res. Toxicol.* 18, 954-969 (2005).

371. Teubner, W., Mehling, A., Schuster, P.X. *et al.* Computer models versus reality: how well do in silico models currently predict the sensitization potential of a substance. *Regul. Toxicol. Pharmacol.* 67, 468-485 (2013).

372. Gerberick, G.F., Vassallo, J.D., Bailey, R.E., Chaney, J.G., Morrall, S.W. and Lepoittevin, J.P. Development of a peptide reactivity assay for screening contact allergens. *Toxicol. Sci.* 81, 332-343 (2004).

373. Gerberick, G.F., Vassallo, J.D., Foertsch, L.M., Price, B.B., Chaney, J.G. and Lepoittevin, J.P. Quantification of chemical peptide reactivity for screening contact allergens: a classification tree model approach. *Toxicol. Sci*. 97, 417-427 (2007).

374. Gerberick, G.F., Troutman, J.A., Foertsch, L.M. *et al.* Investigation of peptide reactivity of pro-hapten skin sensitizers using a peroxidase-peroxide oxidation system. *Toxicol. Sci*. 112, 164-174 (2009).

375. Chipinda, I., Ajibola, R.O., Morakinyo, M.K., Ruwona, T.B., Simoyi, R.H. and Siegel, P.D. Rapid and simple kinetics screening assay for electrophilic dermal sensitizers using nitrobenzenethiol. *Chem. Res. Toxicol.* 23, 918-925 (2010).

376. Cho, S.A., Jeong, Y.H., Kim, J.H. *et al.* Method for detecting the reactivity of chemicals towards peptides as an alternative test method for assessing skin sensitization potential. *Toxicol. Lett.* 225, 185-191 (2014).

377. Troutman, J.A., Foertsch, L.M., Kern, P.S. *et al.* The incorporation of lysine into the peroxidase peptide reactivity assay for skin sensitization assessments. *Toxicol. Sci.* 122, 422-436 (2011).

378. Joint Research Centre (JRC) of the European Commission: EURL ECVAM recommendation on the Direct Peptide Reactivity Assay (DPRA) for Skin Sensitisation Testing, November 2013. Available at: http://ihcp.jrc.ec.europa.eu/our_labs/eurl-ecvam/eurl-ecvam-recommendations/files-dpra/EURL_ECVAM_Recommendation_DPRA_2013.pdf, accessed 13 September 2014.

379. Aleksic, M., Thain, E., Roger, D. *et al.* Reactivity profiling: covalent modification of single nucleophile peptides for skin sensitization risk assessment. *Toxicol. Sci.* 108, 401-411 (2009).

380. Natsch, A. and Gfeller, H. LC-MS-based characterization of the peptide reactivity of chemicals to improve the in vitro prediction of the skin sensitization potential. *Toxicol. Sci.* 106, 464-478 (2008).

381. Naik, S.M., Cannon, G., Burbach, G.J. *et al.* Human keratinocytes constitutively express interleukin-18 and secrete biologically active interleukin-18 after treatment with pro-inflammatory mediators and dinitrochlorobenzene. *J. Invest. Dermatol*. 113, 766-772 (1999).

382. Smith Pease, C.K., Basketter, D.A. and Patlewicz, G.Y. Contact allergy: the role of skin chemistry and metabolism. *Clin. Exp. Dermatol.* 28, 177-183 (2003).

383. Van Och, F.M., Van Loveren, H., Van Wolfswinkel, J.C., Machielsen, A.J. and Vandebriel, R.J. Assessment of potency of allergenic activity of low molecular weight compounds based on IL-1alpha and IL-18 production by a murine and human keratinocyte cell line. *Toxicology* 210, 95-109 (2005).

384. Corsini, E., Mitjans, M., Galbiati, V., Lucchi, L., Galli, C.L. and Marinovich, M. (2009) Use of IL-18 production in a human keratinocyte cell line to discriminate contact sensitizers from irritants and low molecular weight respiratory allergens. *Toxicol. In Vitro* 23, 789-796.

385. Galbiati, V. and Corsini, E. The NCTC 2544 IL-18 assay for the in vitro identification of contact allergens. *Curr. Protoc. Toxicol.* Chapter 20, Unit 20.8 (2012).

386. Galbiati, V., Martínez, V., Bianchi, S., Mitjans, M. and Corsini E. Establishment of an in vitro photoallergy test using NCTC2544 cells and IL-18 production. *Toxicol. In Vitro* 27, 103-110 (2013).

387. Gibbs, S., Corsini, E., Spiekstra, S.W. *et al.* An epidermal equivalent assay for identification and ranking potency of contact sensitizers. *Toxicol. Appl. Pharmacol.* 272, 529-541 (2013).

388. Teunis, M., Corsini, E., Smits, M. *et al.* Transfer of a two-tiered keratinocyte assay: IL-18 production by NCTC2544 to determine the skin sensitizing capacity and epidermal equivalent assay to determine sensitizer potency. *Toxicol. In Vitro* 27, 1135-1150 (2013).

389. Galbiati, V., Bianchi, S., Martínez, V., Mitjans, M. and Corsini E. NCTC 2544 and IL-18 production: a tool for the in vitro identification of photoallergens. *Toxicol. In Vitro* 28, 13-17 (2014).

390. Teissier, S., Tourneix, F., Del Bufalo, A., Gomes C., Groux, H. and Meunier, J.R. Evaluation of SENS-IS®, an Episkin® based model for Identifying Chemical Sensitizers. Poster presentation on the 51st annual meeting of the Society of Toxicology (SOT), San Francisco, March 11-15 (2012).

391. McKim, J.M.J., Keller III, D.J. and Gorski, J.R. A new in vitro method for identifying chemical sensitizers combining peptide binding with ARE/EpRE-mediated gene expression in human skin cells. *Cutan. Ocul. Toxicol.* 29, 171–192 (2010).

392. McKim, J.M., Keller, D.J. 3rd and Gorski, J.R. An in vitro method for detecting chemical sensitization using human reconstructed skin models and its applicability to cosmetic, pharmaceutical and medical device safety testing. *Cutan. Ocul. Toxicol.* 31, 292-305 (2012).

393. Natsch, A. and Emter, R. Skin sensitizers induce antioxidant response element dependent genes: application to the in vitro testing of the sensitization potential of chemicals. *Toxicol. Sci.* 102, 110-119 (2008).

394. Natsch, A. The Keratinosens Assay: A high-throughput screening assay to assess chemical skin sensitization. In *High-Throughput Screening Methods in Toxicity Testing* (Steinberg, P., ed.), 159-175. John Wiley & Sons, Chichester, UK (2013).

395. Bauch, C., Kolle, S.N., Ramirez, T. *et al.* Putting the parts together: Combining in vitro methods to test for skin sensitizing potentials. *Reg. Tox. Pharmacol.* 63, 489-504 (2012).

396. Emter, R., Ellis, G. and Natsch, A. Performance of a novel keratinocyte-based reporter cell line to screen skin sensitizers in vitro. *Toxicol. Appl. Pharmacol.* 245, 281-290 (2010).

397. Joint Research Centre (JRC) of the European Commission. JRC Scientific and Policy Reports: EURL ECVAM Recommendation on the KeratinoSens™ assay for skin sensitisation testing, February 2014. Available at: http://ihcp.jrc.ec.europa.eu/our_labs/eurl-ecvam/eurl-ecvam-recommendations/file-kerati/JRC_SPR_Keratinosens_Rec_17_02_2014.pdf, accessed 13 September 2014.

398. Ryan, C.A., Gerberick, G.F., Gildea, L.A. *et al.* Interactions of contact allergens with dendritic cells: opportunities and challenges for the development of novel approaches to hazard assessment. *Toxicol. Sci.* 88, 4-11 (2005).

399. Ryan, C.A., Kimber, I., Basketter, D.A., Pallardy, M., Gildea, L.A. and Gerberick, G.F. Dendritic cells and skin sensitization: biological roles and uses in hazard identification. *Toxicol. Appl. Pharmacol.* 221, 384-394 (2007).

400. Dos Santos, G.G., Reinders, J., Ouwehand, K,. Rustemeyer, T., Scheper, R.J. and Gibbs, S. Progress on the development of human in vitro dendritic cell based assays for assessment of the sensitizing potential of a compound. *Toxicol. Appl. Pharmacol.* 236, 372-382 (2009).

401. Ovigne, J.M., Martinozzi-Teissier, S., Verda, D., Abdou, D. Piroird, C., Ade, N. and Rousset, F. The MUSST for in vitro skin sensitization prediction: Applicability domains and complementary protocols to adapt to the physico-chemical diversity of chemicals. *Toxicol. Lett.* 180 (Suppl.) 216 (2008).

402. Python, F., Goebel, C. and Aeby, P. Assessment of the U937 cell line for the detection of contact allergens. *Toxicol. Appl. Pharmacol.* 220, 113-124 (2007).

403. Sakaguchi, H., Ashikaga, T., Miyazawa, M. *et al.* The relationship between CD86/CD54 expression and THP-1 cell viability in an in vitro skin sensitization test--human cell line activation test (h-CLAT). *Cell Biol. Toxicol.* 25, 109-126 (2009).

404. Ashikaga, T., Sakaguchi, H., Sono, S. *et al.* A comparative evaluation of in vitro skin sensitisation tests: the human cell-line activation test (h-CLAT) versus the local lymph node assay (LLNA). *Altern. Lab. Anim.* 38, 275-284 (2010).

405. Hooyberghs, J., Schoeters, E., Lambrechts, N., Nelissen, I., Witters, H., Schoeters, G. and Van Den Heuvel, R. A cell-based in vitro alternative to identify skin sensitizers by gene expression. *Toxicol. Appl. Pharmacol.* 231, 103-111 (2008).

406. Lambrechts, N., Vanheel, H., Nelissen, I. *et al.* Assessment of chemical skin-sensitizing potency by an in vitro assay based on human dendritic cells. *Toxicol. Sci.* 116, 122-129 (2010).

407. Johansson, H., Albrekt, A.S., Borrebaeck, C.A. and Lindstedt, M. The GARD assay for assessment of chemical skin sensitizers. *Toxicol. In Vitro* 27, 1163-1169 (2013).

408. Hitzler, M., Bergert, A., Luch, A. and Peiser, M. Evaluation of selected biomarkers for the detection of chemical sensitization in human skin: a comparative study applying THP-1, MUTZ-3 and primary dendritic cells in culture. *Toxicol. In Vitro* 27, 1659-1669 (2013).

409. Mitjans, M., Galbiati, V., Lucchi, L., Viviani, B., Marinovich, M., Galli, C.L. and Corsini, E. Use of IL-8 release and p38 MAPK activation in THP-1 cells to identify allergens and to assess their potency in vitro. *Toxicol. In Vitro* 24, 1803-1809 (2010).

410. Martínez, V., Galbiati, V., Corsini, E., Martín-Venegas, R., Vinardell, M.P. and Mitjans, M. Establishment of an in vitro photoassay using THP-1 cells and IL-8 to discriminate photoirritants from photoallergens. *Toxicol. In Vitro* 27, 1920-1927 (2013).

411. Guironnet, G., Dalbiez-Gauthier, C., Rousset, F., Schmitt, D. and Péguet-Navarro, J. In vitro human T cell sensitization to haptens by monocyte-derived dendritic cells. *Toxicol. In Vitro* 14, 517-522 (2000).

412. Rougier, N., Redziniak, G., Mougin, D., Schmitt, D. and Vincent, C. In vitro evaluation of the sensitization potential of weak contact allergens using Langerhans-like dendritic cells and autologous T cells. *Toxicology* 145, 73-82 (2000).

413. Peiser, M., Hitzler, M. and Luch, A. On the role of co-inhibitory molecules in dendritic cell: T helper cell coculture assays aimed to detect chemical-induced contact allergy. *EXS* 104, 115-135 (2014).

414. Vocanson, M., Cluzel-Tailhardat, M., Poyet, G. *et al.* Depletion of human peripheral blood lymphocytes in CD25+ cells allows for the sensitive in vitro screening of contact allergens. *J. Invest. Dermatol.* 128, 2119-2122 (2008).

415. Vocanson, M., Achachi, A., Mutez, V. *et al.* Human T cell priming assay: depletion of peripheral blood lymphocytes in CD25(+) cells improves the in vitro detection of weak allergen-specific T cells. *EXS* 104, 89-100 (2014).

416. Martin, S.F., Esser, P.R., Schmucker, S. *et al.* T-cell recognition of chemicals, protein allergens and drugs: towards the development of in vitro assays. *Cell Mol. Life Sci.* 67, 4171-4184 (2010).

417. Aeby, P., Ashikaga, T., Bessou-Touya, S. *et al.* Identifying and characterizing chemical skin sensitizers without animal testing: Colipa's research and method development program. *Toxicol. In Vitro* 24, 1465-1473 (2010).

418. Bauch, C., Kolle, S.N., Fabian, E. *et al.* Intralaboratory validation of four in vitro assays for the prediction of the skin sensitizing potential of chemicals. *Toxicol. In Vitro* 25, 1162-1168 (2011).

419. OpenStax College, Anatomy & Physiology. OpenStax College, 25 April 2013. http://cnx.org/content/col11496/latest/, accessed at 13 September 2014.

420. Langhals, H. and Fuchs, K. Sonnenstrahlung, Hautreaktionen und Sonnenschutz (Sun radition, skin reactions and sun protection). *Chem. unserer Zeit* 39, 98-112 (2004).

421. Slominski, A., Tobin, D.J., Shibahara, S. and Wortsman, J. Melanin pigmentation in mammalian skin and its hormonal regulation. *Physiol. Rev.* 84, 1155-1228 (2004).

422. Hennino, A., Vocanson, M., Chavagnac, C., Saint-Mezard, P., Dubois, B., Kaiserlian, D. and Nicolas, J.-F. Update on the pathophysiology with special emphasis on CD8 effector T cells and CD4 regulatory T cells. *An. Bras. Dermatol*. 80, 335-347 (2005).

Aim and structure of the work

Sunscreens play an important role in protecting the skin against harmful UV radiation. The efficacy and tolerability of sun protection products mainly depend on the stability and the protection ability of the included UV filters. The letter can not only be influenced by photodegradation processes but also by possible reactions of UV filters and their photoproducts with skin constituents, e.g. proteins.

Various previous studies have contributed to achieve a better understanding of the cellular and molecular mechanisms behind protein binding, especially in the context of skin sensitization. Accordingly, a large number of substances were tested for their sensitizing potential and some of the underlying reaction processes were identified [1-6].
However, although UV filters are the main topical photosensitizers [7-9], skin proteins as quantitatively significant reaction partners were previously hardly and not extensively considered in this context [10,11].

Therefore, the overall purpose of this thesis was it to gain more knowledge about the (photo) chemical processes behind UV filter-protein reactions, using various model systems and appropriate analytical tools to identify possible protein adducts and their influence on the UV-protective ability. As lysine residues are seen as typical reaction sites in the context of hapten binding [12-14], reactions of common UV filters with amine side chains of multiple reactants were the starting point of this research.

First, it was the aim to develop a rapid and simple screening tool to estimate the reactivity of common UV filter substances towards amino structures under the conditions of slightly heating or UV irradiation. As protein reactions play a central role in skin sensitization, the results of the screening may allow first conclusions about a possible allergic potential of the UV filters.

To identify the underlying chemical mechanisms, the objective of the second part of the work was to investigate the reactivity of UV filters towards the amino acid analogues ethanolamine and butylamine at different temperatures and under additional irradiation. Products formed under the influence of heat and/or UV irradiation should be identified by mass spectrometry (MS), fourier transform infrared spectroscopy (FTIR), and nuclear magnetic resonance spectroscopy (NMR). Changes of the respective UV filter spectra during the reactions could give first evidence of the influence of amine reactions on the protection ability of the UV filters.

The usage of further reaction partners with primary amino groups, e.g. Boc-protected lysine, lysine-containing peptides and more complex proteins like bovine serum albumin (BSA) should subsequently substantiate the initial results.

Using appropriate extraction and determination methods, e.g. high-performance liquid chromatography with diode array detection (HPLC-DAD) or matrix-assisted laser desorption/ionization time-of-flight mass spectrometry (MALDI-TOFMS), the binding amounts of the UV filters to the reactants

could be determined to compare the overall reactivity and therefore the sensitization potential of the used UV filters with the results of the initial screening.

In a next step, in order to reflect realistic application conditions, an elastic porcine gelatin layer may be used as appropriate skin model, using UV irradiation to initiate possible reactions between the UV filters and the protein. A valid extraction method or the usage of deuterium labeled UV-filter analogues seems to be promising to examine the actual binding amount of the UV filters to gelatin by HPLC-DAD or isotope-ratio mass spectrometry (IRMS) and may also be applicable for further skin models.

At last, attempts should be made to examine, to what extent the results of the model studies coincide with examinations on prepared fresh porcine skin using various commercial sunscreen and day care products with integrated UV protection. Differences in the recoveries of the UV filters from skin or glass plates may indicate the occurrence of skin-typical reactions (e.g. protein binding), which are currently not covered by existing *in-vitro* methods.

References

1. Breitbart, E.W., Greinert, R. and Volkmer, B. Effectiveness of information campaigns. *Prog. Biophys. Mol. Biol.* 92, 167-172 (2006).
2. Divkovic, M., Peasel, C.K., Gerberick, G.F. and Basketter, D.A. Hapten–protein binding: from theory to practical application in the in vitro prediction of skin sensitization. *Contact Dermatitis* 53, 189–200 (2005).
3. Chipinda, I., Hettick, J.M. and Siegel, P.D. Haptenation: chemical reactivity and protein binding. *J. Allergy (Cairo)* 2011, 839682 (2011).
4. Aleksic, M., Thain, E., Roger, D., Saib, O., Davies, M.., Li, J., Aptula, A. and Zazzeroni, R. Reactivity profiling: covalent modification of single nucleophile peptides for skin sensitization risk assessment. *Toxicol. Sci.* 108, 401-411 (2009).
5. Aleksic, M., Pease, C.K., Basketter, D.A., Panico, M., Morris, H.R. & Dell, A. Investigating protein haptenation mechanisms of skin sensitisers using human serum albumin as a model protein. *Toxicol. In Vitro* 21, 723-733 (2007).
6. Migdal, C., Botton, J., El Ali, Z., Azoury, M.E., Guldemann, J., Giménez-Arnau, E., Lepoittevin, J.P., Kerdine-Römer, S. and Pallardy, M. Reactivity of chemical sensitizers toward amino acids in cellulo plays a role in the activation of the Nrf2-ARE pathway in human monocyte dendritic cells and the THP-1 cell line. *Toxicol. Sci.* 133, 259-274 (2013).
7. Schauder, S. and Ippen, H. Contact and photocontact sensitivity to sunscreens. Review of a 15-year experience and of the literature. *Contact Dermatitis* 37, 221-232 (1997).
8. Scheuer, E. and Warshaw, E. Sunscreen allergy: A review of epidemiology, clinical characteristics, and responsible allergens. *Dermatitis* 17, 3-11 (2006).
9. Chuah, S.Y., Leow, Y.H., Goon, A.T., Theng, C.T. and Chong, W.S. Photopatch testing in Asians: a 5-year experience in Singapore. *Photodermatol. Photoimmunol. Photomed.* 29, 116-120 (2013).
10. Karlsson, I., Persson, E., Mårtensson, J. and Börje, A. Investigation of the sunscreen octocrylene's interaction with amino acid analogs in the presence of UV radiation. *Photochem. Photobiol.* 88, 904-912 (2012).
11. Karlsson, I., Vanden Broecke, K., Mårtensson, J., Goossens, A. and Börje A. (2011) Clinical and experimental studies of octocrylene's allergenic potency. *Contact Dermatitis* 64, 343-352.
12. Gerberick, G.F., Vassallo, J.D., Bailey, R.E., Chaney, J.G., Morrall, S.W. and Lepoittevin, J.P. Development of a peptide reactivity assay for screening contact allergens. *Toxicol. Sci.* 81, 332-343 (2004).
13. Gerberick, G.F., Vassallo, J.D., Foertsch, L.M., Price, B.B., Chaney, J.G. and Lepoittevin, J.P. Quantification of chemical peptide reactivity for screening contact allergens: a classification tree model approach. *Toxicol. Sci*. 97, 417-427 (2007).

14. Troutman, J.A., Foertsch, L.M., Kern, P.S., Dai, H.J., Quijano, M., Dobson, R.L., Lalko, J.F., Lepoittevin, J.P. and Gerberick, G.F. The incorporation of lysine into the peroxidase peptide reactivity assay for skin sensitization assessments. *Toxicol. Sci.* 122, 422-436 (2011).

II Rapid screening method to study the reactivity of UV filter substances towards skin proteins by high-performance thin-layer chromatography

Constanze Stiefel, Wolfgang Schwack

Reprinted with permission from: *International Journal of Cosmetic Science* 2013, 35, 588–599.

SYNOPSIS

OBJECTIVE: Most UV filters used in sunscreens and other cosmetic products contain carbonyl groups, which generally are able to react with peptides or free amino acids of the human skin. To estimate their reactivity, we studied different prominent UV filter substances, octocrylene, ethylhexyl salicylate, 4-t-butyl-4′-methoxydibenzoylmethane, ethylhexyl methoxycinnamate, benzophenone- 3, hydroxymethylbenzoyl sulphonic acid, octyldimethyl p-aminobenzoic acid, 3-benzylidene camphor, 4-methylbenzylidene camphor, diethylhexyl butamido triazone and ethylhexyl triazone.

METHODS: A simple screening method using an amino HPTLC plate as protein model was established. The influence of different reaction conditions like heating and irradiation was determined.

RESULTS: The ketones BP-3, HMBS and BM-DBM revealed the highest binding rates after both irradiation and heating. After 1 h of irradiation, 82%, 28% and 96%, respectively, were bonded to the amino phase, while heating resulted in values of 52%, 36% and 16%. For BP-3 and HMBS, even storage in the dark at room temperature resulted in a low binding. Contrarily, for the two camphor derivatives 3-BC and 4-MBC, only irradiation led to a slightly turnover. UV filters with ester groups also showed a different behaviour depending on their main skeleton. While OCR especially reacted under heating with the amino phase, resulting in 36% of bound species after one hour, UV irradiation particularly encouraged a reaction of the other esters. After 1 h irradiation, 15% of EHMC, 38% of EHS and 48% of OD-PABA were bonded to the amino groups of the HPTLC plate, whereas the reactivity of the two triazones, EHT and DEBT, was comparatively low.

CONCLUSION: Especially the UV filters BP-3, BM-DBM, HMBS, EHMC or OCR, which are commonly known to cause contact dermatitis, showed a high tendency to form adducts with the amino layer. Thus, the amino plate seems to be a proper tool to screen for skin sensitizers.

RÉSUMÉ

OBJECTIFS: La plupart des filtres UV utilisés dans les crèmes solaires et autres produits cosmétiques contiennent des groups carbonyle, qui sont généralement capables de réagir avec des peptides ou des acides aminés libres de la peau humaine.

Pour estimer leur réactivité, nous avons étudié différentes substances éminents de filtre UV, octocrylène, le salicylate d'éthylhexyle, 4-t-butyl-4-méthoxy, hexyle méthoxycinnamate, la benzophénone-3, l'acide hydroxymethylbenzoyl, l'acide p-aminobenzoïque octyldiméthyl, 3,4 benzylidène camphre camphre méthylbenzylidène, diethylhexyl butamido triazone et éthylhexyle triazone.

MÉTHODES: Une méthode de criblage simple à l'aide d'une plaque HPTLC amine comme modèle de protéine a été établie. L'influence des différentes conditions de réaction comme le chauffage et l'irradiation a été déterminée.

RÉSULTATS: Les cétones BP 3, HMBS et BM DBM ont révélé des taux de liaison les plus élevés après deux irradiation et le chauffage. Après 1 heure d'irradiation, 82, 28 et 96%, respectivement, ont été liés à la phase aminée, tandis que le chauffage a abouti à des valeurs de 52, 36 et 16%. Pour HMBS BP-3, même le stockage dans l'obscurité à la température ambiante a entraîné une faible liaison. Au contraire, pour les deux dérivés du camphre 3-BC et 4-MBC, seulement l'irradiation a conduit à une légère dérivatisation.. Les filtres UV avec des groupes ester ont également montré un comportement différent en fonction de leur squelette principal. Alors qu'OCR réagit surtout à chaud avec la phase aminée, entraînant 36% des espèces liées au bout d'une heure, l'irradiation UV particulièrement encourage une réaction des autres esters. Après une irradiation de 1 heure, 15% des EHMC, 38% des EHS, et 48% des OD-PABA ont été liés aux groupes aminés de la plaque HPTLC, alors que la réactivité des deux triazones, ISE et DEBT, a été relativement faible.

CONCLUSION: En particulier, les filtres UV BP-3, BM-DBM, HMBS, EHMC, ou OCR, qui sont communément connus pour provoquer des dermatites de contact, ont montré une forte tendance à former des adduits avec la couche aminée. Ainsi, la plaque aminée semble être un bon outil pour dépister des sensibilisants cutanés.

KEYWORDS: amino phase, HPTLC, protein binding, screening method, UV filters, UV irradiance

INTRODUCTION

Consumers increasingly are aware of the negative effects that intensive sunlight can have on the human skin. Acute injuries like sunburn, photodermatosis or photoallergic contact eczema are highly visible [1, 2], induced by UVB radiation penetrating mainly into the superficial layers of the epidermis. Nowadays, however, the major attention is paid to chronic effects of intensive sun exposures like skin pigmentation [3, 4], skin ageing [5, 6] and at worst skin cancer [7–10]. Particularly, UVA radiation (320– 400 nm) reaches deeper skin layers (corium and subcutis) and induces the formation of reactive oxygen species (ROS) [11, 12], responsible for biological damages [13]. As sun protection formerly concentrated on the category of sunscreen products, actually a variety of daily personal care products like lipsticks, vanishing creams or even shampoos claim UV protection properties that are achieved by the addition of UV filters [14–16]. The increased application of such products results in an accumulated contact time of UV filters with the human skin during the whole year and can quite be considered as critical. Not only the fate of UV filters in the environment is questioned [17, 18], but also reactions of filter substances and their photodegradation products with human tissues. Thus, it is known that some UV filters can penetrate the human skin [19–22], whereas others show a certain adsorption tendency [23, 24].

This behaviour is the basis to consider the reaction potential of UV filters or their photodegradation products with components of the human skin. Many of the UV filters approved in Europe provide reactive carbonyl groups, which are possible reaction partners for amino groups of peptides or free amino acids. The formation of protein adducts with different electrophilic agents is multiply described [25–29], but UV filters as reaction partners previously were rarely considered [30]. Recent considerations conclude that such interactions with the human skin may possibly be associated with the formation of contact allergies [31–33].

The aim of this study was to develop a rapid and simple *in vitro* method to estimate the possible reactivity of UV filter substances with amino groups of skin constituents. An HPTLC amino plate seemed to be a promising model. Therefore, we applied the common UV filters, octocrylene (OCR), ethylhexyl methoxycinnamate (EHMC), benzophenone-3 (BP-3), hydroxymethylbenzoyl sulphonic acid (HMBS), ethylhexyl salicylate (EHS), 4-t-butyl-4′-methoxydibenzoylmethane (BM-DBM), octyldimethyl p-aminobenzoic acid (OD-PABA), 3-benzylidene camphor (3-BC), 4-methylbenzylidene camphor (4-MBC), diethylhexyl butamido triazone (DEBT) and ethylhexyl triazone (EHT), onto an HPTLC plate and initialized the reactions both by UV irradiation and by slight heating. Thus, we took into account that the usage of UV filters is not limited to sunscreen products but also includes daily care products. For these products, which are also regularly used without necessarily being in the sun, the energy for a possible reaction primarily is provided by the natural warmth of the skin and additionally by artificial and natural UV sources. Finally, the HPTLC plate was developed, and the still migrating, non-bonded UV filters were quantified by a TLC scanner, whereas bound species remained at the start zones.

MATERIALS AND METHODS

4-t-Butyl-4′-methoxydibenzoyl methane (BM-DBM, Eusolex 9020), ethylhexyl methoxycinnamate (EHMC, Eusolex 2292), benzophenone- 3 (BP-3, Eusolex 4360), octyldimethyl p-aminobenzoic acid (OD-PABA, Eusolex 6007), octocrylene (OCR, Eusolex OCR), 4-methylbenzylidene camphor (4-MBC, Eusolex 6300), toluene (≥98%), petroleum ether (bp 40–60°C, p.a.) and methanol (HPLC grade) were obtained from Merck (Darmstadt, Germany). Hydroxymethylbenzoyl sulphonic acid (HMBS, Uvinul MS 40), triethylamine (≥98.5%), potassium hydroxide (pearls, p.a.) and 4-methylbenzaldehyde (≥96%) were obtained from Fluka (Neu-Ulm, Germany). Dimethyl sulphoxide (DMSO) (HPLC grade), ethanol (≥99.8%, p.a.), n-hexane (≥95%) and acetic acid (100%, p.a.) were purchased from Carl Roth (Karlsruhe, Germany). 2-Ethylhexyl salicylate (EHS), *tert*-butyl methyl ether (≥99.8%), acetonitrile (≥99.9%) and DL-camphor (≥97%) were obtained from Sigma-Aldrich (Steinheim, Germany). Magnesium chloride hexahydrate (99–102%, p.a.) was purchased from VWR International (Bruchsal, Germany). Ethylhexyl triazone (EHT, Uvinul T 150) was kindly provided by BASF (Ludwigshafen, Germany) and diethylhexyl butamido triazone (DEBT) by 3V Sigma (Bergamo, Italy). All solvents used for planar chromatography were at least HPLC grade or distilled prior to

use. HPTLC glass plates silica gel 60 F_{254}, 20 x 10 cm, HPTLC glass plates amino F_{254}, 10 x 10 cm, and HPTLC glass plates RP_{18} WF_{254}, 10 x 10 cm, all with a layer thickness of 200 µm, were obtained from Merck. They generally were prewashed by development with methanol, dried at 100°C for 30 min, wrapped into aluminium foil and stored in a proper TLC chamber until use to prevent contamination.

Synthesis of 4-methylbenzylidene camphor (4-MBC)

As 4-MBC was no longer commercially available, it was synthesized according to a previously published method [34]. Briefly, camphor (9.13 g, 60 mmol) and 4-methylbenzaldehyde (7.21 g, 60 mmol) were suspended in 100 mL DMSO, and finely ground potassium hydroxide (3.4 g, 60 mmol) was added by degrees. The reaction mixture was stirred for 3 h and then stored overnight. Pure water (100 mL) was added, and the formed precipitate was vacuum filtered through a Büchner funnel, washed with 100 mL of ethanol and dried for 6 h at 80°C (yield 45%). Melting point (68°C) and TLC-ESI/MS data were compared with those of a residue of a commercial Eusolex 6300 sample (Merck) and proved the identity of the synthesized product.

Standard solutions

For the preparation of standard solutions, 15 mg of BM-DBM, BP-3, OCR, EHS, EHMC, OD-PABA, DEBT, 3-BC and 4-MBC were individually dissolved in 10 mL acetonitrile and diluted to a final concentration of 150 mg L^{-1}. HMBS (15 mg) was dissolved in 10 mL methanol, EHT (15 mg) in a mixture of ethanol/acetonitrile/ toluene (40/40/20). Both solutions were also diluted to a final concentration of 150 mg L^{-1}.

High performance thin-layer chromatography (HPTLC)

Sample application was performed with an Automatic TLC Sampler 4 (ATS4) (CAMAG, Muttenz, Switzerland). Heating of the TLC plates was performed with a TLC plate heater (CAMAG). Plate images were documented by a DigiStore 2 Documentation System (CAMAG) consisting of illuminator Reprostar 3 with digital camera Baumer optronic DXA252. Densitometry was performed by a TLC Scanner 3 (CAMAG) with a slit dimension of 4 x 0.3 mm^2. The data obtained were processed with WINCATS software, version 1.4.2 (CAMAG). Mobile phase was generally petroleum ether/*tert*-butyl methyl ether/methanol 70/20/10 (v/v/v) + 1% triethylamine. In case of HMBS, methanol/acetic acid 90/10 (v/v) was used.

Irradiation

Solar simulator

Irradiations were performed with a Suntest CPS+ from Atlas Material Testing Technology (Linsengericht, Germany) equipped with a xenon lamp and a filter combination of coated quartz glass with UV special glass (simulation of solar global radiation outdoors at daylight, Atlas) using the following settings: irradiation intensity 350 W m^{-2}, ventilation temperature 33°C. A custom-made, watercooled base plate was held at 20°C.

Natural sunlight

Irradiation under natural sunlight was performed at different days in May and June 2010 between 10 a.m. and 4 p.m. in Stuttgart- Hohenheim, Germany. Irradiation was performed under cloudless conditions. Average temperatures at the test days were between 26 and 33°C. The average irradiation intensity was 512 W m^{-2}.

Reactions of UV filters on the HPTLC plates

For each UV filter, three bands (4 mm width, 8 mm distance from lower edge, 10 mm distance from left edge, 8 mm distance between tracks) of the standard solution (2 µL) were applied on a 7 x 5 cm^2 HPTLC glass plate amino. Thereafter, the plates were immediately developed to determine recoveries or differently treated up to 120 min: stored in the dark at ambient temperature, heated at 33°C on a plate heater protected from light and irradiated with sunlight or under the Suntest CPS+. The corresponding light doses for 1 h of irradiation were 1260 kJ m^{-2} (4.4 kJ/HPTLC plate) for the sun simulator and on average 1843 kJ m^{-2} (6.5 kJ/HPTLC plate) under natural sunlight.
Afterwards, a series of the respective standard solutions (0.2–2.9 µL) was applied on the same plate for calibration purposes. The chromatography was carried out in a twin-trough chamber to a migration distance of 48 mm; thereafter, the plates were dried in a stream of cold air for 2 min. The amount of the UV filter bonded to the sorbent layer at the starting zone ($hR_F = 0$) was calculated by quantifying the migrated amount at the corresponding hR_F value (BP-3: 67, BM-DBM: 51, EHMC: 81, OCR: 69, HMBS: 33, EHS: 72, OD-PABA: 75, 3-BC: 77, 4-MBC: 81, EHT: 29, DEBT: 58) by densitometry at 254 nm. Additionally, plate images were documented under illumination by UV light (254 nm).
As a negative control, samples of each UV filter were applied on 7 x 5 cm^2 HPTLC silica gel 60 and RP 18 plates and were treated under the same conditions as described for the amino plates.

RESULTS AND DISCUSSION

Concept of the study

An HPTLC amino plate never was used as a simple protein model layer to study the reactivity of ingredients of cosmetics towards main skin constituents. However, the sorbent consists of propylamine

chains covalently attached to a silica gel surface, which like proteins generally are able to react with carbonyl groups. The studied UV filter substances, BP-3, HMBS, BM-DBM, 3-BC, 4-MBC, EHMC, OCR, EHS, OD-PABA, EHT and DEBT (Fig. 1), provide ketone or ester groups, which may undergo condensation reactions with primary amines, yielding azomethins or amides, respectively.

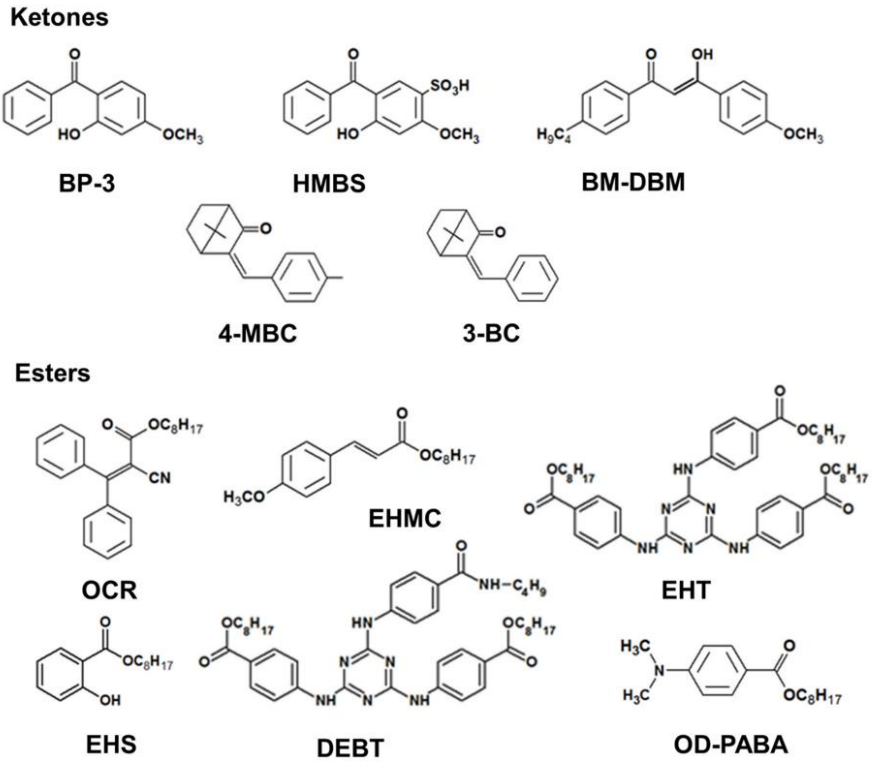

Figure 1 Structure formulas of the studied UV filter substances.

Therefore, standard solutions of UV filters were applied bandwise onto an HPTLC amino glass plate, followed by different treatments to induce a possible reaction. During each series of experiments, one HPTLC plate was developed immediately after the application of standards to determine recoveries, which generally were between 97% and 102% (data not shown); thus, systematic losses were not observed. Slightly heating at 33°C should respect the temperature of the epidermis [35], whereas a dark control at ambient temperatures should show, if even such conditions result in reactions of the UV filters with the amino plate. UV irradiation both under a sun simulator and in natural sunlight could reveal, if excited states especially support reactions with amino groups of skin constituents. After each experiment on the plate, calibration standards were applied, the plate was developed, and the migrated UV filters, not bonded at the start zones, were quantified by densitometry as exemplarily shown in Figs 2–5. For BP-3, BM-DBM and OCR, the bonded part of the UV filter substances at the start zones is clearly detectable, both on the plate images and from the corresponding scans. Accordingly, the peak areas at the respective hR_F values of the chromatographed UV filters decreased. It holds true for heat treatments and UV irradiations, and except BM-DBM (Fig. 3) even for the dark control experiments at ambient temperature. The sharp ‘double-peaks’ at the start zones are a result of the spray application, as a strongly eluting solvent was used for the preparation of the standard solutions.

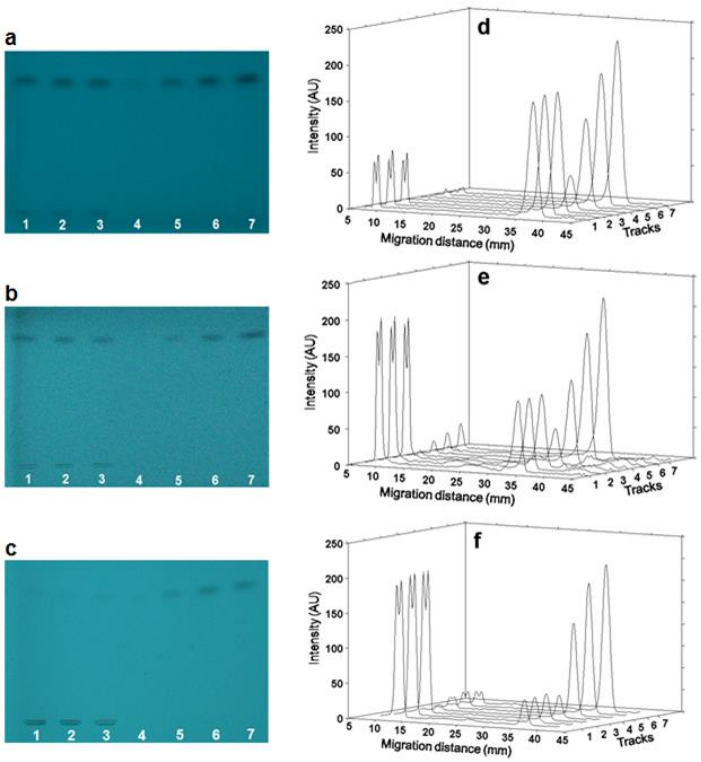

Figure 2 HPTLC results for the example of a ketone (BP-3), images of plates stored for 60 min in the dark at ambient temperature (a), heated at 33°C for 60 min (b) and irradiated for 60 min at 350 W m^{-2} (c); associated scans of the densitometric evaluation at 254 nm (d-f). Track 1–3: 2 µL of BP-3 standard solution (150 mg L^{-1}), applied before treatment, Track 4–7: 0.2–2.9 µL of the BP-3 standard solution, applied after treatment for calibration.

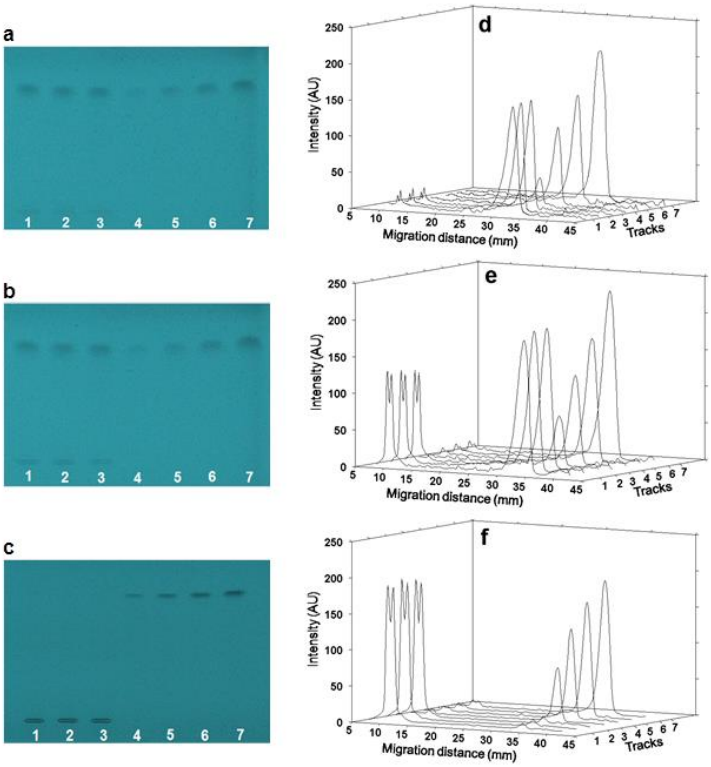

Figure 3 HPTLC results for the example of a dibenzoylmethane (BM-DBM), images of plates stored for 60 min in the dark at ambient temperature (a), heated at 33°C for 60 min (b) and irradiated for 60 min at 350 W m^{-2} (c); associated scans of the densitometric evaluation at 254 nm (d–f). Track 1–3: 2 µL of BM-DBM standard solution (150 mg L^{-1}), applied before treatment, Track 4–7: 0.2–2.9 µL of the BM-DBM standard solution, applied after treatment for calibration.

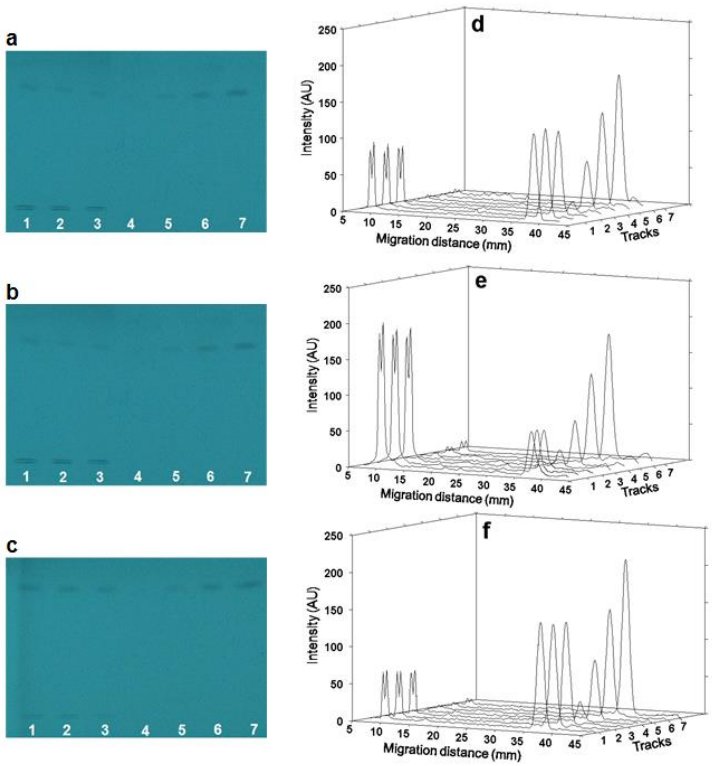

Figure 4 HPTLC results for the example of an ester (OCR), images of plates stored for 60 min in the dark at ambient temperature (a), heated at 33°C for 60 min (b) and irradiated for 60 min at 350 W m^{-2} (c); associated scans of the densitometric evaluation at 254 nm (d–f). Track 1–3: 2 µL of OCR standard solution (150 mg L^{-1}), applied before treatment, Track 4–7: 0.2–2.9 µL of the OCR standard solution, applied after treatment for calibration.

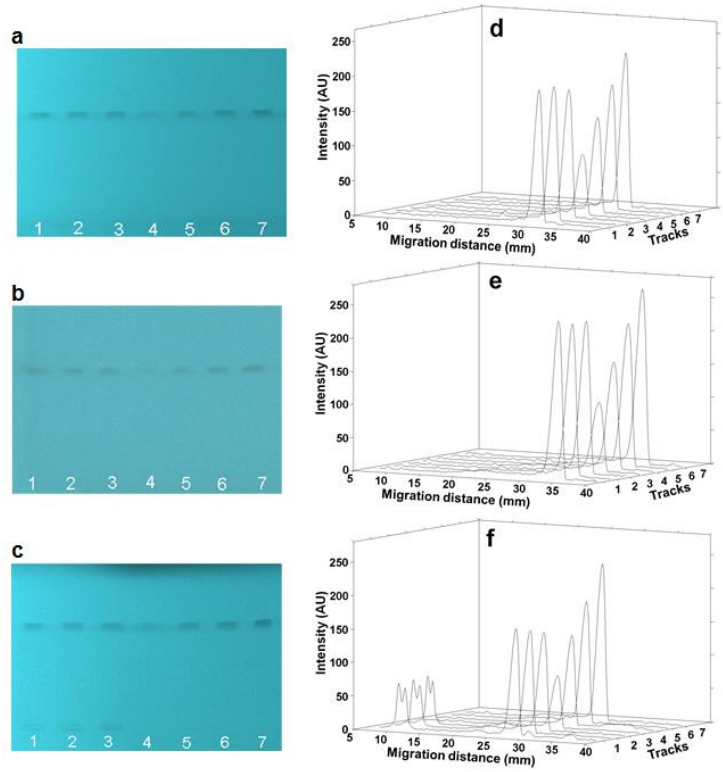

Figure 5 HPTLC results for the example of a triazone (DEBT), images of plates stored for 60 min in the dark at ambient temperature (a), heated at 33°C for 60 min (b) and irradiated for 60 min at 350 W m^{-2} (c); associated scans of the densitometric evaluation at 254 nm (d–f). Track 1–3: 2 µL of DEBT standard solution (150 mg L^{-1}), applied before treatment, Track 4–7: 0.2–2.9 µL of the DEBT standard solution, applied after treatment for calibration.

In contrast to the former examples, the triazone DEBT was rather reaction-resistant on the amino plate; just UV irradiation slightly afforded bonded species at the start zone (Fig. 5). Generally, also a second development of the amino plates with a strong polar solvent (methanol) or a very lipophilic solvent (n-hexane) did not show a change of the obtained and presented figures, which supports that a covalent bond to the amino groups of the start zones was formed. However, to additionally prove that the amino groups are responsible for the covalent retardation instead of other reactions to be assumed like oxidations, polymerizations or even reactions with free silanol groups, the experiments were repeated on HPTLC silica gel 60 and RP18 plates. In any case, bound UV filter species could not be detected at the start zones, exemplarily shown for BP-3 in Fig. 6. Only the amino plate was able to react with BP-3 forming adducts at the start zone during UV irradiation.

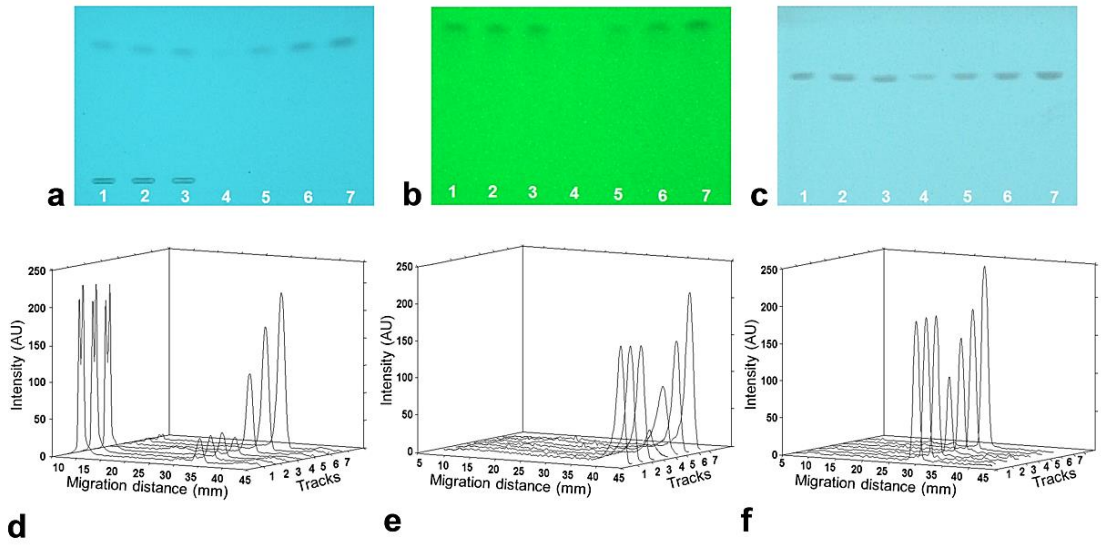

Figure 6 Comparison of the reactivity of BP-3 on different HPTLC plates after irradiation for 60 min at 350 W m^{-1} and subsequent development: plate images of silica amino (a), normal phase silica (b) and silica RP 18 (c); associated scans of the densitometric evaluation at 254 nm (d-f). Track 1–3: 2 µL of a BP-3 standard solution (150 mg L^{-1}), applied before treatment, Track 4–7: 0.2–2.9 µL of the BP-3 standard solution applied after treatment for calibration.

Ketones and diketones (BP-3, HMBS, BM-DBM, 3-BC, 4-MBC)

Among the UV filter substances under study, the group of ketones and diketones almost revealed the highest reactivity with the amino plate under the conditions used. Clear linear correlations were found plotting the absolute amount of plate-bound UV filters against the time of the respective treatments (Fig. 7a). As the aminopropyl groups were present in high excess as compared to the applied UV filters (generally 300 ng), the kinetics may be understood as pseudo-first order. For BP-3 and HMBS, even one hour storage in the dark at ambient temperature significantly led to the formation of adducts (Table I).

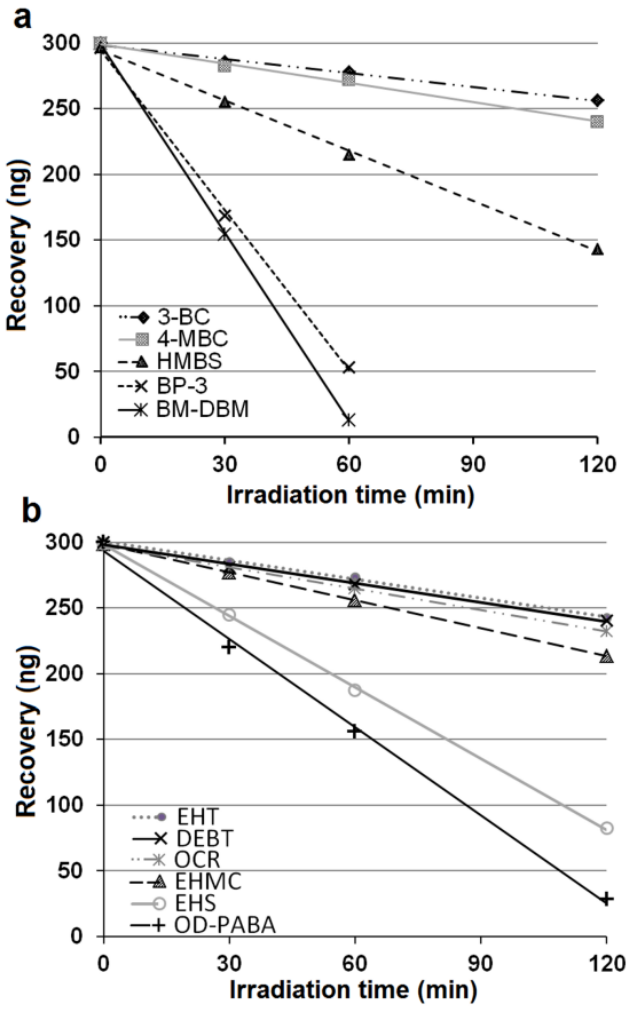

Figure 7 Decrease in the recovered amounts of the UV filter ketones (a) and esters (b) from the HPTLC amino plate, exemplarily shown after different irradiation times in the Suntest CPS+ system followed by plate development.

Table I Amounts of UV filter substances, ketones (a) and esters (b), bonded to an HPTLC amino plate after different treatments for 1 h

	bonded to the amino plate (%) ± SD[a]					
(a)	**3-BC**	**4-MBC**	**HMBS**	**BP-3**	**BM-DBM**	
dark storage	0.2 ± 0.01	0.6 ± 0.02	15.1 ± 0.11	12.6 ±0.20	1.0 ± 0.01	
heating (33°C)	0.7 ± 0.04	0.8 ± 0.01	35.9 ± 0.31	51.9 ± 0.81	15.6 ± 0.31	
sunlight	4.5 ± 0.07	6.0 ± 0.10	20.1 ± 0.32	63.3 ± 1.64	69.8 ± 2.20	
Suntest CPS+	7.4 ± 0.16	9.4 ± 0.18	28.3 ± 0.40	82.3 ± 1.60	95.6 ± 3.55	
LOD[†]	34	26	11	11	31	
(b)	**EHT**	**DEBT**	**EHMC**	**EHS**	**OCR**	**OD-PABA**
dark storage	n.d.	n.d.	0.8 ± 0.01	3.2 ± 0.13	8.6 ± 0.28	2.1 ± 0.09
heating (33°C)	0.3 ± 0.01	0.4 ± 0.01	10.0 ± 0.16	6.6 ± 0.20	35.6 ± 0.20	3.3 ± 0.17
sunlight	5.6 ± 0.08	6.6 ± 0.18	11.5 ± 0.26	30.8 ± 0.74	9.8 ± 0.74	31.0 ± 1.05
Suntest CPS+	8.8 ± 0.33	10.5 ± 0.09	14.7 ± 0.63	37.6 ± 1.52	11.8 ± 1.52	48.0 ± 4.42
LOD[†]	11	7	34	45	33	62

[a]Standard deviation (n = 3).
[†]Limit of detection in ng/zone.
n.d., not detectable (below LOD).

Slightly heating at 33°C strongly increased the turnover for BP-3 and HMBS, but only moderately for BM-DBM. Irradiation under natural sunlight or in the sun simulator especially affected BP-3 and BM-DBM, last of which was nearly completely bonded to the amino phase after one hour in the suntest system. Owing to the steady radiation energy and the enclosed test chamber, the suntest system resulted in most distinct reactions.

Regarding the high photoinstability of BM-DBM [36, 37], one could argue that also photodegradation on the plate may be responsible for losses, but zones of compounds other than the parent could not be detected (Fig. 3).

Additionally, photofragmentation of BM-DBM is not to be expected in the polar environment of a silica amino plate [36]. In contrast, after 60 min irradiation on the RP18 plate, we could separate four photodegradation products with 31%, 32%, 74% and 93% of the area of the BM-DBM peak. As compared to the two benzophenones and the dibenzoylmethane, the two camphor derivatives 3-BC and 4-MBC significantly showed a lower reactivity, which was solely initiated by UV irradiation. Steric hindrance of the cyclic ketones might give an explanation.

Esters (EHMC, EHS, OCR, OD-PABA, EHT, DEBT)

The studied UV filters with ester groups not only generally revealed the same reaction kinetics as found for the ketones, but also quite different reactivities (Fig. 7b). Storage in the dark and slight heating almost did not generate adducts with the amino plate (Table I). After heating for one hour, significant amounts of bound species were only found for EHMC, whereas UV irradiation resulted in very similar reactivities. However, OCR remarkably reacted with the amino plate after heating, even during dark storage at ambient temperature. Vice versa, only about 10% of the applied OCR was bound to the amino plate after a one hour treatment by UV irradiation, which may be in accordance with the high photostability of OCR [38, 39]. Contrarily, highest binding rates after UV irradiation could be determined for EHS and OD-PABA, both under natural sunlight and in the sun simulator (Table I), whereas heating only played a minor role for the binding of both esters to the amino plate. Additionally, a highly fluorescence quenching substance zone at hR_F 60, thus slightly more polar, was detected on the irradiated and developed plate of OD-PABA. By TLC-MS experiments, we could identify two known OD-PABA photodegradation products, 4-dimethylamino-(2/3)-methylbenzoic acid 2-ethylhexyl ester and 4-monomethylaminobenzoic acid 2-ethylhexyl ester [39]. These products were also formed on the silica gel 60 and the RP18 plates, where they clearly could be separated and assigned. Although the peak at the start zone, that is, bound OD-PABA had a relatively large peak area, the formation of the additional photoproducts (together approximately the same peak area as the migrated OD-PABA) certainly pretends a higher binding rate that was just calculated from the recovered OD-PABA. Both triazones, EHT and DEBT, generally were least reactive, although they are also p-aminobenzoates like OD-PABA and even present three ester groups.

Just UV irradiation led to the formation of adducts with the amino plate in the range of approximately 6–10% (Table I). The well-known photostability of EHT and DEBT [40] possibly can again explain the findings.

Comparison with dermatological data

As the formation of protein adducts is known as a central mechanism in the development of allergies [41–43], an important question was whether binding to the amino plate can provide a first indication for an allergic potential of the studied UV filters. Therefore, the obtained results were compared with recently published patch and photopatch data [44–49]. The top five UV filters (BP-3, HMBS, OCR, BMDBM and EHMC) identified as allergens during patch tests (Table II) also showed the highest binding rates on the amino plate under the conditions of slight heating. Binding under irradiating conditions additionally well correlate with photopatch test data (Table II). The most reactive UV filters on the amino plate (BMDBM, BP-3, HMBS, EHMC and OCR) also were the most common allergens in photopatch tests, whereas for the likewise reactive EHS, the available dermatological data are very limited. In the case of OD-PABA, however, the additional formation of photodegradation products on the amino plate pretends a greater amount of binding than actually occurred.

Table II Summary of patch (a) and photopatch (b) test results for the observed UV filters ordered by prevalence of skin reactions

(a)	Bryden et al. [44]	Kerr et al. [45]	Pigatto et al. [46]	Total (%)
OCR	n.o.	7/1031 (0.7)	9/1082 (0.8)	16/2113 (0.8)
BP-3	9/1155 (0.8)	6/1031 (0.6)	6/1082 (0.6)	21/3268 (0.6)
HMBS	9/1155 (0.8)	n.o.	1/1082 (0.1)	10/2237 (0.4)
BMDBM	10/1155 (0.9)	3/1031 (0.3)	4/1082 (0.4)	17/3268 (0.4)
EHMC	5/1155(0.4)	2/1031 (0.2)	2/1082 (0.2)	9/3268 (0.3)
OD-PABA	7/1155 (0.6)	n.o.	0/1082 (0)	7/2237 (0.3)
4-MBC	6/1155 (0.5)	4/1031 (0.4)	0/1082 (0)	10/3268 (0.3)
EHT	3/1155 (0.3)	n.o.	1/1082 (0.1)	4/2237 (0.2)
EHS	n.o.	1/1031 (0.1)	n.o.	1/1031 (0.1)
DEBT	n.o.	0/1031	n.o.	0/1031 (0)

(b)	Bryden et al. [44]	Kerr et al. [45]	Rodriguez et al. [47]	Pigatto et al. [46]	Cardoso et al. [48]	Victor et al. [49]	Total (%)
OCR	n.o.	41/1031 (4)	n.o.	23/1082 (2.1)	n.o.	n.o.	64/2113 (3.0)
BP-3	27/1155 (2.3)	37/1031 (3.6)	22/82 (26.8)	15/1082 (1.4)	3/83 (3.6)	3/76 (3.9)	107/3509 (3.0)
HMBS	5/1155 (0.4)	3/1031 (0.3)	2/82 (2.4)	3/1082 (0.3)	3/83 (3.6)	3/76 (3.9)	19/3509 (0.5)
BMDBM	22/1155 (1.9)	18/1031 (1.7)	0/82 (0)	9/1082 (0.8)	1/82 (1.2)	3/76 (2.6)	53/3509 (1.5)
EHMC	8/1155(0.7)	7/1031 (0.7)	8/82 (9.8)	13/1082 (1.2)	1/83 (1.2)	n.o.	37/3433 (1.1)
OD-PABA	3/1155 (0.3)	n.o.	1/82 (1.2)	1/1082 (0.1)	n.o.	2/76 (2.6)	7/2395 (0.3)
4-MBC	4/1155 (0.3)	3/1031 (0.3)	1/82 (1.2)	1/1082 (0.1)	1/83 (1.2)	n.o.	10/3433 (0.3)
EHT	2/1155 (0.2)	3/1031 (0.3)	n.o.	2/1082 (0.2)	n.o.	n.o.	7/3268 (0.2)
EHS	n.o.	2/1031 (0.2)	n.o.	n.o.	n.o.	n.o.	2/1031 (0.2)
DEBT	n.o.	0/1031 (0)	n.o.	n.o.	n.o.	n.o.	0/1031 (0)

n.o., not observed

CONCLUSION

The present study showed that amino HPTLC plates are a suitable screening tool to determine the binding potential of different common UV filters to peptides of the human skin. It could be shown that there are great differences between the studied UV filters concerning the formation of adducts with the amino plates. Obviously, no simple rules could be derived, if, for example, ketones or benzoates preferably react with amino groups under heating or UV irradiation. However, known photostability presumably prevented UV filters also from photoaddition to the HPTLC amino plate. Nevertheless, it is highly interesting that especially the UV filters like BP-3, BM-DBM, HMBS, EHMC or OCR, which are commonly known to cause contact dermatitis, showed a high tendency to form adducts with the amino layer. This supports the assumption that there is a direct correlation between the formation of protein adducts and contact or photoallergic contact dermatitis. Thus, the amino plate seems to be a proper tool to screen for skin sensitizers.

During the ongoing studies, the focus will especially be laid on which reaction mechanisms are responsible for the formation of UV filter protein adducts and if the results of the present first screening are also transferable to more complex protein models and other substance groups.

ACKNOWLEDGEMENTS

The authors express many thanks to Merck (Darmstadt, Germany) and CAMAG (Berlin, Germany) for support regarding plate material and instrumental equipment, respectively. The authors declare no conflicts of interest.

REFERENCES

1. Bayerl, C., Taake, S., Moll, I. and Jung, E.G. Characterization of sunburn cells after exposure to ultraviolet light. *Photodermatol. Photoimmunol. Photomed.* 11, 149–154 (1995).
2. Ichihashi, M. Mechanisms of aging and photoageing of skin-how wrinkles are formed. *Fragr. J.* 32, 24–30 (2004).
3. Mommaas, A.M. Effects of ultraviolet radiation on human skin. SOFW J. 124, 882–888 (1998).
4. Moyal, D. Prevention and ultraviolet-induced skin pigmentation. *Photodermatol. Photoimmunol. Photomed.* 20, 243–247 (2004).
5. Gniadecka, M. and Jemec, G.B. Quantitative evaluation of chronological ageing and photoageing in vivo: studies on skin echogenicity and thickness. Br. J. Dermatol. 139, 815–821 (1998).
6. Puizina-Ivic, N. Skin aging. *Acta Dermatovenerol. Alp. Panonica Adriat.* 17, 47–54 (2008).
7. Ullrich, S.E. Sunlight and skin cancer: lessons from the immune system. *Mol. Carcinog.* 46, 629–633 (2007).
8. Ivry, G.B., Ogle, C.A. and Shim, E.K. Role of sun exposure in melanoma. *Dermatol. Surg.* 32, 481–492 (2006).
9. Armstrong, B.K. and Kricker, A. How much melanoma is caused by sun exposure? *Melanoma Res.* 3, 395–401 (1993).
10. Coelho, S.G., Choi, W., Brenner, M. et al. Short- and long-term effects of UV radiation on the pigmentation of human skin. *J. Investig. Dermatol. Symp. Proc.* 14, 32–35 (2009).
11. Gilchrest, B.A., Soter, N.A., Hawk, J.L. et al. Histologic changes associated with ultraviolet A–induced erythema in normal human skin. *J. Am. Acad. Dermatol.* 9, 213–219 (1983).
12. Herrling, T., Zastrow, L., Fuchsand, J and Groth, N. Electron spin resonance detection of UVA-induces free radicals. Skin Pharmacol. Appl. Skin Physiol. 15, 381–383 (2002).
13. Jung, K., Seifert, M., Herrling, T. and Fuchs, J. UV-generated free radicals (FR) in skin: their prevention by sunscreens and their induction by self-tanning agents. *Spectrochim. Acta. A Mol. Biomol. Spectrosc.* 133, 1423–1428 (2008).
14. Seite, S., Fourtanier, A. and Rougier, A. Photoprotection in moisturizers and dailycare products. *G. Ital. Dermatol. Venereol.* 145, 631–636 (2010).
15. Seité, S., Colige, A., Piquemal-Vivenot, P., Montastier, C., Fourtanier, A., Lapière, C. and Nusgens, B. A full-UV spectrum absorbing daily use cream protects human skin against biological changes occurring in photoaging. *Photodermatol. Photoimmunol. Photomed.* 16, 147–155 (2000).
16. Gaspar, L.R. and Campos, P.M. Photostability and efficacy studies of topical formulations containing UV-filters combination and vitamins A, C and E.. *Int. J. Pharm.* 343, 181–189 (2007).
17. Poiger, T., Buser, H., Balmer, M.E., Bergqvist, P. and Müller, M.D. Occurrence of UV filter compounds from sunscreens in surface waters: regional mass balance in two Swiss lakes. *Chemosphere* 55, 951–963 (2004).

18. Gago-Ferrero, P., Díaz-Cruz, S. and Barceló, D. An overview of UV-absorbing compounds (organic UV filters) in aquatic biota. *Anal. Bioanal. Chem.* 404, 2597–2610 (2012).
19. Gonzales, H., Farbrot, A., Larkö, O. and Wennberg, A. Percutaneous absorption of the sunscreen benzophenone-3 after repeated whole-body applications, with and without ultraviolet irradiation. *Br. J. Dermatol.* 154, 337–340 (2006).
20. Schlumpf, M., Kypke, K., Wittassek, M. et al. Exposure patterns of UV filters, fragrances, parabens, phthalates, organochlor pesticides, PBDEs, and PCBs in human milk: correlation of UV filters with use of cosmetics. *Chemosphere* 81, 1171–1183 (2010).
21. Klinubol, P., Asawanonda, P. and Wanichwecharungruang, S.P. Transdermal penetration of UV filter. *Skin Pharmacol. Physiol.* 21, 23–29 (2008).
22. Treffel, P. and Gabard, B. Skin penetration and sun protection factor of ultra-violet filters from two vehicles. *Pharm. Res.* 13, 770–774 (1996).
23. Potard, G., Laugel, C., Schaefer, H. and Marty, J. The stripping technique: in vitro absorption and penetration of five UV filters on excised fresh human skin. *Skin Pharmacol. Appl. Skin Physiol.* 13, 336–344 (2000).
24. Hagedorn-Lewekw, U. and Lippold, B.C. Absorption of sunscreens and other compounds through human skin in vivo: derivation of a method to predict maximum fluxes. *Pharm. Res.* 12, 1354–1360 (1995).
25. Natsch, A. and Gfeller, H. LC-MS-based characterization of the peptide reactivity of chemicals to improve the in vitro prediction of the skin sensitization potential. *Toxicol. Sci.* 106, 464–478 (2008).
26. Hoffmann, T., Meyer, R.J., Sorrell, M.F. and Tuma, D.J. Reactions of acetaldehyde with proteins: formation of stable fluorescent adducts. *Alcohol. Clin. Exp. Res.* 17, 69–74 (1993).
27. Tuma, D.J., Newman, M.R., Donohue, T.M. and Sorrell, M.F. Covalent binding of acetaldehyde to proteins: participation of lysine residues. *Alcohol. Clin. Exp. Res.* 11, 579–584 (1987).
28. Törnqvist, M., Fred, C., Haglund, J., Helleberg, H., Paulsson, B. and Rydberg, P. Protein adducts: quantitative and qualitative aspects of their formation, analysis and applications. *J. Chromatogr. B Analyt. Technol. Biomed. Life Sci.* 778, 279–308 (2002).
29. Lalko, J.F., Kimber, I., Dearman, R.J., Api, A.M. and Gerberick, G.F. The selective peptide reactivity of chemical respiratory allergens under competitive and non-competitive conditions. *J. Immunotoxicol* 10, 292–301 (2013).
30. Karlsson, I., Persson, E., Mårtensson, J. and Börje, A. Investigation of the sunscreen octocrylene's interaction with amino acid analogs in the Presence of UV radiation. *Photochem. Photobiol.* 88, 904–912 (2011).
31. Andreu, I., Mayorga, C. and Miranda, M.A. Generation of reactive intermediates in photoallergic dermatitis. *Curr. Opin. Allergy Clin. Immunol.* 10, 303–308 (2010).

32. Karlsson, I., Vanden Broecke, K., Mårtensson, J., Goossens, A. and Börje, A. Clinical and experimental studies of octocrylene's allergenic potency. *Contact Dermatitis* 64, 343–352 (2011).
33. Karlsson, I., Hillerström, L., Stenfeldt, A.L., Mårtensson, J. and Börje, A. Photodegradation of dibenzoylmethanes; potential cause of photocontact allergy to sunscreens. *Chem. Res. Toxicol.* 22, 1881–1892 (2009).
34. Vashenko, V., Kutulya, L. and Krivoshey, A. Simple and effective protocol for Claisen-Schmidt condensation of hindered cyclic ketones with aromatic aldehydes. *Synthesis* 14, 2125–2134 (2007).
35. Kagetsu, N., Gange, R.W. and Parrish, J.A. UVA-induced erythema, pigmentation, and skin surface temperature changes are irradiance dependent. *J. Invest. Dermatol.* 85, 445–447 (1985).
36. Schwack, W. and Rudolph, T. Photochemistry of dibenzoyl methane UVA filters Part 1. *J. Photochem. Photobiol.* 28, 229–234 (1995).
37. Sayre, R.M. and Dowdy, J.C. Photostability of avobenzone. *Cosmetics & Toiletries* 114, 85–91 (1999).
38. Ricci, A., Chretien, M.N., Maretti, L. and Scaiano, J.C. TiO2-promoted mineralization of organic sunscreens in water suspension and sodium dodecyl sulfate micelles. *Photochem. Photobiol. Sci.* 2, 487–492 (2003).
39. Rosario, R., Moeder, M., Altenburger, R. and Schmitt-Jansen, M. Photostability and phototoxicity of selected sunscreen agents and their degradation mixtures in water. *Anal. Bioanal. Chem.* 395, 1513–1524 (2009).
40. Kockler, J., Oelgemöller, M., Robertson, S. and Glass, B.D. Photostability of sunscreens. *J. Photochem. Photobiol. C: Photochem. Rev.* 13, 91–110 (2012).
41. Divkovic, M., Peasel, C.K., Gerberick, G.F. and Basketter, D.A. Hapten–protein binding: from theory to practical application in the in vitro prediction of skin sensitization. *Contact Dermatitis* 53, 189–200 (2005).
42. Gerberick, G.F., Vassallo, J.D., Foertsch, L.M., Price, B.B., Chaney, J.G. and Lepoittevin, J.P. Quantification of chemical peptide reactivity for screening contact allergens: a classification tree model approach. *Toxicol. Sci.* 97, 417–427 (2007).
43. Elahi, E.N., Wright, Z., Hinselwood, D., Hotchkiss, S.A., Basketter, D.A. and Pease, C.K. Protein binding and metabolism influence the relative skin sensitization potential of cinnamic compounds. *Chem. Res. Toxicol.* 17, 301–310 (2004).
44. Bryden, A.M., Moseley, H., Ibbotson, S.H. et al. Photopatch testing of 1155 patients: results of the U.K. multicentre photopatch study group. *Br. J. Dermatol.* 155, 737–747 (2006).
45. Kerr, A.C., Ferguson, J., Haylett, A.K. et al. A european multicentre photopatch test study. *Br. J. Dermatol.* 166, 1002–1009 (2012).
46. Pigatto, P.D., Guzzi, G., Schena, D. et al. Photopatch test: an Italian multicentre study from 2004-2006. *Contact Dermatitis* 59, 103–108 (2008).

47. Rodríguez, E., Valbuena, M., Rey, M. and Porras de Quintana, L. Causal agents of photoallergic contact dermatitis diagnosed in the national institute of dermatology of Colombia. *Photodermatol Photoimmunol Photomed.* 22, 189–192 (2006).
48. Cardoso, J., Canelas, M., Goncalo, M. and Figueiredo, A. Photopatch testing with an extended series of photoallergens: a 5-year study. *Contact Dermatitis* 60, 314–319 (2009).
49. Victor, F.C., Cohen, D.E. and Soter, N.A. A 20-year analysis of previous and emerging allergens that elicit photoallergic contact dermatitis. *J. Am. Acad. Dermatol.* 62, 605–610 (2010).

III Reactions of cosmetic UV filters with skin proteins: model studies of ketones with primary amines

Constanze Stiefel, Wolfgang Schwack

Reprinted with permission from: *Trends in Photochemistry & Photobiology* 2013, 15, 63-75.

ABSTRACT

As most UV filter substances approved for usage in sunscreens have reactive carbonyl groups, the possibility of their reaction with amino groups of proteins or free amino acids of the human skin cannot be precluded. An initial screening on high performance thin layer chromatography (HPTLC) amino plates showed that benzophenones and dibenzoylmethanes were strongly bound to the amino phase after heating and/or UV irradiation, while camphor derivatives were less reactive. To understand the underlying mechanisms and to identify reaction products, the reactions of benzophenone-3 (BP-3), dibenzoylmethane (DBM), 4-t-butyl-4'-methoxydibenzoylmethane (BM-DBM), hydroxymethylbenzoyl sulfonic acid (HMBS), 3-benzylidene camphor (3-BC), and 4-methylbenzylidene camphor (4-MBC) in the presence of butyl amine or ethanolamine as protein models were studied. Heating the reaction batches transformed BP-3 and HMBS into benzophenone imines with high yields, while DBM and BM-DBM afforded enamines and, due to α-clevages, acetophenone and benzamide derivatives. An additional UV irradiation of the reaction batches affected the product distribution in the cases of BM-DBM and DBM, but not for BP-3 and HMBS. The amine reactions generally had great influence on the UV absorption spectra. For both BP-3 and HMBS, a significant bathochromic shift together with increased absorbance was observed, thus an increased UVA protection, while the dibenzoylmethanes clearly lost UVA efficiency. According to the slight binding to the HPTLC amino layer, 3-BC and 4-MBC did not yield any reaction product with butylamine or ethanolamine.

KEYWORDS: UV filters, UV irradiance, protein binding, ketone-amine-adducts, mass spectrometry, NMR, UV absorbance

INTRODUCTION

Moderate exposure to direct sunlight has various positive effects on skin [1-5] and the human psyche [6-9], mostly associated with the generation of vitamin D3. Besides these positive effects, different undesirable consequences such as sunburn, premature skin aging or wrinkle formation are described and attributed to extensive exposure to sunlight [10-13]. Of particular importance are serious long-term effects of extensive sun exposure, like skin cancer or irreversible eye damages, which become manifest only after several years [14-18].To avoid such negative consequences at an early stage, there are currently 27 UV filter substances permitted for usage in cosmetic products in the European Union [19]; only a balanced combination of several UV filters offers a broad protection against UVA and

UVB radiation by a sunscreen [20-22]. Therefore in 2006, the European Commission issued a recommendation on the efficacy of sunscreen products, including that the level of UVA protection provided by a product should be at least 1/3 ratio of its sun protection factor (SPF) [23]. However, the usage of these UV filters is not limited to special sunscreen products. A variety of daily care products like face creams, lipsticks etc. often include two or more UV filters to claim a particular UV and antiaging protection [24, 25].

Although most of the UV filter substances are not known to be common contact allergens, there are various case reports and patch test study results over the last few years, which suspect UV filter substances becoming more and more responsible as triggers for allergies [26-32]. This is certainly a result of the steadily increasing usage of UV filters in daily care products, leading to a long contact time of UV filters with the skin. The formation of protein adducts is seen as one important step in the incidence of allergic skin reactions [33, 34]. Therefore, the identification of typical reactive groups responsible for the reaction of a substance with proteins and the underlying reaction processes were the subject of several publications [35-39]. Thus, it could be confirmed that both UV radiation as well as heating can initiate or accelerate a reaction with proteins due to the formation of reactive groups. However, UV filter substances as possible reaction partners of proteins have hardly been considered previously [40-42].

To get a first evaluation of the overall reactivity of different UV filter substances towards proteins, we developed a fast and simple screening method using an HPTLC amino plate as protein model system [43]. The screening results showed that the studied UV filters significantly differ in their reaction potential and their response to different reaction initiators such as heating or UV irradiation.

The aim of the present study was to further explore the underlying reaction processes for the UV filters benzophenone-3 (BP-3), hydroxylmethylbenzoyl sulfonic acid (HMBS), 3-benzylidene camphor (3-BC), 4-methylbenzylidene camphor (4-MBC), 4-t-butyl-4'-methoxydibenzoylmethane (BM-DBM), and the unsubstituted dibenzoylmethane (DBM), all providing keto or diketo groups. As reaction partners and simple models for amino acids or proteins, two primary amines, ethanolamine and butylamine, were selected. The obtained reaction products formed under different conditions were identified and examined for their influence on the UV spectra of the UV filters.

MATERIALS AND METHODS

4-t-Butyl-4'-methoxydibenzoylmethane (BM-DBM, Eusolex 9020), 1,3-diphenylpropan-1,3-dion (≥98%) (dibenzoylmethane, DBM), benzophenone-3 (BP-3, Eusolex 4360) and methanol (HPLC grade) were obtained from Merck (Darmstadt, Germany). 3-Benzylidene camphor (3-BC) was obtained from Chemos GmbH (Regenstauf, Germany). Hydroxymethylbenzoyl sulfonic acid (HMBS, Uvinul MS 40), ethanolamine (≥99%) and toluene-4-sulfonic acid monohydrate (~99%) were obtained from Fluka (Neu-Ulm, Germany). Acetonitrile (HPLC grade) and dimethyl sulfoxide (DMSO) (HPLC grade) were purchased from Carl Roth (Karlsruhe, Germany).

Butyl amine (≥99.5%), dimethyl sulfoxide-d_6, ammonium formate (≥99.0%) and deutero-chloroform ($CDCl_3$) were purchased from Aldrich (Steinheim, Germany). 4-Methylbenzylidene camphor (4-MBC) was synthesized according to a previously published method [43].

High-performance liquid chromatography (HPLC)

HPLC analyses were performed on an 1100 liquid chromatograph (Agilent, Waldbronn, Germany), consisting of a degasser (G 1315A), a quaternary HPLC pump (G 1311A), an autosampler (G 1313A), a column oven (G 1316A) set to 30 °C, and a diode array detector (G 1315B). DAD detection wavelengths were 275 nm, 313 nm and 360 nm (spectral bandwidth (SBW) 8 nm), while the reference wavelength was 500 nm (SBW 8 nm). Data processing was performed by Agilent ChemStation software (rev. A.04.02). As stationary phase, a Eurospher 100-5 C 18 HPLC column, 250 mm x 3 mm (Knauer, Berlin, Germany) was used. The mobile phase (0.5 mL/min) consisted of 10 mM ammonium formate buffer pH 4.0 (A) and acetonitrile (B). Gradient % A (t(min)): 40 (0) – 40 (4) – 25 (9) – 25 (13) – 10 (17) – 24 (40) – 26 (40). The injection volume was 10 µL.

HPLC-Electrospray ionization mass spectrometry (LC/ESI-MS)

The LC/MS system consisted of an identical Agilent 1100 chromatograph as described above, coupled to a G1956B MSD single-quadrupole mass spectrometer (Agilent) equipped with an electrospray ionization (ESI) interface, operated under the following conditions: capillary voltage 4 kV, skimmer voltage 35 V, source temperature 100 °C, nebulizer gas pressure 20 psig, drying gas temperature 300 °C, drying gas flow rate 10 L/min^{-1}, fragmentor voltage 80 V, gain 1, threshold 100, step size 0.1. Data processing for MS measurements was carried out with ChemStation software (Agilent). Mass spectra were recorded in the positive and negative (for HMBS) full scan mode (*m/z* 50-1000). Column and gradient were as described under section HPLC.

Spectroscopy

Infrared (IR) spectra were recorded between 4000 and 500 cm^{-1} on a diamond crystal of a Dura Sampler SMART ATR installed at the Avatar 320 FT-IR-Spectrometer (Thermo Nicolet, Madison, USA). A minimum of 32 scans was signalaveraged with a resolution of 2 cm^{-1}. UV spectra were measured with a Perkin-Elmer Lambda 2 (Überlingen, Germany).

^{13}C and ^{1}H nuclear magnetic resonance (NMR) spectra were recorded on a Varian Unity Inova-300 spectrometer (Varian, Darmstadt, Germany) at 300 MHz (^{1}H) and 75 MHz (^{13}C). The samples were dissolved in $CDCl_3$, or DMSO-d_6. The signal assignments were based on chemical shifts related to tetramethylsilane (TMS) and H-H and C-H correlation data; s = singlet, d = dublet, t = triplet, q = quartet, and m = multiplet.

Thermal reaction of UV filters with amines

The respective UV filter (0.5 mmol) was weighed into a 10-mL screw-capped glass tube (SCHOTT AG, Mainz, Germany) and suspended in acetonitrile (5 mL). Toluene-4-sulfonic acid monohydrate (1 mg, 5 µmol) and 1 mL of butyl amine (10 mmol) or 0.8 mL of ethanolamine (10 mmol) were added. After heating the mixture for 3 h at 40 or 80 °C, the reaction was stopped by cooling the tubes under running tap water. Additionally, a reaction batch was stored in the dark at ambient temperature.
To determine if the amount of amine has an impact on the reaction, different amounts of ethanolamine were used (equimolar, 2.5-fold, and 5-fold excess for BP-3 and HMBS, and 5-fold, 10-fold, and 20-fold excess for BM-DBM and DBM).

Photoreaction of UV filters in the presence of amines

The respective UV filter (2 mmol) was weighed into a 50-mL quartz beaker (diameter 38 mm, Th. Geyer, Renningen, Germany) and suspended in acetonitrile (20 mL). Toluene-4-sulfonic acid monohydrate (3.8 mg, 20 µmol) and either butyl amine or ethanolamine (40 mmol) were added, and the beaker was covered by a teflon cap and irradiated for 3 h. To maintain a constant temperature (20 °C or 60 °C), the beaker was placed in a chamber of quartz glass, which was flushed with water provided by a chiller (Model RML 6, Lauda, Germany). Irradiation was performed by a modified sun simulator SOL 500 with a metal halide lamp (430 W) (Dr. Höhnle, Gräfelfing, Germany). The modification consisted of the replacement of the front filter glass by an aluminum plate with two gaps (each 16 cm^2) to hold WG 295 glass filters (Schott, Mainz, Germany). The irradiation intensity was 0.55 mW/cm^2 in the UVB and 12.5 mW/cm^2 in the UVA range. The corresponding light doses for 3 hours of irradiation were 1410 kJ/m^2 (2.3 kJ/quartz beaker). The solutions were stirred with a magnetic stirrer, Variomag Micro (Thermo Scientific). To distinguish between the effect of UV radiation or heat on the reaction, a second identical batch was prepared in another quartz beaker, which was completely covered by aluminum foil and placed aside the irradiated sample.

Isolation of reaction products

The reaction solutions were evaporated at a temperature of 35 °C to dryness in a LABCONCO (Kansas City, USA) CentriVap concentrator equipped with a CentriVap cold trap. For HMBS and BP-3, the obtained residues could be directly used for NMR spectroscopy. For the DBM batches, the residues were taken up in 5 mL methanol, and 1 mL of the methanolic solution was subjected to preparative HPLC (five injections). The HPLC system consisted of a Kronlab (Sinsheim, Germany) HD 2-200 HPLC pump, a Variable Wavelength Monitor (Knauer, Berlin, Germany), a C-R3A Chromatopac integrator (Shimadzu), and a YMC (Dinslaken, Germany) HPLC column (ODS-A, RP 18, 5 µm, 20 mm x 25 cm). The eluent was acetonitrile/water (60/40) for 14 min followed by flushing the column with pure acetonitrile for 3 min. The flow rate was 8 mL/min, the detection wavelength 275 nm.

Reaction products isolated from batches at 80 °C for three hours

BP-3

2-[(Z)-[(2-Hydroxyethyl)imino](phenyl)methyl]-5-methoxyphenol. 133 mg (98% yield) of pure **1a** were obtained as yellow, viscous liquid. UV/Vis (methanol) λ_{max} (nm) (log ε) 302 (4.11), 384 (3.87). IR (ATR) ν (cm^{-1}): 3380-3050 (m), 3075 (w), 2940-2850 (w), 2860 (w), 1589 (s), 1535 (m), 1485 (m), 1464 (m), 1343 (w), 1261 (w), 1232 (s), 1113 (m), 1076 (w), 1031 (w), 972 (w), 831 (m), 772 (m), 698 (m). LC-MS (ESI^+) (t_R = 6.07) *m/z* (relative intensity) = 543 ($2MH^+$, 10), 272 (MH^+, 100), 106 (55). ^{1}H-NMR ($CDCl_3$, 300 MHz) δ (ppm) 16.14 (NH, bs, 1H), 7.51 (m, 3H, ^{3}J = 2.88 Hz), 7.27 (m, 2H, ^{3}J = 3.45 Hz), 6.62 (d, 1H, ^{3}J = 9.2 Hz), 6.32 (d, 1H, ^{3}J = 2.5 Hz), 6.07 (dd, 1H, ^{3}J = 9.0, 2.3 Hz), 3.82 (t, 2H, ^{3}J = 5.4 Hz), 3.78 (s, 3H), 3.42 (t, 2H, ^{3}J = 5.37 Hz). ^{13}C-NMR ($CDCl_3$, 300 MHz) δ (ppm) 174.6, 172.3, 164.9, 133.2, 132.5, 129.5, 129.4, 128.7, 127.7, 105.8, 102.2, 61.6, 55.2, 50.9.

2-[(Z)-(Butylimino)(phenyl)methyl]-5-methoxyphenol. 139 mg (98% yield) of pure **1b** were obtained as yellow, very viscous liquid. UV/Vis (methanol) λ_{max} (nm) (log ε) 302 (4.12), 385 (3.94). IR (ATR) ν (cm^{-1}): 3338 (w), 3077 (w), 2953 (m), 2931 (m), 2864 (w), 1595 (s), 1535 (m), 1490 (w), 1434 (w), 1343 (w), 1268 (m), 1209 (m), 1165 (m), 1113 (m), 1076 (w), 1031 (m), 968 (w), 842 (w), 804 (w), 775 (w), 708 (m). LC-MS (ESI^+) (t_R = 14.72) *m/z* (relative intensity) = 589 ($2MH^+$, 10), 284 (MH^+, 100), 106 (50). ^{1}H-NMR ($CDCl_3$, 300 MHz) δ (ppm) 7.50 (m, 3H), 7.26 (m, 2H), 6.65 (dd, 1H, ^{3}J = 9.1, 2.4 Hz), 6.37 (d, 1H, ^{3}J = 2.4 Hz), 6.11 (dd, 1H, ^{3}J = 9.1, 2.4 Hz), 3.78 (s, 3H), 3.27 (t, 2H, ^{3}J = 6.8 Hz), 1.61 (m, 2H), 1.39 (m, 2H), 0.88 (t, 3H, ^{3}J = 7.3 Hz). ^{13}C-NMR ($CDCl_3$, 300 MHz) δ (ppm) 173.4, 173.1, 165.0, 133.2, 132.9, 129.7, 129.6, 128.9, 127.8, 105.8, 102.5, 55.5, 48.3, 32.7, 20.5, 13.9.

HMBS

4-Hydroxy-5[(Z)-[(2-hydroxyethyl)imino](phenyl)methyl]-2-methoxybenzenesulfonic acid. 170 mg (97% yield) of pure **2a** were obtained as light yellow, fine powder. UV/Vis (methanol) λ_{max} (nm) (log ε) 303 (4.05), 384 (3.85). IR (ATR) ν (cm^{-1}): 3450-3250 (m), 2930 (w), 2871 (w), 1578 (s), 1534 (m), 1491 (w), 1430 (w), 1415 (w), 1306 (w), 1219 (s), 1176 (s), 1078 (s), 1014 (s), 834 (w), 779 (w), 749 (w), 687 (m), 601 (m). LC-MS (ESI^-) (t_R = 2.56) *m/z* (relative intensity) = 350 (M^-, 100). ^{1}H-NMR (DMSO-d_6, 300 MHz) δ (ppm) 7.58 (m, 3H), 7.32 (m, 2H), 7.13 (s, 1H), 6.20 (s, 1H), 3.72 (s, 3H), 3.38 (t, 2H, ^{3}J = 5.4 Hz), 3.55 (t, 2H, ^{3}J = 5.4 Hz); ^{13}C-NMR (DMSO-d_6, 300 MHz) δ (ppm) 174.5, 174.0, 162.2, 133.0, 132.4, 130.3, 129.5, 128.3, 125.5, 109.7, 101.9, 60.9, 56.0, 51.1.

5[(Z)-(Butylimino)(phenyl)methyl]-4-hydroxy-2-methoxybenzenesulfonic acid. 178 mg (98% yield) of pure **2b** were obtained as yellow, fine powder. UV/Vis (methanol) λ_{max} (nm) (log ε) 303 (4.08), 383 (3.89). IR (ATR) ν (cm^{-1}): 3450-3420 (w), 2957 (m), 2925 (m), 2871 (w), 1578 (s), 1520 (m), 1486 (w), 1472 (w), 1420 (w), 1225 (s), 1171 (s), 1078 (s), 1013 (s), 921 (w), 825 (w), 774 (w), 745 (w), 686 (w), 604 (w).

LC-MS (ESI^-) (hR_F = 2.96) *m/z* (relative intensity) = 362 (M^-, 100). ^{1}H-NMR (DMSO-d_6, 300 MHz) δ (ppm) 7.59 (m, 3H), 7.32 (m, 2H), 7.13 (s, 1H), 6.20 (s, 1H), 3.73 (s, 3H), 3.21 (t, 2H, ^{3}J = 6.7 Hz), 1.51 (m, 2H), 1.30 (m, 2H), 0.84 (t, 3H, ^{3}J = 7.3 Hz); ^{13}C-NMR (DMSO-d_6, 300 MHz) δ (ppm) 174.1, 174.0, 162.2, 132.9, 132.2, 130.4, 129.6, 128.1, 125.5, 109.6, 102.0, 56.1, 47.8, 29.7, 20.2, 14.1.

DBM

N-(2-Hydroxyethyl)benzamide. 45 mg (54 mol%) of pure **3a** were obtained as light-brown, very viscous liquid. UV/Vis (isopropanol) λ_{max} (nm) (log ε) 226 (4.10). IR (ATR) ν (cm^{-1}) 3380-3100 (s), 3057 (w), 2938 (w), 2872 (w), 2360 (w), 1632 (s), 1536 (s), 1491 (m), 1425 (w), 1306 (m), 1217 (w), 1068 (m), 801 (w), 712 (w), 690 (w). LC-MS (ESI^+) (t_R = 2.72) *m/z* (relative intensity) = 353 ($2MNa^+$, 10), 166 (MH^+, 100), 106 (5). ^{1}H-NMR (DMSO-d_6, 300 MHz) δ (ppm) 8.41 (t, 1H, ^{3}J = 5.0 Hz), 7.81 (m, 2H), 7.47 (m, 3H), 4.83 (s, 1H), 3.50 (m, 2H), 3.32 (m, 2H).

N-Butylbenzamide. 23 mg (26 mol%) of pure **3b** were obtained as dark-brown, viscous liquid. UV/Vis (isopropanol) λ_{max} (nm) (log ε) 225 (4.08). IR (ATR) ν (cm^{-1}) 3350-3250 (m), 3061 (w), 2957 (m), 2935 (m), 2868 (m), 2364 (w), 1636 (s), 1532 (s), 1494 (w), 1464 (w), 1310 (m), 1146 (w), 1080 (w), 1028 (w), 849 (w), 805 (w), 694 (m); LC-MS (ESI^+) (t_R = 4.47) *m/z* (relative intensity) = 355 ($2MH^+$, 10), 178 (MH^+, 100), 106 (55). ^{1}H-NMR (DMSO-d_6, 300 MHz) δ (ppm) 7.75 (m, 2H), 7.44 (m, 3H), 6.20 (2, 1H), 3.40 (q, 2H, ^{3}J = 13.1, 6.3 Hz), 1.59 (m, 2H), 1.42 (m, 2H), 0.95 (t, 3H, ^{3}J = 7.3 Hz); ^{13}C-NMR ($CDCl_3$, 300 MHz) δ (ppm) 167.8, 135.1, 131.5, 128.8, 127.1, 40.1, 32.0, 20.4, 14.0.

(2Z)-3-[(2-Hydroxyethyl)amino]-1,3-diphenylprop-2-en-1-one. 49 mg (36 mol%) of pure **9a** were obtained as brown, very viscous liquid. UV/Vis (isopropanol) λ_{max} (nm) (log ε) 244 (3.99), 252 (3.97), 342 (4.42). IR (ATR) ν (cm^{-1}) 3390-3180 (s), 3054 (w), 2928 (w), 2876 (w), 2364 (w), 1591 (s), 1569 (s), 1480 (m), 1435 (w), 1324 (m), 1295 (m), 1228 (w), 1153 (w), 1065 (m), 1030 (w), 887 (w), 746 (w), 694 (w); LC-MS (ESI^+) (t_R = 6.27) *m/z* (relative intensity) = 268 (MH^+, 100), 106 (50). ^{1}H-NMR (DMSO-d_6, 300 MHz) δ (ppm) 11.46 (s, 1H), 7.88 (m, 2H), 7.43 (m, 3H), 7.40 (m, 2H), 7.39 (m, 3H), 5.78 (s, 1H), 3.74 (t, 2H, ^{3}J = 5.3 Hz), 3.38 (q, 2H, ^{3}J = 11,2, 5.6 Hz); ^{13}C-NMR ($CDCl_3$) δ (ppm) 188.8, 167.6, 140.5, 135.7, 131.1, 129.8, 128.8, 128.5, 128.1, 127.4, 94.3, 62.3, 47.2.

(2Z)-3-(Butylamino)-1,3-diphenylprop-2-en-1-one. 50 mg (36 mol%) of pure **9b** were obtained as orange, very viscous liquid. UV/Vis (isopropanol) λ_{max} (nm) (log ε) 243 (4.09), 349 (4.39). IR (ATR) ν (cm^{-1}) 3065 (m), 2953 (m), 2924 (m), 2872 (m), 2660 (s), 1588 (s), 1573 (s), 1477 (m), 1328 (m), 1298 (m), 1217 (m), 1143 (s), 1054 (s), 1034 (s), 1002 (s), 927 (s), 742 (m), 690 (m), 616 (s); LC-MS (ESI^+) (t_R = 14.51) *m/z* (relative intensity) = 280 (MH^+, 100), 106 (10). ^{1}H-NMR (DMSO-d_6, 500 MHz) δ (ppm) 11.43 (s, 1H), 7.88 (m, 2H, ^{3}J = 7.8 Hz), 7.44 (m, 3H), 7.40 (m, 1H), 7.42 (m, 2H), 7.38 (m, 2H), 5.74 (s, 1H), 3.21 (q, 2H, ^{13}J = 13.0, 6.6 Hz), 1.56 (m, 2H), 1.37 (m, 2H), 0.87 (t, 3H, ^{3}J = 7.2

Hz); ^{13}C-NMR ($CDCl_3$, 500 MHz) δ (ppm) 188.8, 167.6, 140.5, 135.7, 131.1, 129.8, 128.8, 128.4, 127.9, 127.3, 93.4, 44.7, 33.1, 20.2, 13.9.

1-Phenylethanone (acetophenone). 30 mg (59 mol%) and 15 mg (25 mol%) of pure **5** were obtained as coloAvailable atess viscous liquid from the reaction with ethanolamine and butylamine, respectively. UV/Vis (isopropanol) λ_{max} (nm) (log ε) 240 (4.1), 319 (1.7). LC-MS (ESI^+) (t_R = 1.70) *m/z* (relative intensity) = 241 ($2MH^+$, 3), 121 (MH^+, 100), 106 (6). IR (ATR) ν (cm^{-1}) 3600 (w), 3352 (w), 3090-2870 (m), 1685 (s), 1601 (s), 1588 (m), 1451 (s), 1432 (m), 1362 (s), 1315 (m), 1270 (s), 1182 (m), 1080 (m), 967 (m), 762 (s), 691 (s), 589 (s). ^{1}H-NMR ($CDCl_3$, 300 MHz) δ (ppm) 7.92 (m, 2H), 7.53-7.36 (m, 3H), 2.55 (s, 3H); ^{13}C-NMR ($CDCl_3$, 300 MHz) δ (ppm) 196.1, 136.7, 131.8, 128.5, 128.4, 24.9.

By-products assigned by mass spectrometry:

2-{[(1E)-1-Phenylethylidene]amino}ethanol (12a). LC-MS (ESI^+) (t_R = 4.71) *m/z* (relative intensity) = 327 ($2MH^+$, 4), 164 (MH^+, 100), 148 (5).

N-[(1E)-1-Phenylethylidene]butan-1-amine (12b). LC-MS (ESI^+) (t_R = 5.96) *m/z* (relative intensity) = 351 ($2MH^+$, 3), 176 (MH^+, 100), 106 (50).

BM-DBM

***N*-(2-Hydroxyethyl)-4-methoxybenzamide (4a).** LC-MS (ESI^+) (t_R = 1.56), *m/z* (relative intensity) = 391 ($2MH^+$, 14), 196 (MH^+, 100), 135 (5), 106 (3).

***N*-Butyl-4-methoxybenzamide (4b).** LC-MS (ESI^+) (t_R = 4.46), *m/z* (relative intensity) = 415 ($2MH^+$, 17), 208 (MH^+, 100), 135 (4), 106 (3).

1-(4-*tert*-Butylphenyl)ethanone (6). LC-MS (ESI^+) (t_R = 2.11), *m/z* (relative intensity) = 353 ($2MH^+$, 81), 177 (MH^+, 100), 106 (2).

4-*tert*-Butyl-*N*-(2-hydroxyethyl)benzamide (7a). LC-MS (ESI^+) (t_R = 17.86), *m/z* (relative intensity) = 443 ($2MH^+$, 48), 222 (MH^+, 100), 106 (2).

***N*-Butyl-4-*tert*-butylbenzamide (7b).** LC-MS (ESI^+) (t_R = 8.27), *m/z* (relative intensity) = 467 ($2MH^+$, 35), 234 (MH^+, 100), 106 (2).

1-(4-Methoxyphenyl)ethanone (8). LC-MS (ESI^+) (t_R = 1.96), *m/z* (relative intensity) = 301 ($2MH^+$, 75), 151 (MH^+, 100), 106 (4).

(2*Z*)-3-[(2-Hydroxyethyl)amino]-1-(4-*tert*-butylphenyl)-3-(4-methoxyphenyl)prop-2-en-1-one (10a). LC-MS (ESI^+) (t_R = 4.62), *m/z* (relative intensity) = 707 ($2MH^+$, 46), 354 (MH^+, 100).

(2*Z*)-3-(2-Butylamino)-1-(4-*tert*-butylphenyl)-3-(4-methoxyphenyl)prop-2-en-1-one (10b). LC-MS (ESI^+) (t_R = 20.66), *m/z* (relative intensity) = 731 ($2MH^+$, 43), 366 (MH^+, 100).

(2*Z*)-3-[(2-Hydroxyethyl)amino]-3-(4-*tert*-butylphenyl)-1-(4-methoxyphenyl)prop-2-en-1-one (11a). LC-MS (ESI^+) (t_R = 5.41), *m/z* (relative intensity) = 707 ($2MH^+$, 76), 354 (MH^+, 100).

2*Z*)-3-(2-Butylamino)-3-(4-*tert*-butylphenyl)-1-(4-methoxyphenyl)prop-2-en-1-one (11b). LC-MS (ESI^+) (t_R = 21.82), *m/z* (relative intensity) = 731 ($2MH^+$, 82), 366 (MH^+, 100).

2-{[(1*E*)-1-(4-*tert*-Butylphenyl)ethylidene]amino}ethanol (13a). LC-MS (ESI^+) (t_R = 20.58), *m/z* (relative intensity) = 439 ($2MH^+$, 20), 220 (MH^+,100).

***N*-[(1*E*)-1-(4-*tert*-Butylphenyl)ethylidene]butan-1-amine (13b).** LC-MS (ESI^+) (t_R = 22.20), *m/z* (relative intensity) = 463 ($2MH^+$, 18), 232 (MH^+, 100).

2-{[(1*E*)-1-(4-Methoxyphenyl)ethylidene]amino}ethanol (14a). LC-MS (ESI^+) (t_R = 5.38), *m/z* (relative intensity) = 387 ($2MH^+$, 26), 194 (MH^+, 100).

***N*-[(1*E*)-1-(4-Methoxyphenyl)ethylidene]butan-1-amine (14b).** LC-MS (ESI^+) (t_R = 1.82), *m/z* (relative intensity) = 411 ($2MH^+$, 22), 206 (MH^+, 100).

RESULTS AND DISCUSSION

During the reactions of the selected UV filters (Table 1) with butylamine or ethanolamine, different temperatures (20, 40, 60, and 80 °C) were selected. The higher temperatures should enforce the reactions and increase the yield of products, while the lower temperatures should assure that reactions also took place at moderate terms, which can be reached on the skin surface in direct summer midday sunlight within 15–20 min [44]. Comparing the two primary amines, it generally was observed that ethanolamine was clearly more reactive than butylamine (Figure 1), which is difficult to explain, but might be attributable to the inductive effect of the hydroxyl group.

Table 1. UV filter substances under study

Name (shortcut)	Chemical structure
Benzophenone-3 (BP-3)	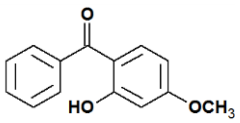
Hydroxymethylbenzoyl sulfonic acid (HMBS)	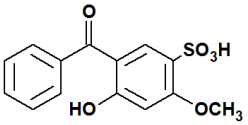
4-t-butyl-4'-methoxydibenzoyl methane (BM-DBM)	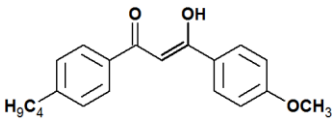
Dibenzoylmethane (DBM)	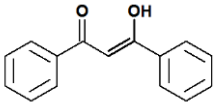
3-benzylidene camphor (3-BC)	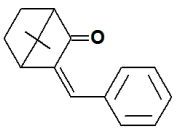
4-methylbenzylidene camphor (4-MBC)	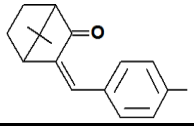

BP-3 and HMBS showed the highest reaction rates with both amines (Figure 2). Already 60 min at 80 °C led to a nearly complete conversion with ethanolamine (Figure 2A).

With butylamine, the same conversion was achieved only after 2 hours (Figure 2B). In the presence of ethanolamine, the same results were also obtained after 3 h at 40 °C and even at room temperature (Figure 1B), while in the presence of butylamine at room temperature a conversion of only about 40% (Figure 1A) was obtained. As compared to benzophenones, the reaction rates of the dibenzoylmethanes were clearly lower (Figure 2). Additionally, there was no apparent spontaneous conversion at room temperature, but heating to 40 °C significantly increased the turnover in the presence of both ethanolamine and butylamine (Figure 1A/B).

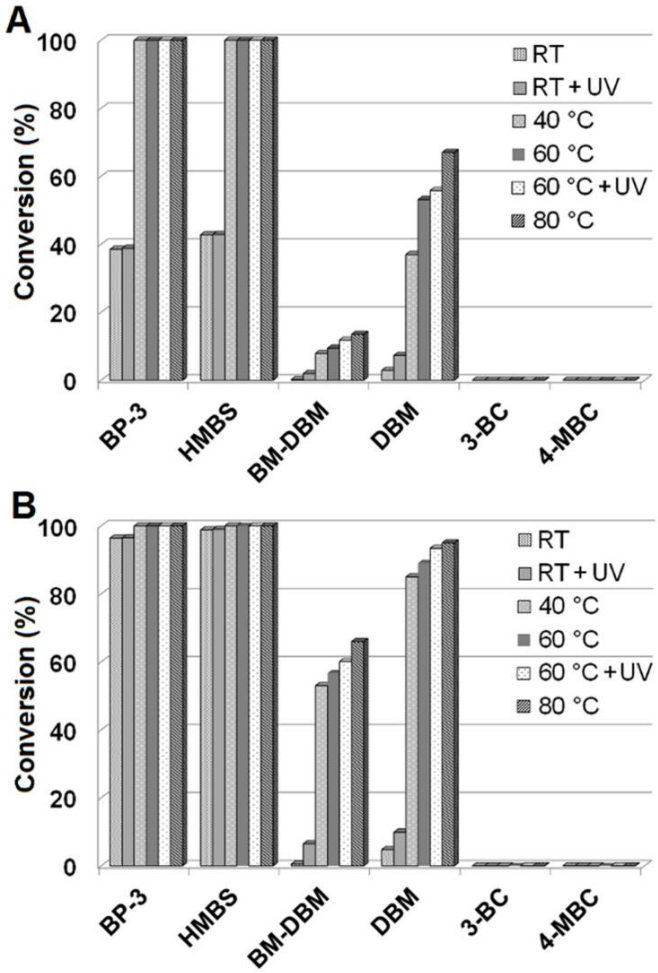

Figure 1. Conversion rates for the reactions of the studied UV filter substances with butylamine (A) or ethanolamine (B) after 3 hours under different conditions; RT (room temperature), UV (UV irradiation).

As should be expected, the amount of amine used for the reaction strongly influenced the reaction-rates; the more amine, the faster the reaction. After 1 hour heating at 40 °C in the presence of equimolar amounts of ethanolamine, nearly 30% of BP-3 was transformed (Figure 3). With a 2.5-fold or a 5-fold excess of ethanolamine, the reaction conversion doubled or even tripled. For HMBS, the results were nearly the same (Figure 3). In case of the dibenzoylmethanes, however, an excess of amines only had a minor effect on the conversions (Figure 3), which is in agreement with the generally lower reactivity.

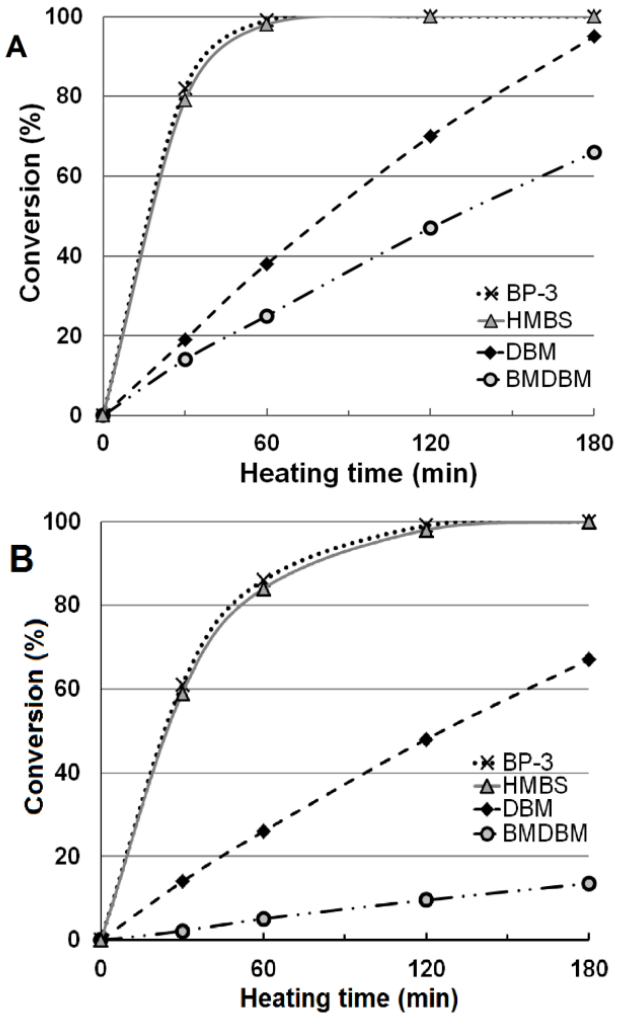

Figure 2. Reactions rates of the studied UV filter substances in the presence of ethanolamine (A) or butylamine (B) at 80 °C.

An additional UV irradiation of the reaction batches had no influence on the reactions of BP-3 and HMBS (Figure 1). For the dibenzoylmethanes, additional radiation led to a slightly increased conversion of up to 5% and 6% for DBM and BM-DBM, respectively, both at room temperature and at 60 °C, when the difference was more pronounced at ambient temperature (Figure 1).

In contrast to the highly reactive benzophenones, the two camphor derivatives 3-BC and 4-MBC (both also ketones) did not afford detectable reaction products under the used conditions with both amines. HPLC analyses resulted in recoveries of >98% of the UV filters in any case.

The differences in the reaction behaviour obviously depend on sterical hindrance or on the cyclic keto group. During the former HPTLC screening, 3-BC and 4-MBC also showed only a slight binding to the amino phase [43].

HPLC analyses resulted in recoveries of >98% of the UV filters in any case. The differences in the reaction behaviour obviously depend on sterical hindrance or on the cyclic keto group. During the former HPTLC screening, 3-BC and 4-MBC also showed only a slight binding to the amino phase [43].

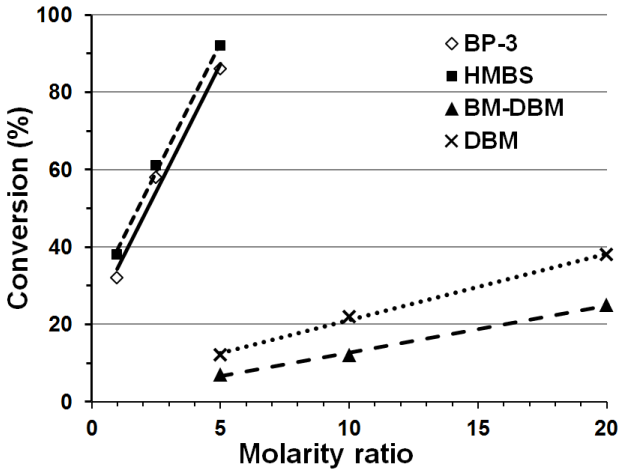

Figure 3. Conversion rates of the studied UV filter substances in the presence of ethanolamine at different molar ratios after 1 hour at 40 °C (BP-3 and HMBS) and at 80 °C (BM-DBM and DBM).

Reaction products

The reaction of BP-3 and HMBS with both amines only led to the respective imines **1a/b** and **2a/b** (Figure 4). Any by-products could not be detected, and an additional UV irradiation had also no influence on the reactions of both BP-3 and HMBS.

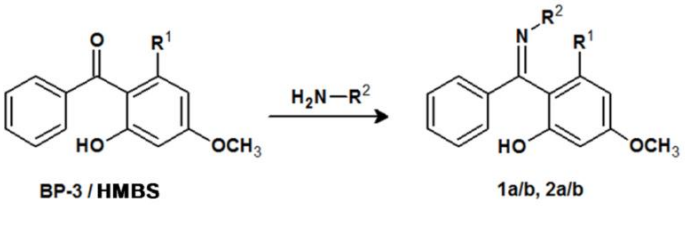

	R^1	R^2
BP-3	H	-
1a	H	C_2H_4OH
1b	H	C_4H_9
HMBS	SO_3H	-
2a	SO_3H	C_2H_4OH
2b	SO_3H	C_4H_9

Figure 4. Reaction products of BP-3 and HMBS with butylamine and ethanolamine.

BM-DBM, however, afforded a multiplicity of reaction products (Figure 5), which were assigned by LC-MS. The benzamides with both methoxy (**4a/b**) and t-butyl substituents (**8a/b**), the corresponding acetophenone derivatives (**6** and **7**), and the constitution isomers of the enamines **10a/b** and **11a/b** were detected. In the presence of an amine excess, two imines (**13a/b** and **14a/b**) were additionally identified, resulting from a further reaction of products **6** and **7** with the amines.

For an easier preparative isolation of the different reaction products and clear confirmation by NMR spectroscopy, the unsubstituted DBM was chosen. The two amides **3a/b**, the cleavage product acetophenone (**5**), and the enamines **9a/b** unequivocally could be identified (Figure 5). The additional imine by-products **12a/b** were assigned by LC-MS. As for the imine formation of BP-3 and HMBS, the formation of the dibenzoylmethane enamines generally was depending on temperature and the reaction time. Accordingly, after 3 hours at room temperature, enamines were not detectable (Figure 6). Heating at 60 °C yielded the respective enamines as main products, while an additional UV irradiation had no significant influence on their amount. Contrarily, both temperature and irradiation affected the formation of the amide products (Figure 6).

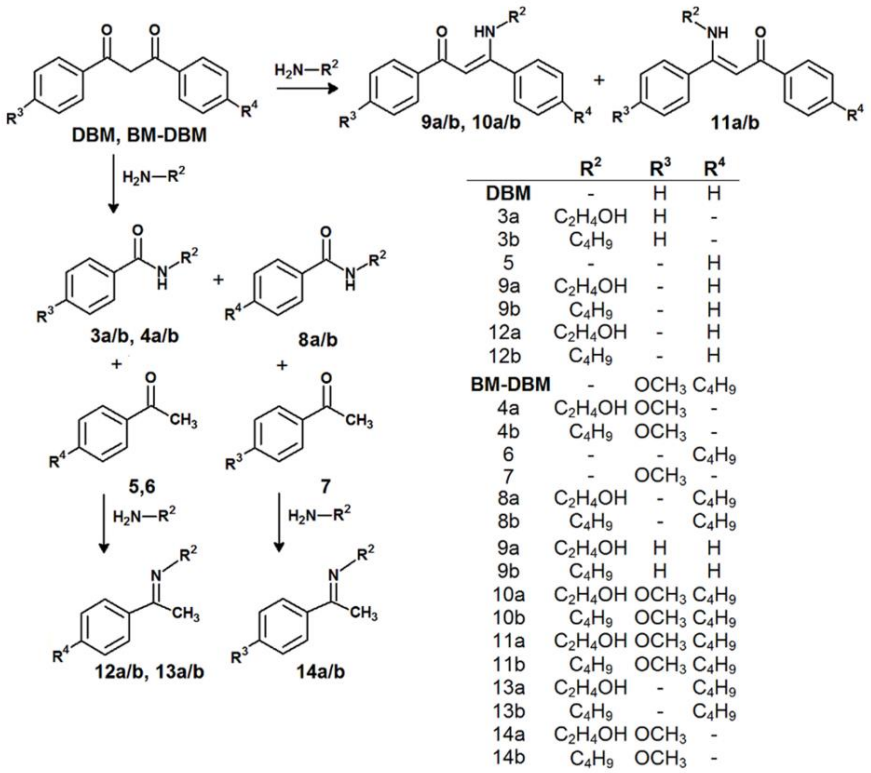

	R^2	R^3	R^4
DBM	-	H	H
3a	C_2H_4OH	H	-
3b	C_4H_9	H	-
5	-	-	H
9a	C_2H_4OH	-	H
9b	C_4H_9	-	H
12a	C_2H_4OH	-	H
12b	C_4H_9	-	H
BM-DBM	-	OCH_3	C_4H_9
4a	C_2H_4OH	OCH_3	-
4b	C_4H_9	OCH_3	-
6	-	-	C_4H_9
7	-	OCH_3	-
8a	C_2H_4OH	-	C_4H_9
8b	C_4H_9	-	C_4H_9
9a	C_2H_4OH	H	H
9b	C_4H_9	H	H
10a	C_2H_4OH	OCH_3	C_4H_9
10b	C_4H_9	OCH_3	C_4H_9
11a	C_2H_4OH	OCH_3	C_4H_9
11b	C_4H_9	OCH_3	C_4H_9
13a	C_2H_4OH	-	C_4H_9
13b	C_4H_9	-	C_4H_9
14a	C_2H_4OH	OCH_3	-
14b	C_4H_9	OCH_3	-

Figure 5. Reaction products of DBM and BM-DBM with butylamine and ethanolamine.

At 20 °C, irradiation of the ethanolamine reaction batch yielded 10 and 7 mol% amides from DBM and BM-DBM, respectively. Also at 60 °C, the additional UV irradiation resulted in slightly increased amide formation (Figure 1).

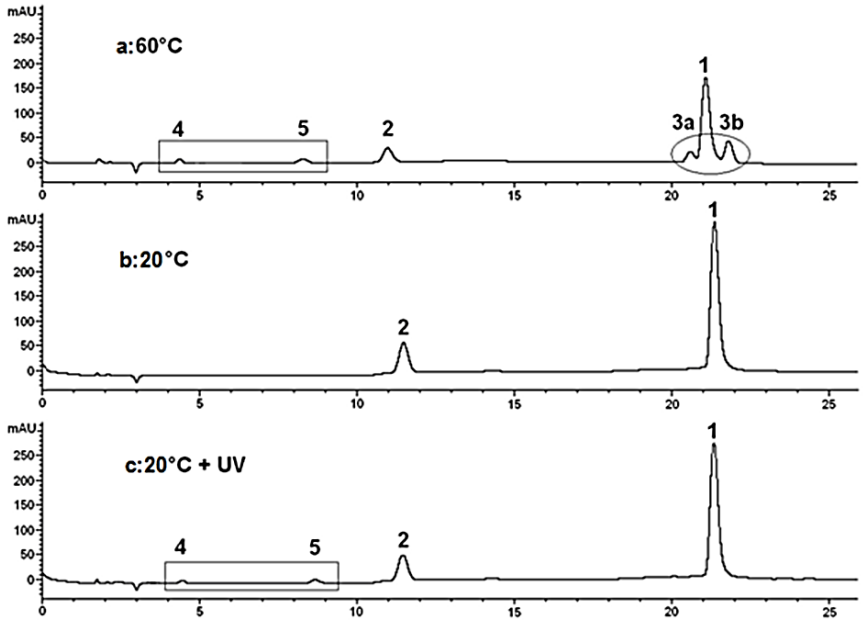

Figure 6. HPLC chromatograms of reaction batches of BM-DBM with butylamine after (a) heating for 3 hours at 60 °C under light protection, (b) 3 hours storage in the dark at 20 °C, and (c) UV irradiation at 20 °C. Detection wavelength: 250 nm; measured concentrations: 0.7 mmol/L.
1: BM-DBM keto-enol form; 2: BM-DBM diketo form; 3a /3b: enamines **10b** and **11b**; 4: 4-Methoxybenzamide (**4b**); 5. 4-*t*-Butylbenzamide (**8b**)
Contrary to previous assumptions [45, 46] that the diketo form of BM-DBM arises only under irradiation, it was already detectable in untreated standard solutions at the appropriate wavelength.

Influence of amine reactions on the UV spectra

For BP-3 and HMBS, the bonded amines participate in the resonance delocalisation process, which resulted in strong bathochromic shifts (Figure 7). A strong increase of absorbance in the UVA range was calculated for both the butylamine and ethanolamine reaction batches, which was at the expense of UVB absorption, but nevertheless resulted in an increased absorption of approximately 10% for the whole UVA+B range (Table 2).

The isolated enamines **9a/9b** showed only a small bathochromic shift and a slightly reduced absorbance (log ε = 4.46 at 359 nm). Thus, the effect was not as distinct as in the case of the benzophenones. Obviously, the enamines provide a nearly identical chromophore as the keto-enol forms of dibenzoylmethanes. The amides **3a/3b**, however, completely lost the dibenzoylmethane chromophore, leading to a strong spectrum change. The absorption maximum was located at 225 nm and 226 nm, respectively, and the absorption coefficient decreased considerably to log ε 4.07 and 4.10 for the butylamine and ethanolamine derivatives, respectively.

Therefore, the spectra of the reaction batches of both DBM and BM-DBM with ethanolamine showed a strong decrease in absorbance over the whole UVA+B range by 84 and 59%, respectively. According to the lower conversion rates, the decrease in absorbance was also lower for the reaction batches with butylamine (Table 2).

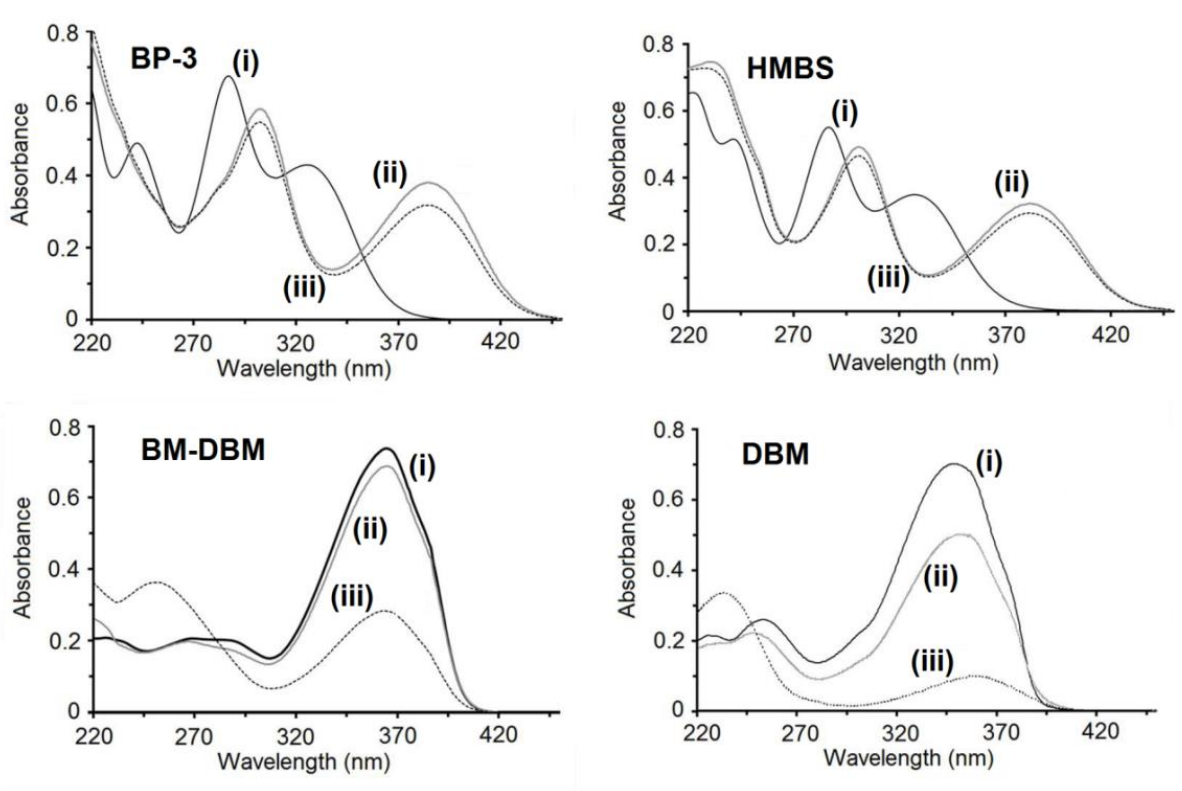

Figure 7. UV spectra of the respective UV filter standard solutions (i) and of reaction batches with butylamine (ii) and ethanolamine (iii) after 3 hours heating at 80 °C. Measured concentrations: about 5 mg/L.

Table 2. UV absorbance characteristics of the pure UV filter substances and the reactions mixtures with ethanolamine (EA) or butylamine (BA) after heating for 3 hours at 80 °C, measured at concentrations of 5 mg/L and calculated as area under the curve (AUC).

	UV-A range		UV-B range		UV-A and UV-B	
	AUC	Percentage change	AUC	Percentage change	AUC	Percentage change
BP-3	13.3		20.6		34.0	
+ EA	17.8	+ 34 %	17.9	- 13 %	35.8	+ 5 %
+ BA	20.8	+ 56 %	18.9	- 8 %	39.7	+ 17 %
HMBS	9.1		12.5		21.6	
+ EA	12.1	+ 18 %	24.7	-11 %	23.2	+ 7 %
+ BA	13.0	+ 43 %	11.6	- 7 %	24.7	+ 14 %
DBM	83.8		28.1		111.9	
+ EA	12.1	- 82 %	2.2	- 89 %	14.3	- 84 %
+ BA	67.1	- 20 %	19.7	- 30 %	86.8	- 22 %
BM-DBM	39.0		8.1		46.8	
+ EA	14.8	- 62 %	4.3	- 47 %	19.0	- 59 %
+ BA	36.3	- 7 %	7.2	- 11 %	43.2	- 8 %

CONCLUSION

The present study shows that the UV filter substances BP-3, HMBS, DBM, and BM-DBM (all with a functional carbonyl group) indeed were able to react with primary amines. Under the influence of heat and/or UV irradiation, the generation of different reaction products like imines, amides, and enamines could be detected, which are also to be expected in the presence of skin proteins. With a molar excess of amine (corresponding to the conditions after application on the skin), the reaction rates increased significantly.

Reactions with primary amines clearly affect the UV spectra. In the case of DBM and BM-DBM, reactions are associated with a significant decrease of absorption strength and a loss of the UVA protection. On the contrary, for BP-3 and HMBS the conversions lead to bathochromic shifts and hence to approved UVA protection.

The observation that the camphor derivatives 3-BC and 4-MBC did not form detectable reaction products with amines under the conditions used reflects the results of our previous HPTLC screenings.

Further studies with proteins and skin models will have to show, if the results obtained in this study are transferable to more complex skin model systems. In addition, experiments with further UV filters, e. g. with ester structures, will show, whether the already developed fast screening actually allows direct conclusions about the reactivity of sunscreen filter substances with proteins. Ideally, the screening is also suitable for a first assessment of other cosmetic ingredients having moieties reactive towards proteins.

CONFLICT OF INTEREST STATEMENT

The authors of this publication declare that there is no conflict of interest.

REFERENCES

1. Zittermann, A. and Gummert, J. F. 2010, J. Photochem. Photobiol. B, 101, 124.
2. Keményа, L. and Korecka, A. 2007, J. Photochem. Photobiol. B, 87, 58.
3. Hart, P. H., Gorman, S. and Finlay-Jones, S. J. 2011, Nat. Rev. Immunol., 11, 584.
4. Holick, M. F. 2004, Am. J. Cli. Nutr., 80, 1678.
5. Mehta, B. K. 2010, J. Neuroln. Sci., 292, 5.
6. Kent, S. T., McClure, L. A., Crosson, W. L., Arnett, D. K., Wadley, V. G. and Sathiakumar, N. 2009, Environ. Health, 8, 34. doi: 10.1186/1476-069X-8-34.
7. Partonen, T. 1994, J. Affect. Disorders, 30, 47.
8. Lambert, G. W., Reid, C., Kaye, D. M., Jennings, G. L. and Esler, M. D. 2002, Lancet, 360, 1840.
9. Khoraminya, N., Tehrani-Doost, M., Jazayeri, S., Hosseini, A. and Djazayery, A. 2012, Aust. N. Z. J. Psychiatry, 47, 271.
10. Murphy, G., Young, A. R., Wulf, H. C., Kulms, D. and Schwarz, T. 2001, Exp. Dermatol., 10, 155.
11. Davies, M. J. 2003, Biochem. Bioph. Res. Co., 305, 761.
12. Polefka, T. G., Meyer, T. A., Agin, P. P. and Bianchini, R. J. 2012, J. Cosmet. Dermatol., 11, 134.
13. Rabe, J. H., Mamelak, A. J., McElgunn, P. J. S., Morison, W. L. and Sauder, D. N. 2006, J. Am. Acad. Dermatol., 55, 1.
14. Leiter, U. and Garbe, C. 2008, Adv. Exp. Med. Biol., 624, 89.
15. Traianou, A., Ulrich, M., Apalla, Z., De Vries, E., Bakirtzi, K., Kalabalikis, D., Ferrandiz, L., Ruiz-de-Casas, A., Moreno-Ramirez, D., Sotiriadis, D., Ioannides, D., Aquilina, S., Apap, C., Micallef, R., Scerri, L., Pitkänen, S., Saksela, O., Altsitsiadis, E., Hinrichs, B., Magnoni, C., Fiorentini, C., Majewski, S., Ranki, A., Proby, C. M., Stockfleth, E. and Trakatelli, M.; EPI-DERM Group. 2012, Br. J. Dermatol., 167, 36.
16. Iannacone, M. R., Wang, W., Stockwell, H. G., O'Rourke, K., Giuliano, A. R., Sondak, V. K., Messina, J. L., Roetzheim, R. G., Cherpelis, B. S., Fenske, N. A. and Rollison, D. E. 2012, BMC Cancer, 12, 417. doi: 10.1186/1471-2407-12-417.
17. Saccà, S. C., Roszkowska, A. M. and Izzotti, A. 2013, Mutat. Res., 752, 153-171.
18. Roberts, J. E. 2011, Eye Contact Lens, 37, 249.
19. Regulation (EC) No. 1223/2009 of the European Parliament and of the Council of 30 November 2009 on cosmetic products.
20. Moyal, D. 2012, Indian J. Dermatol. Venereol. Leprol., 78, 24.
21. Bernerd, F. C., Marionnet, C. and Duval, C. 2012, Indian J. Dermatol. Venereol. Leprol., 78, 15.
22. Gaspar, L. R. and Campos, R. M. 2007, Int. J. Pharm., 343, 181.

23. Official Journal of the European Commission, Recommendation on the efficacy of sunscreen products and the claims made relating thereto, 22 September 2006.
24. Seité, S. and Fourtanier, A. M. 2008, J. Am. Acad. Dermatol., 58, 160.
25. Manová, E., von Goetz, N., Hauri, U., Bogdal, C. and Hungerbühler, K. 2012, Int. J. Hyg. Environ. Health, 216, 508.
26. Singh, M. and Beck, M. H. 2007, Contact Dermatitis, 56, 48.
27. Kerr, A. and Ferguson, J. 2010, Photodermatol. Photoimmunol. Phoromed., 26, 56.
28. Avenel-Audran, M., Dutartre, H., Goossens, A., Jeanmougin, M., Comte, C., Bernier, C., Benkalfate, L., Michel, M., Ferrier-Lebouëdec, M. C., Vigan, M., Bourrain, J. L., Outtas, O., Peyron, J. L. and Martin, L. 2010, Arch. Dermatol., 146, 753.
29. Greenspoon, J., Ahluwalia, R., Juma, N. and Rosen, C. F. 2013, Dermatitis, 24, 29.
30. Hughes, T. M. and Stone, N. M. 2007, Contact Dermatitis, 56, 153.
31. Landers, M., Law, S. and Storrs, F. J. 2003, Am. J. Contact Dermatol., 14, 33.
32. Rodríguez, E., Valbuena, M. C., Rey, M. and Porras de Quintana, L. 2006, Photodermatol. Photoimmunol. Photomed., 22, 189.
33. Divkovic, M., Pease, C. K., Gerberick, G. F. and Basketter, D. A. 2005, Contact Dermatitis, 53, 189.
34. Aleksica, M., Pease, C. K., Basketter, D. A., Panicoa, M., Morrisa, H. R. and Della, A. 2007, Toxicol. In Vitro, 21, 723.
35. Elahi, E. N., Wright, Z., Hinselwood, D., Hotchkiss, S. A., Basketter, D. A. and Pease, C. K. 2004, Chem. Res. Toxicol., 17, 301.
36. Natsch, A., Gfeller, H., Haupt, T. and Brunner, G. 2012, Chem. Res. Toxicol., 25, 2203.
37. Melles, D., Vielhaber, T., Baumann, A., Zazzeroni, R. and Karst, U. 2013, J. Chromatogr. B Analyt. Technol. Biomed. Life Sci., 913-914, 106.
38. Aleksic, M., Pease, C. K., Basketter, D. A., Panico, M., Morris, H. R. and Dell, A. 2008, Toxicol. In Vitro, 22, 1169.
39. Andreu, I., Mayorga, C. and Miranda, M. A. 2010, Curr. Opin. Allergy Clin. Immunol., 10, 303.
40. Karlsson, I., Hillerström, L., Stenfeldt, A. L., Mårtensson, J. and Börje, A. 2009, Chem. Res. Toxicol., 22, 1881.
41. Karlsson, I., Vanden Broecke, K., Mårtensson, J., Goossens, A. and Börje, A. 2010, Contact Dermatitis, 64, 343.
42. Karlsson, I., Persson, E., Mårtensson, J. and Börje, A. 2012, Photochem. Photobiol., 88, 904.
43. Stiefel, C. and Schwack, W. 2013, Int. J. Cosmetic Sci., 35, 588.
44. Kagetsu, N., Gange, R. W. and Parrish, J. A. 1985, J. Invest. Dermatol., 85, 445.
45. Damiani, E., Baschong, W. and Greci, L. 2007, J. Photochem. Photobiol. B, 87, 95.
46. Vallejo, J. J., Mesa, M. and Gallardo, C. 2011, Vitae-Columbia, 18, 63.

.

IV Reactions of cosmetic UV filters with skin proteins: model studies of esters with primary amines

Constanze Stiefel, Wolfgang Schwack

Reprinted with permission from: *Trends in Photochemistry & Photobiology* 2013, 15, 105-116.

ABSTRACT

Cosmetic UV filter substances are known triggers for contact or photocontact allergies. UV filters contain reactive carbonyl groups, which are possible reaction partners for free amino acids or proteins from human skin, through which they can act as haptens. Prior screening using high performance thin layer chromatography (HPTLC) amino phase showed that commonly used UV filters with responsive ester groups were able to bind covalently to the amino side chains of the plate after heating and/or UV irradiation. The aim of the study presented here was to investigate the underlying reaction mechanisms and to assign possible reaction products for the UV filter substances octocrylene (OCR), ethylhexyl methoxycinnamate (EHMC), ethylhexyl salicylate (EHS), octyldimethyl-p-aminobenzoic acid (OD-PABA), and ethylhexyl triazone (EHT), using two primary amines, namely ethanolamine and butylamine, as reaction partners. Heating of the reaction batches completely transformed OCR into its corresponding benzophenone imines, while for EHS, EHT, and EHMC, ester aminolysis mainly yielded their respective amides. In the case of EHMC, a Michael-type addition reaction also occurred, which resulted in addition of the primary amines to the conjugated double bond. Further UV irradiation of the reaction batches slightly affected the product distribution of OCR and of EHMC, but not of EHS and EHT. The observed reactions generally had great influences on the absorption spectra. For EHS, a significant bathochromic shift and an increased absorbance were observed, while for EHMC, and especially for OCR, UVA+B efficiency was clearly lost. In contrast, for OD-PABA, no reaction products could be generated under the conditions used.

KEYWORDS: UV filters, UV irradiance, protein binding, ester-amine adducts, mass spectrometry, NMR, OCR, EHMC, UV absorbance

INTRODUCTION

Various case reports, patch test and photopatch test data published in recent years suggest that synthetic UV filter substances are often the cause of allergic and photoallergic contact reactions of the skin [1-8]. This certainly is, among other things, attributed to the increasing use of UV filters in a variety of cosmetic products, including specific sun protection products and also in many daily body care products such as hand and face cream, hair spray and make-up products. These products advertise UV protection to prevent early signs of skin aging triggered by daily sun exposure [9, 10].

UV filters are important cosmetic ingredients. However, their extended usage with increased skin contact time challenges their behavior and stability, including photostability, and hence their protection capability [11-13]. As a result, their protection capability could be quite different on the skin than in a comparable *in vitro* test [14].

Indeed, reactions of UV filters and their photodegradation products with skin proteins are to be expected. The formation of protein adducts is associated with a certain hapten activity and the incidence of contact allergic skin reactions [15-17]. Several publications have focused on the identification of reactive groups and elucidation of possible underlying reaction mechanisms [18-20]. However, the reaction potential of cosmetic UV filter substances with proteins has not been extensively examined [21-23].

Recently, we developed a fast and simple screening method using an HPTLC amino plate as a protein model layer to get an initial evaluation of the reactivity of different UV filter substances towards amino groups of skin constituents [24]. The tested UV filters were either ketones or esters, and they revealed a different degree of reactivity after heating or irradiation. To further examine the underlying reaction mechanisms, we applied two primary amines as reaction partners for the common UV filters butylmethoxydibenzoylmethane (BM-DBM), benzophenone-3 (BP-3), 3-benzylidene camphor (3-BC), 4-methylbenzylidene camphor (4-MBC), and hydroxy-4-methoxybenzophenone-5-sulfonic acid (HMBS), all of which provide reactive keto or diketo groups. Different reaction products and conversion rates could be identified, which depended on the UV filter skeletons and the reaction conditions [25].

Therefore, the aim of the present study was to extend these studies to UV filter substances containing ester groups, such as ethylhexyl methoxycinnamate (EHMC), octocrylene (OCR), ethylhexylsalicylate (EHS), octyldimethyl-paminobenzoic acid (OD-PABA), and ethylhexyl triazone (EHT). Using butylamine and ethanolamine as reaction partners and simple models for amino acids or proteins of the skin, reaction products formed under the conditions of UV irradiation and/or under slight heating were isolated and identified. Finally, the UV spectra of reaction batches were recorded to determine the effects of reaction products on the UVA and UVB absorbance.

MATERIALS AND METHODS

Ethylhexyl methoxycinnamate (EHMC, Eusolex 2292), octyldimethyl-p-aminobenzoic acid (OD-PABA, Eusolex 6007), octocrylene (OCR, Eusolex OCR) and methanol (HPLC grade) were obtained from Merck (Darmstadt, Germany). Toluene-4-sulfonic acid monohydrate (~99%) and ethanolamine (≥99%) were obtained from Fluka (Neu-Ulm, Germany). Acetonitrile (HPLC grade) was purchased from Carl Roth (Karlsruhe, Germany). 2-Ethylhexyl salicylate (EHS), butylamine (≥99.5%), ammonium formate (≥99%), dimethyl sulfoxide-d_6 (DMSO-d_6, 99.96 atom% D), D_2O (99.99 atom % D), acetone-d_6 (99.9 atom% D) and deutero-chloroform ($CDCl_3$, 99.8 atom% D) were purchased from

Aldrich (Steinheim, Germany). Ethylhexyl triazone (EHT, Uvinul T 150) was kindly provided by BASF (Ludwigshafen, Germany).

High-performance liquid chromatography (HPLC)

HPLC measurements were carried out on a 1100 liquid chromatograph (Agilent, Waldbronn, Germany), using a quaternary HPLC pump (G 1311A), a degasser (G 1315A), an autosampler (G 1313A), a column oven set to 30 °C (G 1316A), and a diode array detector (G 1315B) with DAD detection wavelength of 275 nm, 313 nm, and 360 nm (spectral bandwidth (SBW) 8 mm). The reference wavelength was 500 nm (SBW 8 mm). For data processing, the HP ChemStation software (rev. A.04.02) was used. The stationary phase was a Eurospher 100-5 C 18 HPLC column, 250 mm x 3 mm (Knauer, Berlin, Germany). The mobile phase (0.5 mL/min) consisted of acetonitrile (A) and 10 mM ammonium formate buffer set to pH 4.0 (B). For EHT, isocratic elution (90% A / 10% B) was used. For the other UV filters the gradient was % B (t(min)): 40 (0)-40 (4)-25 (9)-25 (13)-10 (17)-24 (40)-26 (40). The injection volume was 10 µL.

HPLC-electrospray ionization mass spectrometry (LC/ESI-MS)

LC/MS measurements were performed on an identical Agilent 1100 chromatograph as described above, coupled with an MSD single-quadrupole mass spectrometer (G1956B, Agilent) equipped with an electrospray ionization (ESI) interface. Mass spectra were generally recorded in the ESI positive full scan mode (*m/z* 50-1200), and in the case of OCR reactions, additionally in the ESI negative full scan mode (*m/z* 50-800) using the following settings: capillary voltage 4 kV, skimmer voltage 35 V, nebulizer gas pressure 20 psig, source temperature 100 °C, drying gas temperature 300 °C, drying gas flow rate 10 L/min, fragmentator voltage 80 V, gain 1, threshold 100, and step size 0.1. For data processing, ChemStation software (Agilent) was used.

Spectroscopy

Infrared (IR) spectra were recorded on a Dura Sampler SMART ATR installed at the Avatar 320 FT-IR-Spectrometer (Thermo Nicolet, Madison, USA). The samples were applied on a diamond crystal and were recorded between 4000 and 500 cm^{-1}. A minimum of 32 scans was signalaveraged with a resolution of 2 cm^{-1}.

UV spectra were measured using a Perkin-Elmer Lambda 2 (Überlingen, Germany). ^{13}C and ^{1}H nuclear magnetic resonance (NMR) spectra were recorded at 300 MHz (^{1}H) and 75 MHz (^{13}C) on a Varian Unity Inova-300 spectrometer (Varian, Darmstadt, Germany). The samples were dissolved in $CDCl_3$, DMSO-d_6, D_2O, or acetone-d_6. The signal assignments were made based on chemical shifts related to tetra-methylsilane (TMS) and H-H and C-H correlation data; s = singlet, d = doublet, t = triplet, q = quartet and m = multiplet.

Thermal reaction of UV filters with amines

Each UV filter (0.5 mmol) was weighed into a 10 mL screw-capped glass tube (Schott, Mainz, Germany) and suspended in acetonitrile (5 mL), except for EHT, which was suspended in 5 mL acetonitrile/toluene (80/20). Butylamine (1 mL, 10 mmol) or 0.6 mL of ethanolamine (10 mmol) and toluene-4-sulfonic acid monohydrate (1 mg, 5 µmol) were added. The mixture was heated for 3 h at 40 or 80 °C. Afterwards, the reaction was stopped by cooling the tubes under running tap water. As controls, reaction batches were stored in the dark, at an ambient temperature of approximately 20 °C.
To determine the impact of the quantity of amine on the reaction, different amounts of ethanolamine were used (equimolar, 3- and 5-fold excess for OCR, 5-, 10- and 20-fold excess for EHS and EHMC, and 10-, 20- and 30-fold excess for EHT).

Photoreaction of UV filters in the presence of amines

Each UV filter (2 mmol) was weighed into a 50 mL quartz beaker with a diameter of 38 mm (Th. Geyer, Renningen, Germany) and suspended in acetonitrile (20 mL), except for EHT, where acetonitrile/toluene (80/20, 20 mL) was used. Either butylamine or ethanolamine (40 mmol) and toluene-4-sulfonic acid monohydrate (3.8 mg, 20 µmol) were added. The beaker was tightly closed by a teflon cap and irradiated for 3 h. To maintain a consistent temperature (20 °C or 60 °C), the beaker was placed inside a quartz glass flow chamber, which was connected to a chiller (Model RML 6, Lauda, Germany). For irradiation, a modified sun simulator SOL 500 with a 430 W metal halide lamp (Dr. Höhnle, Gräfelfing, Germany) was used. The modification involved the front filter glass being replaced by an aluminum plate with two 16 cm^2 gaps to hold two WG 295 glass filters (Schott, Mainz, Germany). The irradiation intensities were 12.5 mW/cm^2 in the UVA and 0.55 mW/cm^2 in the UVB range. For 3 hours of irradiation, the corresponding light doses were 1410 kJ/m^2 (2.3 kJ/quartz beaker). The solutions were stirred continuously using a Variomag Micro stirrer (Thermo Scientific). To distinguish between the effects of heat or UV radiation on the reaction, a second batch was prepared in another quartz beaker in the same manner, but was completely covered by aluminum foil and placed aside the irradiated sample.

Isolation of the reaction products

The reaction solutions were evaporated to dryness in a Labconco (Kansas City, USA) CentriVap concentrator equipped with a CentriVap cold trap at a temperature of 35 °C. For OCR, the obtained residues could be directly used for NMR spectroscopy. For the reaction batches of the other UV filters, the residues were dissolved in 5 mL methanol. To isolate the reaction products, 1 mL of the methanolic solution (five injections) was subjected to a preparative Kronlab HPLC system (Sinsheim, Germany) consisting of a HD 2-200 HPLC pump, a C-R3A Chromatopac Integrator (Shimadzu), and a Variable Wavelength Monitor (Knauer, Berlin, Germany).

For separation, a YMC (Dinslaken, Germany) HPLC column (ODS-A, RP 18, 5 µm, 20 mm x 25 cm) was used. For the first 14 min elution was performed with acetonitrile/water (60/40), followed by a 3 min flushing of the column with pure acetonitrile. The detection wavelength was 275 nm and the flow rate 8 mL/min. The respective fractions were collected, the solvent was evaporated and the residue dried over phosphorus pentoxide. The purity of the products was examined by HPLC/DAD.

Reaction products isolated from the respective batches after 3 hours at 80 °C

EHS

N-(2-Hydroxyethyl)-2-methoxybenzamide. 90 mg (99 mol%) of purewas obtained as reddishbrown, highly viscous oil. UV/Vis (methanol) λ_{max} (nm) (log ε) 315 (3.60). IR (ATR) ν (cm^{-1}): 3355-3270 (m), 3055 (w), 2932 (m), 2862 (m), 1609 (s), 1554 (2), 1448 (m), 1322 (m), 1243 (w), 1144 (w), 1070 (m), 1030 (m), 853 (w), 766 (w), 700 (w). LC-MS (ESI^+) (t_R = 2.77) *m/z* (relative intensity) = 182 (MH+, 100), 147 (22), 121 (10), 106 (21). ^1H NMR (D_2O, 300 MHz) δ (ppm) 7.82 (m, 1H), 7.31 (m, 1H), 6.77 (m, 1H), 6.65 (m, 1H), 3.77 (t, 2H, ^3J = 5.6 Hz), 3.55 (t, 2H, ^3J = 5.6 Hz). ^{13}C NMR (D_2O, 300 MHz) δ (ppm) 171.2, 168.8, 134.0, 129.7, 122.2, 118.4, 114.2, 60.7, 41.3.

N-Butyl-2-methoxybenzamide. 87 mg (90 mol%) of pure **1b** was obtained as yellow-brown viscous oil. UV/Vis (methanol) λ_{max} (nm) (log ε) 317 (3.63). IR (ATR) ν (cm^{-1}): 3505-3270 (m), 3055 (w), 2956 (s), 2929 (m), 2870 (m), 1633 (s), 1597 (s), 1538 (s), 1498 (m), 1456 (m), 1365 (w), 1306 (m), 1227 (m), 1144 (w), 1034 (w), 865 (w), 754 (m), 699 (w). LC-MS (ESI^+) (t_R = 4.69) *m/z* (relative intensity) = 194 (MH^+, 100), 147 (22), 121 (3), 106 (32). ^1H NMR (acetone-d_6, 300 MHz) δ (ppm) 7.82 (m, 1H), 7.37 (m, 1H), 6.89 (m, 1H), 6.81 (1H, m), 3.41 (2H, t, ^3J = 7.0 Hz), 1.61 (2H, m), 1.39 (2H, m), 0.93 (3H, t, ^3J = 7.3). ^{13}C NMR (acetone-d_6, 300 MHz) δ (ppm) 170.4, 162.7, 134.4, 127.6, 118.8, 118.6, 115.9, 39.6, 32.2, 20.7, 14.0.

EHMC

(2E)-N-(2-Hydroxyethyl)-3-(4-methoxyphenyl)-prop-2-enamide. 21.6 mg (20 mol%) of pure **2a** was obtained as yellow, very viscous liquid. UV/Vis (methanol) λ_{max} (nm) (log ε) 291 (4.27), 224 (4.21). IR (ATR) ν (cm^{-1}): 3320-3270 (s), 2930 (m), 2865 (m), 2355 (w), 1649 (m), 1595 (s), 1551 (m), 1508 (s), 1247 (m), 1225 (m), 1171 (m), 1062 (w), 1030 (w), 976 (w), 824 (m). LC-MS (ESI^+) (t_R = 3.21) *m/z* (relative intensity) = 465 ($2MNa^+$, 35), 244 (MNa^+, 5), 222 (MH^+, 100), 161 (20%). ^1H NMR (DMSO-d_6, 300 MHz) δ (ppm) 8.09 (t, 1H, ^3J = 5.5 Hz), 7.51 (m, 2H), 7.36 (d, 1H, ^3J = 15.8 Hz), 6.96 (m, 2H), 6.51 (d, 1H, ^3J = 15.8 Hz), 3.77 (s, 3H), 3.46 (t, 2H, ^3J = 5.9 Hz), 3.24 (m, 2H); ^{13}C NMR (DMSO-d_6, 300 MHz) δ (ppm) 166.5, 161.0, 139.3, 129.9, 128.1, 120.2, 115.1, 60.6, 56.0, 42.3.

(2E)-N-Butyl-3-(4-methoxyphenyl)-prop-2-enamide. 8.2 mg (7 mol%) of pure **2b** was obtained as light-brown, very viscous liquid. UV/Vis (methanol) λ_{max} (nm) (log ε) 290 (4.29), 225 (3.99). IR (ATR) ν (cm^{-1}): 3290-3210 (m), 3071 (w), 2952 (m), 2930 (m), 2865 (w), 2344 (w), 1649 (m), 1595 (s), 1551 (m), 1508 (s), 1453 (w), 1301 (w), 1286 (w), 1247 (m), 1225 (m), 1171 (m), 1029 (w), 976 (w), 824 (w). LC-MS (ESI^+) (t_R = 5.43) *m/z* (relative intensity) = 467 ($2MH^+$, 20), 234 (MH^+, 100), 161 (3%). ^1H NMR ($CDCl_3$, 300 MHz) δ (ppm) 7.57 (d, 1H, ^3J = 15.5 Hz), 7.44 (m, 2H), 6.68 (m, 2H), 5.55 (t, 1H, ^3J = 6.1 Hz), 6.25 (d, 1H, ^3J = 15.5 Hz), 3.83 (m, 3H), 3.39 (m, 2H), 1.55 (m, 2H), 1.40 (m, 2H), 0.95 (t, 3H, ^3J = 7.2 Hz); ^{13}C NMR ($CDCl_3$, 300 MHz) δ (ppm) 166.4, 161.1, 140.6, 129.5, 127.9, 118.7, 114.5, 55.6, 39.7, 32.1, 20.4, 14.0.

N-(2-Hydroxyethyl)-3-[(2-hydroxyethyl)-amino]-3-(4-methoxyphenyl)propanamide. 14.4 mg (10 mol%) of pure **4a** was obtained as lightbrown, very viscous liquid. UV/Vis (methanol) λ_{max} (nm) (log ε) 226 (4.17), 201 (4.37). IR (ATR) ν (cm^{-1}): 3390-3280 (s), 2953 (m), 2920 (m), 2863 (w), 1716 (w), 1632 (m), 1594 (s), 1545 (m), 1508 (s), 1453 (w), 1306 (w), 1247 (m), 1225 (m), 1170 (m), 1057 (w), 1029 (w), 975 (w), 823 (w). LCMS (ESI^+) (t_R = 4.12) *m/z* (relative intensity) = 283 (MH^+, 100), 222 (5%).

N-Butyl-3-(butylamino)-3-(4-methoxyphenyl)-propanamide. 6.3 mg (4 mol%) of pure **4b** was obtained as bright yellow, fine powder. UV/Vis (methanol) λ_{max} (nm) (log ε) 226 (4.23), 201 (4.43). IR (ATR) ν (cm^{-1}): 3299 (w), 2952 (m), 2919 (m), 2865 (w), 1714 (m), 1627 (m), 1594 (m), 1540 (w), 1508 (s), 1453 (w), 1440 (w), 1247 (m), 1160 (m), 1030 (w), 824 (w). LC-MS (ESI^+) (t_R = 10.21) *m/z* (relative intensity) = 307 (MH^+, 100), 234 (5%). ^1H NMR ($CDCl_3$, 300 MHz) δ (ppm) 7.21 (m, 2H), 6.88 (m, 2H), 3.79 (2, 3H), 3.89 (m, 1H), 3.22 (m, 2H), 2.48 (m, 2H), 2.43 (m, 2H), 1.42 (m, 4H), 1.31 (m, 4H), 0.89 (m, 6H); ^{13}C NMR ($CDCl_3$, 300 MHz) δ (ppm) 171.7, 159.1, 135.2, 127.8, 114.2, 59.7, 55.5, 47.0, 44.4, 39.1, 32.5, 31.9, 20.7, 20.4, 14.2, 14.0.

By-products (identified by mass spectrometry):

2-Ethylhexyl 3-[(2-hydroxyethyl)amino]-3-(4-methoxyphenyl)propionate (3a). LC-MS (ESI^+) (t_R = 5.16) *m/z* (relative intensity) = 352 (MH^+, 100).

2-Ethylhexyl 3-(butylamino)-3-(4-methoxyphenyl)propionate (3b). LC-MS (ESI^+) (t_R = 16.20) *m/z* (relative intensity) = 364 (MH^+, 100).

OCR

2-[(Diphenylmethylene)imino]ethanol. 111 mg (98 mol%) of pure **5a** was obtained as yellow highly viscous oil. UV/Vis (methanol) λ_{max} (nm) (log ε) 245 (4.11). IR (ATR) ν (cm^{-1}): 3500-3250 (m), 3080-3010 (m), 2919 (m), 2872 (m), 1656 (s), 1620 (s), 1593 (m), 1573 (m), 1442 (s), 1314 (m), 1271 (s), 1068 (w), 1024 (w), 941 (w), 762 (w), 695 (s), 639 (w). LC-MS (ESI^+) (t_R = 4.08) *m/z* (relative intensity) = 226 (MH^+, 100), 106 (4). ^1H NMR ($CDCl_3$, 300 MHz) δ (ppm) 7.61 (m, 4H), 7.30-7.48 (m, 6H), 3.84 (t, 2H, ^3J = 5.3 Hz), 3.49 (2H, t, ^3J = 5.3 Hz). ^{13}C NMR ($CDCl_3$, 300 MHz) δ (ppm) 169.9, 136.7, 130.2, 128.3, 127.7, 62.9, 55.5.

N-Butyl-1,1-diphenylmethanimine. 115 mg (97 mol%) of pure **5b** was obtained as yellow highly viscous oil. UV/Vis (methanol) λ_{max} (nm) (log ε) 244 (4.12). IR (ATR) ν (cm^{-1}): 3500-3200 (w), 3080-3015 (w), 2961 (s), 2921 (s), 2859 (s), 1659 (m), 1617 (s), 1593 (m), 1576 (m), 1442 (m), 1311 (w), 1278 (m), 1070 (w), 1029 (w), 780 (m), 764 (m), 694 (s), 637 (w). LC-MS (ESI^+) (t_R = 14.46) *m/z* (relative intensity) = 238 (MH^+, 100), 106 (3). ^1H NMR ($CDCl_3$, 300 MHz) δ (ppm) 7.59 (m, 4H), 7.31-7.49 (m, 6H), 3.37 (2H, t, ^3J = 7.0 Hz), 1.65 (2H, m), 1.34 (2H, m), 0.87 (3H, m). ^{13}C NMR ($CDCl_3$, 300 MHz) δ (ppm) 167.7, 137.1, 129.7, 128.4, 127.9, 53.6, 33.4, 20.6, 13.9.

By-products (identified by mass spectrometry):

2-Ethylhexyl cyanoacetate (6). LC-MS (ESI^-) (t_R = 4.19) *m/z* (relative intensity) = 196 ($[M-H]^-$, 100).

2-Cyano-N-(2-hydroxyethyl)acetamide(7a).C-MS (ESI^-) (t_R = 3.12) *m/z* (relative intensity) = 127 ($[M-H]^-$, 100).

N-Butyl-2-cyanoacetamide(7b). LC-MS (ESI^-) (t_R = 3.38) *m/z* (relative intensity) = 139 ($[M-H]^-$, 100).

By-products formed under additional UV irradiation (identified by mass spectrometry):

2-Hydroxyethyl-2-cyano-3,3-diphenyl-2-propenamide (8a). LC-MS (ESI^+) (t_R = 2.86) *m/z* (relative intensity) = 293 (MH^+, 100), 315 (MNa^+, 5).

2-Butyl-2-cyano-3,3-diphenyl-2-propenamide (8b). LC-MS (ESI^+) (t_R = 12.68) *m/z* (relative intensity) = 305 (MH^+, 100), 327 (MNa^+, 6), 631 ($2MNa^+$, 30).

EHT

4-[[4,6-Bis[[4-(2-ethylhexoxy-oxomethyl)-phenyl]amino]-1,3,5-triazin-2-yl]amino]benzoic acid 2-hydroxyethyl amide. 20.3 mg (5 mol%) of pure **9** was obtained as colorless powder. UV/Vis (methanol) λ_{max} (nm) (log ε) 313 (5.02). IR (ATR) ν (cm^{-1}): 3500-3200 (s), 2958 (m), 2924 (s), 2855 (m), 2360 (s), 2341 (m), 1693 (w), 1609 (m), 1490 (m), 1414 (m), 1310 (w), 1278 (m), 1248 (w), 1177 (w), 1111 (w), 851 (w), 768 (w), 668 (w). LC-MS (ESI^+) (t_R = 17.91) *m/z* (relative intensity) = 754 (MH^+, 100), 308 (10). ^1H NMR ($CDCl_3$, 300 MHz) δ (ppm) 8.02 (t, 1H, ^3J = 5.51 Hz), 7.81 (m, 2H), 7.74-7.66 (m, 10H), 4.25 (m, 4H), 3.89 (t, 2H, ^3J = 5.4 Hz), 3.66 (t, 2H, ^3J = 5.4 Hz), 1.73 (m, 2H), 1.45-1.20 (m, 16H), 0.96 (m, 6H), 0.90 (m, 6H). ^{13}C NMR ($CDCl_3$, 300 MHz) δ (ppm) 167.8, 166.3, 164.2, 150.5, 142.4, 130.7, 129.8, 128.0, 125.2, 119.9, 119.4, 67.8, 62.6, 42.9, 38.9, 30.6, 28.9, 24.0, 23.1, 14.0, 11.1.

RESULTS AND DISCUSSION

The reactions of the UV filter substances that were analyzed (Table 1) with the amino acid models butylamine and ethanolamine were conducted at different temperature levels: 20, 40, 60, and 80 °C. The moderate temperatures were chosen to reflect standard environmental conditions such as natural warming of the skin in direct summer sunlight within 20 min [26].

Table 1. UV filter substances under study.

Name (shortcut)	Structure
Octocrylene (OCR)	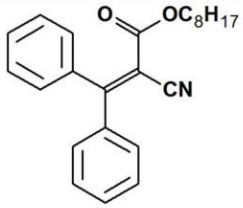
Ethylhexyl methoxycinnamate (EHMC)	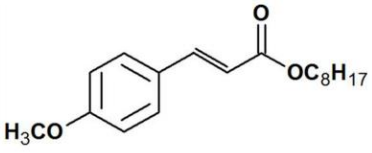
Ethylhexyl salicylate (EHS)	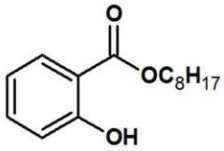
Octyl dimethyl PABA (OD-PABA)	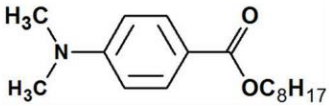
Ethylhexyl triazone (EHT)	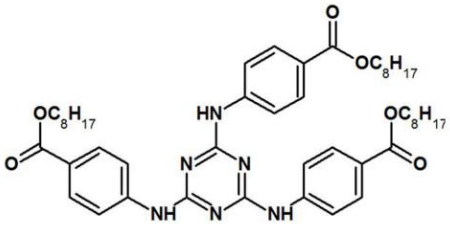

The higher temperatures should accelerate the reactions and increase the yield of the products to be isolated and elucidated. To observe the influence of UV radiation on the reactions, the batches at 20 °C and 60 °C were additionally irradiated, and the results compared to the non-irradiated samples. As already observed during the experiments with ketones [25], ethanolamine was significantly more reactive towards esters than butylamine (Figure 1).

Among the selected UV filters, OCR and EHS showed the highest reaction rates with both butylamine and ethanolamine (Figure 2), which is in good agreement with the results obtained during the previous amino HPTLC screening [24]. After only 10 min at 80 °C, OCR completely reacted with ethanolamine (Figure 2B), while with butylamine the conversion was complete within 20 min (Figure 2A).

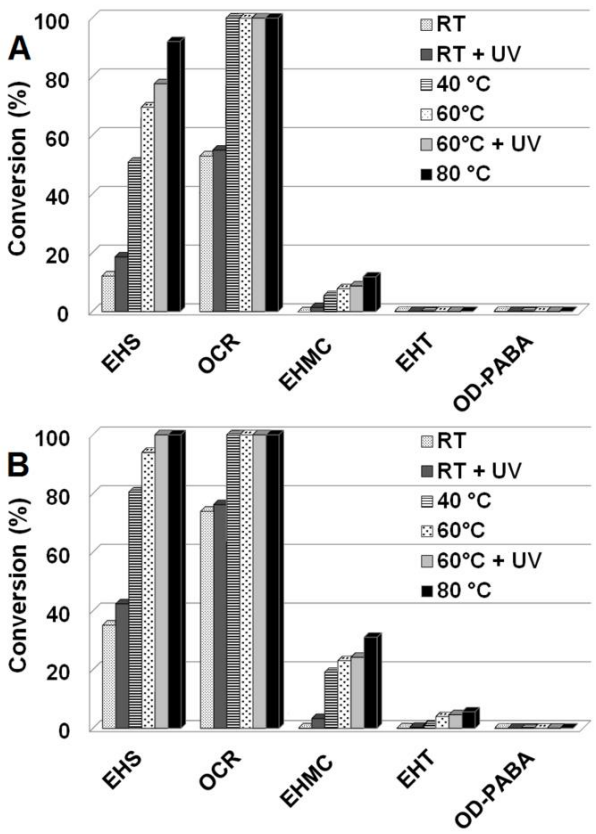

Figure 1. Conversion rates of the studied UV filters in the presence of a 20-molar excess of butylamine (A) or ethanolamine (B) under different conditions after 3 h; UV (UV irradiation), RT (room temperature).

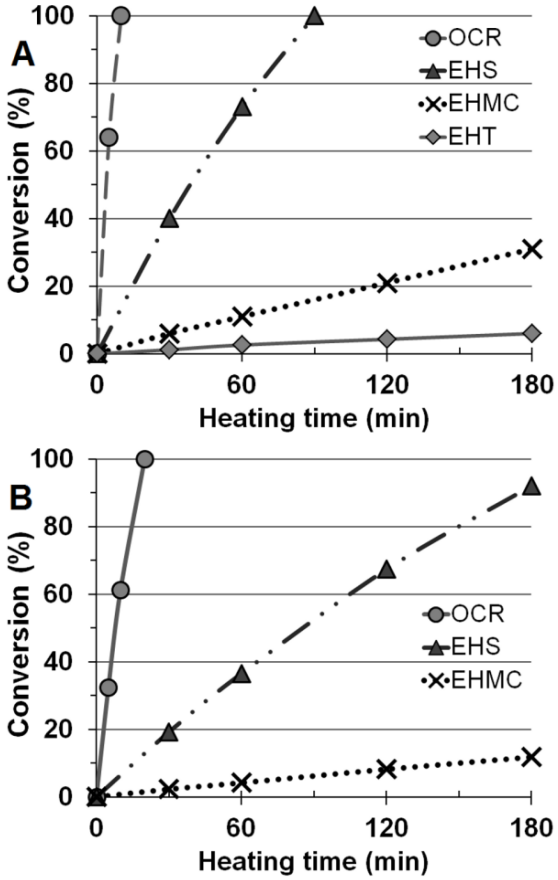

Figure 2. Reaction kinetics for the conversion of the studied UV filters in the presence of a 20-molar excess of ethanolamine (A) or butylamine (B) at 80 °C.

Even at room temperature, a high conversion of >70% or >50% was observed in the presence of ethanolamine and butylamine, respectively, after a reaction time of 3 h (Figure 1). EHS showed the same tendency as OCR, but an overall lower reactivity. At room temperature, 35% and 12% of the initial EHS reacted with ethanolamine and butylamine, respectively, within 3 h. As forOCR, heating increased the conversion significantly (Figure 1). In the presence of ethanolamine, a complete conversion of EHS was achieved after 90 min, while it took >180 min with butylamine (Figure 2). Compared to OCR and EHS, reaction rates of EHMC were clearly lower (Figure 2). At room temperature, no spontaneous conversion could be observed, but even marginal heating to 40 °C or 60 °C increased the conversion in the presence of both butylamine and ethanolamine (Figure 1). The two p-aminobenzoates, EHT and OD-PABA, showed the lowest reactivity or generally no reactivity (Figure 1). For EHT, any reactivity was limited to the reactions with ethanolamine at high temperatures, only leading to a low conversion of up to 6%. In the presence of butylamine, EHT was completely recovered, even after 3 h at 80 °C. Reaction products of OD-PABA could not be identified under the conditions used, neither with butylamine nor with ethanolamine. HPLC analyses resulted in recoveries of >99% for OD-PABA. During the former HPTLC screening, OD-PABA seemed to show a moderate binding to the amino phase, but it was already suspected that the additional formation of two photodegradation products on the plate overestimated the determined binding rate [24]. Obviously, good resonance stabilization prevents the ester moieties of EHT and OB-PABA from nucleophilic attacks including aminolysis. Otherwise, an intermolecular self-aminolysis of at least OB-PABA, resulting in a polyamide, had to be expected in cosmetic formulations.

As expected, a higher amine/UV filter ratio accelerated the reactions and increased the conversions (Figure 3). After 60 min at 40 °C with an equimolar amount of ethanolamine, approximately 40% of the provided OCR was transformed. With 3-fold and 5-fold excess of ethanolamine, the conversion rate nearly doubled and tripled, respectively. For the other UV filter substances, an excess of amine increased the conversions, but due to the overall lower reactivity, the effect was less pronounced, especially for EHMC and EHT (Figure 3).

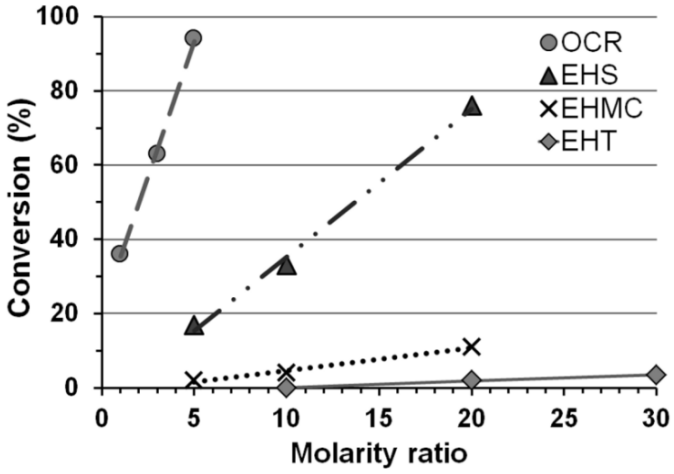

Figure 3. Conversion rates of the studied UV filters in the presence of ethanolamine at different molar ratios after 1 h at 40 °C (OCR) and at 80 °C (EHS, EHMC and EHT).

Additional UV irradiation of the reaction batches with EHS, EHMC, and EHT partly affected the reaction rates, but did not create new reaction products, except the respective Z-isomers of EHMC and **2a/b** due to the known photoisomerization [27]. This corresponds to the behavior of the ketones during the former study [25]. For OCR, however, two additional reaction products (**8a/b**) were formed under UV irradiation (Figure 4).

UV irradiation resulted in a slightly increased conversion of up to 8% for EHS, and 4% for OCR, both at room temperature and at 60 °C (Figure 1). Corresponding to the overall lower reactivity, the influence of UV irradiation on the conversion of EHMC and EHT was concurrently lower. At 20 °C, irradiation of the ethanolamine reaction batches only increased the conversion rates to 0.3% and 3% for EHT and EHMC, respectively (Figure 1). At 60 °C, the effect of additional UV irradiation was also insignificant. UV irradiation also could not activate OD-PABA in terms of reactions with primary amines.

Reaction products

The reaction of EHS with both ethanolamine and butylamine only generated the respective amides **1a/b** in high yields (Figure 4). Further byproducts could not be detected, and an additional UV irradiation had an influence on the rate of conversion, but not on the kind of products.

EHMC reacted by both ester aminolysis and Michael-type addition. As main products, the amides **2a/b** and the products **4a/b**, which resulted from a twofold reaction with the primary amines, could be isolated. The pure Michael adducts **3a/b** could only be detected by LC/MS as by-products in relatively low amounts. The kinetic data suggests that the products **4a/b** were mainly formed from **2a/b** (data not shown). The formation of the amines **3a/b** was solely dependent on temperature and reaction time. Additional UV irradiation did not significantly influence their yields (approximately the same peak areas were observed). On the contrary, both temperature and irradiation affected the formation of the amide products and the aminated amides. Irradiation of the ethanolamine reaction batch at 20 °C yielded 2 mol% of the amide **2a** and its Z-isomer (calculated as E-isomer) and 1 mol% of the aminated amide **4a**, while under dark conditions no conversion occurred. At 60 °C the additional irradiation led to an increased formation of **2a** and its Z-isomer (calculated as E-isomer) by about 8% as compared to the non-irradiated batch. This was partly at the expense of **4a**, which decreased by 5%.

For OCR, the benzophenone imines **5a/b** were the only reaction products under dark conditions, in terms of conversion influenced by reaction temperature and time (Figure 2). With additional UV irradiation at 20 °C a small amount of the amide by-products **8a/b** was detectable. At higher temperatures, however, the formation of the imines **5a/b** predominated and the amides were not formed. Regarding the surprising formation of **5a/b**, a Michael-type addition of the primary amine must first be assumed, followed by elimination of ethylhexyl cyanoacetate (**6**), which could be identified by LC/MS.

Regarding the reaction type, it is comparable to a retro-aldol cleavage. In the presence of an amine excess, the amides **7a/b** were additionally identified, resulting from a further reaction of product **6** with the amines.

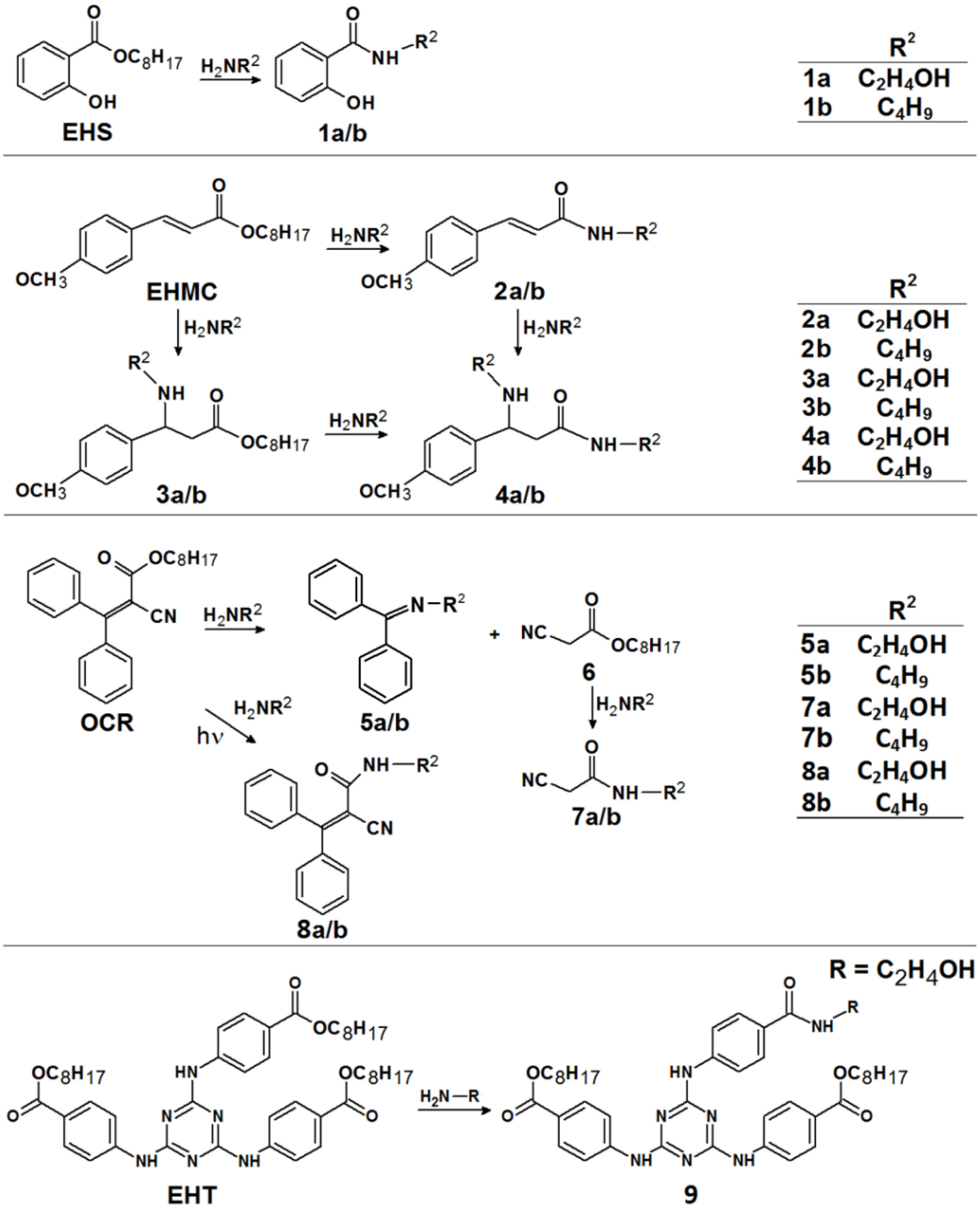

	R^2
1a	C_2H_4OH
1b	C_4H_9

	R^2
2a	C_2H_4OH
2b	C_4H_9
3a	C_2H_4OH
3b	C_4H_9
4a	C_2H_4OH
4b	C_4H_9

	R^2
5a	C_2H_4OH
5b	C_4H_9
7a	C_2H_4OH
7b	C_4H_9
8a	C_2H_4OH
8b	C_4H_9

Figure 4. Overview of the reaction products of EHS, EHMC, OCR and EHT with butylamine and ethanolamine.

While there was no reaction between EHT and butylamine, in the presence of ethanolamine EHT was only transformed into the amide **9** (Figure 4), after only one ester group had reacted. For its formation, temperature and irradiation played a role. However, temperature had a much greater impact (Figure 1). Reactions at the two other available ester groups of EHT could not be observed, even in the presence of a high excess ofethanolamine. Evidently, the findings are in agreement with the high (photo) stability of EHT.

Influence of amine reactions on the UV spectra

As expected, the bonded amines participate in the resonance delocalization process of EHS, resulting in a significant bathochromic shift (Figure 5). For both amine reaction batches, a strong increase of absorbance in the UVA range of about 200% was observed, which was partly at the expense of UVB absorption. However, over the whole UVA+B range, an increase of the absorption strength of nearly 30% was calculated (Table 2).

In contrast to EHS, noticeable shifts of absorption maxima could not be detected for the reaction batches of EHMC with both amines. However, depending on the percentage of conversion, a significant decrease of the absorption strength over the whole UVA+B range could be calculated (Table 2).

Since for OCR, the benzophenone imines **5a/b** were the main reaction products resulting in loss of conjugation, the spectral changes of the reaction batches directly correlated with the percentage of conversion (data not shown).

The absorption maxima of the benzophenone imines were at 245 nm; accordingly, the spectra of the reaction batches with both ethanolamine and butylamine showed a strong absorbance decrease over the whole UVA+B range by nearly 100%.

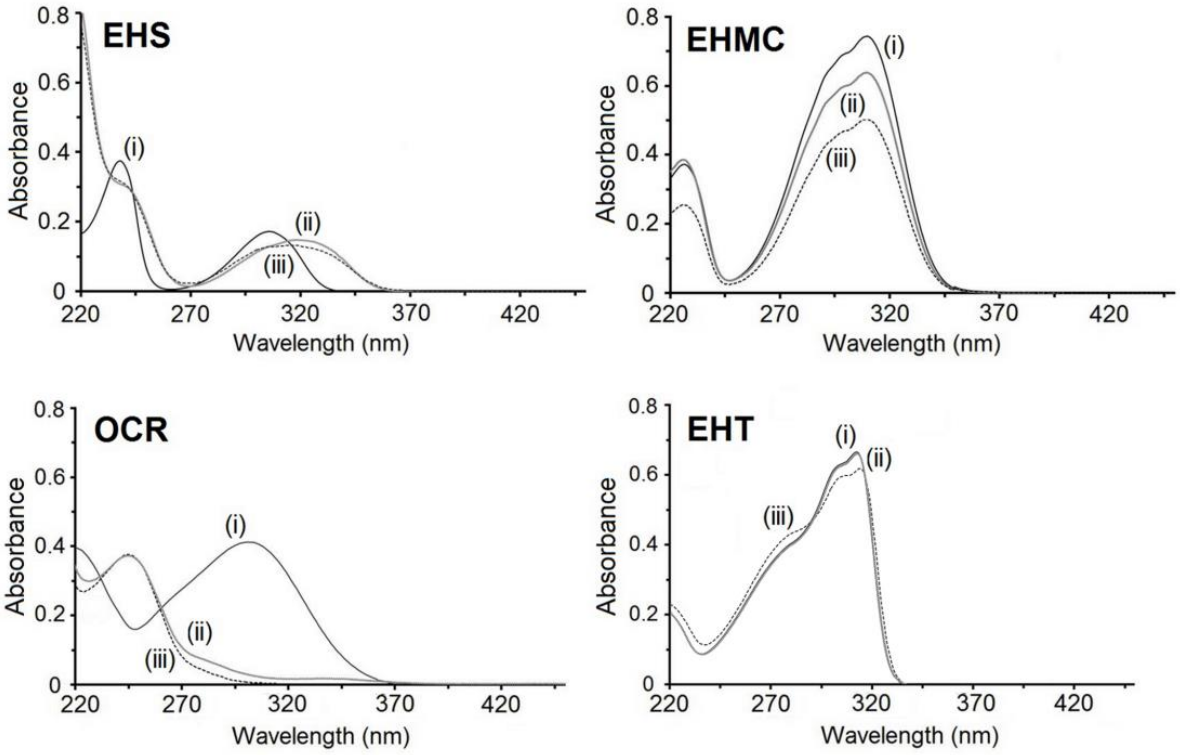

Figure 5. UV spectra of standard solutions of the studied UV filters (i) and of 20-molar reaction batches with butylamine (ii) and ethanolamine (iii) after 3 h at 80 °C; concentrations about 5 mg/L relating to the UV filter.

Due to the rather low conversion of EHT, the change in the UV spectrum of the reaction batches was insignificant. After the reaction with ethanolamine, there was only a marginal bathochromic shift of the spectrum to an adsorption maximum at 316 nm, and a small decrease of absorbance in the UVA+B range of about 2% (Table 2).

Table 2. UV absorbance characteristics of the studied UV filter substances and the reaction mixtures with an 20-molar excess of ethanolamine (EA) or butylamine (BA) after heating for 3 h at 80 °C, calculated as area under the curve (AUC), measured at concentrations of 5 mg/L.

		UVA range		UVB range		UVA and UVB	
		AUC	Percentage change	AUC	Percentage change	AUC	Percentage change
EHS		1.4		4.4		5.8	
	+ EA	3.8	+ 171%	3.5	- 20%	7.3	+ 26%
	+ BA	4.2	+ 200%	3.3	- 25%	7.5	+ 29%
EHMC		10.3		22.8		33.1	
	+ EA	7.0	- 32%	15.4	- 32%	22.4	- 32%
	+ BA	8.6	- 17%	19.8	- 13%	28.4	- 14%
OCR		6.0		9.5		15.4	
	+ EA	0.1	- 98%	0.3	- 97%	0.4	- 97%
	+ BA	0.7	- 88%	0.9	- 91%	1.6	- 90%
EHT		5.6		18.9		24.5	
	+ EA	5.3	- 5%	18.7	- 1%	24.0	- 2%
	+ BA	5.5	- 2%	18.9	± 0%	24.4	- 0.4%

CONCLUSION

The study presented here shows that the UV filter substances EHS, OCR, EHMC and EHT (which all contain a functional ester group), but not OD-PABA, were able to react with primary amines. Under the influence of UV radiation and/or heat, different reaction products could be assigned. They primarily resulted from ester aminolysis and, in the cases of EHMC and OCR, from Michael-type additions, when OCR surprisingly lost the cyanoacetate moiety. The identified reactions generally are also conceivable in the presence of proteins. The reaction rates increased significantly after applying a molar excess of amines corresponding to the conditions for skin applications.

The time-dependent conversions led to a bathochromic shift of the respective UV spectra, especially for EHS, whereas for OCR a hypsochromic shift and a nearly complete loss of UVA+B protection were observed. For EHS, the amine reactions led to an improved UVA protection, while the conversions were associated with a decrease of the absorbance strength of EHMC and to some extent of EHT.

The results of this study and our previous study with common UV filters with keto or diketo groups confirm that the recently developed fast screening HPTLC method allows direct conclusions about the reactivity of sunscreen substances with protein structures, and consequently about their possible allergic potential. It is still unclear if the results obtained in this study are likely transferable to more complex skin model systems but further studies using proteins and skin analogs to confirm this are planned for the future.

CONFLICT OF INTEREST STATEMENT

The authors of this publication declare that there is no conflict of interest.

REFERENCES

1. Singh, M. and Beck, M. H. 2007, Contact Dermatitis, 56, 48.
2. Kerr, A. and Ferguson, J. 2010, Photodermatol. Photoimmunol. Phoromed., 26, 56.
3. Avenel-Audran, M., Dutartre, H., Goossens, A., Jeanmougin, M., Comte, C., Bernier, C., Benkalfate, L., Michel, M., Ferrier-Lebouëdec, M. C., Vigan, M., Bourrain, J. L., Outtas, O., Peyron, J. L. and Martin, L. 2010, Arch. Dermatol., 146, 753.
4. Greenspoon, J., Ahluwalia, R., Juma, N. and Rosen, C. F. 2013, Dermatitis, 24, 29.
5. Hughes, T. M. and Stone, N. M. 2007, Contact Dermatitis, 56, 153.
6. Landers, M., Law, S. and Storrs, F. J. 2003, Am. J. Contact Dermatol., 14, 33.
7. Rodríguez, E., Valbuena, M. C., Rey, M. and Porras de Quintana, L. 2006, Photodermatol. Photoimmunol. Photomed., 22, 189.
8. Gilbert, E., Pirot, F., Bertholle, V., Roussel, L., Falson, F. and Padois, K. 2013, Int. J. Cosmetic Sci., 35, 208.
9. Seité, S. and Fourtanier, A. M. 2008, J. Am. Acad. Dermatol., 58, 160.
10. Manová, E., von Goetz, N., Hauri, U., Bogdal, C. and Hungerbühler, K. 2013, Int. J. Hyg. Environ. Health, 216, 508.
11. Gaspar, L. R. and Maia Campos, P. M. 2006, Int. J. Pharm., 13, 123.
12. Dondi, D., Albini, A. and Serpone, N. 2006, Photochem. Photobiol. Sci., 5, 835.
13. Schwack, W. and Rudolph, T. 1995, J. Photochem. Photobiol., 28, 229.
14. Stokes, R. and Diffey, B. 1999, Int. J. Cosmet. Sci., 21, 341.
15. Divkovic, M., Pease, C. K., Gerberick, G. F. and Basketter, D. A. 2005, Contact Dermatitis, 53, 189.
16. Elahi, E. N., Wright, Z., Hinselwood, D., Hotchkiss, S. A., Basketter, D. A. and Smith Pease, C. K. 2004, Chem. Res. Toxicol., 17, 301.
17. Aleksica, M., Pease, C. K., Basketter, D. A., Panicoa, M., Morrisa, H. R. and Della, A. 2007, Toxicol. In Vitro, 21, 723.
18. Natsch, A., Gfeller, H., Haupt, T. and Brunner, G. 2012, Chem. Res. Toxicol., 25, 2203.
19. Melles, D., Vielhaber, T., Baumann, A., Zazzeroni, R. and Karst, U. 2013, J. Chromatogr. B, 913-914, 106.
20. Andreu, I., Mayorga, C. and Miranda, M. A. 2010, Curr. Opin. Allergy Clin. Immunol., 10, 303.
21. Karlsson, I., Vanden Broecke, K., Mårtensson, J., Goossens, A. and Börje, A. 2011, Contact Dermatitis, 64, 343.
22. Karlsson, I., Hillerström, L., Stenfeldt, A. L., Mårtensson, J. and Börje, A. 2009, Res. Toxicol., 22, 1881.
23. Karlsson, I., Persson, E., Mårtensson, J. and Börje, A. 2011, Photochem. Photobiol., 88, 904.
24. Stiefel, C. and Schwack, W. 2013, Int. J. Cosmetic Sci., 35, 588.
25. Stiefel, C. and Schwack, W. 2013, Trends Photochem. Photobiol., 15, 63.

26. Kagetsu, N., Gange, R. W. and Parrish, J. A. 1985, J. Invest. Dermatol., 85, 445.

27. Huong, S. P., Andrieu, V., Reynier, J. P., Rocher, E. and Fourneron, J. D. 2007, Photochem. Photobiol. A, 186, 65.

V Reactivity of cosmetic UV filters towards skin proteins: Model studies with Boc-lysine, Boc-Gly-Phe-Gly-Lys-OH, BSA and gelatin

Constanze Stiefel, Wolfgang Schwack

Reprinted with permission from: *International Journal of Cosmetic Science* 2014, 36, 561–570.

SYNOPSIS

OBJECTIVE: Organic UV filters are used as active ingredients in most sunscreens and also in a variety of daily care products. Their good (photo) stability is of special interest to guarantee protective function and to prevent interactions with the human skin. Due to the mostly electrophilic character of the UV filters, reactions with nucleophilic protein moieties like lysine side chains are conceivable. Prior studies showed that the UV filters octocrylene (OCR), butyl methoxydibenzoylmethane (BM-DBM), ethylhexyl salicylate (EHS), ethylhexyl methoxycinnamate (EHMC), benzophenone-3 (BP-3), ethylhexyl triazone (EHT) and dibenzoylmethane (DBM) were able to covalently bind to an HPTLC amino phase and the amino acid models ethanolamine and butylamine after slightly heating and/or radiation.

METHODS: Boc-protected lysine, the tetrapeptide Boc-Gly-Phe-Gly- Lys-OH, bovine serum albumin (BSA) and porcine gelatin were used as more complex models to determine the reactivity of the mentioned UV filters towards skin proteins under thermal or UV irradiation conditions.

RESULTS: After gentle heating at 37°C, benzophenone imines were identified as reaction products of BP-3 and OCR with Boc-lysine and the tetrapeptide, whereas DBM and BM-DBM yielded enamines. For EHMC, a Michael-type reaction occurred, which resulted in addition of Boc-lysine or the tetrapeptide to the conjugated double bond. Ester aminolysis of EHS and EHT mainly afforded the corresponding amides. Reactions of the UV filters with BSA changed the UV spectrum of BSA, generally associated with an increase of the absorption strength in the UVA or UVB range. For all protein models, the UV filters showed an increasing reactivity in the order EHT < EHMC < EHS < BP-3 < OCR < DBM < BM-DBM.

CONCLUSION: Especially the UV absorbers BM-DBM, OCR and BP-3, which are seen as common allergens or photoallergens, showed a high reactivity towards the different skin protein models. As the formation of protein adducts is recognized as important key element in the induction of skin sensitization, the results of this study can contribute to a better understanding of the underlying chemical mechanisms of such reactions.

RÉSUMÉ

OBJECTIF: Les filtres UV organiques sont utilisés comme ingredients actifs dans la plupart des écrans solaires et également dans une variété de produits de soins quotidiens. Leur bonne (photo-) stabilité est d’un intérêt particulier pour garantir la fonction de protection et d’éviter les interactions

avec la peau humaine. En raison du caractère électrophile de la plupart des filtres UV, des réactions avec des fragments protéiques nucléophiles tels que des chaînes latérales de lysine sont envisageables. Des études antérieures ont montré que le filtre UV octocrylene (OCR), butyl methoxydibenzoylmethane (BM-DBM), éthylhexyle salicylate (EHS), éthylhexyle méthoxycinnamate (EHMC), la benzophénone-3 (BP-3), éthylhexyle triazone (EHT), et dibenzoylméthane (DBM) sont capables de se lier de manière covalente à une phase CCM-HP d'amine et aux modèle d'acide aminé tels l'éthanolamine et la butylamine, après un léger chauffage et / ou la radiothérapie.

MÉTHODES: la lysine protégée par Boc, le tétrapeptide de Boc-Gly-Phe-Gly-Lys-OH, l'albumine de sérum bovin (BSA) et de la gélatine de porc ont été utilisés comme des modèles plus complexes afin de déterminer la réactivité des filtres UV mentionnés vers les protéines de la peau sous des conditions thermiques ou UV irradiation.

RÉSULTATS: Après un léger chauffage à 37°C, des benzophénonimines ont été identifiés en tant que produits de réaction de 3-BP et OCR avec Boc-lysine et le tétrapeptide, tandis que DBM et BM-DBM ont donné des énamines. Pour EHMC, une réaction de type Michael s'est produite, ce qui a entraîné l'addition de Boc-lysine ou le tétrapeptide de la double liaison conjuguée. L' aminolyse d'ester d'EHS et EHT a principalement donné les amides correspondants. Les réactions des filtres UV avec de la BSA ont changé le spectre UV de BSA, généralement associée à une augmentation de l'intensité de l'absorption dans la gamme des UVA ou UVB. Pour tous les modèles de protéines, les filtres UV ont montré une réactivité croissante dans l'ordre EHT <EHMC <EHS <BP 3 <OCR <DBM <BM-DBM.

CONCLUSION: Surtout les absorbeurs UV comme BM-DBM, OCR, et BP-3, qui sont considérés comme des allergènes ou photoallergens communs, ont montré une forte réactivité à l'égard des différents modèles de protéines de la peau. Comme la formation de produits d'addition de protéine est reconnue comme élément clé important dans l'induction de la sensibilisation de la peau, les résultats de cette étude peuvent contribuer à une meilleure compréhension des mécanismes chimiques sous-jacentes de ces réactions.

KEYWORDS: chemical analysis, safety testing, skin sensitization, spectroscopy, sun protection, UV absorbers

INTRODUCTION

For more than 80 years, sunscreens are available on the market. The efficacy and safety of these products depend on the kind and amount of active ingredients, especially the used UV filters and the overall formulation of the products [1–3]. Most sunscreens act through a combined chemical and physical UV protection and should meet particular requirements like, for example balanced UVA/UVB protection, good water resistance, high stability and good tolerability [4–6]. Therefore, studies on the photochemical behaviour of different UV filter substances are an important part of sunscreen development [7–9]. Through interaction with sunlight or artificial light sources it may come to photodegradation of the UV filters, resulting in decreased protection ability and the formation of new products with possi-

bly different properties [9–14]. In addition, most UV filters approved within the EU contain electrophilic carbonyl groups, which may react with nucleophilic groups of free amino acids or proteins of the skin [15–17]. In this case, not only photochemistry, but also thermal chemistry may influence the reactivity of UV filters on the skin. This may be of particular interest when using personal care products with integrated UV protection, since during a normal working day, the skin is hardly exposed to direct UV light [18,19]. As the formation of protein adducts is understood as the key step in the formation of contact allergies [20–22], the widespread usage of UV filters in a variety of cosmetics and consumer products [23] should be examined critically.

First studies with common UV filters either on an high-performance thin-layer chromatography (HPTLC) amino layer [24] or in the presence of butylamine and ethanolamine [25,26] confirmed that the UV filters octocrylene (OCR), ethylhexyl salicylate (EHS), ethylhexyl methoxycinnamate (EHMC), benzophenone-3 (BP–3), butyl methoxydibenzoylmethane (BM–DBM), ethylhexyl triazone (EHT) and dibenzoylmethane (DBM) were generally able to react with primary amines under UV radiation and/or gentle heating. Imines, amides or amines could be identified as possible reaction products. Depending on the type of reaction, there partly was a strong influence on the respective UV filter spectra. The aim of this study was to explore, if the identified reactions could also be observed in the presence of peptides and complex proteins. Therefore, Boc-protected lysine, the tetrapeptide Boc-Gly-Phe-Gly-Lys-OH (Boc-GFGK), bovine serum albumin (BSA) and porcine gelatin were applied as reaction partners for OCR, BM–DBM, EHMC, BP–3, EHS and EHT. After gentle heating or UV radiation, the covalently bound UV filters were quantified and reactions products identified.

MATERIALS AND METHODS

4-t-Butyl-40-methoxydibenzoyl methane (BM-DBM, Eusolex 9020), 1,3-diphenylpropan-1,3-dion (≥98%) (DBM), ethylhexyl methoxycinnamate (EHMC, Eusolex 2292), benzophenone-3 (BP– 3, Eusolex 4360), octocrylene (OC, Eusolex OCR), sodium *tert*-butoxide (~98%), 2–ethylhexyl acetate (≥99%), silica gel 60 (0.06–0.2 mm), Bondesil-PSA (40 µm), *n*-hexane (HPLC grade), toluene (99%), ethanol (≥99.5%), methanol (HPLC grade), dichloromethane (99.7%), cyclohexane (99%), sulphuric acid (95–97%), hydrochloric acid (37%) and sodium hydroxide (pearls, 97 %) were obtained from VWR (Darmstadt, Germany). Cartridges with Teflon frits (ID 2 cm, volume 25 mL), 2–ethylhexyl salicylate (EHS), bovine serum albumin (BioReagent, ≥96%), ethyl benzoate (≥99%), monopotassium phosphate (≥99%), disodium hydrogen phosphate (≥99%), trifluoroacetic acid (≥99%), magnesium perchlorate (≥99%), Nα-Boc-L-lysine (≥99%), L-glutamic acid (≥99%), D(+)–sucrose (≥99.5%), sodium sulphate (≥99%) and tween 20 were purchased from Sigma-Aldrich (Steinheim, Germany). Tetrahydrofuran (≥99.9%) was obtained from Carl Roth (Karlsruhe, Germany). Acetonitrile (≥99.8%) was purchased from J.T. Baker (Deventer, Netherlands), acetophenone-2,3,4,5,6-d_5 (99 atom% D) and benzaldehyde-2,3,4,5,6-d_5 (99 atom% D) from ISOTEC (Miamisburg, OH, U.S.A.). The Boc-protected tetrapeptide (Boc-GFGK) was obtained from Bachem (Heidelberg, Germany), gelatin (food quality, water content 12%) from Ruf Lebensmittel KG (Quakenbrück, Germany). Ethylhexyl triazone

(EHT, Uvinul T 150) was kindly provided by BASF. HPTLC plates silica 60 F_{254}, 20 x 10 cm (layer thickness 200 µm) were obtained from Merck.

Solar simulator

Irradiations were performed with a Suntest CPS+ from Atlas Material Testing Technologies (Linsengericht, Germany) equipped with a xenon lamp and a filter combination of coated quartz glass with UV special glass (simulation of solar global radiation outdoors at daylight, Atlas) using the following settings: irradiation intensity 350 W m^{-2}, ventilation temperature 33°C. A custom-made, watercooled base plate was held at 20°C.

Accelerated solvent extraction

Accelerated solvent extraction was performed on an Accelerated solvent extraction (ASE) 200 from Dionex (Idstein, Germany) under the following conditions: preheat time 0 min, heating time 5 min, static time 5 min, flushing volume 11 mL (100% of the extraction cell), purge time 60 s (nitrogen), number of cycles 1, solvent methanol, pressure 35 bar and temperature 40°C.

Freezer mill

Grinding of gelatin samples was accomplished by a cryogenic mill with a self-container liquid nitrogen bath (6800 Freezer Mill) from SPEX CertiPrep (Metuchen, New Jersey, U.S.A.). Each of the four cylindrical grinding vials (internal volume 25 mL) consisted of a polycarbonate centre tube, a magnetic impactor and two end plugs of stainless steel. The magnetic bar was introduced into the polycarbonate tube with a sample mass of approximately 0.5 g. The tubes were closed and after 15 min precooling of the sampling vials, which were immersed in liquid nitrogen, the alternating magnetic field was applied. The grinding was carried out in four cycles of 2 min using a grinding frequency of 10 Hz. After each grinding cycle, the magnetic field was turned off for 1 min to allow re-cooling of the samples.

High-performance liquid chromatography-diode array detection

High-performance liquid chromatography measurements were performed on an 1100 liquid chromatograph (Agilent, Waldbronn, Germany), consisting of a degasser (G 1315A), a quaternary HPLC pump (G 1311A), an autosampler (G 1313A), a column oven (G 1316A) set to 30°C and a diode array detector (G 1315B) with detection wavelengths of 275 nm, 315 nm and 360 nm (spectral bandwidth 8 nm) and a reference wavelength of 500 nm. Data processing was performed by Agilent ChemStation software (rev. A.04.02). As stationary phase, an XTerra MS C_{18} 5 µm HPLC column, 250 x 3 mm, (Waters, Milford, NE, U.S.A.) was used. The mobile phase (0.5 mL min^{-1}) consisted of 10 mM ammonium formate pH 4.0 (A) and acetonitrile (B). Gradient: % A (t(min)): 40 (0)– 40 (4)–30 (9)–30 (13)–10 (17)–10 (26)–40 (28)–40 (33). Injection volume was 10 µL.

Liquid chromatography–mass spectrometry

The Liquid chromatography–mass spectrometry (LC-MS) system consisted of an identical Agilent 1100 chromatograph as described above, coupled to a MSD single-quadrupole mass spectrometer (G 1956B, Agilent) equipped with an electrospray ionization interface (ESI), operated under the following conditions: capillary voltage 3 kV, skimmer voltage 35 V, source temperature 100°C, nebulizer gas pressure 40 psig, drying gas temperature 300°C, drying gas flow rate 8 L min^{-1}, fragmentator voltage 80 V, gain 1, threshold 100 and step size 0.1. Data processing for MS measurements was carried out with ChemStation software (Agilent). Mass spectra were recorded in the positive full scan mode (*m/z* 80-1300). Column and gradient were as described above.

High-performance thin-layer chromatography

Sample application was performed with an Automatic TLC Sampler 4 (ATS4) (CAMAG, Muttenz, Switzerland), followed by plate development in a twin-through chamber (10 x 10 cm) with 8 mL dichloromethane/cyclohexane (50 : 50, v/v). Plate images were documented by a DigiStore 2 Documentation System (CAMAG) consisting of illuminator Reprostar 3 with digital camera Baumer optronic DXA252.

Gas chromatography

Gas chromatography (GC) measurements were carried out on an AutoSystem XL gas chromatograph (PerkinElmer, Rodgau, Germany), equipped with a flame ionization detector and a DB-5 (30 m x 0.25 mm x 0.25 µm) capillary column (Agilent). The carrier gas hydrogen was set to a constant flow of 2.0 mL min^{-1}. The oven was programmed as follows: 80°C (1 min), at 40°C min^{-1} to 300°C, 15 min at 300°C. Samples (1 µL) were manually injected into the injection port heated at 270°C. Data processing was performed by PerkinElmer Turbochrom Navigator software.

Matrix-assisted laser desorption/ionization time-of-flight mass spectrometry

Mass spectra were acquired on an orthogonal Bruker Autoflex III MALDI-TOF-TOF-system (Bruker Daltonics, Bremen, Germany) equipped with a nitrogen laser (337 nm, 3 ns pulse width) in the mass range 10–140 kDa in the positive reflector mode using an accelerating voltage of 21 kV and combining at least 600 laser shots per sample. Data processing was performed using flex analysis 3.0 and biotools 3.0 software (Bruker Daltonics).

Isotope-ratio mass spectrometry

For $^{2}H/^{1}H$ isotope ratio measurements, a DeltaPlus-XP isotope-ratio mass spectrometer (Thermo Scientific, Bremen, Germany) was coupled to a Euro EA 3000 elemental analyser (Hekatech, Wegberg, Germany) through a Conflo III interface.

The pyrolysis reactor tube (Hekatech) comprised of an outer ceramic tube, and an inner graphite tube filled with glassy carbon and nickel coated carbon. Reactor temperature was set to 1400°C. The carrier gas helium (10 kPa) was set to a constant flow of 120 mL min^{-1}. As working reference gas, hydrogen (5 kPa) was used, which was calibrated against the international calibration material VSMOW (δ^2H_{VSMOW} = 0‰, IAEA, Vienna, Austria). For data acquisition and processing, Thermo Electron Isodat NT software, version 2.0, was used.

Synthesis of d_5-dibenzoylmethane

Sodium *tert*-butoxide (2 g, 20 mmol) was weighed into a 50-mL round-bottomed flask and dissolved in 20 mL of THF. Ethyl benzoate (2.5 g, 17 mmol) was added in 0.5 g portions under constant magnetic stirring. After further stirring for 5 min, a solution of 1 mL (8 mmol) acetophenone-d_5 in 5 mL of THF was added dropwise under ice cooling. The mixture was stirred for 10 min at room temperature, followed by heating under reflux for 90 min. Afterwards, the cooled reaction mixture was poured into ice water (25 mL), acidified with 20% sulphuric acid to pH 6, and extracted three times with 15 mL *n*-hexane. The combined organic phases were dried over sodium sulphate and poured into a 150-mL glass beaker. The *n*-hexane evaporated from the beaker in a fume hood overnight. The residue was taken up in 2 mL *n*-hexane, poured on a silica gel cartridge (8 g silica gel 60) and eluted with *n*-hexane. Fractions of 2 mL were checked by HPTLC against a DBM standard. Fractions containing d_5-dibenzoylmethane (DBM-d_5) were combined and rotary evaporated to dryness. The crystalline residue was redissolved in 2 mL nhexane and poured on a cartridge packed with Bondesil-PSA (7 g). The cartridge was eluted with *n*-hexane, and fractions of 2 mL were again checked by HPTLC. DBM-d_5 positive fractions were combined, the solvent was rotary evaporated and the remaining residue recrystallized from methanol/water (80 : 20, v/v). Therefore, the yellowcoloured solid was dissolved in a minimum amount of methanol while heating under reflux for 10 min. To this solution, 2 mL hot water was added and the reaction mixture was slowly cooled down to room temperature, while crystals precipitated. Precipitation was completed at -20°C in a freezer. The crystals were filtered, washed with water/methanol (20 : 80, v/v) and dried over phosphorus pentoxide. Pure DBM-d_5 was obtained as light yellow-coloured crystals (yield: 1.1 g (60%), purity: 99%). Purity and identity of the product was confirmed by full scan LC-MS(ESI^+): t_R = 10.2 min, *m/z* 230 (MH^+, 100%), 106 (10%).

Synthesis of d_5-ethylhexyl cinnamate

Sodium *tert*-butoxide (2.4 g, 25 mmol) was weighed into a 50-mL Erlenmeyer flask and dissolved in 25 mL THF. 2-Ethylhexyl acetate (4 mL, 20 mmol) was added in 1-mL portions under magnetic stirring. After further stirring for 5 min, benzaldehyde-d_5 (1 mL, 10 mmol) was added dropwise under stirring. The reaction mixture was stirred for 1 h, then poured on ice water (25 mL), acidified with 20 % sulphuric acid to pH 6 and extracted three times with 15 mL *n*-hexane.

The combined organic phases were dried over sodium sulphate and poured into a 100-mL round-bottomed flask. The *n*-hexane evaporated from the flask in a fume hood overnight.
Afterwards, the residue was vacuum distilled at 0.05 mbar and 90°C to remove excess of 2-ethylhexyl acetate. The remaining residue was dissolved in 2 mL *n*-hexane, poured on a silica gel cartridge (8 g silica gel 60) and eluted with *n*-hexane. Fractions of 2 mL were checked by GC, and fractions containing d_5-ethylhexyl cinnamate (EHC-d_5) were combined and evaporated to dryness. EHC-d_5 was obtained as slightly yellow viscous liquid (yield: 1.3 g (51%), purity: 98%). Identity and purity of the product was confirmed by full scan LC-MS (ESI^+): t_R = 23.8 min, *m/z* 266 (MH^+, 100%), 154 (39%).

Reactions with Boc-lysine

The respective UV filters (15 mg) and Boc-lysine (8 mg) were weighed into 2-mL screw-capped glass vials and suspended with a mixture of 1950 µL ethanol and 50 µL sodium hydroxide solution (3.5 µmol). The mixtures were incubated for up to three days in a BD 53 cell culture incubator (Binder, Tuttlingen, Germany) at 37°C. Aliquots (40 µL) were taken after 0, 8, 24 and 72 h, were diluted to 1500 µL with ethanol, filtered through a syringe filter (0.2 µm) and analysed by high-performance liquid chromatography- diode array detection (HPLC-DAD) to quantify the residual UV filters. LC-MS analyses were performed to identify UV filter-Boclysine adducts.

Reactions with Boc-GFGK

The respective UV filters (5 mg) and the tetrapeptide Boc-GFGK (5 mg) were weighed into 2-mL screw-capped vials and suspended with 720 µL ethanol, 30 µL water and 50 µL sodium hydroxide solution (3.5 µmol). The mixtures were incubated in a BD 53 cell culture incubator (Binder) at 37°C for up to 3 days. For HPLCDAD and LC-MS determination, aliquots (80 µL) of the mixtures, which were incubated for 0, 8, 24 and 72 h, were adjusted to 1500 µL with ethanol and filtered through a syringe filter (0.2 µm) to determine the turnover of the UV filters and to identify UV filter-peptide adducts, respectively.

Reactions with BSA

Individual standard solutions (5 mg mL^{-1}) of BM–DBM, BP–3, OCR, EHS, DBM and EHMC were prepared in ethanol/tween 20 (4 : 1, v/v). EHT (25 mg) was dissolved in 5 mL of ethanol/toluene/ tween 20 (2 : 2 : 1, v/v/v). Bovine serum albumin (25 mg) was weighed into a 10-mL screw-capped glass tube and dissolved in 5 mL phosphate buffer (25 mg KH_2PO_4 and 140 mg $Na_2HPO_4 \cdot 2H_2O$). Afterwards, 800 µL of the respective UV filter standard solution was added, and the mixtures were incubated for up to three days on a rocking platform shaker (5 rpm) in a BD 53 cell culture incubator (Binder) at 37°C. After 0, 8, 24 and 72 h, aliquots of the samples (300 µL) were mixed with 700 µL acetonitrile in a plastic centrifuge tube, resulting in precipitation of the protein.

The tube was placed for 5 min into an ultrasonic bath, followed by centrifugation for 5 min at 7800 g. The supernatant was passed through a syringe filter (0.2 µm) and analysed by HPLC-DAD.

The protein pellets were lyophilized using a Lyovac GT2 (Leybold Heraeus, Hürth, Germany) freeze dryer, extracted by ASE to remove excess UV filters, and afterwards desalted and washed free of tween 20 by dialysis against Milli-Q water (1000 mL) using an pressurized (compressed air at 2 bar) stirred cell (type 8050) from Amicon (Witten, Germany) with a 10 kDa cut-off PBMC membrane (Biomax-10, Millipore, Billerica, MA, U.S.A.) connected to an auxiliary reservoir. Afterwards, the dialysate was lyophilized and stored at -20°C until MALDI-TOF analyses.

For MALDI-TOF analyses, approximately 1.5 mg BSA-UV filter conjugate was reconstituted in 1 mL 0.1% trifluoroacetic acid (TFA). An aliquot of 10 µL was desalted using C18 ZipTips (Millipore, Schwalbach, Germany) according to the manufacturer's protocol. Proteins were eluted from the ZipTips directly onto a stainless steel target using 3 µL of a α-cyano-4-hydroxy-cinnamic acid matrix solution (5 mg mL^{-1} in acetonitrile/0.1% TFA, 50 : 50, v/v) and were allowed to dry and crystallize at room temperature. For UV/VIS spectroscopy, approximately 1.5 mg of the lyophilized dialysate was dissolved in 10 mL of water. Spectra were recorded on a Perkin-Elmer Lambda 2 (Überlingen, Germany).

Reactions with gelatin

For the reaction with gelatin, 160 mg of BM-DBM, BP-3, OCR, EHS and EHMC were individually dissolved in 10 mL of a 4 : 1 (v/v) mixture of ethanol and tween 20. EHT (160 mg) was dissolved in a mixture of ethanol/toluene/tween 20 (2 : 2 : 1, v/v/v).

Leaf gelatin (0.8 g) was soaked in 10 mL of cold water for 10 min. Afterwards, the mixture was heated to 80°C to melt the gelatin and transferred into a glass petri dish (diameter 6 cm). The respective UV filter solution (150 µL) was added and thoroughly mixed with the gelatin with a spatula to obtain a homogeneous distribution. After 30 min solidification of the layer (final thickness about 1.5 mm) at 6°C in the fridge, the samples were irradiated. To avoid drying out, the dishes were cooled by a water-cooled base plate (20°C) and covered by a thin low-density polyethylene (LDPE) foil. The corresponding light doses for 1 h of irradiation were 1260 kJ m^{-2} (3.6 kJ/petri dish). After irradiation, the gelatin gel was transferred into a 50-mL centrifuge tube and melted by adding 10 mL of 80°C hot water. When the temperature reached approximately 30°C, acetonitrile (30 mL) was added to precipitate proteins and to extract excess UV filters. As internal standard, 25 µL of a DBM standard solution in ethanol (80 mg mL^{-1}) was added.

The mixture was shaken vigorously for 1 min and placed into an ultrasonic bath (Sonorex RK 106; Bandelin, Berlin, Germany) for 5 min at 35 kHz. After centrifugation (10 min at 2500 g), the supernatant was filtered through a syringe filter (0.2 µm) and analysed by HPLC-DAD.

To take into account a possible depletion of the UV filters solely caused by photodegradation, samples of 10 mL water spiked with the UV filter solutions were irradiated and treated as described above.

Possible photodegradation of the UV filters was also determined by HPLC-DAD based on the comparison of the irradiated samples with the respective samples before irradiation.

For isotope-ratio mass spectrometry (IRMS) studies, 228 mg EHC (synthesized according to EHC-d_5, but using undeuterated benzaldehyd) or DBM and 12 mg EHC-d_5 or DBM-d_5 were dissolved in 10 mL ethanol/tween 20 (4 : 1, v/v). Preparation and irradiation f the gelatin was carried out as described above, but only 100µL of the EHC/EHC-d_5 or DBM/DBM-d_5 solutions, respectively, were added, and no internal standard was used. After centrifugation, the precipitated protein was washed twice with 20 mL of acetonitrile and lyophilized to dryness. The dry gelatin was finely grounded using a freezer mill, washed twice with 20 mL of TBME, lyophilized and stored over phosphorus pentoxide until IRMS analysis. For pyrolysis, approximately 0.8 mg of the milled gelatin samples or the standard substances (sucrose and glutamic acid) were weighed into silver capsules (3.5 x 5 mm, Hekatech). One test series consisted of 5–8 samples, which were run in replicates of four, preceded and followed by a set of three standard runs.

RESULTS AND DISCUSSION

Boc-lysine, the tetrapeptide Boc-GFGK, and BSA presenting about 30–35 accessible lysine residues were chosen as reaction partners for the common UV filters BM–DBM, OCR, EHMC, EHS, BP–3 and EHT. Reactions were carried out at a moderate temperature of 37°C to include reactions, which are just initiated by the natural skin temperature on a warm day [27]. Afterwards, we used a thin gelatin gel layer as further skin model system, when the influence of UV radiation and heat on the reactivity of UV filters towards gelatin was examined to come close to the natural conditions during sunscreen application and usage.

Reactions with Boc-lysine and Boc-GFGK

Boc-lysine and Boc-GFGK were chosen to measure the ability of the selected UV filters to react with nucleophilic lysine side chains of proteins and thus to screen their possible potential of sensitization. Therefore, the UV filters were incubated with the Boc-protected amino acid or the tetrapeptide at 37°C for up to 3 days. Samples were analysed before the incubation as reference and after 8, 24 and 72 h by HPLC-DAD to monitor the depletion of the respective UV filters. As for respective ‘blank samples’ (without the addition of Boc-lysine and Boc-GFGK) recoveries of 98–101% were observed, the depletion of the UV filters during incubation allowed an assessment of the amount of the respective UV filter bound to the protein models. Among the studied UV filters, OCR and BM–DBM showed the strongest depletion, thus the highest reactivity towards Boc-lysine and Boc-GFGK. Already after 8 h, which corresponds to a normal working day, 54 and 34 mg of OCR were bound to 1 g of Boclysine and the tetrapeptide, respectively (Fig. 1). For BM-DBM, 22 and 17 mg g^{-1} were reached after 8 h. As to be expected, extension of the reaction time also increased the conversion rates. Compared to 8 h, the loss of OCR was about three-fold after 3 days at 37°C in the presence of both models.

BM–DBM even showed a stronger increase in depletion after 3 days of incubation with Boc-lysine and the tetrapeptide. BP–3, DBM and EHS generally revealed a comparable reactivity, whereas the two esters EHMC and EHT showed a comparatively low reactivity, which is in accordance with the results of our previous screening [24]. Only 30 and 24 mg of EHMC and 11 and 8 mg of EHT were bond to Boc-lysine or the tetrapeptide after 3 days at 37°C (Fig. 1).

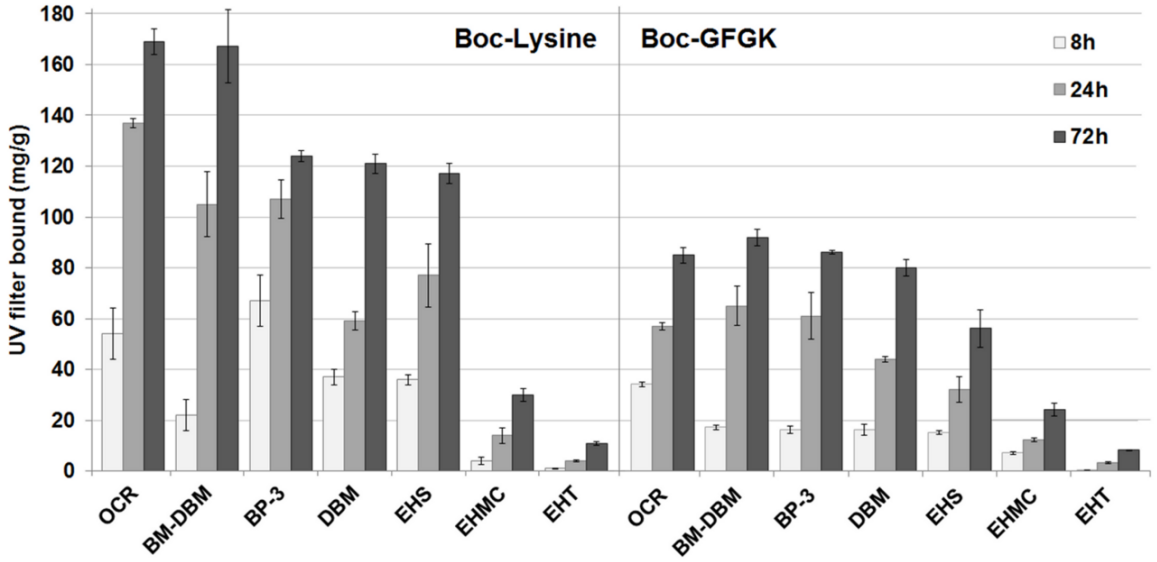

Figure 1 Depletion of the UV filters after different times of incubation at 37°C with Boc-lysine and Boc-GFGK. Error bars represent the SD (n = 3).

At first glance, it seemed that the UV filters showed a higher reactivity towards Boc-lysine than towards the tetrapeptide. However, taking into account that both reaction partners have one lysine binding site but a different molecular weight and, therefore, calculating the result on a molar base, the results were quite comparable, but tending to a slightly higher reactivity for Boc-GFGK (Fig. 2).

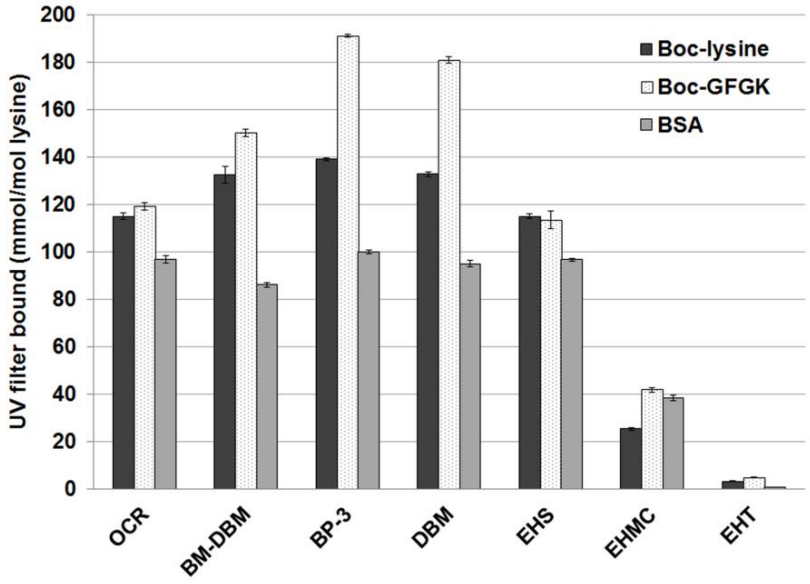

Figure 2 Depletion of the UV filters after 72 h incubation at 37°C in the presence of Boc-lysine, Boc-GFGK and bovine serum albumin (BSA), expressed as molar ratios. Error bars represent the SD (n = 3).

Concerning the different chemical structures of the UV filters, respective reaction products were identified by LC-MS regarding our former experiences [25,26] (Table I). EHS and EHT afforded the respective amides, which is in accordance with the results of our previous studies with butylamine and ethanolamine [26].

For OCR, the respective benzophenone imines were the only reaction products of a Michael-type addition followed by elimination of ethylhexyl cyanoacetate. Also BP–3 only afforded the respective imines. EHMC underwent Michael-type additions at the conjugated double bond and yielded the respective amines, but amides as products of ester aminolysis could not be identified. This is contrary to the previous results of the reactions with ethanolamine und butylamine, when the respective amides were the main products, and the amines only by-products [26]. However, under the conditions described above, Michael addition was the preferred reaction mechanism for EHMC, in the presence of both Boc-lysine and Boc- GFGK. BM–DBM and DBM yielded the respective enamines (Table I), whereas cleavage of the diketo group could not be observed, which occurred during the former studies in the presence of butyl amine and ethanolamine under the influence of UV irradiation or heat [25].

Table I Reaction products of UV filters after incubation (37°C) with Boc-lysine and Boc-GFGK, and the corresponding mass to charge ratios (*m/z*) of the protonated molecules determined by LC-MS

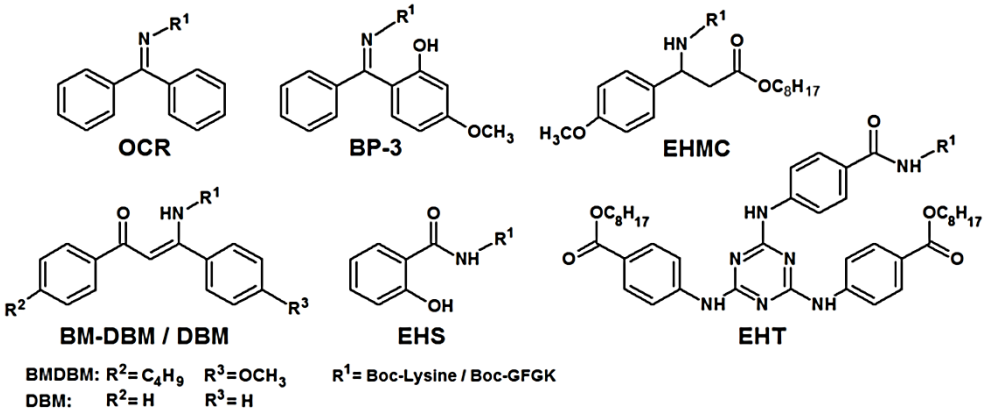

	OCR	BP-3	EHMC	BM-DBM	DBM	EHS	EHT
Boc-Lysine-UV filter adduct $[M+H]^+$	411	457	537	539	453	367	939
Boc-GFGK-UV filter adduct $[M+H]^+$	672	718	798	800	714	628	1200

Reactions with BSA

To extent the studies to a more complex and real protein, bovine serum albumin (BSA) was chosen as further reaction partner. BSA has a total of 59 lysine residues, 30–35 of which are sterically accessible for conjugation [28]. In addition, BSA contains 35 cysteine residues, which could be seen as second important binding site in the context of sensitization. However, as 34 of these cysteine residues form 17 stable disulphide bonds, this reaction pathway is negligible in the following context.

Due to the large number of lysine residues as possible binding sites, BSA was incubate with an approximately 35-fold molar excess of the respective UV filter substances at 37°C for up to 3 days. To follow the turnover, aliquots were taken at the beginning (reference) and after an incubation time of 8, 24 and 72 h. BSA was precipitated by acetonitrile, and the supernatant was analysed by HPLC-DAD.

Recovery rates samples incubated without BSA were between 98 and 99%, thus the depletion of the UV filters could again be used to indirectly determine the UV filters bound to BSA.

As for the simpler models, the UV filters showed a time-dependent turnover in the presence of BSA, when OCR, BM-DBM, BP-3, DBM and EHS showed comparable high reactivity (Fig. 3). In good accordance with the Boc-lysine and Boc-GFGK experiments, EHMC was clearly low reactive towards BSA, whereas EHT again was the most stable UV filter. As compared to Boc-lysine and Boc-GFGK, the obtained values expressed in mg UV filter per gram BSA, ranging 11–19 mg g^{-1} after 72 h incubation for the five most reactive UV filters (Fig. 3), seem to be rather low.

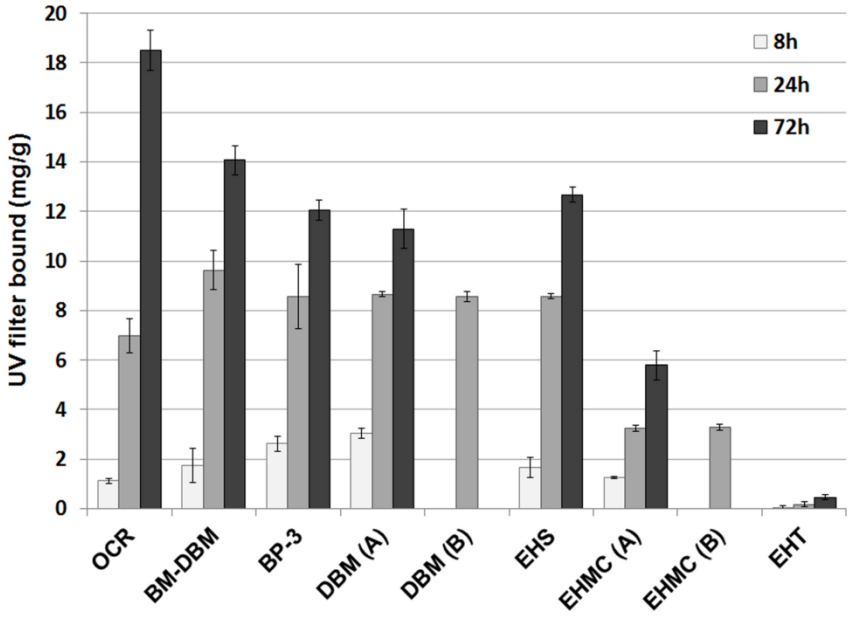

Figure 3 Depletion of the UV filters after different times of incubation at 37°C with bovine serum albumin (BSA). For dibenzoylmethane (DBM) and ethylhexyl methoxycinnamate (EHMC), (A) and (B) indicate the determination with high-performance liquid chromatography-diode array detection (HPLC-DAD) and matrix-assisted laser desorption/ionization time-of-flight mass spectrometry (MALDI-TOFMS), respectively. Error bars represent the SD (n = 3).

When, however, the BSA-bound UV filters are calculated on a molar basis regarding the maximum number of accessible lysine residues (35), the results became well comparable (Fig. 2). To further assess the reactivity of UV filters towards BSA, matrix-assisted laser desorption/ionization time-of-flight mass spectrometry (MALDI-TOFMS) was employed to determine the increase in molecular mass of BSA after incubation with DBM and EHMC as examples in comparison to a blank sample of BSA treated in the same manner. After 24 h of incubation, mean mass increases of approximately 570 and 220 g mol^{-1} were determined for the DBM and EHMC experiment, respectively. These data correspond to 8.6 mg DBM g^{-1} BSA and 3.3 mg EHMC g^{-1} BSA. Thus, the MS results were highly identical to them calculated from the depletion of the two UV filters and only differed by about 1% and 2% for DBM and EHMC, respectively (Fig. 3). This confirmed that the fast and simple HPLC-DAD method, analysing the residual non-transformed UV filters, was quite suitable to indirectly determine the BSA-bound UV filters.

The covalent binding of the UV filters to BSA had influence on the UV spectrum of BSA and of the bound UV filters (Fig. 4). As to be expected, a longer incubation time increased the changes of the

BSA spectrum in the UVA and/or UVB range (data not shown). For the BSA adducts of DBM and BM-DBM, a further absorption maximum at 349 and 359 nm, respectively, could be observed. They correspond to the UVA maxima of BM-DBM and DBM, which were not affected by the enamine formation. The two ethylhexyl esters EHMC and EHT also maintained the UV absorption characteristics after the reaction with BSA. Due to the minimal reactivity of EHT, the changes of the BSA-EHT adduct spectrum were correspondingly low. BSA-bound BP-3 and EHS provided a bathochromic shift compared to the UV filter spectra (Fig. 4), which is well in accordance with our previous observations for the reactions of these UV filters with butylamine or ethanolamine [25,26].

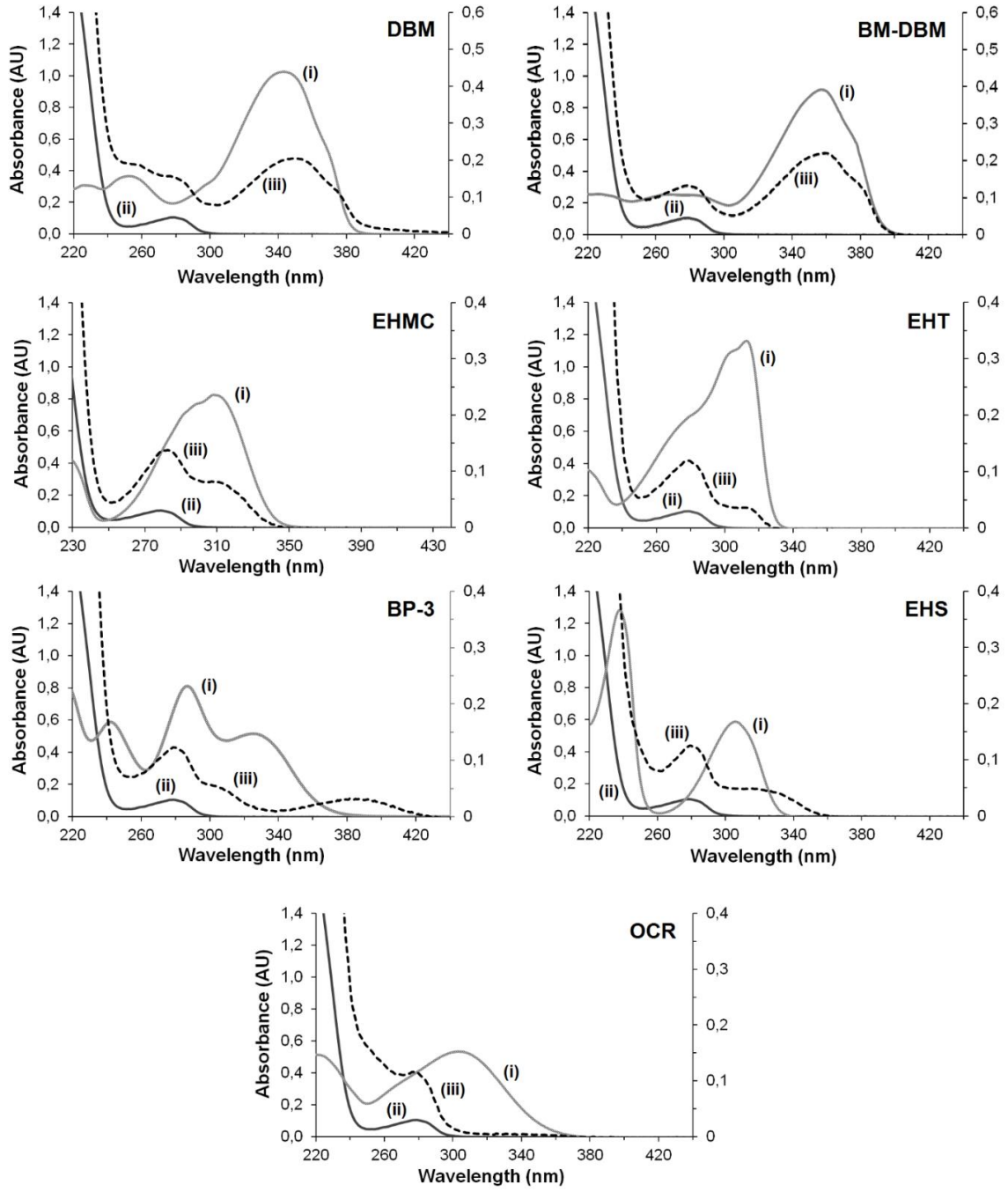

Figure 4 UV spectra of the studied UV filters (i) (about 8 mg L^{-1} in acetonitrile), bovine serum albumin (BSA) (ii), and the respective BSA-UV filter adducts (iii) (each 150 mg L^{-1} in water), isolated after incubation of 72 h at 37°C. Absorbance of (i) and (ii) is shown on the left axis, of (iii) on the right axis.

The UV spectrum of the BSA-OCR adduct showed an increase of the absorption strength mainly between 240 and 265 nm together with the loss of the characteristic absorption maximum (303 nm) of OCR (Fig. 4). This observation reasonably allowed the assumption that, as for the reaction with Boc-lysine and Boc-GFGK, OCR was covalently bound to BSA through Michael addition followed by the elimination of ethylhexyl cyanoacetate. The UV protective properties of BM-DBM, EHMC and EHT will obviously not be influenced by the formation of protein adducts. Protein bound EHS and BP-3 moved their absorption to greater wavelength, increasing UVA protection of EHS or BP-3, respectively. OCR, however, completely lose its UV protective function, if a reaction with lysine side chains of proteins occur.

Reactions with gelatin

Porcine gelatin containing approximately 4% lysine [29] was used as further model system and was chosen to represent connective tissue. In addition, gelatin contains only traces of cysteine, thus reactions with these nucleophilic side chains could be neglected. Furthermore, gelatin forms a stable, elastic gel and was therefore well suited as simplified skin model. The studied UV filters were homogeneously dispersed within the gelatin gel layer, and after solidification, the gel was irradiated using a Suntest CPS+ sun simulator to simulate real-life application conditions. The amount of the UV filters used was adapted to the requirements of the ISO 24444:2010 for the *in vivo* determination of the sun protection factor (2 mg sunscreen cm^{-2} skin area). Binding of the UV filters to gelatin was first indirectly determined from the recovered UV filters after extraction of the irradiated protein layer using HPLC-DAD. Samples were analysed directly and after 0.5, 1, 2 and 4 h of irradiation, using DBM as internal standard. To take a possible photodegradation of the UV filters into account, the photodegradation measured with the corresponding blank samples without gelatin was subtracted from the depletion examined for the samples with gelatin. However, significant photodegradation in the water phase could only be observed for BM–DBM (about 6.5% after 4 h) and EHMC (about 4% after 4 h). The other UV filters were rather photostable, so that the results were hardly affected. All studied UV filters showed a time-dependent binding to the gelatin layer, but revealed partly large differences in reactivity (Fig. 5). As in the presence of the previously used models (lysine, tetrapeptide, BSA), OCR was the most reactive UV filter towards gelatin. After 4 h of irradiation, about 740 µg OCR was bond to 1 g dry gelatin. For the other UV filters, the reactivity decreased in the order BP-3 > EHS > BM-DBM > EHMC > EHT (Fig. 5). Due to the high excess of gelatin, the covalent binding of the UV filters to the gelatin may be understood as reaction of pseudo-first order. To further directly assess the binding of UV filters to gelatin, isotope- ratio mass spectrometry (IRMS) was used to follow changes of the $^{2}H/^{1}H$ isotope ratio ($\delta^{2}H$) of gelatin incubated with synthetized, deuterium-labelled UV filters. Due to their simpler chemical structure and therefore easier synthesis, DBM-d_5 and EHC-d_5 were used as UV filter analogues to examine the general reaction behaviour of dibenzoylmethanes and cinnamates towards gelatin.

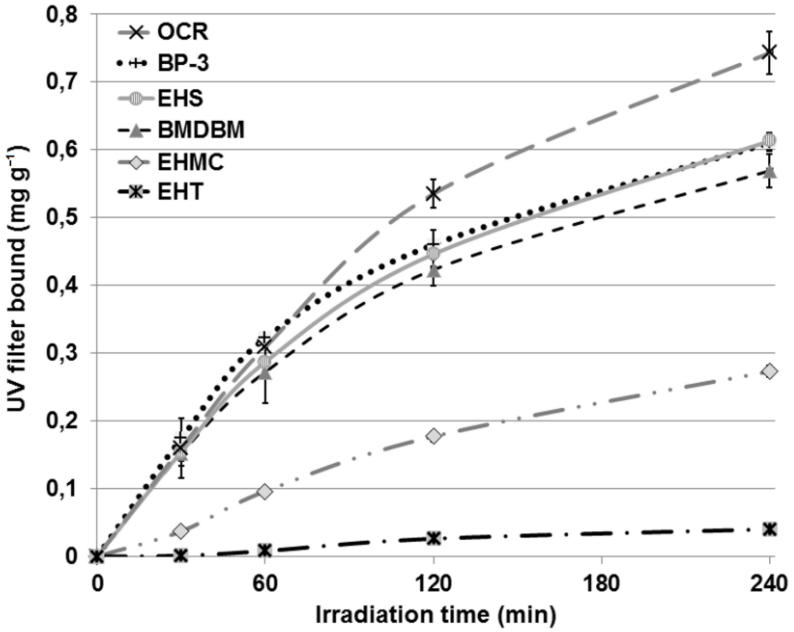

Figure 5 Reaction kinetics of the studied UV filters to gelatin gels (expressed as dry mass) during irradiation with 350 W m^{-2}; means of triplicates, and error bars represent the SD.

After 2 and 4 h of irradiation, the original δ^2H value of approximately -75‰ for gelatin clearly increased, especially for the reaction with d_5-DBM, indicating binding of the UV filters to gelatin (Table II). The changes in the isotope ratio allowed direct calculation of the amount of UV filters bond, which were very well in agreement with the indirect HPLC-DAD results (Table II). Only minor deviations of approximately 2–4% again confirmed that the fast and simple indirect extraction method were well suitable to determine the binding of UV filters to the gelatin layer, which also may be used for further skin models.

Table II Amounts of UV filters bound to gelatin, determined by extraction of the excess UV filters and HPLC-DAD analyses and by IRMS (δ^2H values) measurements of the extracted gelatin, irradiations at 350 W m^{-2}

Sample (irradiation time)	**δ^2H (‰) (±SD, *n*=3)**	**UV filter bound (mg g^{-1} dry gelatin)**		
		IRMS (±SD, *n*=3)	**HPLC-DAD (±SD, *n*=3)**	**Deviation (%)**
Gelatin (2 h)	-77.0 (1.2)	-	-	-
Gelatin (4 h)	-74.4 (0.8)	-	-	-
Gelatin-DBM-d_5 (2 h)	-1,7 (1.7)	0.71 (0.02)	0.74 (0.03)	3.2
Gelatin-DBM-d_5 (4 h)	7.1 (1.1)	0.89 (0.01)	0.90 (0.01)	1.8
Gelatin-EHC-d_5 (2 h)	-60.9 (0.7)	0.17 (0.01)	0.17 (0.01)	2.4
Gelatin-EHC-d_5 (4 h)	-55.5 (1.9)	0.27 (0.02)	0.28 (0.01)	3.7

HPLC-DAD, high-performance liquid chromatography-diode array detection; IRMS, isotope-ratio mass spectrometry; DBM-d_5, d_5-dibenzoylmethane; EHC-d_5, d_5-ethylhexyl cinnamate.

CONCLUSION

The present study confirmed that the common UV filters BM–DBM, OCR, EHS, EHMC, BP–3 and EHT were able to react with lysine side chains of proteins under slightly heating or UV irradiation. The studied UV filters showed great differences in their reactivity in the decreasing order OCR > BM-DBM > DBM > BP–3 > EHS > EHMC > EHT. This gradation is in accordance with the recently developed fast screening HPTLC method, indicating a different contact-allergic potential of the UV filters. Depending on the functional groups of the UV filters, that is ketones, 1,3-diketones and esters, imines, enamines and amides were the products of reactions with lysine residues. As shown for BSA adducts, binding to proteins did not affect the UV absorption properties of dibenzoylmethanes, EHMC and EHT, but gave rise to a more or less bathochromic shift in the cases of BP–3 and EHS. For OCR, however, a strong hypsochromic shift and a nearly complete loss of UVA + B protection were observed. The application of stable- isotope labelled UV filter analogues combined with IRMS analyses was shown a reliable tool to quantify adduct formation in proteins, which should be applicable to excised skin samples, even from volunteers. Further studies are ongoing to test, if the results obtained in this study are transferable to real skin experiments using commercial sunscreen products.

ACKNOWLEDGEMENTS

The authors express many thanks to Sylvia Maïtre for support regarding the preparation of the gelatine samples during her bachelor thesis.

CONFLICTS OF INTEREST

The authors declare no conflicts of interest.

REFERENCES

1. Serpone, N., Dondi, D. and Albini, A. Inorganic and organic UV filters: Their role and efficacy in sunscreens and suncare products. *Inorg. Chim. Acta* 360, 794–802 (2007).
2. Nash, J.F. Human safety and efficacy of ultraviolet filters and sunscreen products. *Dermatol. Clin.* 24, 35-51 (2006).
3. Sambandan, D.R. and Ratner, D. Sunscreens: an overview and update. *J. Am. Acad. Dermatol.* 64, 748-758 (2011).
4. Nash, J.F. and Tanner, P.R. Relevance of UV Filter/Sunscreen Product Photostability to Human Safety. *Photodermatol. Photoimmunol. Photomed.* 30, 88-95 (2014).
5. Bernerd, F., Marionnet, C. and Duval, C. Solar ultraviolet radiation induces biological alterations in human skin in vitro: relevance of a well-balanced UVA/UVB protection. *Indian J. Dermatol. Venereol. Leprol.* 78, 15-23 (2012).
6. El-Boury, S., Couteau, C., Boulande, L., Paparis, E. and Coiffard, L.J. Effect of the combination of organic and inorganic filters on the Sun Protection Factor (SPF) determined by in vitro method. *Int. J. Pharm.* 340, 1-5 (2007).
7. Jansen, R., Osterwalder, U., Wang, S.Q., Burnett, M. and Lim, H.W. Photoprotection: part II. Sunscreen: development, efficacy, and controversies. *J. Am. Acad. Dermatol*. 69, 867.e1-867.e14 (2013).
8. Moyal D. The development of efficient sunscreens. *Indian J. Dermatol. Venereol. Leprol.* 78, 31-34 (2012).
9. Lhiaubet-Vallet, V., Marin, M., Jimenez, O., Gorchs, O., Trullas, C. and Miranda, M.A. Filter-filter interactions. Photostabilization, triplet quenching and reactivity with singlet oxygen. *Photochem. Photobiol. Sci*. 9, 552-558 (2010).
10. Herzog, B., Wehrle, M. and Quass, K. Photostability of UV absorber systems in sunscreens. *Photochem. Photobiol.* 85, 869-878 (2009).
11. Rodil, R., Moeder, M., Altenburger, R. and Schmitt-Jansen, M. Photostability and phytotoxicity of selected sunscreen agents and their degradation mixtures in water. *Anal. Bioanal. Chem.* 395, 1513-1524 (2009).
12. Schwack, W. and Rudolph, T. Photochemistry of dibenzoyl methane UVA filters Part 1. *J. Photochem. Photobiol., B* 28, 229–234 (1995).
13. Santos, A.J., Miranda, M.S. and Esteves da Silva, J.C. The degradation products of UV filters in aqueous and chlorinated aqueous solutions. *Water Res.* 46, 3167-3176 (2012).
14. Shaath, N.A. Ultraviolet filters. *Photochem. Photobiol. Sci.* 9, 464-469 (2010).
15. Enoch, S.J., Ellison, C.M., Schultz, T.W. and Cronin, M.T. A review of the electrophilic reaction chemistry involved in covalent protein binding relevant to toxicity. *Crit. Rev. Toxicol.* 41, 783-802 (2011).

16. Dimitrov, S.D., Low, L.K., Patlewicz, G.Y., Kern, P.S., Dimitrova, G.D., Comber, M.H., Phillips, R.D., Niemela, J., Bailey, P.T. and Mekenyan, O.G. Skin sensitization: modeling based on skin metabolism simulation and formation of protein conjugates. *Int. J. Toxicol.* 24, 189-204 (2005).
17. Karlsson, I., Persson, E., Mårtensson, J. and Börje, A. Investigation of the sunscreen octocrylene's interaction with amino acid analogs in the presence of UV radiation. *Photochem. Photobiol.* 88, 904-912 (2012).
18. Thieden, E., Agren, M.S. and Wulf, H.C. Solar UVR exposures of indoor workers in a Working and a Holiday Period assessed by personal dosimeters and sun exposure diaries. *Photodermatol. Photoimmunol. Photomed.* 17, 249-255 (2001).
19. Diffey, B.L. Human exposure to solar ultraviolet radiation. *J. Cosmet. Dermatol.* 1, 124-130 (2002).
20. Natsch, A. and Gfeller, H. LC-MS-based characterization of the peptide reactivity of chemicals to improve the in vitro prediction of the skin sensitization potential. *Toxicol. Sci.* 106, 464-478 (2008).
21. Divkovic, M., Pease, C.K., Gerberick, G.F. and Basketter, D.A. Hapten-protein binding: from theory to practical application in the in vitro prediction of skin sensitization. *Contact Derm.* 53, 189-200 (2005).
22. Roberts, D.W. and Aptula, A.O. Determinants of skin sensitisation potential. *J. Appl. Toxicol.* 28, 377-387 (2008).
23. Manová, E., von Goetz, N., Hauri, U., Bogdal, C. and Hungerbühler, K. Organic UV filters in personal care products in Switzerland: a survey of occurrence and concentrations. *Int. J. Hyg. Environ. Health* 216, 508-514 (2013).
24. Stiefel, C. and Schwack, W. Rapid screening method to study the reactivity of UV filter substances towards skin proteins by high-performance thin-layer chromatography. *Int. J. Cosmet. Sci.* 35, 588-599 (2013).
25. Stiefel, C. and Schwack, W. Reactions of cosmetic UV filters with skin proteins: model studies of ketones with primary amines. *Trends Photochem. Photobiol.* 15, 63-75 (2013).
26. Stiefel, C. and Schwack, W. Reactions of cosmetic UV filters with skin proteins: model studies of esters with primary amines. *Trends Photochem. Photobiol.* 15, 105-116 (2013).
27. Webb, P. Temperatures of skin, subcutaneous tissue, muscle and core in resting men in cold, comfortable and hot conditions. *Eur. J. Appl. Physiol. Occup. Physiol.* 64, 471-476 (1992).
28. Jacques, P., Régis, M., Mathias, B. and Miginiac, E. Monitoring of hapten protein coupling reactions by capillary zone electrophoresis: improvement of abscisic acid-bovine serum albumin coupling and determination of molar coupling. *J. Chromatogr. A* 723, 381–388 (1996).
29. Eastoe, J.E. The amino acid composition of mammalian collagen and gelatin. *Biochem. J.* 61, 589-600 (1955).

VI Photostability of Cosmetic UV Filters on Mammalian Skin Under UV Exposure

Constanze Stiefel, Wolfgang Schwack, Yen-Thi Hai Nguyen

Reprinted with permission from: *Photochemistry & Photobiology* 2015, 91, 84-91.

ABSTRACT

Previous studies showed that the common UV filter substances benzophenone-3 (BP–3), butyl methoxydibenzoylmethane (BM–DBM), octocrylene (OCR), ethylhexyl methoxycinnamate (EHMC), ethylhexyl salicylate (EHS) and ethylhexyl triazone (EHT) were able to react with amino side chains of different proteins *in vitro*. To transfer the results to mammalian skin conditions, sunscreen products were applied on both prepared fresh porcine skin and glass plates, followed by UV irradiation and the determination of depletion of the respective UV filters. Significantly lower recoveries of the UV filters extracted from skin samples than from glass plates indicated the additional reaction of the UV filters with skin constituents, when proteins will be the most important reactants. Among the products tested, BP-3 showed the greatest differences in recoveries between glass and skin samples of about 13% and 24% after 2 and 4 h of irradiation, respectively, followed by EHS > BMDBM > OCR > EHMC > EHT. The obtained results raise the question, whether the common *in vitro* evaluations of sunscreens, using inert substrate materials like roughened quartz or polymethyl methacrylate (PMMA) plates are really suitable to fully replace *in vivo* methods, as they cannot include skin-typical reactions.

INTRODUCTION

The usage of sunscreen products with adequate broadband UV protection can be an effective way to protect the skin against the harmful effects of UV radiation (1–3). Their efficacy is claimed by different indicators, i.e. a high sun protection factor (SPF), a well-balanced UVA/UVB protection and a high photostability of the used UV filters (4,5). Originally, the application of UV filter substances was mainly concentrated on sunscreen products. However, UV filters nowadays are also important ingredients of personal care products to avoid undesirable short- and long-term effects of direct sun exposure as early as possible (6,7).

As part of the legally required safety evaluation of cosmetic products, the efficacy and safety of sun protection products must be proven by either *in vivo* tests on the skin of human volunteers or alternatively *in vitro* using roughened quartz or polymethyl methacrylate plates as test substrates (8–10). As *in vitro* tests avoid the ethical concerns associated with *in vivo* procedures, provide reproducible results, and are comparatively fast and cost-efficient, they are often used in practice. However, as the results of *in vitro* determinations can be influenced by various parameters like the radiation source, the exact application amount, the substrate material and the distribution of the sample, it complicates the implementation of the test systems and comparability of the results (11–14). In addition, as the usage of inert substrate materials can never exactly represent the natural skin conditions, the transferability

of the results to *in vivo* conditions may be limited. Especially reactions and processes that are attributed to different skin constituents (e.g. proteins) are not taken into account. This is of special interest, as previous studies with different protein and skin models confirmed that the common UV filters octocrylene (OCR), butyl methoxydibenzoylmethane (BM–DBM), benzophenone-3 (BP–3), ethylhexyl salicylate (EHS), ethylhexyl methoxycinnamate (EHMC) and ethylhexyl triazone (EHT) were generally able to react with amino side chains of proteins under thermal and/or irradiation conditions (15–19). Depending on the reaction products formed, a strong influence on the respective UV filter spectra was partly observed, confirming the importance of such reactions for the determination of efficacy.

Furthermore, as the formation of protein adducts is seen as an important key element of sensitization processes (20–22), the observed reactions may also be interesting in the context of safety testing and may challenge the increasingly widespread usage of UV filters in nearly all types of cosmetic products.

The aim of this study was to explore, if the identified protein reactions also play a role during the application of sunscreen products under "real life" conditions of use. Therefore, different commercially available sunscreens and skin care products with integrated UV protection were applied onto both prepared fresh porcine skin and glass plates, afterward irradiated, and extracted to determine the recoveries of the UV filters. Differences in the depletion of the UV filters extracted from skin or glass samples indicate additional reactions of the UV filters, attributed to natural skin constituents.

MATERIALS AND METHODS

4-t-Butyl-4'-methoxydibenzoylmethane (BM-DBM, Eusolex 9020), 1,3-diphenylpropan-1,3-dion (≥98%) (DBM), ethylhexyl methoxycinnamate (EHMC, Eusolex 2292), benzophenone–3 (BP–3, Eusolex 4360) and octocrylene (OCR, Eusolex OCR) were obtained from VWR (Darmstadt, Germany). Tween 20, 2–ethylhexyl salicylate (EHS), ammonium formate (>99%), dimethyl sulfoxide (≥99.7%) and ethanol (≥99.8%) were purchased from Sigma Aldrich (Steinheim, Germany). Ethylhexyl triazone (EHT, Uvinul T 150) was kindly provided by BASF (Ludwigshafen Germany). Cetyl alcohol (≥95%) was obtained from Carl Roth (Karlsruhe, Germany). Tegomuls was purchased from Spinnrad (Bad Segeberg, Germany), acetonitrile (≥99.8%) from J.T. Baker (Deventer, the Netherlands). C_{12}–C_{15} alkyl benzoate and caprylic/capric triglycerides (Miglyol 812) were kindly provided by Sasol (Hamburg, Germany). Samples of commercial products (15 sunscreens, 7 personal care products) were purchased from German drugstores and supermarkets. Porcine ears were freshly obtained from a local butcher (Gerlingen, Germany).

Standard solutions

Stock solutions (1 g L^{-1}) of BM–DBM, BP–3, OCR, EHS and EHMC were prepared in ethanol, of EHT in acetonitrile, and stored at 6°C. For calibration purposes, working standard solutions (2.5–140 mg L^{-1}) were prepared by appropriate dilution with ethanol or acetonitrile, respectively.

For standard mixture 1, BM–DBM (60 mg), OCR (150 mg) and EHS (80 mg) were dissolved in 2 mL of a 6:4 (v/v) mixture of capric/caprylic triglyceride and ethanol. For standard mixture 2, BP-3 (100 mg), EHMC (90 mg) and EHT (40 mg) were prepared in 2 mL of the same solvent mixture. As internal standard, a solution of DBM (50 mg mL^{-1}) was prepared in acetonitrile.

Sunscreen test formulations

Capric/caprylic triglyceride (6 g), C_{12-15} alkyl benzoate (6 g), Tegomuls (2 g) and cetyl alcohol (0.7 g) were melted in a 50 mL glass beaker, not exceeding the temperature of 80°C. Afterward, BP–3 (1.7 g), EHT (1.2 g) and EHMC (2.8 g) (sunscreen test formulation 1) or BM–DBM (1.4 g), OCR (2.5 g) and EHS (1.5 g) (sunscreen test formulation 2) were added and completely dissolved in the lipid phase. Hot water (80°C, 40 g) was added in 10 mL portions under constant stirring. After the complete addition of water the mixture was stirred vigorously for further 2 min. The resulting emulsion was cooled to room temperature under occasional stirring and stored at 6°C until usage.

Solar simulator

Irradiations were performed with a Suntest CPS+ from Atlas Material Testing Technology (Linsengericht, Germany) equipped with a xenon lamp and a filter combination of coated quartz glass with UV special glass (simulation of solar global radiation outdoors at daylight, Atlas) using the following settings: irradiance set to 350 W m^{-2}, ventilation temperature to 33°C. A custom-made, watercooled base plate was held at 20°C. Total UV irradiance (280–400 nm) in the test chamber was measured with a Dr. Höhnle UV meter (Gräfelfing, Germany) and was determined to 43 W m^{-2}.

High-performance liquid chromatography

High-performance liquid chromatography (HPLC) measurements were performed on a liquid chromatography (Agilent, Waldbronn, Germany), using a quaternary HPLC pump (G 1311A), a degasser (G 1315A), an autosampler (G 1313A), a column oven (G 1316A) set to 30°C and a diode array detector (G 1315B) with DAD detection wavelength of 300 nm and 350 nm (spectral bandwidth (SBW) 8 nm). As reference wavelength 500 nm was chosen (SBW 8 nm). Data processing was performed by Agilent ChemStation software (Agilent) (rev. A.04.02). As stationary phase, an XterraMS C 18 HPLC column (5 µm, 250 x 3 mm) (Waters, Milford, MA) was used. The injection volume was 10 µL. The mobile phase (0.3 mL min^{-1}) consisted of 10 mM ammonium formate buffer set to pH 4.0 (A) and acetonitrile (B). Isocratic elution (10% A/90% B) was used. For the determination of the UV filters BM–DBM, OCR, EHS, BP–3 and EHMC a run time of 14 min was sufficient, whereas for samples with EHT an extension of the run time to 30 min was necessary. For the separation of the UV filters, it was taken into account that EHMC (E isomer) forms the additional Z isomer during irradiation.

Determination of UV filters by HPLC

To determine the precision of the HPLC method used, three aliquots (8 mg) of the sunscreen test formulations 1 and 2 were accurately weighed into 15 mL screw-cap glass vials, 10 µL of the internal standard solution were added and the extraction was performed with 10 mL acetonitrile under sonication (5 min) at 35 kHz (Sonorex RK 106; Branson, Teltow, Germany). After centrifugation for 5 min at 2500 g, the clear supernatant was filtered through a syringe filter (0.2 µm), and analyzed by HPLC to calculate the means and standard deviations. To examine the accuracy of the method, the results of the triplicate measurements were compared to the theoretically calculated amounts of the respective UV filters in the sunscreen test formulations (recovery test).
Samples of commercial sunscreens and skin care products (approximately 10 mg) were weighed into a 50 mL centrifuge tubes, and 10 mL of acetonitrile and 10 µL of the internal standard solution were added. Samples were extracted under 10 min sonication (Sonorex RK 106, Branson) and centrifuged for 5 min at 2500 g. The clear supernatant was analyzed by HPLC after filtering through a syringe filter (0.2 µm).

Preparation of porcine skin

Excised full-thickness porcine ear skin was used. For the experiments, only ears without macroscopically visible damages or other changes (e.g. a peeling of the skin or rashes) were used. Ears were washed with cold water, dried with paper towels, and were carefully shaven to remove any visible hairs or bristles. Afterward, the outer skin membrane (dermis and epidermis) was carefully removed from the cartilage with a scalpel. The skin was cut into pieces of 2 x 2 cm^2. As it has been shown that freezing and storage at subzero temperatures does not influence the permeability properties and the quality of the skin (23), the prepared skin samples were stored at -20°C in a freezer until use.

Extraction tests for porcine skin samples

The sunscreen test formulation 1 and 2 (approximately 8 mg) were individually applied on the prepared porcine skin and evenly spread with a small spatula. After 30 min in the dark, skin samples were transferred into 50 mL centrifuge tubes, 10 µL of the internal standard solution and 20 mL of acetonitrile, ethanol, dimethyl sulfoxide or a mixture of water and ethanol (1:1 v/v) were added. The samples were shaken vigorously for 1 min and extracted under sonication (Sonorex RK 106, Branson) for 10 min. After centrifugation (5 min at 2500 g), the clear supernatant was filtered through a syringe filter (0.2 µm) and analyzed by HPLC to determine the recoveries of the UV filters from the skin in comparison to the directly extracted sunscreen test formulations.

Comparison between porcine skin and glass plates

The two standard mixtures (20 µL) were evenly spread onto the prepared porcine skin samples and in parallel on glass plates cut to the same size. Samples of commercial sunscreens and skin care products (approximately 8 mg) were uniformly distributed on the skin and the glass plates with a small spatula. A set of the respective samples was placed into a petri dish (diameter 8 cm) and covered by a thin low-density polyethylene (LDPE) cling film. After 30 min, the samples were irradiated for up to 4 h. The corresponding light doses for 1 h of irradiation were 155 kJ m^{-2} (62 J per sample). After 0, 0.5, 1, 2 and 4 h of irradiation, the samples were transferred into 50 mL centrifuge tubes, 10 µL of the internal standard solution were added and extraction was conducted with 10 mL of acetonitrile under sonication (10 min), followed by centrifugation for 5 min at 2500 g. The supernatant was passed through a syringe filter (0.2 µm) and measured by HPLC. Differences in the recoveries for each UV filter were assessed by ANOVA analysis

RESULTS AND DISCUSSION

Analysis of UV filters

Chromatography

To determine the recoveries of the UV filters, an appropriate HPLC method was used, allowing the simultaneous determination of the UV filters under study. Typical chromatograms of a standard mixture and the sunscreen sample No. 9 are shown in Figure S1. It was taken into account that EHMC, which is mainly found in its E form under dark conditions, is in equilibrium with the respective Z isomer under UV irradiation, resulting in an additional peak (Fig. S1). The ratio of absorbance between the Z and E isomer at 300 nm was 0.59, which is in good accordance with data found in literature (24). As the stable E/Z ratio already developed after 10 min of irradiation and was stable over the whole irradiation time, the peak area of Z-EHMC was multiplied by the factor 1.7 and was added to the peak area of E-EHMC for the evaluation of the irradiated samples. The linearity of the used HPLC-DAD method was determined by a six-point calibration. Regression equations were obtained by linear regression analysis, using the peak area ratio (sample to internal standard) as a function of concentration. Linear calibration curves for BM-DBM, BP–3, EHMC, EHS, OCR and EHT were obtained in the concentration range 2.5–140 mg L^{-1}. All correlation coefficients were greater or equal than 0.995 (Fig. S2). The calculated limits of quantitation (LOQ), defined as 10 times the signal-to-noise ratio (S/N = 10), were between 2.7 and 5.2 mg L^{-1}, the calculated limits of detection (LOD), defined as S/N = 3, between 0.8 and 1.6 mg L^{-1} (Table 1). The accuracy (recoveries) of the method was found to be 99.4–100.3% for all UV filters in the sunscreen test formulations (Table 1). The precision of the method (repeatabilities) was expressed as relative standard deviation (% RSD, n = 3) of the recoveries and was determined to ≤1.5% for all six UV filters (Table 1).

Table 1. Analytical parameters for the validation of the HPLC-DAD determination.

	LOD/LOQ (mg L^{-1})	Accuracy* (% Recovery)	Repeatability (% RSD, *n*=3)
BP-3	1.2 / 3.9	99.7 ± 0.03	1.12
EHMC	1.6 / 5.2	99.7 ± 0.05	1.13
BM-DBM	1.1 / 3.5	99.4 ± 0.01	0.86
OCR	0.8 / 2.7	99.6 ± 0.05	1.10
EHS	1.0 / 3.4	100.3 ± 0.02	1.49
EHT	1.3 / 4.4	99.7 ± 0.04	0.42

LOD/LOQ = Limit of detection/quantification; RSD = Relative standard deviation. *Related to the sunscreen test formulations

Extraction of the UV filters from porcine skin

To determine the most suitable solvent, which ensures a complete extraction of the unbound UV filters from the porcine skin, sunscreen test formulations were extracted from the skin with different solvents after 30 min, which corresponds to the usually recommended waiting time before sun exposure (25). Considering all six UV filters under study, acetonitrile was the most suitable solvent, showing high recovery rates and low standard deviations (Table 2), thus confirming the good applicability and accuracy of the extraction method.

Table 2. Recovery rates for the application and extraction of the sunscreen test formulations from porcine skin using different solvents.

	Recovery of the studied UV filters (% ± SD)*					
	BP-3	OCR	BM-DBM	EHMC	EHS	EHT
H_2O/Ethanol 1:1 (v/v)	91.2 ± 1.0	59.8 ± 2.7	46.7 ± 2.0	60.2 ± 1.5	58.8 ± 2.5	33.7 ± 3.0
Dimethyl sulfoxide	98.3 ± 2.6	86,4 ± 0.6	99.1 ± 1.5	98.5 ± 1.1	99.2 ± 1.2	94.9 ± 0.9
Acetonitrile	97.7 ± 1.6	99.2 ± 0.9	98.2 ± 0.7	99.6 ± 1.1	100.9 ± 0.6	97.3 ± 2.3
Ethanol	92.7 ± 3.6	97.0 ± 1.7	80.4 ± 1.1	95.1 ± 3.6	98.1 ± 1.6	90.1 ± 3.3

* Standard deviation (*n*=3)

Determination of the UV filters in commercial products

The UV filter content of commercial sunscreens and skin care products was determined by external calibration, using internal standard correction. The UV filter combinations and the SPF of the samples tested are shown in Table 3. The most frequently detected UV filters were BM–DBM and OCR, in 21 (95%) and 16 (73%) of the products tested. EHMC was only present in two of the examined skin care products (Table 3). All samples contained at least one organic UV filter, however, some products contained up to five different UV filter substances. The determined concentration ranges of the UV filters in the products were 0.2–7.1%, 1.4–10.1%, 2.2–4.3%, 1.1–2.7%, 2.3–5.5% and 0.7–5.9% for BM-DBM, OCR, EHS, EHT, EHMC and BP–3, respectively (Table 3). The UV filter content of the products generally complied with the maximum allowed concentration of the EU Cosmetics Regulation (26).

Table 3. UV filter combinations and claimed sun protection factors (SPF) of the studied sunscreens and skin care products.

	Main protection range		Active ingredients of the 15 investigated sunscreens and 7 skin care products, UV filter amount in g per 100g																			
	UVA	UVB	1	2	3	4	5	6	7	8	9	10	11	12	13	14	15	16	17	18	19	20	21	22
BM-DBM	x		2.6	3.0	7.1	4.2	3.6	4.0	2.6	4.9	0.4	4.2	2.6	2.9	1.2	2.3	3.1	1.6	1.3	2.0	1.3	0.2	1.1	
OCR		x	9.9	6.4	9.9	10.1	4.7	5.5	6.5	8.3		3.9	5.9	10	6.4	5.8	9.2	3.0			1.4			
EHS		x			4.2		2.2	2.8		4.3					4.0	2.9				2.5				
EHMC		x																				2.3	5.5	
EHT		x									1.1								2.7					
BP-3	(x)	x											5.9											0.7
Further UV filters in the products, according to the respective INCI declaration:																								
TiO_2		x	x	x	x	x	x	x	x	x		x		x	x	x	x						x	
TDSA	x		x																					
BEMT	x	x		x		x			x			x	x											
PBSA		x			x																x		x	
Homosalate		x											x											
SPF			30	50+	10	30	25	30	30	30	6	20	15	20	30	25	15	6	n.s.	n.s.	6	n.s.	n.s.	n.s.

TDSA = Terephthalylidene dicamphor sulfonic acid; n.s. = not specified; BEMT = Bis-Ethylhexyloxyphenol methoxyphenyl triazine;
PBSA = Phenylbenzimidazole sulfonic acid

Irradiation on glass or porcine skin

In former studies (15–19) it could be shown that the common UV filters BM–DBM, OCR, EHMC, EHS, BP–3 and EHT were able to react with different proteins and skin models under UV irradiation (Fig. 1). To assess, whether those reactions play also a role during the irradiation of the UV filters on the skin, different commercially available sunscreens and UV filter containing personal care products were applied onto prepared fresh porcine skin. Porcine skin was frequently used as surrogate for human skin in research due to its similar histological and biochemical properties and structure (27,28). The sunscreen amounts used were adapted to the requirements of the ISO 24444:2010 for the *in vivo* determination of the SPF (2 mg sunscreen per cm^{-2} skin area) (29). In parallel, the respective samples were applied onto glass plates and treated in the same manner, to take possible side effects into account, particularly photodegradation processes not influenced by the presence of skin proteins.

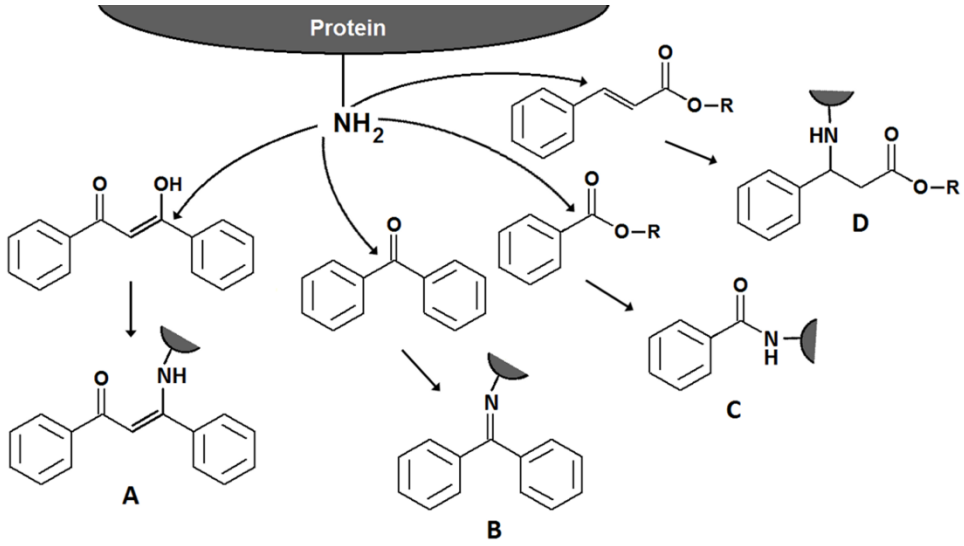

Figure 1. Schematic representation of possible reactions between skin proteins and UV filters with (A) diketo (e.g. BM-DBM), (B) benzophenone (e.g. BP-3), (C) ester (e.g. EHS), and (D) cinnamate structure (e.g. EHMC); according to the results of (18).

Photostability of the UV filters

Regarding the recoveries of the UV filters from glass plates after UV irradiation, an estimation of their photostability was possible. For EHT, OCR and BP-3 a relatively good photostability with mean recoveries of >85% after 4 h irradiation could be observed (Table 4). In contrast, EHS, BM-DBM and EHMC showed a comparatively higher photodegradation trend. However, in the case of EHS, this degradation may have limited influence on the overall UVB protection ability, as EHS is mostly used in the combination with other UVB filters. Because it is well known that the combination of EHMC with the UVA filter BM–DBM has a negative impact on the photostability of both UV filters (30,31), it is not surprisingly that for the 2 day care products (sample No. 20 and 21) combining EHMC and BM–DBM, a high photodegradation of both UV filters could be observed (Table 4). For EHMC, mean recoveries of 69 and 48% were determined after 2 and 4 h of irradiation for the two samples, when also the recoveries of BM–DBM were strongly reduced.

Table 4 Recoveries (% ± standard deviation) of the UV filters extracted from glass and skin after 2 h and 4 h of irradiation at 43 W m^{-2}.

Sample	BM-DBM						OCR						EHMC					
	2h glass	2h skin	4h glass	4h skin	Δ 2h	Δ 4h	2h glass	2h skin	4h glass	4h skin	Δ 2h	Δ 4h	2h glass	2h skin	4h glass	4h skin	Δ 2h	Δ 4h
1	87.0±1.0	80.9±1.0	77.6±0.6	58.0±0.6	6.1	19.6	94.1±0.9	90.9±0.9	91.4±1.3	83.1±0.1	3.2	8.3	-	-	-	-	-	-
2	91.4±1.5	88.3±1.5	85.7±0.6	77.8±1.1	3.1	7.9	99.3±1.3	95.9±0.3	99.1±0.7	91.5±0.9	3.4	7.6	-	-	-	-	-	-
3	85.0±4.5	73.5±0.9	76.2±5.1	55.0±2.4	11.5	21.2	95.5±1.5	91.3±0.6	92.7±1.8	82.0±0.7	4.2	10.7	-	-	-	-	-	-
4	95.2±1.5	88.3±1.1	90.0±0.8	74.5±0.8	6.9	15.5	97.9±0.4	90.4±0.6	95.0±1.2	83.3±0.8	7.5	11.7	-	-	-	-	-	-
5	90.1±3.6	84.0±1.8	82.5±0.4	73.1±1.1	6.1	9.4	98.2±0.6	93.6±0.6	95.3±0.5	87.6±0.5	4.6	7.7	-	-	-	-	-	-
6	89.9±0.4	84.7±3.0	79.5±0.6	67.0±2.3	5.2	12.5	97.6±1.8	94.1±1.8	96.9±0.4	89.4±0.5	3.5	7.5	-	-	-	-	-	-
7	96.8±0.7	90.1±1.4	90.7±0.5	78.8±2.0	6.7	11.9	99.1±1.3	95.8±1.0	98.7±0.4	91.4±1.3	3.3	7.3	-	-	-	-	-	-
8	90.6±1.4	85.7±0.1	80.7±1.2	67.7±1.4	4.9	13.0	96.4±0.9	92.2±0.3	94.9±1.7	85.1±0.8	4.2	9.8	-	-	-	-	-	-
9*	**71.3±1.5**	**58.6±2.7**	**42.7±0.4**	**30.4±1.8**	12.7	12.3	-	-	-	-	-	-	-	-	-	-	-	-
10	89.4±2.4	75.7±1.0	74.6±0.8	57.4±0.8	13.7	17.2	96.2±1.7	90.8±1.5	92.4±1.2	84.3±0.9	5.4	8.1	-	-	-	-	-	-
11	94.0±0.9	90.0±0.5	87.7±0.5	76.5±2.5	4.0	11.2	98.0±1.9	93.8±0.3	97.1±0.1	90.0±2.5	4.2	7.1	-	-	-	-	-	-
12	94.2±0.6	86.7±0.7	89.3±1.0	74.8±1.5	7.5	14.5	98.0±0.7	92.6±1.2	96.7±0.8	85.6±1.5	5.4	11.1	-	-	-	-	-	-
13	92.5±1.7	82.4±1.7	86.3±1.1	65.7±2.2	10.1	20.6	99.0±1.0	94.9±0.8	97.4±0.7	86.0±2.2	4.1	11.4	-	-	-	-	-	-
14	92.5±1.4	83.9±0.6	84.1±1.4	72.2±1.4	8.6	11.9	97.8±1.1	95.2±1.3	96.3±0.2	88.8±0.9	2.6	7.5	-	-	-	-	-	-
15	91.0±1.6	84.0±1.0	84.2±3.4	70.6±1.8	7.0	13.6	98.7±0.6	95.1±1.0	97.0±1.5	88.1±1.6	3.6	8.9	-	-	-	-	-	-
16	81.5±1.2	71.6±1.0	63.0±1.00	46.2±0.8	9.9	16.8	97.8±1.3	89.5±2.1	94.5±1.3	81.9±0.7	8.3	12.6	-	-	-	-	-	-
17*	**57.6±0.5**	**49.0±0.7**	**25.9±0.4**	**14.4±1.3**	8.6	11.5	-	-	-	-	-	-	-	-	-	-	-	-
18*	**57.3±2.2**	**48.8±1.6**	**25.8±0.6**	**20.7±0.4**	8.5	5.1	-	-	-	-	-	-	-	-	-	-	-	-
19	88.7±3.1	69.0±2.1	73.2±3.0	48.1±1.2	19.7	25.1	98.8±4.5	90.1±1.6	96.3±3.4	84.4±0.1	8.7	11.9	-	-	-	-	-	-
20*	**12.1±0.1**	**6.0±0.6**	**n.d.**	**n.d.**	6.1	-	-	-	-	-	-	-	**74.6±0.6**	**69.5±0.3**	**58.8±0.7**	**49.8±0.7**	5.1	9.0
21*	**17.4±0.5**	**15.5±0.2**	**n.d.**	**n.d.**	1.9	-	-	-	-	-	-	-	**64.0±0.8**	**58.3±1.0**	**37.8±0.3**	**28.7±0.2**	5.7	9.1
22	-	-	-	-	-	-	-	-	-	-	-	-	-	-	-	-	-	-
Average	79.3	71.3	73.7	59.4	8.0	14.3	97.7	92.9	95.7	86.4	4.8	9.3	69.3	63.9	48.3	39.3	5.4	9.1

Table 4 continued

Sample	EHS						BP-3						EHT					
	2h glass	2h skin	4h glass	4h skin	Δ 2h	Δ 4h	2h glass	2h skin	4h glass	4h skin	Δ 2h	Δ 4h	2h glass	2h skin	4h glass	4h skin	Δ 2h	Δ 4h
1	-	-	-	-	-	-	-	-	-	-	-	-	-	-	-	-	-	-
2	-	-	-	-	-	-	-	-	-	-	-	-	-	-	-	-	-	-
3	87.2±4.7	71.7±1.2	71.2±2.9	47.5±0.6	15.5	23.7	-	-	-	-	-	-	-	-	-	-	-	-
4							-	-	-	-	-	-	-	-	-	-	-	-
5	85.4±3.6	78.6±2.3	75.0±1.7	58.3±1.8	6.8	16.7	-	-	-	-	-	-	-	-	-	-	-	-
6	78.7±1.8	66.3±0.6	56.8±0.6	25.6±0.4	12.4	31.2	-	-	-	-	-	-	-	-	-	-	-	-
7	-	-	-	-	-	-	-	-	-	-	-	-	-	-	-	-	-	-
8	82.0±1.6	72.4±2.5	66.5±1.8	38.4±13	9.6	28.1	-	-	-	-	-	-	-	-	-	-	-	-
9	-	-	-	-	-	-	-	-	-	-	-	-	97.4±1.5	95.9±0.8	94.3±0.9	90.0±1.8	1.5	4.3
10	-	-	-	-	-	-	-	-	-	-	-	-	-	-	-	-	-	-
11	-	-	-	-	-	-	95.4±1.7	84.4±0.7	88.3±0.1	67.4±0.8	11.0	20.9	-	-	-	-	-	-
12	-	-	-	-	-	-	-	-	-	-	-	-	-	-	-	-	-	-
13	81.8±2.4	73.1±1.4	73.2±0.5	37.8±1.2	8.7	35.4	-	-	-	-	-	-	-	-	-	-	-	-
14	85.3±0.5	82.0±0.2	77.1±0.7	66.5±0.2	3.3	10.6	-	-	-	-	-	-	-	-	-	-	-	-
15	-	-	-	-	-	-	-	-	-	-	-	-	-	-	-	-	-	-
16	-	-	-	-	-	-	-	-	-	-	-	-	-	-	-	-	-	-
17	-	-	-	-	-	-	-	-	-	-	-	-	98.4±0.7	95.9±0.5	93.8±0.9	88.9±1.3	2.5	4.9
18	93.8±2.1	82.7±2.5	84.0±1.8	68.3±2.0	11.1	15.7	-	-	-	-	-	-	-	-	-	-	-	-
19	-	-	-	-	-	-	-	-	-	-	-	-	-	-	-	-	-	-
20	-	-	-	-	-	-	-	-	-	-	-	-	-	-	-	-	-	-
21	-	-	-	-	-	-	-	-	-	-	-	-	-	-	-	-	-	-
22	-	-	-	-	-	-	95.2±1.0	79.5±1.6	83.5±1.0	57.3±1.1	15.7	26.2	-	-	-	-	-	-
Average	84.9	75.3	72.0	48.9	9.6	23.1	95.3	82.0	85.9	62.4	13.4	23.6	97.9	95.9	94.1	89.5	2.0	4.6

n.d. = not detectable *Bold values indicate strong photodegradation

After 2 h, only about 15% of the initially applied BM–DBM could be recovered from the glass, and after 4 h of irradiation, the degradation of BM–DBM was complete (Table 4). The observed photodegradation of both UV filters may have a great influence on the UVA and UVB protection ability of the day care products, particularly with regard to their long-term protection. Also for the two products containing a combination of BM–DBM and EHT (sample No. 9 and 17), recoveries of only 26 and 43% could be observed for BM–DBM after an irradiation time of 4 h. Similarly, the personal-care product (sample No. 18) that contained BM-DBM and EHS only revealed 26% of the initial BM–DBM after 4 h of irradiation (Table 4). These results suggest that not only the combination of BM–DBM and EHMC, but also combinations of BM–DBM with EHS or EHT have a rather negative impact on the UVA protection performance of the products. In contrast, for all products containing BM–BDM in combination with OCR, a good photostability of the UVA filter was observed, which is in good accordance with the existing literature (32).

Differences between porcine skin and glass plates

After irradiation of the samples and extraction of the UV filters, differences in the depletion of the respective UV filters on both substrates (skin and glass) allowed first conclusions about the reactivity of the different UV filters toward the skin.

In a first step, the two standard mixtures were applied and uniformly distributed on either porcine skin or the glass plates to exclude possible side effects caused by interactions with further cosmetic ingredients. The standard solutions were allowed to dry and the samples were irradiated for up to 4 h afterward. The different UV filters showed an individual binding tendency toward the skin, to be derived from the different recoveries for the extraction from glass or skin (Fig. 2). EHS showed the most significant difference between glass and skin, followed by BP-3 > BM–BDM > EHMC > OCR > EHT.

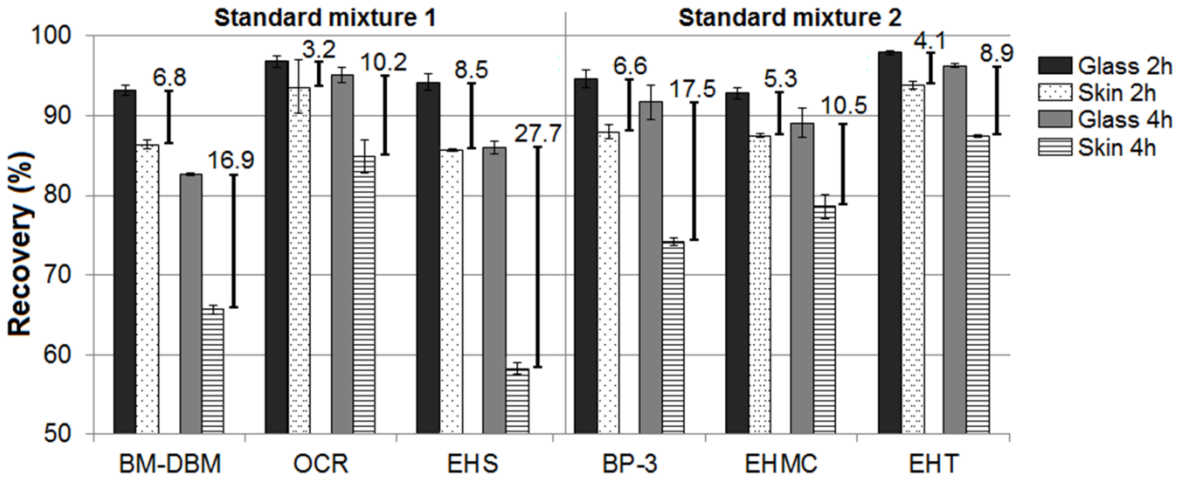

Figure 2. Recoveries of the UV filters applied as two standard mixtures from glass and porcine skin after 2 h and 4 h of irradiation at 43 W m^{-2}. Error bars represent the standard deviation (*n*=3), adjacent bars show the respective difference between glass and skin.

.

In a second step, 22 commercial products were examined, the obtained results are summarized in Table 4. Figure 3 exemplarily shows the different recoveries for the UV filters OCR, BM–DBM and BP-3 of sunscreen sample No. 11, extracted from the skin and the glass plates after 2 and 4 h of irradiation. Significant differences between the recoveries from the skin samples and glass plates (ΔR) were determined by ANOVA analysis for OCR ($\Delta R_{2\,h}$ = 4.2%, $\Delta R_{4\,h}$ = 7.1%), BM–DBM ($\Delta R_{2\,h}$ = 4.0%, $\Delta R_{4\,h}$ = 11.2%), and for BP–3 ($\Delta R_{2\,h}$ = 11.0%, $\Delta R_{4\,h}$ = 20.9%), the letter showing the highest reactivity (Fig. 3).

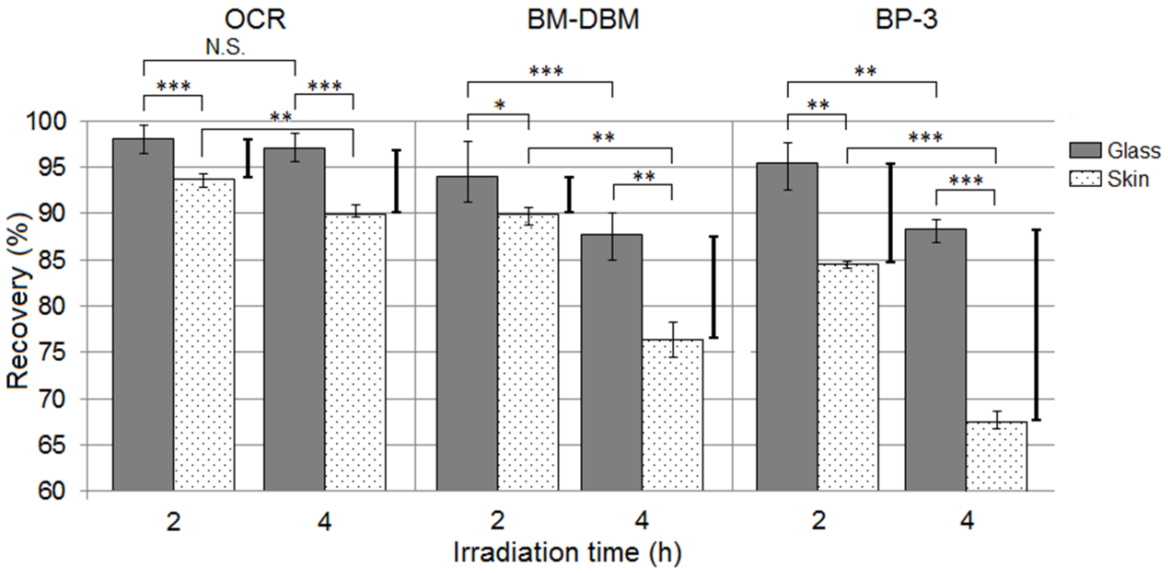

Figure 3. Recoveries of the UV filters from glass and porcine skin after 2 h and 4 h of irradiation at 43 W m^{-2}; exemplary shown for sunscreen sample No.11. Error bars represent the standard deviation (*n*=3). Data that are not significantly different (N.S.; > 0.05) and data that are significant (* p < 0.05, ** p < 0.01, *** p < 0.001) are marked accordingly.

There was no statistically significant difference between the recoveries from the glass plates after 2 and 4 h irradiation for OCR, confirming its good photostability. For BM–DBM and BP–3, however, there was a certain photodegradation of approximately 5% and 12% after 2 and 4 h of irradiation, respectively. The results obtained with the personal care products are exemplarily discussed for product No. 17, containing the UV filters BM–DBM and EHT. EHT was very photostable and less reactive ($\Delta R_{2\,h}$ = 2.5%, $\Delta R_{4\,h}$ = 4.9%), whereas BM–DBM showed a significant reactivity ($\Delta R_{2\,h}$ = 8.6%, $\Delta R_{4\,h}$ = 11.5%) but especially a high photodegradation of approximately 75% after 4 h irradiation (Fig. 4). The example illustrates that a high degradation tendency under UV exposure was generally associated with a decreased difference between the recovery results (ΔR) after 2 and 4 h, as the photodegradation competes with protein-adduct formations. However, from this study design it cannot be excluded that products of photodegradation also react with skin proteins and possibly result in skin sensitization (33).

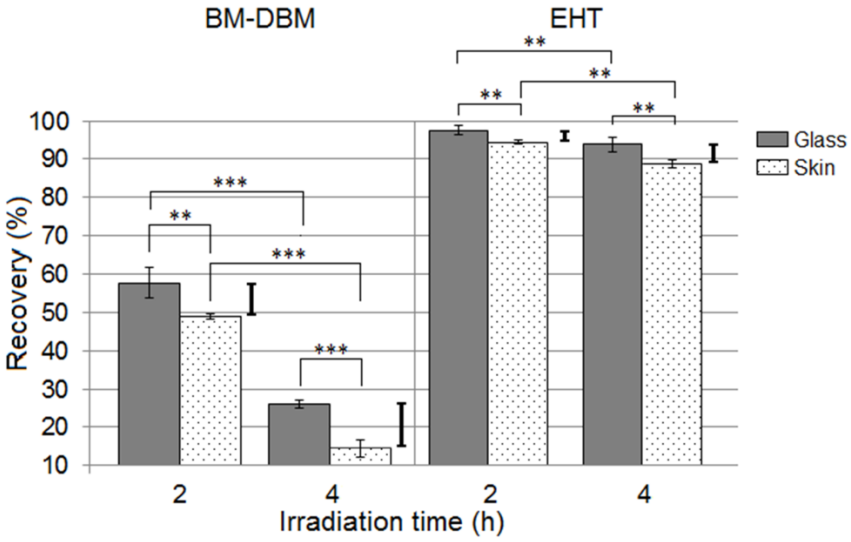

Figure 4. Recoveries of the UV filters from glass and porcine skin after 2 and 4 h of irradiation at 43 W m^{-2}; exemplary shown for face cream No.17. Error bars represent the standard deviation (n = 3). Data that are significant (**P < 0.01, ***P < 0.001) are marked accordingly.

For all UV filters, a time-dependent nearly linear increase in ΔR was observable, when the results for all samples were averaged (Fig. 5), indicating the occurrence of certain skin-typical reaction, e.g. protein-adduct formation initiated by UV irradiation (Fig. 1). However, comparing the different UV filters, partly large differences in their reactivity were observed, which were comparable to the previous results from the application of standard solutions. Considering the arithmetic mean of UV filter recoveries for the different commercial samples examined, BP–3 obviously showed the largest differences between the recoveries calculated from the glass plates and the skin, followed by EHS and BM–DBM (Fig. 5).

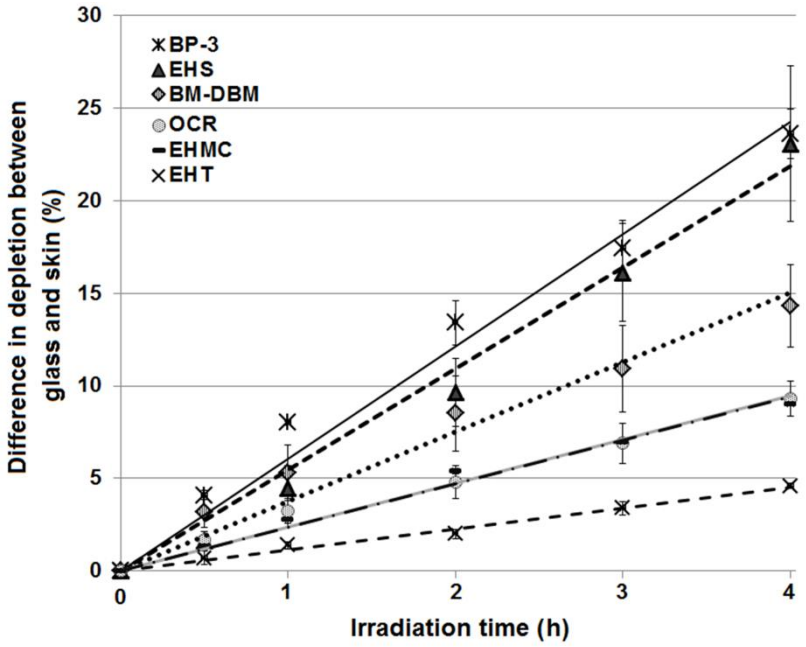

Figure 5. Mean differences in the depletion of UV filters for the commercial samples under study on glass and porcine skin after different irradiation times (43 W m^{-2}). Error bars represent the standard deviation, for BP-3 (n=2), EHS (n=7), BM-DBM (n=19, sample 20 and 21 excluded due to extreme photodegradation), OCR (n=16), EHMC (n=2), and EHT (n=2).

However, as there were only two samples containing BP–3, its reactivity cannot be conclusively assessed. EHMC and EHT were the two UV filters with the lowest reactivity toward the porcine skin, which is in good accordance with the results of our developed HPTLC screening (15).

The same applied for OCR; its moderate reactivity corresponds also well to the HPTLC screening under UV radiation conditions, although in further studies with the amino acid models ethanolamine and butylamine (17), BSA and gelatine (18), OCR was identified as highly reactive binding partner. The difference in the reactivity of OCR toward the various substrates was quite surprising, but presently is difficult to explain. It is noticeable that the different recoveries from glass and skin were sample dependent for each UV filter. After 4 h of irradiation, OCR for example showed ΔR values of 7–13% for all sunscreen samples under study. For BM–DBM, a larger margin of 5–25% was determined under the same conditions (Table 4). It is likely that the different UV filter combinations, the photostability and the overall composition of the products may influence the respective results.

As the differences between the recoveries determined by extraction from the glass plates and the skin were mostly significant and not only UV filter but also product dependent, it raises the question, how suitable the existing *in vitro* methods are to reflect *in vivo* conditions. Due to the usage of quartz or PMMA plates to determine the SPF, the UVA protection ability and the photostability, skin-typical reactions, which may have a direct influence on the accuracy of the results, are not covered by the existing *in vitro* methods.

CONCLUSION

This study shows that for the common UV filter substances BP-3, BM–DBM, EHS, OCR, EHMC and EHT, differences in their recoveries could be observed when sunscreen samples were irradiated on either glass plates or porcine skin. The time-dependent increasing differences between the recoveries from glass and skin indicate the occurrence of certain skin-typical reactions, as the formation of protein adducts. The studied UV filters showed remarkable differences in their reactivity toward the skin, listed in decreased order as follows: BP–3 > EHS > BM–DBM > OCR > EHMC > EHT. This gradation is in good accordance with the results of the recently developed HPTLC screening method, indicating a different photocontact allergenic potential of the UV filters. Which impact a binding of the UV filters to the skin may have on the respective UV spectra of the applied products cannot be derived directly, as also the bound, nonextractable UV filters or their cleavage products may have a certain absorption potential. Recent methods, which are used to examine the sunscreen performance *in vitro*, cannot take such skin-typical reactions into account. Therefore, the validity of those testing results for the practical usage needs to be questioned.

Especially for some of the studied day care products, a partly high photodegradation of the included UV filters was observed. This raises the question, if such products are really effective and if it is necessary that also for day care products advertising with UV protection, certain minimum requirements for the stability of the used UV filters should apply.

REFERENCES

1. Seité, S., Fourtanier, A., Moyal, D. and Young, A.R. (2010) Photodamage to human skin by suberythemal exposure to solar ultraviolet radiation can be attenuated by sunscreens: a review. *Br. J. Dermatol.* 163, 903-914.

2. Moyal, D.D. and Fourtanier, A.M. (2008) Broad-spectrum sunscreens provide better protection from solar ultraviolet-simulated radiation and natural sunlight-induced immunosuppression in human beings. *J. Am. Acad. Dermatol.* 58, 149-154.

3. Cole, C., Appa, Y. and Ou-Yang, H. (2014) A broad spectrum high-SPF photostable sunscreen with a high UVA-PF can protect against cellular damage at high UV exposure doses. *Photodermatol. Photoimmunol. Photomed.* (2014), 30, 212-219.

4. Forestier, S. (2008) Rationale for sunscreen development. *J. Am. Acad. Dermatol.* 58, 133-138.

5. Antoniou, C., Kosmadaki, M.G., Stratigos, A.J. and Katsambas, A.D. (2008) Sunscreens--what's important to know. *J. Eur. Acad. Dermatol. Venereol.* 22, 1110-1118.

6. Manová, E., von Goetz, N., Hauri, U., Bogdal, C. and Hungerbühler, K. (2013) Organic UV filters in personal care products in Switzerland: a survey of occurrence and concentrations. *Int. J. Hyg. Environ. Health* 216, 508-514.

7. Seité, S. and Fourtanier, A.M. (2008) The benefit of daily photoprotection. *J. Am. Acad. Dermatol.* 58, 160-166.

8. Cole, C. (2014) Sunscreens--what is the ideal testing model? *Photodermatol. Photoimmunol. Photomed.* 30, 81-87.

9. Crovara Pescia A., Astolfi, P., Puglia, C., Bonina, F., Perrotta, R., Herzog, B. and Damiani, E. (2012) On the assessment of photostability of sunscreens exposed to UVA irradiation: from glass plates to pig/human skin, which is best? *Int. J. Pharm.* 427, 217-223.

10. Pelizzo, M., Zattra, E., Nicolosi, P., Peserico, A., Garoli, D. and Alaibac, M. (2012) In vitro evaluation of sunscreens: an update for the clinicians. *ISRN Dermatol.* 2012, Article ID 352135.

11. Schrader, K. (2001) Die Sonnenschutzfaktorbestimmung Kritische Bewertung aus der Sicht eines Prüfinstitutes. *Bundesgesundheitsblatt Gesundheitsforschung Gesundheitsschutz* 44, 457-462.

12. Stokes, R. and Diffey, B. (1999) In vitro assessment of sunscreen photostability: the effect of radiation source, sunscreen application thickness and substrate. *Int. J. Cosmetic Sci.* 21, 341-351.

13. Garoli, D., Pelizzo, M.G., Nicolosi, P., Peserico, A., Tonin, E. and Alaibac, M. (2009) Effectiveness of different substrate materials for in vitro sunscreen tests. *J. Dermatol. Sci.* 56, 89-98.

14. Rohr, M., Klette, E., Ruppert, S., Bimzcok, R., Klebon, B., Heinrich, U., Tronnier, H., Johncock, W., Peters, S., Pflücker, F., Rudolph, T., Flösser-Müller, H., Jenni, K., Kockott, D., Lademann, J., Herzog, B., Bielfeldt, S., Mendrok-Edinger, C., Hanay, C. and Zastrow, L. (2010) In vitro sun protection factor: still a challenge with no final answer. *Skin Pharmacol. Physiol.* 23, 201-212.

15. Stiefel, C. and Schwack, W. (2013) Rapid screening method to study the reactivity of UV filter substances towards skin proteins by high-performance thin-layer chromatography. *Int. J. Cosmet. Sci.* 35, 588-599.

16. Stiefel, C. and Schwack, W. (2013) Reactions of cosmetic UV filters with skin proteins: model studies of ketones with primary amines. *Trends Photochem. Photobiol.* 15, 63-75.

17. Stiefel, C. and Schwack, W. (2013) Reactions of cosmetic UV filters with skin proteins: model studies of esters with primary amines. *Trends Photochem. Photobiol.* 15, 105-116.

18. Stiefel, C. and Schwack, W. (2014) Reactivity of cosmetic UV filters towards skin proteins: Model studies with Boc-lysine, Boc-Gly-Phe-Gly-Lys-OH, BSA and gelatin. *Int. J. Cosmet. Sci.* 36, 561-570.

19. Karlsson, I., Persson, E., Mårtensson, J. and Börje, A. (2012) Investigation of the sunscreen octocrylene's interaction with amino acid analogs in the presence of UV radiation. *Photochem. Photobiol.* 88, 904-912.

20. Roberts, D.W. and Aptula, A.O. (2008) Determinants of skin sensitisation potential. J. *Appl. Toxicol.* 28, 377-387.

21. Chipinda, I., Hettick, J.M. and Siegel, P.D. (2011) Haptenation: chemical reactivity and protein binding. *J. Allergy* 2011, Article ID 839682.

22. Divkovic, M., Pease, C.K., Gerberick, G.F. and Basketter, D.A. (2005) Hapten-protein binding: from theory to practical application in the in vitro prediction of skin sensitization. *Contact Dermatitis* 53, 189-200.

23. Franz, T.J. (1975) On the relevance of in vitro data. *J. Invest. Dermatol.* 93, 633–640.

24. Huonga, S.P., Andrieua, V., Reyniera, J.P., Rocherb, E. and Fourneronb, J.D. (2007) The photoisomerization of the sunscreen ethylhexyl p-methoxy cinnamate and its influence on the sun protection factor. *J. Photochem. Photobiol.* A 186, 65-70.

25. Elsner, P., Hölzle, E., Diepgen, T., Grether-Beck, S., Hönigsmann, H., Krutmann, J., Scharffetter-Kochanek, K., Schwarz, T. and Luger, T. (2007) Recommendation: daily sun protection in the prevention of chronic UV-induced skin damage. *J. Dtsch. Dermatol. Ges.* 5, 166-73.

26. European Parliament and Council (2009) Regulation (EC) No. 1223/2009. *Off. J. Eur. Union L* 342, 59-209.

27. Godin, B. and Touitou, E. (2007) Transdermal skin delivery: predictions for humans from in vivo, ex vivo and animal models. *Adv. Drug Deliv. Rev.* 59, 1152-1161.

28. Barbero, A.M. and Frasch, H.F. (2009) Pig and guinea pig skin as surrogates for human in vitro penetration studies: a quantitative review. *Toxicol. In Vitro* 23, 1-13.

29. International Organization for Standardization, ISO 24444:2010, Cosmetics - Sun protection test methods - In vivo determination of the sun protection factor (SPF), Geneva, Switzerland, 2010.

30. Sayre, R.M., Dowdy, J.C., Gerwig, A.J., Shields, W.J. and Lloyd, R.V. (2005) Unexpected photolysis of the sunscreen octinoxate in the presence of the sunscreen avobenzone. *Photochem. Photobiol.* 81, 452-456.

31. Dondi, D., Albini, A. and Serpone, N. (2006) Interactions between different solar UVB/UVA filters contained in commercial suncreams and consequent loss of UV protection. *Photochem. Photobiol. Sci.* 5, 835-843.

32. Gaspar, L.R., Maia, P. and Campos, M. (2006) Evaluation of the photostability of different UV filter combinations in a sunscreen. *Int. J. Pharm.* 307, 123-128.

33. Karlsson, I., Hillerström, L., Stenfeldt, A.L., Mårtensson, J. and Börje, A. (2009) Photodegradation of dibenzoylmethanes: potential cause of photocontact allergy to sunscreens. *Chem. Res. Toxicol.* 22, 1881-1892.

SUPPORTING INFORMATION

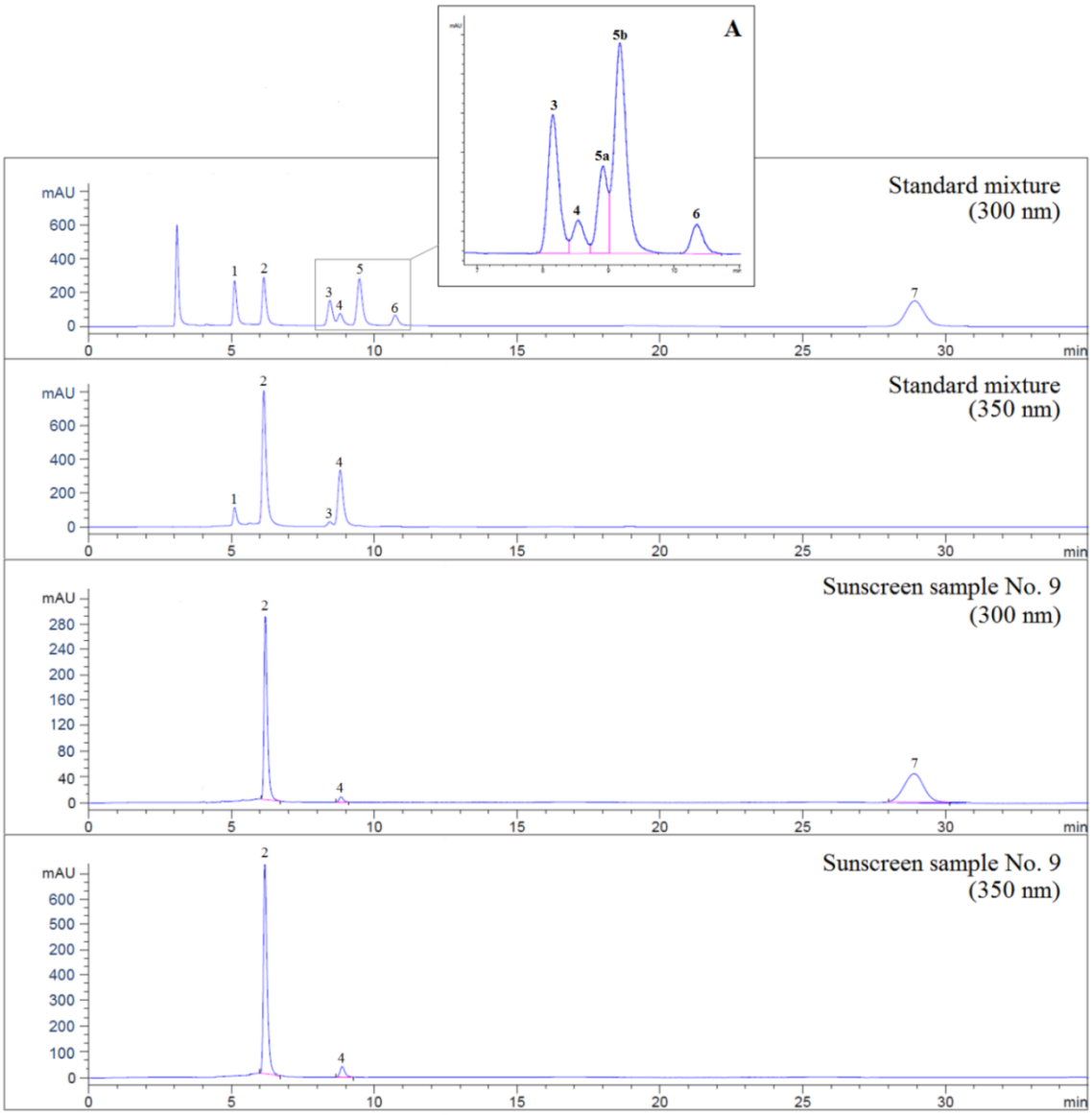

Figure S1 HPLC chromatogram of a standard mixture (50 mg L^{-1}) and exemplarily of the extracted UV filters of sunscreen sample No. 9, detected at 300 nm and 350 nm. 1: BP 3, 2: DBM (ISTD), 3: OCR, 4: BM DBM, 5: EHMC, 6: EHS, and 7: EHT. Enlarged section (A) after 1 h irradiation at 43 W m^{-2}, showing the two isomers *Z*-EHMC (5a) and *E*-EHMC (5b).

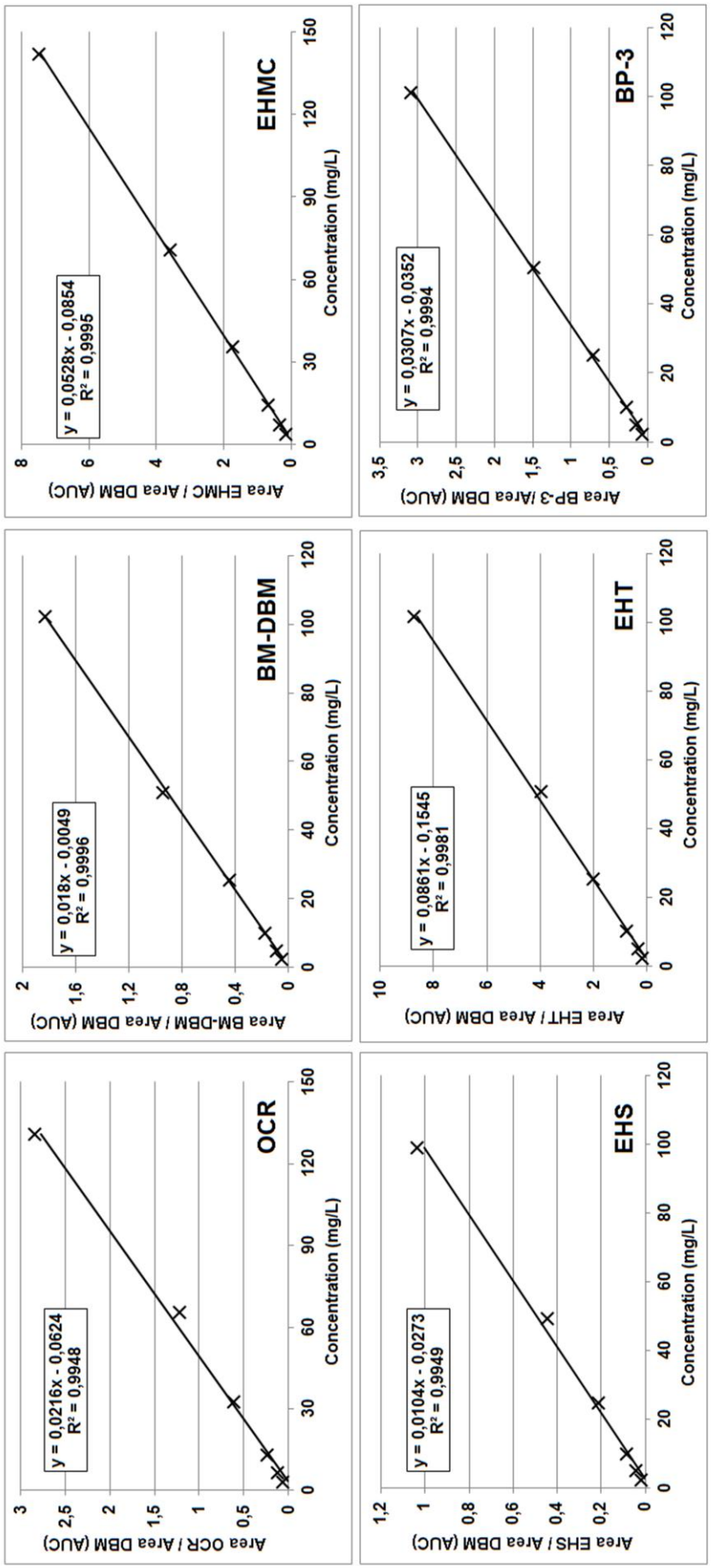

Figure S2 Calibration curves for the respective UV filters, measured at 300 nm for OCR, EHMC, EHS, EHT, and BP-3, and at 350 nm for BM-DBM.

VII Summary

Undoubtedly, the usage of sunscreens is one of the most important ways to protect the skin against the harmful effects of UV radiation. To secure their safety and efficacy, sun protection products must provide, *inter alia*, a well-balanced UVA/UVB protection, a high photostablity of the used UV filters, and a good tolerability.

Some properties like the sun protection factor (SPF), the UVA protection ability (UVAPF) and the photostability can be determined either *in vivo*, on human skin, or *in vitro* by using roughened quartz or polymethylmethacrylate (PMMA) plates as recommended substrate material. As *in vitro* techniques show a good reproducibility, are comparatively cheap, and can refrain from the use of human volunteers, they are often the method of choice in practice. However, as the used substrates are chemical inert and have a completely different structure than human skin, they cannot take into account any reactions, which may be attributed to natural skin structure and its constituents.

For the determination of a possible sensitizing potential of a cosmetic ingredient, however, exactly such interactions between the substances applied and the skin play a crucial role. In particular, the binding of electrophilic reactants to nucleophilic amino groups of skin proteins (haptenization) plays a key role in the development of allergic and photoallergic reactions.

Although UV filters are important, widespread used cosmetic ingredients, their reaction potential towards skin proteins has hardly been studied so far. Therefore, the aim of the present thesis was to contribute closing this gap of knowledge in the field of basic research and to investigate the reactivity of widespread UV filter substances towards skin proteins. For this purpose, increasingly complex protein or skin model systems were applied to examine the underlying chemical mechanisms by means of different analytical techniques.

At first, the development of a rapid high-performance thin-layer chromatographic (HPTLC) screening method on an amino phase as protein model provided an easy and rapid way to estimate the reactivity of different common UV filters, namely benzophenone-3 (BP-3), hydroxymethoxybenzoyl sulfonic acid (HMBS), butyl methoxydibenzoylmethane (BM-DBM), 3-benzylidene camphor (3-BC), 4-methylbenzylidene camphor (4 BMC), octocrylene (OCR), ethylhexyl methoxycinnamate (EHMC), ethylhexyl salicylate (EHS), diethylhexyl butamido triazone (DEBT), ethylhexyl triazone (EHT), and octyldimethyl p-aminobenzoic acid (OD-PABA) towards amino groups or skin proteins under thermal and/or irradiation conditions. A direct comparison of the results of the screening with patch and photopatch test data of the dermatological practice showed that especially the UV filters BP-3, HMBS, OCR, BM-DBM, and DBM, which are known to be common triggers for allergic an photoallergic reactions, showed the highest tendency to bind to the amino phase. This indicates that the screening may be well suited to identify possible skin sensitizers as part of a multistage testing strategy.

The observation that the reactivity of the different UV filters used can be influenced by both heat and UV irradiation was verified during the subsequent studies with the amino acid models butylamine and ethanolamine. The UV filters showed individual, partly very different, time- and temperature-dependent reactivities towards the two amines. An additional irradiation resulted only in a small increase of the respective conversions and in a slightly different distribution of the amine adducts, except in the case of OCR, for which the respective amide as additional by-product was detectable.

Benzophenone imines, enamines, and amides were identified as typical reaction products by means of electrospray ionization mass spectrometry (ESI-MS), Fourier transform infrared (FTIR), and nuclear magnetic resonance (NMR) spectroscopy. BP-3, HMBS, the dibenzoylmethanes, OCR, and EHS showed by far the highest reactivity what was in good correlation with the previous screening, indicating a different contact-allergic potential of the UV filters. For BP-3, HMBS, and OCR, already room temperature was sufficient to initiate the conversion. In contrast, the esters EHMC and EHT showed a significantly lower reactivity, and for the UV filters 3-BC, 4-MBC, and OD-PABA no conversion was observable at all.

The formation of the reaction products had partly big influence on the respective UV filter spectra. In the case of BP-3, HMBS, and EHS, the conversions led to a strong bathochromic shift and hence to approved UVA protection. In contrary, in the case of DBM and BM-DBM, a breakage of the diketo structure was observed, resulting in a significant decrease of the respective absorption strength (up to 80 and 60 %) and a loss of UVA protection. The most significant difference was apparent in the case of OCR, which was converted to the respective benzophenone imines associated with the cleavage of its cyanoacetate moiety, resulting in a nearly complete loss of its UVB protection ability.

The same reaction tendencies could also be observed, when using Boc-protected lysine, the tetrapeptide Boc-Gly-Phe-Gly-Lys-OH (Boc-GFGK), and bovine serum albumin (BSA) as increasingly complex protein or skin models. As seen for the ethanolamine and butylamine, OCR and BM-DBM confirmed to be most reactive towards the lysine side chains of the mentioned model systems, followed by DBM > BP 3 > EHS > EHMC > EHT in decreasing order. The determination of the conversions or rather the binding amount of the UV filters was performed by analyzing the remaining unbound UV filters by high-performance liquid chromatography coupled to diode-array detection (HPLC-DAD). Adducts formed with Boc-lysine and Boc-GFGK were determined by ESI-MS.

In contrast to the previous reactions with the amines, for BM-DBM and DBM enamines were the only detectable reaction products with Boc-lysine and Boc-GFGK, whereas no cleavage of the diketo-structure occurred. Also EHMC showed some differences: due to Michael-type additions at the conjugated double bond the respective amines were formed, whereas no ester aminolysis was observed. In the case of EHS, EHT and OCR, the same reaction products were identified.

To determine the covalent binding of the UV filters to the protein BSA, beside the extraction of the unbound UV filters, the increase of the molar mass of the formed BSA-adducts was additionally exemplarily determined for EHMC and DBM by matrix-assisted laser desorption/ionization time-of-flight mass spectrometry (MALDI-TOFMS). The mass increase allowed a direct conclusion about the binding amount of the respective UV filters. The results of the MALDI determinations were highly identical to the results calculated from the depletion of the two UV filters, confirming that the fast HPLC-DAD method was quite suitable to determine the amounts of the UV filters bound to BSA.
As the formation of the enamines and amines only had small influence on the UV characteristics of the respective UV filters, the binding to BSA did not affect the UV absorption properties of BM-DBM, EHMC, and EHT, but led to a bathochromic shift in the cases of BP-3 and EHS. Binding to BSA led again to a strong hypsochromic shift and a nearly complete loss of UVA+B protection in the case of OCR.

To better reflect the usual application conditions, in a next step, a thin gelatine layer was chosen as skin model. The UV filter amounts applied were adapted according to the existing ISO norm for the determination of the SPF. Afterwards, UV irradiation was performed. Beside the determination of the binding amounts by extraction of the unbound UV filters, two specially synthetized, stable-isotope labelled UV filter analogues (EHC-d_5 and DBM-d_5) were used to additionally determine the binding of the UV filters by isotope-ratio mass spectrometry (IRMS) due to the changes of the $^2H/^1H$ isotope ratio (δ^2H). The resulting δ^2H values after 4 hours of irradiation (-55.5 ‰ and 7.1 ‰ against Vienna Standard Mean Ocean Water (VSMOW)) were significantly enriched in ^2H compared to pure gelatin (-74.4 ‰ against VSMOW), confirming a binding of the deuterium-labeled UV filters. Again, the results of the IRMS measurements showed a good correlation to the results of the extraction and subsequent HPLC-DAD determination. In contrast to the esters EHMC and EHT, which showed comparatively small binding amounts, for the other UV filters (OCR, BP-3, EHS, and BM-DBM) significant reaction tendencies towards gelatin were observed.

Finally, it was observed to what extent the results of the model studies coincide with observations on fresh skin. For this purpose, various commercial sunscreens and personal care products with integrated UV protection were applied on either prepared porcine skin or glass plates, followed by UV irradiation. Significant differences were observed for the amounts of UV filters extracted from glass and skin. The lower recoveries in the case of the porcine skin indicated some additional reaction of the UV filters towards the skin samples. Due to the previous studies, it can be suggested that protein binding may be mainly responsible for the observed discrepancy. Also in the case of the skin, the UV filters differed in their reactivity, whereas BP-3 showed the highest discrepancy between the recoveries from glass and skin of an average of 13 % and 24 % after 2 and 4 h irradiation, followed by EHS > BM-DBM > OCR > EHMC > EHT in decreasing order.

Whereas for nearly all sun protection products included in the study a relatively high photostability was observed, some of the studied day care products showed a high photodegradation tendency, especially in the case of the combination of BM-DBM and EHMC.

The present dissertation showed that cosmetic UV filters were able to react with amino structures of different proteins under thermal and irradiation conditions. As the formation of protein adducts is seen as key event in the development of allergic and photoallergic reactions, the results indicate a specific skin sensitization potential of the UV filters. This is confirmed by the experience of dermatological practice. Since such reactions have partly strong influence on the respective UV filter spectra, the existing *in vitro* methods using PMMA plates or quartz glass as substrates have to be questioned, since those methods cannot capture such skin-typical reactions.
Since this work investigated basic chemical processes of protein reactions, the results of this work may also be helpful for the assessment of further chemical ingredients. Existing structural similarities can give information on possible reactions occurring and may help to estimate a possible sensitization potential of different chemical substances.

VIII Zusammenfassung

Ohne Zweifel ist die Verwendung von Sonnencremes eine der wichtigsten Möglichkeiten, die Haut vor den negativen Auswirkungen übermäßiger UV-Strahlung zu schützen. Um ihre Sicherheit und Wirksamkeit zu gewährleisten, müssen Sonnenschutzprodukte unter anderem einen ausgewogenen UVA- und UVB-Schutz ausweisen, sollten photostabile UV-Filtersubstanzen enthalten und eine gute Verträglichkeit zeigen.
Einige Paramater wie der Sonnenschutzfaktor (SPF), die UVA-Schutzleistung und die Photostabilität der Produkte können sowohl *in vivo*, heißt auf menschlicher Haut, oder *in vitro* auf geeigneten Modellsystemen, z.B. Methacrylat- oder Quarzplättchen, bestimmt werden. Da *in vitro* Methoden gut reproduzierbare Ergebnisse liefern, in vielen Fällen vergleichsweise günstig sind und ohne den Einsatz von menschlichen Probanden auskommen, werden diese in der Praxis häufig bevorzugt. Da das im Test verwendete Plattenmaterial jedoch chemisch inert ist und völlig anders aufgebaut ist als die menschliche Haut, können jegliche Reaktionen, die auf die natürliche Hautstruktur zurückzuführen sind, nicht erfasst werden.

Bei der Bestimmung eines möglichen sensibilisierenden Potentials eines chemischen Stoffes spielen hingegen genau solche Wechselwirkungen zwischen den aufgebrachten Substanzen und der Haut eine entscheidende Rolle. So stellt insbesondere die Bindung elektrophiler Reaktionspartner an nukleophile Aminogruppen von Hautproteinen (Haptenisierung) eine Schlüsselrolle bei der Entstehung allergischer und photoallergischer Reaktionen dar.

Obwohl UV-Filter wichtige und vielfach verwendete kosmetische Inhaltsstoffe sind, wurde ihr Reaktionsvermögen gegenüber Hautproteinen bisher kaum untersucht. Das Ziel der vorliegenden Doktorarbeit war es daher, dazu beizutragen, diese Wissenslücke im Bereich der Grundlagenforschung zu schließen und die Reaktivität weit verbreiteter UV-Filtersubstanzen gegenüber Hautproteinen zu untersuchen. Hierfür wurden unterschiedliche, komplexer werdende Protein- und Hautmodelle herangezogen und die zugrundeliegenden chemischen Mechanismen mit Hilfe geeigneter analytischer Methoden untersucht.

Im ersten Schritt wurde eine schnelle hochleistungsdünnschichtchromatographische (HPTLC) Screening-Methode auf Basis einer Aminophase als Proteinmodell entwickelt. Durch die Bestimmung des Bindungsvermögens der UV-Filtersubstanzen Benzophenon-3 (BP-3), 2-Hydroxy-4-methoxybenzophenon-5-sulfonsäure (HMBS), Octocrilen (OCR), Butylmethoxydibenzoylmethan (BM-DBM), Dibenzoylmethan (DBM), Ethylhexylsalicylsäure (EHS), 3-Benzylidencampher (3-BC), 4-Methylbenzylidencampher (4-MBC), Ethylhexylmethoxyzimtsäure (EHMC), Diethylhexylbutamidotriazon (DEBT), Ethylhexyltriazon (EHT) und Octyldimethyl-*p*-aminobenzoesäure (OD-PABA) an die Aminoschicht konnte die generelle Reaktivität der UV-Filter gegenüber Proteinstrukturen unter dem Einfluss von Wärme und UV-Bestrahlung bestimmt werden.

Ein direkter Vergleich der Ergebnisse des Screenings mit Patch- und Photopatchtest-Daten aus der dermatologischen Praxis zeigte, dass insbesondere die UV-Filter BP-3, HMBS, OCR, BM-DBM und DBM, die als typische Auslöser allergischer bzw. photoallergischer Reaktionen gelten, auch auf der Aminophase die größte Bindungstendenz zeigten. Dies legt die Vermutung nahe, dass das entwickelte Screening als Teil einer Testbatterie dazu beitragen kann, mögliche sensibilisierende Stoffe zu identifizieren.

Die Beobachtung, dass die Reaktivität der untersuchten UV-Filter gegenüber Aminstrukturen sowohl durch Wärmeeinwirkung sowie UV-Bestrahlung beeinflusst werden kann, wurde bei den folgenden *in vitro* Untersuchungen mit den Aminosäuremodellen Butylamin und Ethanolamin überprüft. Die UV-Filter zeigten eine individuell sehr unterschiedliche, zeit- und temperaturabhängige Reaktivität gegenüber den beiden Aminen. Eine zusätzliche Bestrahlung mit UV-Licht äußerte sich für fast alle UV-Filter lediglich in einer geringen Erhöhung des Umsatzes und einer geringfügig unterschiedlichen Mengenverteilung der Aminaddukte. Eine Ausnahme bildete hier lediglich OCR, für welches das entsprechende Amid als weiteres Nebenprodukt nach Bestrahlung detektierbar war. Mittels Elektrospray-Ionisations-Massenspektrometrie (ESI-MS), Infrarotspektroskopie (IR) und Kernspinresonanzspektroskopie (NMR) konnten Benzophenonimine, Enamine und Amide als typische Reaktionsprodukte identifiziert werden. Ähnlich dem vorangegangenen Screening zeigten BP-3, HMBS, die beiden Dibenzoylmethane, OCR und EHS bei weitem die größte Reaktivität. Im Fall von BP-3, HMBS und OCR waren bereits bei Raumtemperatur deutliche Reaktionsumsätze feststellbar. Die beiden Ester EHMC und EHT hingegen zeigten eine deutlich geringere Reaktivität und für die beiden Campferderivate 3-BC und 4-MBC und für OD-PABA konnte unter den angewandten Bedingungen keinerlei Umsatz mit den Aminen detektiert werden. Wie bereits für das Screening erwähnt, lässt die unterschiedliche Reaktivität der einzelnen UV-Filter erste Rückschlüsse auf Unterschiede im Sensibilisierungspotential der Substanzen zu.
Die Bildung der unterschiedlichen Reaktionsprodukte führte zum Teil zu starken Veränderungen im Absorptionsspektrum der jeweiligen UV-Filter. Im Falle von BP-3, HMBS und EHS wurde eine deutliche bathochrome Verschiebung der Spektren und damit eine erhöhte UVA-Schutzwirkung festgestellt. Im Gegensatz dazu war im Falle von DBM und BM-DBM ein Bruch der Diketostruktur feststellbar, was zu einem deutlichen Verlust der Absorptionsstärke (bis zu 80 % bzw. 60 %) und damit auch der UVA-Schutzleistung führte. Die größten Unterschiede waren im Falle von OCR feststellbar. Durch die Bildung des entsprechenden Benzophenonimins, einhergehend mit dem Verlust der Cyanoacetat-Seitenkette, zeigte der UV-Filter einen fast vollständigen Verlust seiner Schutzleistung im UVB-Bereich.

Ähnliche Reaktionstendenzen der einzelnen UV-Filter waren auch für die komplexer werdenden Reaktionspartner Boc-Lysin, das Tetrapeptid Boc-Gly-Phe-Gly-Lys-OH (Boc-GFGK) und Rinderserumalbumin (BSA) feststellbar, die als weitere Protein- bzw. Hautmodelle dienten.

Wie in den vorangegangenen Versuchen zeigten OCR und BM-DBM auch gegenüber den Lysin-Seitenketten der genannten Modellsysteme die größte Reaktivität, gefolgt von den UV-Filtern DBM > BP 3 > EHS > EHMC > EHT in abnehmender Reihenfolge. Die Bindungsmenge der jeweiligen UV-Filter wurde anhand der verbleibenden, nicht umgesetzten UV-Filter mittels Hochleistungsflüssigkeitschromatographie, gekoppelt mit Diodenarray-Detektor (HPLC-DAD), bestimmt. Mit Boc-Lysin und Boc-GFGK gebildete Addukte wurden mittels ESI-MS identifiziert.

Im Gegensatz zu den vorangegangenen Aminreaktionen waren im Falle von DBM und BM-DBM die jeweiligen Enamine die einzigen detektierbaren Reaktionsprodukte mit Boc-Lysin und dem Tetrapeptid. Die zuvor beobachtete Spaltung der Diketostruktur war nicht feststellbar. Auch im Falle von EHMC waren Unterschiede zu den vorherigen Ergebnissen erkennbar: Durch eine Michael-Addition der Aminogruppe an die freie Doppelbindung des Zimtsäureesters wurde das jeweilige Amin gebildet, eine Aminolyse des Esters fand dagegen nicht statt. Im Falle von EHS, EHT und OCR waren dieselben Reaktionsprodukte wie bei den vorangegangenen Aminversuchen identifizierbar.

Um die kovalente Bindung der UV-Filter an das Protein BSA festzustellen, wurde zusätzlich zur Extraktion der ungebundenen UV-Filter die Veränderung der molaren Masse des Proteins beispielhaft für die Reaktion mit dem Ester EHMC und dem Diketon DBM mittels Matrix-unterstützter Laser-Desorption/Ionisation (MALDI-TOFMS) bestimmt. Aus der Massenzunahme konnte direkt auf die Menge an gebundenem UV-Filter geschlossen werden. Die Ergebnisse der MALDI-Messungen zeigten eine sehr gute Übereinstimmung mit den Ergebnissen, die mittels HPLC-DAD bestimmt wurden und bestätigten die gute Anwendbarkeit der Extraktionsmethode zur Bestimmung der UV-Filter-Bindung an das Protein.

Da sich durch die Enamin- und Aminbildung die UV-Absorptionscharakteristika der jeweiligen UV-Filter nur geringfügig änderten, konnten für die Bindung von BM-DBM, EHMC und EHT an BSA keine deutlichen Unterschiede in den UV-Spektren festgestellt werden. Wie bereits im Falle von Butyl- und Ethanolamin beobachtet, war hingegen bei EHS und BP-3 eine bathochrome Verschiebung der ursprünglichen Absorptionsspektren der UV-Filter zu beobachten. Für OCR führte die Bindung an BSA erneut zu einer deutlichen hypsochromen Verschiebung des UV Spektrums und damit zu einem fast vollständigen Verlust der UVB-Schutzwirkung des UV-Filters.

Um im nächsten Schritt die realen Anwendungsbedingungen noch besser abbilden zu können, wurde eine dünne Gelatineschicht als Hautmodell verwendet. Die Menge der aufgetragenen UV-Filter wurde entsprechend der bestehenden ISO-Norm zur Bestimmung des Lichtschutzfaktors (LSF) angepasst. Anschließend erfolgte die Bestrahlung unter Simulation natürlicher Sonnenstrahlung. Neben der Bestimmung der Bindungsmenge mittels Extraktion der ungebundenen UV-Filter wurde mithilfe zweier eigens synthetisierter, stabilisotopen-markierter UV-Filteranaloga (EHC-d_5 und DBM-d_5) die Bindung der beiden UV-Filter an das Protein mittels Isotopenverhältnis-Massenspektrometrie (IRMS) anhand der Änderungen des $^2H/^1H$-Isotopenverhältnisses (δ^2H) bestimmt. Die resultierenden δ^2H-Werte nach vierstündiger Bestrahlung (-55.5 ‰ and 7.1 ‰ gegen Vienna Standard Mean Ocean Water

(VSMOW)) zeigten im Gegensatz zu reiner Gelatine (-74.4 ‰ gegen VSMOW) eine deutliche Anreicherung and ^{2}H, was die Bindung der deuterierten UV-Filter bestätigte. Die Ergebnisse der IRMS Messungen zeigten erneut eine gute Übereinstimmung mit den Ergebnissen der Extraktion und anschließenden HPLC-DAD Bestimmung. Im Gegensatz zu den beiden Estern EHMC und EHT, für die eher geringe Bindungsmengen festgestellt wurden, zeigten die übrigen UV-Filter (OCR, BP-3, EHS und BM-DBM) eine deutliche Bindungstendenz gegenüber der Gelatineschicht.

Abschließend wurde untersucht, inwieweit sich die Ergebnisse der durchgeführten Modellstudien mit Beobachtungen auf Echthaut decken. Dafür wurden unterschiedliche handelsübliche Sonnencremeprodukte und Pflegepräparate mit integriertem UV-Schutz auf präparierte Schweinehautstücke sowie Glasplättchen aufgetragen und anschließend bestrahlt. Bei der sich anschließenden Extraktion der UV-Filter wurden signifikante Unterschiede zwischen den jeweils ermittelten UV-Filtergehalten festgestellt. Die geringeren Wiederfindungen im Falle der Schweinehaut lassen auf eine zusätzliche Reaktion der UV-Filter auf der Haut schließen, wobei die vorausgegangenen Ergebnisse vermuten lassen, dass Proteinreaktionen hier von entscheidender Bedeutung sind. Auch im Falle des Reaktionspartners Haut zeigten die untersuchten UV-Filter unterschiedliche Reaktivitäten, wobei für die untersuchten Proben im Falle von BP-3 der deutlichste Unterschied der Wiederfindung zwischen Glas und Haut (13 % bzw. 24 % nach 2- und 4-stündiger Bestrahlung) feststellbar war, gefolgt von EHS > BM-DBM > OCR > EHMC > EHT in absteigender Reihenfolge.
Im Falle der untersuchten Sonnenschutzprodukte konnte für nahezu alle Proben eine gute Photostabilität der verwendeten UV-Filter gezeigt werden. Für einige der Tagespflegeprodukte war hingegen ein teils deutlicher Photoabbau feststellbar, insbesondere bei der Kombination der beiden UV-Filter BM-DBM und EHMC.

Mit der vorliegenden Dissertation konnte gezeigt werden, dass kosmetische UV-Filter unter dem Einfluss von Wärme und UV-Licht in der Lage sind, mit Aminostrukturen unterschiedlicher Proteine zu reagieren. Da die Bildung von Proteinaddukten als entscheidender Schritt bei der Ausbildung von Allergien und Photoallergien gilt, lassen die Ergebnisse ein mögliches Sensibilisierungspotential dieser kosmetischen Inhaltsstoffe vermuten. Dies wird durch die Erfahrungen aus der dermatologischen Praxis bestätigt. Da sich derartige Reaktionen teils stark auf die UV-Spektren der jeweiligen UV-Filter und damit auch deren Schutzleistung auswirken, sollten die existierenden *in vitro* Methoden zur Bestimmung der Wirksamkeit von Sonnenschutzprodukten kritisch hinterfragt werden, da beim Einsatz inerter Substratmaterialien wie PMMA oder Quarzglas der Einfluss hautspezifischer Reaktionen nicht berücksichtigt wird.
Da im Zuge dieser Arbeit grundlegende chemische Prozesse von Proteinreaktionen untersucht wurden, können die Ergebnisse auch bei der Bewertung weiterer kosmetischer Inhaltsstoffe hilfreich sein. Anhand vorhandener Strukturähnlichkeiten können Rückschlüsse auf mögliche ablaufende Reaktionen und damit auch auf ein gewisses Sensibilisierungspotential der Substanzen gezogen werden.